Trinity College Dublin
Coláiste na Tríonóide, Baile Átha Cliath
The University of Dublin

Comparing Pathways for Retinal and Neuronal Degeneration in *Drosophila melanogaster*

Thesis submitted to the

University of Dublin

for the degree of

Doctor in Philosophy

Guillaume Charles Thuéry

Supervisor:

Prof. Mani Ramaswami

School of Genetics and Microbiology

and

Trinity College Institute of Neuroscience

Trinity College Dublin

August 2023

Declaration

I declare that this thesis has not been submitted as an exercise for a degree at this or any other university and it is my original research work. Wherever contributions of others were involved, every effort was made to indicate this clearly, with due reference to the literature, and acknowledgment of collaborative research and discussions.

I agree to deposit this thesis in the University's open access institutional repository or allow the Library to do so on my behalf, subject to Irish Copyright Legislation and Trinity College Library conditions of use and acknowledgement.

I consent to the examiner retaining a copy of the thesis beyond the examining period, should they so wish (EU GDPR May 2018).

Guillaume C. Thuéry

August 2023

Summary

Cellular degeneration is the result of molecular processes triggered by external or internal stimuli which manifests as deleterious changes to cell structure or function, and can eventually cause cell death. In an attempt to improve cell survivability, cellular pathways activate in response to specific stimuli. Such pathways include the integrated stress response (ISR), the unfolded protein response (UPR), and the formation of ribonucleoprotein (RNP) granules containing RNA and RNA-binding proteins (RBP). With overlapping components, both the ISR and the UPR activate in response to endoplasmic reticulum (ER) stress and lead to the expression of stress response genes. In addition, many stressful factors can affect nucleic content. For this reason, the cell will initiate the formation of stress-granules, dense in RNA molecules and RBPs, protecting sensitive nucleic content and stall protein translation until cellular homeostasis is returned.

These evolutionarily conserved pathways have been shown to exacerbate cytotoxicity in models of neurodegenerative diseases, for instance, amyotrophic lateral sclerosis, and Huntington's disease (HD). Likewise, there is accumulating evidence that these pathways are implicated in retinal degenerative diseases, with more work having been conducted on the role of ER stress and the ISR in this field. The fact that these pathways are involved is undisputed. Nevertheless, it remains unclear how they relate to pathogenesis, whether chronic activation may exacerbate or protect against cytotoxicity. It has also not been determined to what extent these pathways and their contribution to disease progression overlap between retinal and neuronal degeneration. The primary aim of this thesis was to gain additional insights on overlapping pathways involved in retinal and neuronal degeneration using *Drosophila melanogaster* by modulating the expression of genes involved in the ISR, RNA metabolism, and RNP granule formation.

In the first results chapter of this thesis, retinal degeneration was induced using a mutation in the *rdgB* gene, leading to the visible degeneration of photoreceptor cells. The molecular cascade initiated by mutations of the *rdgB* gene leading to retinal degeneration is unclear. Although activation of the ISR and its components was not detected in the *rdgB* mutant flies, decreasing the expression of PERK, an ISR

component, led to a stark reduction in the retinal degeneration phenotype. In addition, decreasing the expression of a novel RBP known as SF3B2, and two RNP granule components: ATX2 and Rin, led to varying degrees of phenotypic rescue. These novel observations suggest that these proteins and pathways contribute to the cytotoxicity induced by the mutation in the *rdgB* gene, further clarifying the mechanisms underlying this model of retinal degeneration.

In the second results chapter, the requirement of these same proteins for disease progression was assessed in a neurodegeneration model induced by expressing a CAG expanded form of the human *Huntingtin* gene (*Htt*Q138), specifically in a small population of neurons required for a functional circadian rhythm in constant darkness. Decreasing the expression of PERK led to an slightly improved circadian rhythm in flies also expressing *Htt*Q138, suggesting that the ISR could contribute to this form of cytotoxicity, in agreement with previous literature. However, decreasing the expression of RNP granule components, ATX2 and Rin, led to two different effects. As previously reported, a powerful improvement of the circadian rhythm was observed with a reduction of ATX2 expression, but counterintuitively caused an increase in observed neuronal death, and a clearance of HTT aggregation. Decreasing the expression of Rin, however, exacerbated the neurodegenerative phenotype by worsening the circadian rhythm and increasing cell death. These last results either suggest a protective role for Rin against cytotoxicity, or an essential role in neuronal survivability in general. Overall, these observations suggest that RNP granule components are involved in neurodegeneration, but have vastly different roles in disease progression.

These experiments taken together provide evidence that PERK and ATX2 are activated and exacerbate disease progression in both models of cellular degeneration; providing possible overlapping pathways between retinal degeneration and neurodegeneration through the ISR and the dysfunctional formation of RNP granules. Future studies are required to further elucidate the mechanisms underlying these pathways and whether chronic activation of these pathways are significant contributors to disease progression. Future intervention studies should explore whether inhibitors targeting these pathways could slow disease progression in different models of retinal degeneration and neurodegeneration.

Acknowledgements

First, I am deeply indebted to my supervisor, Prof. Mani Ramaswami, for his guidance and expertise throughout this research project. I sincerely appreciate all the opportunities he has given me to learn and mature as a researcher.

I am grateful to my thesis committee, Dr. Sarah Doyle and Prof. Frank Wellmer, for giving me crucial feedback during the early stages of my project; and to Dr. Tamara Boto for helping me approach the study of sleep and circadian rhythms, and for encouraging me during challenging times.

To the postdocs in our lab and in the NCBS: Jens, Jörn, Márcia, and Aman, thank you for your experienced insights, feedback, encouragement, and friendship throughout my PhD journey. Your contributions and support were instrumental in helping me navigate the challenges of research.

This endeavour would not have been possible without my brilliant fellow PhD students, Arnas, Camilla, Daniel, and Georgia. Thank you for your invaluable friendship and support. Our discussions in the lab, and in pubs, have shaped me and my project, and I am grateful for the memories we have shared over the years. I was also lucky to work with talented undergraduate students: Sadhbh, thank you for helping me establish the groundwork for this thesis, and Jasmine, for keeping my flies well fed.

I am thankful for my parents Jacques and Betty, my siblings Anne and Philippe, and their partners Olivier and Anna, for their love, support, and feedback throughout this academic and personal journey. I could not have achieved this milestone without them.

I am grateful for Michael, Cora, and Michelle, for having effectively adopted me and helping me to call Ireland my home.

My friend Teddy, thank you for our conversations and for making me laugh when I needed it most.

Words cannot express my gratitude to Elaine for her love and presence in my life. You have been a source of strength and positivity. I could not have done this without you.

Finally, although he may not read this, I am grateful for my beloved cat, Frisco, reminding me to focus on the present moment whenever I looked up from my screen.

Table of Contents

Declaration i

Summary ii

Acknowledgements iv

Table of Contents v

List of Figures vii

List of Tables ix

List of Abbreviations x

Chapter 1 Introduction 1

1.1. Cellular degeneration 2

1.2. Retinal degeneration 2

1.2.1. Background 2

1.2.2. Photoreceptors 3

1.2.3. Animal opsins 4

1.2.4. Phototransduction in ciliary photoreceptors 6

1.2.5. Phototransduction in microvillar photoreceptors 7

1.2.6. Retinal degenerative models 8

1.3. Neurodegeneration 13

1.3.1. Neurodegenerative diseases 13

1.3.2. Huntington's disease 14

1.4. Integrated stress response 20

1.4.1. ISR pathway 20

1.4.2. ISR in diseases 23

1.5. Aims and objectives 25

Chapter 2 Materials and Methods 28

2.1. Materials 29

2.1.1. *Drosophila* lines 29

2.1.2. General laboratory chemicals and consumables 30

2.1.3. Equipment 30

2.2. Methods 31

2.2.1. *Drosophila* stock maintenance and fly husbandry 31

2.2.2. Gal4/UAS system 31

2.2.3. Retinal degeneration assessment 32

2.2.4. Monitoring translational activation of ATF4 34

2.2.5. Immunohistochemistry 34

2.2.6. RNA analysis 36

2.2.7. Circadian rhythm 41

Chapter 3 Modulation of *rdgB*^{9}-Induced Retinal Degeneration 43

3.1. Introduction 44

3.1.1. The *Drosophila* eye 44

3.1.2. Assessing retinal degeneration in the *Drosophila* retina 45

3.1.3. Aims 47
3.2. Results 48
3.2.1. *rdgB*^{9} mutation causes retinal degeneration 48
3.2.2. Stress pathway activation in *rdgB* mutants 50
3.2.3. Modulating the RdgB^{9} retinal degeneration phenotype 55
3.3. Discussion 69
3.3.1. Stress pathway activation in *rdgB* mutants 70
3.3.2. Efficiency of knockdown and overexpression 72
3.3.3. Pathways involved in *rdgB*^{9}-induced retinal degeneration 75
3.3.4. Conclusion 84
Chapter 4 Modulation of Neurodegeneration Induced by an Expanded Form of HTT 86
4.1. Introduction 87
4.1.1. Circadian rhythm 87
4.1.2. Huntington's disease 92
4.1.3. Aims 95
4.2. Results 96
4.2.1. PERK mediates huntingtin toxicity in circadian rhythm neurons 96
4.2.2. Novel RBPs may mediate huntingtin toxicity in circadian rhythm neurons 106
4.2.3. Ataxin-2 mediates huntingtin toxicity in circadian rhythm neurons 115
4.2.4. Rasputin may play a protective role against Huntingtin toxicity 124
4.3. Discussion 133
4.3.1. Pathways involved in *Htt*Q138-induced neurodegeneration 134
4.3.2. Further studies 142
4.3.3. Conclusion 144
Chapter 5 General Discussion and Future Directions 145
5.1. General discussion 146
5.1.1. Pathways involved in the RdgB^{9} model of retinal degeneration 147
5.1.2. Pathways involved in the *Htt*Q138 model of neurodegeneration 148
5.1.3. Overlapping mechanisms in cellular degeneration 152
5.2. Future directions 155
5.3. Concluding remarks 157
Bibliography 159
Appendices 179
Appendix 1. Presence of two UAS constructs does not lead to a reduction in the power of rhythmicity 180
Appendix 2. *Rin* knockdown does not affect stress-induced transcription 182
Appendix 3. Novel RNA-binding protein alignments, and RNAi targets 184

List of Figures

Figure 1-1 Phylogenetic tree of metazoans showing photoreceptor types in representative animal groups or species 4
Figure 1-2 Diagram of microvillar and ciliary photoreceptors 5
Figure 1-3 Diagram of the ciliary phototransduction pathway 6
Figure 1-4 Diagram of the microvillar phototransduction pathway 7
Figure 1-5 Diagram of the phosphatidylinositol (PI) cycle in *Drosophila melanogaster*. 10
Figure 1-6 Diagram of the domains found in RDGB and its mutant form *rdgB*^{9} 11
Figure 1-7 Diagram of the unfolded protein response and the integrated stress response in *Drosophila* 22
Figure 2-1 Diagram of the UAS/Gal4 system 31
Figure 2-2 Representative images and diagram of retinal degeneration observed in RdgB^{9} flies 33
Figure 2-3 Run used for the Real-Time Quantitative Polymerase Chain Reactions (RT-qPCR) 40
Figure 2-4 DAM2 *Drosophila* Activity Monitor 41
Figure 3-1 The *rdgB*^{9} mutation leads to a significant and quantifiable degeneration of photoreceptors compared to controls 49
Figure 3-2 Representative images of the retina of a 10 day old *rdgB*^{2}*/ ;tubulin(p)ATF4.5'UTR > dsRed/CyO; +/+* fly with an ATF4 reporter staining 51
Figure 3-3 An ATF4 reporter was used to assess ISR activation depending on light exposure and the presence of the *rdgB*^{2} mutation 52
Figure 3-4 Expression of stress-related genes exhibited high variability across replicate experiments in RdgB^{9} flies 54
Figure 3-5 The ISR is involved in RdgB^{9}-related retinal degeneration through the kinase PERK 58
Figure 3-6 The involvement of novel RBPs in *rdgB*^{9}-induced retinal degeneration 62
Figure 3-7 The RNP granule formation pathway may be involved in *rdgB*^{9}-induced retinal degeneration. 66
Figure 3-8 The intrinsically disordered domain of ATX2 suppresses *rdgB*^{9}-induced retinal degeneration. 68
Figure 3-9 Model for mechanisms underlying *rdgb*^{9}-induced retinal degeneration 85
Figure 4-1 The neuronal circuitry of clock neurons in *Drosophila* 90
Figure 4-2 Activity plot showing PERK knockdown could rescue Huntingtin-mediated circadian rhythm dysfunction 98

Figure 4-3 PERK is required for huntingtin-mediated arrhythmicity 101
Figure 4-4 PERK knockdown is not sufficient to rescue *Htt*Q138-induced cell death 103
Figure 4-5 PERK does not modulate *Htt*Q138 aggregate formation in the brain 105
Figure 4-6 Activity plot showing that CG42458 knockdown does not seem to rescue Huntingtin-mediated circadian rhythm dysfunction 108
Figure 4-7 CG42458 may be required for Huntingtin-mediated arrhythmicity 110
Figure 4-8 CG42458 does not modulate cell death induced by *Htt*Q138 112
Figure 4-9 CG42458 does not modulate *Htt*Q138 aggregate formation in the brain 114
Figure 4-10 Activity plot showing that Ataxin-2 is required for Huntingtin-mediated circadian rhythm dysfunction 116
Figure 4-11 Ataxin-2 is required for *Htt*Q138-mediated arrhythmicity 119
Figure 4-12 Ataxin-2 knockdown aggravates cell death induced by *Htt*Q138 121
Figure 4-13 Ataxin-2 modulates *Htt*Q138 aggregate formation in the brain 123
Figure 4-14 Activity plot showing that Rasputin may play a protective role against Huntingtin-mediated circadian rhythm dysfunction 126
Figure 4-15 Rin knockdown aggravates *Htt*Q138-induced arrhythmicity 128
Figure 4-16 Rasputin knockdown does not affect cell death induced by *Htt*Q138 130
Figure 4-17 Rasputin modulates *Htt*Q138 aggregate formation in the brain 132
Figure 4-18 Molecular pathways involved in retinal degeneration and neurodegeneration 158

List of Tables

Table 2-1 List of *Drosophila* strains 29
Table 2-2 List of antibodies and reagents 29
Table 2-3 List of chemicals and consumables 30
Table 2-4 List of equipment 30
Table 2-5 Insertion sites of RNAi lines 32
Table 2-6 Reaction mix for cDNA synthesis 37
Table 2-7 Primer pairs used for qPCR 38
Table 2-8 Reaction mix for RT-qPCR reaction 39
Table 3-1 qPCR results for *perk*, *gcn2*, and *gadd34* expression modulation 57
Table 3-2 qPCR results for *CG42458* and *sf3b2* expression modulation 61
Table 3-3 qPCR results for *atx2* and *rin* expression modulation 65

List of Abbreviations

ALS	Amyotrophic lateral sclerosis
ANOVA	Analysis of variance
ATF4	Activating transcription factor 4
CAG	Polyglutamine repeat
CHOP	C/EBP homologous protein
CLK	Clock
CRC	Cryptocephal
CRY	Cryptochrome
CYC	Cycle
DAM	*Drosophila* activity monitor
DAPI	4′,6-diamidino-2-phenylindole
DD	Dark:Dark
DN	Dorsal neuron
DSHB	Developmental studies hybridoma bank
eIF2α	Eukaryotic translation initiation factor 2 subunit 1
ER	Endoplasmic reticulum
ERG	Electroretinogram
FBS	Foetal bovine serum
FFAT	Two phenylalanines in an acidic tract
FTD	Frontotemporal dementia
G3BP	Ras (GTPase-activating protein) SH3 domain binding protein
GADD34	Growth arrest and DNA damage-inducible protein
Gal4	Gal4 transcription factor
GCN2	General control nonderepressible-2
GFP	Green fluorescent protein
GMR	Glass multiple receptor
HD	Huntington's disease

HMF	Hazardous material facility
HRI	Haemin regulated inhibitor
HTT	Huntingtin protein
IDR	Intrinsically disordered region
IRE1	Inositol-requiring enzyme 1
ISR	Integrated stress response
ISRIB	Integrated stress response inhibitor
LD	Light:Dark
lLNv	Large ventral lateral neuron
LN	Lateral neuron
LNS2	Lipin/Ned1/Smp2
LPN	Lateral posterior neurons
MCS	Membrane contact site
mRFP	Monomeric red fluorescent protein
PA	Phosphatidic acid
PB	Processing bodies
PBS	Phosphate buffered saline
PCR	Polymerase chain reaction
PD	Parkinson's disease
PDF	Pigment dispersing factor
PER	Period
PERK	Protein kinase RNA (PKR)-like ER kinase
PI	Phosphatidylinositol
PIP	Phosphatidylinositol phosphate
PITP	Phosphatidylinositol transfer protein
PITPd	Phosphatidylinositol transfer protein domain
P-S	Power – Significance
RBP	RNA-Binding protein
RDGB	Retinal degeneration B
RH1	Rhodopsin-1 (*Drosophila*)
RHO	Rhodopsin (mammalian)
Rin	Rasputin

RNAi	Interfering RNA
RNP	Ribonucleoprotein
S2	Schneider-2 cells
SCA2	Spinocerebellar ataxia 2
SCN	Suprachiasmatic nucleus
SF3B2	Splicing factor 3 B2
SG	Stress granule
sLNv	Small ventral lateral neuron
SMC	Sub-microvillar cisternae
SOD1	Superoxide dismutase 1
TIM	Timeless
TRiP	Transgenic RNAi project
UAS	Upstream activating sequence
UPR	Unfolded protein response
VAP	Vesicle-associated membrane protein-associated protein
VDRC	Vienna *Drosophila* Research Center
VRN1	Neo-vascular inflammatory vitreoretinopathy
WT	Wild type

Chapter 1
Introduction

1.1. Cellular degeneration

A cell exposed to non-lethal injury from external or internal factors may exhibit various functional and morphological issues. This process is known as cellular degeneration and inevitably occurs during the lifetime of a living organism. If the factor initiating this degeneration is not effectively managed, it could result in cell death. Cellular degeneration plays an essential role in most pathologies, but it can be initiated by different factors, and different molecular pathways are involved.

This work focuses on two major forms of cellular degeneration, retinal and neuronal. Although these two forms of degeneration affect different cells, recent independent studies describe features which appear to be common to both retinal degeneration and central neurodegeneration, such as misfolded proteins, cellular stress, unfolded protein response (UPR) activation, and integrated stress response (ISR) activation (Athanasiou et al., 2017; Bugallo et al., 2020; Fan et al., 2017; Griciuc et al., 2011; McLaughlin et al., 2022; Starr et al., 2018; Xiang et al., 2016). However, retinal degeneration is not usually included in the broader field of central neurodegenerative diseases. The cellular localisation of misfolded proteins, as well as the affected brain region, differ between these degenerative processes, but all likely cause endoplasmic reticulum (ER) dysfunction, suggesting common pathways for both diseases.

1.2. Retinal degeneration

1.2.1. Background

Retinal degenerative diseases affect the eye structure responsible for converting light into neuronal signals. In vertebrates, the retina is located in the innermost part of the eye, where light converges due to the optical nature of the lens and the cornea. In vertebrates, the retina is usually organised into ten distinct retinal layers, with the light-sensitive cells known as photoreceptors located at the back of the retina (Wassle & Boycott, 1991). In certain vertebrates including humans, an area in the retina known as the fovea possesses much higher acuity of sight and is particularly affected in macular degeneration (Penfold et al., 2001).

Globally, inherited human retinal degeneration affects approximately one in 2000 individuals, for whom a progressive loss of photoreceptors leads to retinal degeneration (Berger et al., 2010). This can be caused by conditions such as diabetic

retinopathy, or genetic diseases such as retinitis pigmentosa (Khan et al., 2017). Common symptoms of retinal degeneration include night blindness, loss of peripheral vision, and general progressive loss of vision in later stages (Wert et al., 2014). The main causes of inherited retinal degeneration involve perturbations of the phototransduction pathway or of the synthesis and folding of key proteins. In humans, retinal degeneration largely originates from mutations in the transmembrane protein known as Rhodopsin. Autosomal dominant retinitis pigmentosa (ADRP) is the most common genetically inherited form, affecting 1 in 4000 people (Daiger et al., 2014). Roughly 20 to 30 percent of ADRP cases originate from point mutations in rhodopsin (Sullivan et al., 2006).

1.2.2. Photoreceptors

Phototransduction is a highly conserved ability in which photoreceptor cells can convert electromagnetic wavelengths into a neuronal response, leading to the conscious visual perception of the surrounding environment. Photoreceptor cells are highly specialised in the processing of visual information, with a unique cellular structure optimising the amount of photons that they are capable of capturing, and a unique molecular and neuronal pathway (Wassle & Boycott, 1991). The specific molecular pathway differs between vertebrates and invertebrates, but some similarities exist. This is due to a common ancestral photoreceptor cell that diverged into two different classes of photoreceptors (Fain et al., 2010). These two classes can roughly be separated into two phyla; microvillar photoreceptors are most common in protostomes (such as arthropods), whereas ciliary photoreceptors dominate the principal eyes of chordates (including vertebrates). However, both ciliary and microvillar photoreceptors are found in most phyla, usually with one playing an accessory role, such as melanopsin-containing ganglion cells that are involved in pupillary contraction in mammalian retinas (Koyanagi et al., 2005; Nasir-Ahmad et al., 2019). Although the morphology of photoreceptor cells can vary drastically across species (Figure 1-1)(Fain et al., 2010), they all express opsin proteins capable of changing their conformation depending on light exposure.

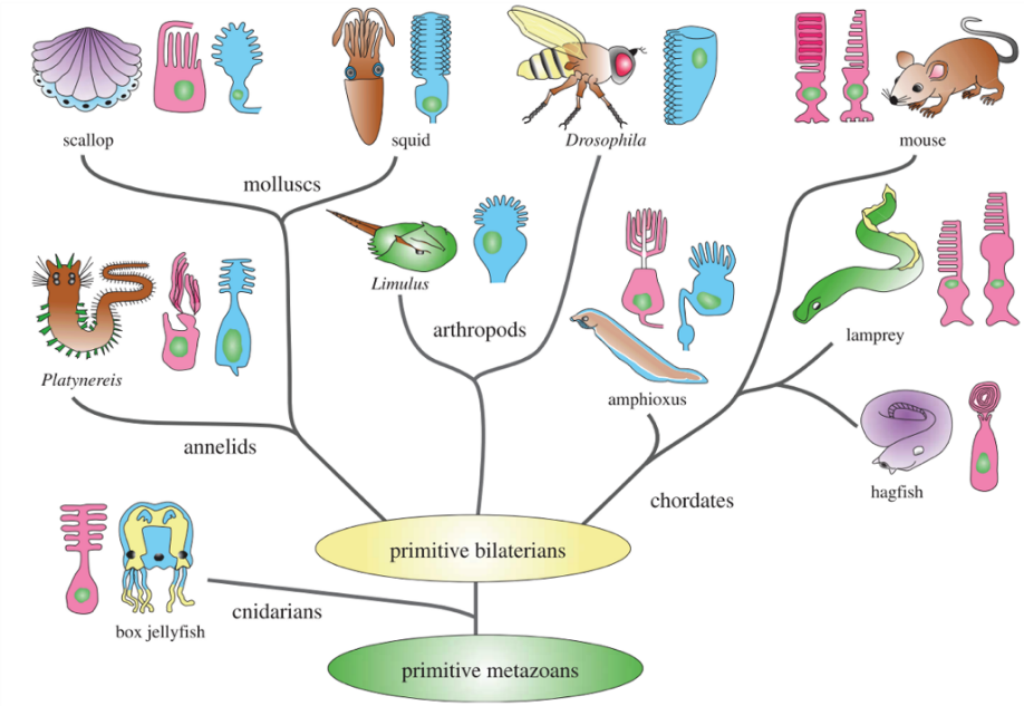

Figure 1-1 Phylogenetic tree of metazoans showing photoreceptor types in representative animal groups or species.

Ciliary (red) or microvillar (blue) photoreceptors (Fain et al., 2010).

1.2.3. Animal opsins

Opsins are G-protein coupled receptors that are light-sensitive when associated to the chromophore retinaldehyde (Shichida & Matsuyama, 2009). Interestingly, opsins also have unconventional light-independent roles, such as in thermosensation, mechanoreception, and chemosensation (Leung & Montell, 2017). Opsins can be categorised into three groups: ciliary opsins, rhabdomeric opsins and photoisomerases (Shichida & Matsuyama, 2009).The former two classes are the main focus of this work. Ciliary opsins are expressed in specific ciliary structures found in vertebrates such as rods and cones. On the other hand, rhabdomeric opsins are found in microvillar structures known as rhabdomeres. All opsins differ in their sensitivity to different wavelengths of light.

Humans possess nine different opsins including Rhodopsin (RHO), which is expressed in rod photoreceptor cells and crucial for vision in low-light environments, and melanopsin, which plays a role in regulating the circadian rhythm (Shichida & Matsuyama, 2009).

In *Drosophila melanogaster*, seven different opsins have been identified thus far (Wang & Montell, 2007). *ninaE* (neither inactivation nor afterpotential E) was first identified through its electroretinogram-defective phenotype (O'Tousa et al., 1995). This gene encodes Rhodopsin-1 (*Rh1*), the *Drosophila* form of RHO, expressed in specific photoreceptors in the retina.

The *Drosophila* compound eye contains around 800 stereotypically organised units known as ommatidia (Wang & Montell, 2007). These contain eight photoreceptors designated as R1 through R8, with various Rhodopsin (Rh) forms being expressed (Figure 1-2). R1 through R6 are known as the outer photoreceptors and predominantly express Rh1. R7 and R8 are both inner photoreceptors stacked on top of each other. R7 expresses either Rh3 or Rh4, whereas R8 expresses Rh5 or Rh6. Rh2 is expressed in the secondary visual system known as ocelli. Rh7 has recently been discovered and is yet to be fully characterised (Senthilan & Helfrich-Förster, 2016). All of these Rhodopsin proteins have a distinct absorption maxima that ranges from ultraviolet (331nm) to visible green light (515nm) (Stavenga & Arikawa, 2008). The sequence identity of *Drosophila* Rh1 with vertebrate opsins is only 36%, but contains several regions of high-sequence identity (Pak, 1995).

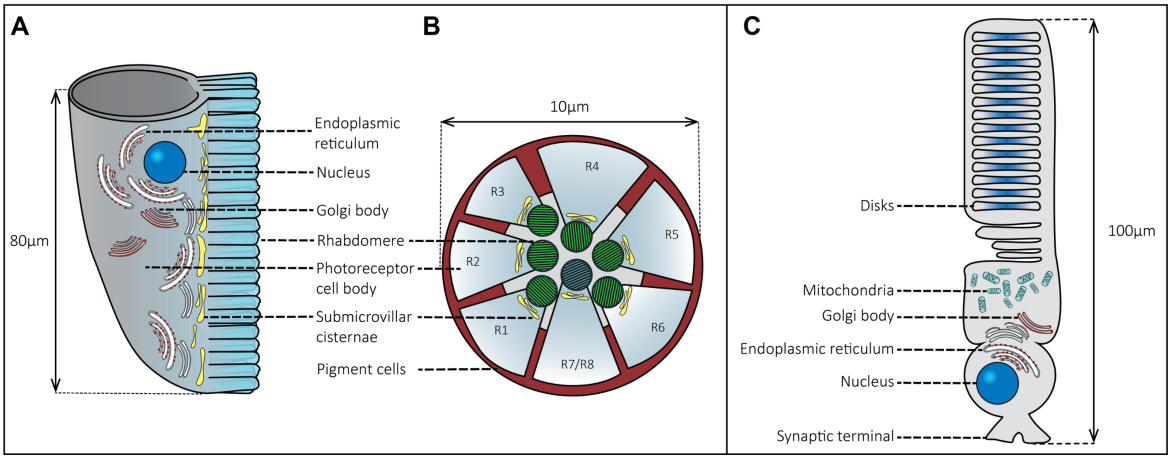

Figure 1-2 Diagram of a microvillar and ciliary photoreceptor.

(A) Microvillar photoreceptor and (B) top view of an ommatidia with photoreceptors labelled R1 through R8, with the rhabdomeres of the outer photoreceptor labelled in green to show a normal Rh1-GFP staining. (C) Schematic of a vertebrate rod, an example of a ciliary photoreceptor. Adapted from Fain et al., 2010.

1.2.4. Phototransduction in ciliary photoreceptors

For the purpose of this section, phototransduction will be explained in the context of activation of RHO (Figure 1-3). In ciliary photoreceptors, phototransduction starts in ciliary disks with the isomerization of an opsin molecule located inside the RHO protein (Fain et al., 2010). This isomerization changes the configuration of RHO, which activates transducin, a G protein. This activated G protein dissociates from a bound GDP molecule, and instead binds to GTP, further dissociating the three subunits. The α-subunit, still bound to the GTP molecule, activates the phosphodiesterase enzyme that will convert cyclic GMP into GMP. The decrease in concentration of cGMP closes transmembrane channels permeable to sodium and calcium, hyperpolarising the photoreceptor cell. This hyperpolarisation causes voltage-gated calcium channels to close. As calcium is required for the fusion of vesicles containing glutamate with the cell membrane, there is a decrease in the amount of glutamate released by the cell, depolarising and hyperpolarising on-centre and off-centre bipolar cells, respectively.

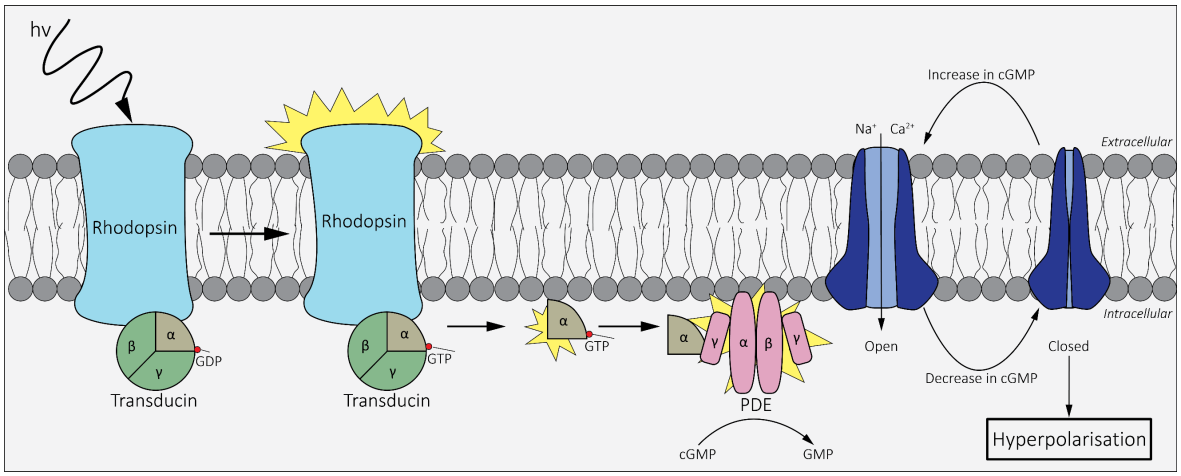

Figure 1-3 Ciliary phototransduction.

Isomerisation of an opsin molecule located inside of the RHO protein will activate RHO and subsequently activate its associated G protein, transducin. A GDP bound to the α-subunit will be exchanged with a GTP molecule. This α-subunit will delocalise to and activate a phosphodiesterase enzyme, converting cyclic GMP into GMP. Transmembrane channels sensitive to intracellular cGMP concentration close, decreasing the influx of sodium and calcium, leading to the hyperpolarisation of the cell and a decrease in glutamate release. hv: light, GDP: guanosine diphosphate, GTP: guanosine triphosphate, PDE: phosphodiesterase, cGMP: cyclic guanosine monophosphate, GMP: guanosine monophosphate.

1.2.5. Phototransduction in microvillar photoreceptors

Phototransduction in microvillar photoreceptors differs significantly in its molecular cascade. Once again, the phototransduction cascade will be explained in the context of Rh1 activation (Figure 1-4). Phototransduction is initiated in rhabdomeres, which are stacked microvilli extensions (Figure 1-2). A high concentration of Rh1 is located in the rhabdomeres, along with other variants of Rhodopsin depending on the localisation of the photoreceptor cell in reference to the ommatidia, as previously mentioned. The G-protein, once activated, binds to and initiates phospholipase-Cβ (PLCβ). This enzyme converts phosphatidylinositol-4,5-bisphosphate (PIP_2) into inositol triphosphate (IP_3) and diacylglycerol (DAG). Thereafter, it remains unclear what metabolite is responsible for opening transient receptor potential channels (TRP) and predominantly allowing calcium ions to flow into the cell and cause depolarisation.

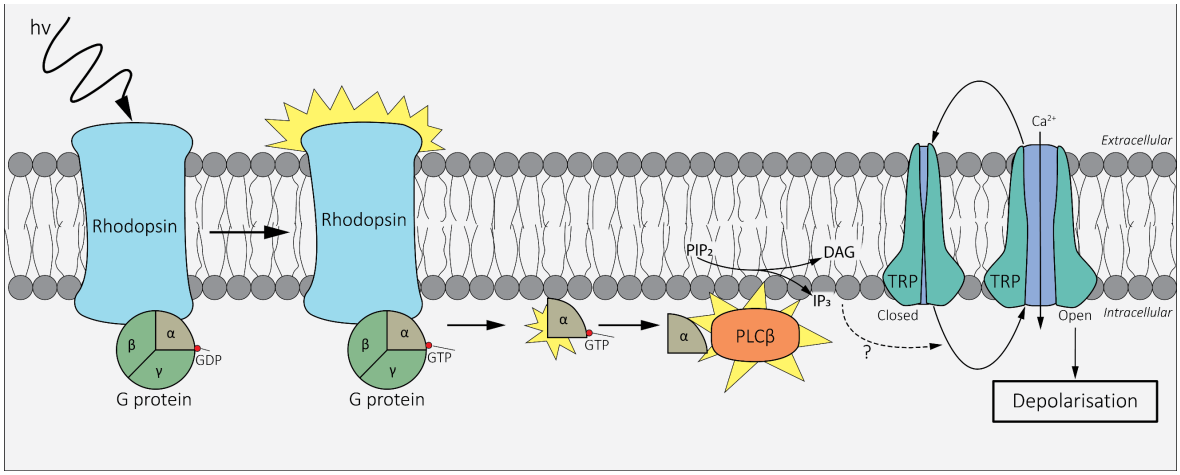

Figure 1-4 Microvillar phototransduction.

Isomerisation of an opsin molecule located inside of the Rh1 protein will activate Rh1 and subsequently activate its associated G-protein. A GDP bound to the α-subunit will be exchanged with a GTP molecule. This α subunit will delocalise to and activate a phospholipase-C enzyme, converting cyclic PIP_2 into IP_3 and DAG. Transmembrane TRP and TRPL channels eventually open through an undetermined pathway, increasing intracellular calcium concentration, leading to the depolarisation of the cell. Abbreviations: hv: light, GDP: guanosine diphosphate, GTP: guanosine triphosphate, PLCβ: phospholipase Cβ, TRP: transient receptor potential channel, PIP_2: phosphatidylinositol-4,5-bisphosphate, IP_3: inositol triphosphate, DAG: diacylglycerol.

Importantly, a biochemical amplification of the original signal occurs in all phototransduction cascades, which occurs at distinct stages of phototransduction depending on the organism. In ciliary photoreceptors, activation of a single rhodopsin molecule will activate numerous transducin G-proteins (Arshavsky & Burns, 2014). This, in turn, translates to the hydrolysis of thousands of cGMP molecules, thus amplifying the original signal. Interestingly, microvillar photoreceptors show a more sensitive transduction with a rapid response to a single photon (Hardie et al., 2002). However, the amplification occurs later in the cascade, downstream of PLCβ activation, but is not fully understood (Fain et al., 2010; Henderson et al., 2000).

1.2.6. Retinal degenerative models

The *Drosophila* compound eye has many morphological and molecular differences when compared to the human eye. Similarities exist in the cellular structure (melanopsin retinal ganglion cells and rhabdomeric photoreceptors) and in the phototransduction pathway (GPCR-initiated). It is these exact similarities that are affected by retinal degeneration in both humans and *Drosophila*. Since the first mutation in *Rhodopsin* was discovered, over 3000 mutations in approximately 70 genes have been identified in humans, with a majority having an ortholog in *Drosophila* (Gaspar et al., 2019).

1.2.6.1. Rh1 mutations

Mutations of the gene Rhodopsin (*RHO*) account for 15% of all types of retinal degeneration and 25% of autosomal dominant retinal degeneration, such as retinitis pigmentosa (Berson et al., 1991). The first mutation identified related to the development of retinal degeneration was in Rh1 (Dryja et al., 1990; Farber et al., 1991). Mutations discovered in *ninaE*, the *Drosophila* homolog for RHO, were almost identical to that of vertebrate RHO that causes retinitis pigmentosa (Pak, 1995). Some of these identified mutations could result in a truncated form of the protein at the third cytoplasmic loop, leading to the elimination of the sixth and seventh transmembrane domains (Colley et al., 1995; Shieh, 2011). In both humans and *Drosophila*, this leads to the degeneration of photoreceptors suggesting some form of conservation in the mechanisms underlying retinal degeneration. Missense mutations and misfolding of the protein are the most common effects of mutations in *RHO* and *Rh1* (Fanelli & Seeber, 2010; Saliba et al., 2002). Among them, an etiologically prevalent and well-

studied mutation of *RHO* is the P23H mutation, where the proline in position 23 has been substituted with a histidine (*Rh1*P37H in *Drosophila*). This is a commonly used genetic mutation to study retinal degeneration in animal models. This mutation leads to an accumulation of a misfolded form of Rhodopsin in the ER, and an age-dependent retinal degeneration (Mendes et al., 2005). There exist other *RHO* mutations, many of which were first discovered in *Drosophila* in *Rh1*, but were then found to be identical in ADRP patients (fly/human residues: G119E/G106R, P184L/P171L, E194K/E181K, and G195S/G182S) (Colley et al., 1995). Interestingly, these mutations do not lead to a degenerative phenotype in animal models when expressed in homozygous mutants, even though there is a decrease in the expression of Rh1 (Kurada & O'Tousa, 1995). This suggests that the toxicity arises from the formation of a complex containing both wild-type and mutant Rhodopsin that is resistant to degradation pathways. Recent studies have found that mutations of RNA-binding proteins (RBP), such as CERKL or PRPF31, can lead to retinitis pigmentosa in humans (Tanackovic et al., 2011; Tuson et al., 2004), one of which found abnormal cytoplasmic RBP aggregation that included the protein TDP-43 in stress granules (Yamoah et al., 2023). These results suggest that RBPs and RNA homeostasis may play a key role in retinal degeneration.

Disrupting the RHO synthesis pathway, its transport, or degradation can all lead to retinal degeneration. This can be seen with mutations of other genes that are essential to RHO dynamics and homeostasis, such as *PRPF31* and *TULP1* in humans (Xiong & Bellen, 2013). In *Drosophila*, there are a number of other genes involved in the normal function of Rh1 that have been found to lead to retinal degeneration when mutated. These include genes involved in Rh1 folding and maturation (*ninaA*), in Rh1 transport (*rab6, ninaC*), Rh1 inactivation (*arr2, rdgC*), and Rh1 endocytosis (*car*, *cm*) (Shieh, 2011). The mechanisms leading to retinal degeneration in these mutants are either reduced Rh1 levels, misfolding of Rh1, Ca^{2+}-mediated excitotoxicity, or transport defects.

Although mutations of the Rh1 protein in *Drosophila* can closely mimic human diseases such as retinitis pigmentosa, they tend to exhibit degenerative phenotypes late in the life of the flies. For this reason, in this work, retinal degeneration was initiated by mutating a different gene: *rdgB*.

1.2.6.2. Retinal degeneration B

The gene *retinal degeneration B* (*rdgB*) encodes for a 116 kD transmembrane protein (RDGB) that plays a critical role in *Drosophila* photoreceptors. *rdgB* was first discovered through a mutagenesis screen conducted by Hotta and Benzer (Hotta & Benzer, 1970), where they identified a retinal degeneration phenotype when this gene was defective. Harris and Stark later characterised the defects caused by this and other loss-of-function mutants in detail (Harris & Stark, 1977). One of the mutants that they identified was originally called $rdgB^{KS222}$, but later renamed $rdgB^{9}$.

The RDGB protein is a phosphatidylinositol transfer protein (PITP), and is crucial for the regeneration of PIP2, a core molecule in the phosphatidylinositol (PI) cycle and in *Drosophila* phototransduction (Section 1.2.5). In *Drosophila*, this protein is highly expressed in the retina, specifically in photoreceptor cells, as well as in the ocelli. RDGB is localised in the membrane contact site (MCS) between the sub-microvillar cisternae (SMC, an ER extension) and the rhabdomeric membrane where it will transport a PI molecule from the ER membrane to the rhabdomeric membrane (Trivedi & Padinjat, 2007; Yadav et al., 2018) (Figure 1-5).

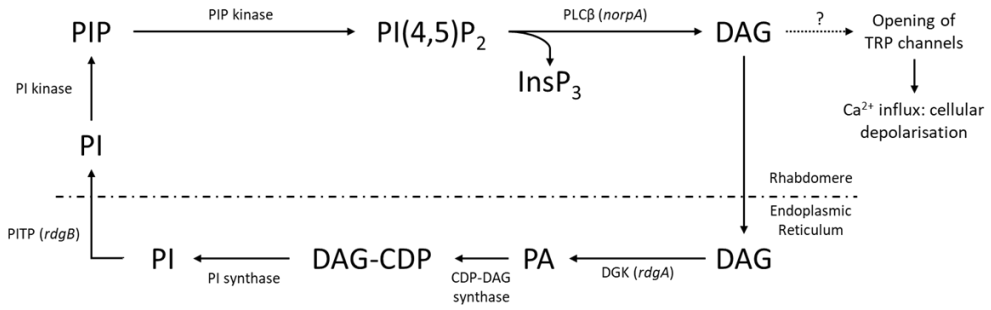

Figure 1-5 The phosphatidylinositol (PI) cycle in Drosophila melanogaster.

This cycle occurs in the membrane contact site (MCS) between the membrane formation known as rhabdomeres and the endoplasmic reticulum. When PLC is activated, it hydrolyses PIP_2 into IP_3 and DAG. This opens TRP channels through an unknown messenger leading to cellular depolarisation. DAG is then transported to the ER and deactivated by transforming it into phosphatidic acid (PA) by the DGK enzyme. The PA molecule is transformed into DAG-CDP by a synthase, which is transformed into PI. This lipid is transported back to the rhabdomere membrane by the transport protein RDGB, and converted by a PI kinase into PI(4)P. PIP is converted into PI(4,5)P by the PIP kinase.

The *Drosophila* protein RDGB has been extensively studied and the following functional domains have been identified (Figure 1-6):

- The PITP domain at the N-terminal carries out the primary function of transporting phosphatidic acid (PA) from the plasma membrane to the sub-microvillar cisternae (SMC). This domain has an unusually high conservation between mammalian and invertebrate *rdgB* (62% amino acid identity), higher than between either of these proteins and any of the known PITP proteins, suggesting a key conserved biological function (Chang et al., 1997).
- The FFAT motif, essential for proper localisation at the MCS between the rhabdomeric membrane and the SMC (Yadav et al., 2018). This motif binds to the major sperm protein domain found in the protein family vesicle-associated membrane protein–associated proteins (VAP).
- The LNS2 domain, found at the C- terminal, needed for proper docking to the plasma membrane through interactions with PA (Cockcroft & Raghu, 2018).
- The DDHD domain is needed for stabilisation of the FFAT motif's interaction with VAP (Cockcroft & Raghu, 2018).

Besides the PITP domain and the FFAT motif, the function of the other domains of *Drosophila rdgB* remain mostly unclear and are based on sequence-based predictions.

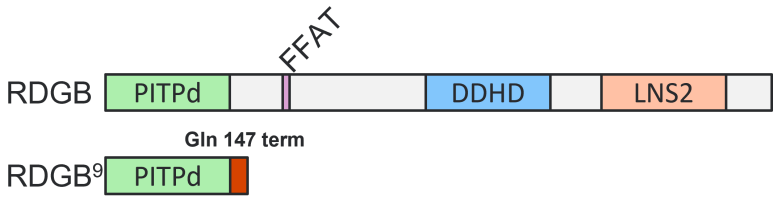

Figure 1-6 Representation of the domains found in RDGB and its mutant form RDGB^{9}.
PITPd: phosphatidylinositol transfer protein domain, FFAT: acronym for two phenylalanines (FF) in an Acidic Tract, DDHD: Asp; Asp; His; Asp, LNS2: Lipin/Ned1/Smp2. Adapted from Yadav et al., (2018).

There exist mammalian homologs to *Drosophila rdgB*, part of the larger family of PITPs, but these show significant differences compared to the *Drosophila* counterpart. The known mammalian PITPs have been divided into three classes. In brief, Class I consists of small and soluble proteins, which are ubiquitously expressed and play a role in the regulation of phosphoinositide metabolism: PITPN, PITPNB, and PITPNC1 (*rdgB*-β*)*. Class II consists of proteins that show high sequence similarities to the *Drosophila rdgB* gene; they contain a PITP domain and are membrane bound: PITPNM1 (*MrdgB*/Nir-2), PITPNM2 (*MrdgB2*/Nir-3), and PITPNM3 (Nir-1). Finally, Class III are also able to transport phosphatidylinositol but are unrelated to the other classes in structure and sequences (Ocaka et al., 2005). These mammalian homologs of the *Drosophila rdgB* do not play a role in the classical phototransduction pathway due to the differences between ciliary and microvillar photoreceptors described earlier. Although, recent work in rodents identified PITPNM2 (M*rdgB2*) being expressed in specific mammalian retinal ganglion cells (Walker et al., 2015). *RdgB2*$^{-/-}$ mutants displayed defects in the circadian rhythm and pupillary responses, suggesting a possible role for this specific PITP in the mammalian visual system (Walker et al., 2015). In addition, an initial study found that the PITPNM1 gene maps at or near the site of four retinal diseases: Bardet-Biedl syndrome 1, vitelliform macular dystrophy, Criswick-Schepens syndrome, and dominant neo-vascular inflammatory vitreoretinopathy (VRN1) (Chang et al., 1997). A later study found that the genetic map positions of PITPNM1 and PITPNM2 coincided with the retinal diseases VRN1 and dominant central areolar choroidal dystrophy, respectively (Ocaka et al., 2005). A conclusive link remains to be demonstrated between these retinal diseases and *rdgB* as these genes are also expressed in many other tissues. There is therefore a strong possibility for these genes to not be involved in retinal diseases (Fitzgibbon & Hunt, 1995). However, if mutations in these PITPs are found to be responsible, the *Drosophila* mutants of *rdgB* may be of particular use to assess the underlying mechanism of these diseases.

As the name suggests, mutations of the gene *rdgB* can lead to a rapid onset of light-dependent retinal degeneration. This degeneration can be detected by electroretinogram one day after eclosion as a decreased electrical response to light, and can be observed visually three days after eclosion (Harris & Stark, 1977). The work in this thesis primarily used the *rdgB*^{9} mutation, introducing a premature stop codon located inside its PITP domain (Figure 1-6). This hypomorphic allele is translated to a

protein unable to properly localise in the photoreceptors, and thus unable to complete its function in the PI cycle leading to a rapid degeneration of these cells (Yadav et al., 2018).

The exact molecular pathway leading from this mutation to retinal degeneration is still unclear. Importantly, independent studies have found methods to rescue the electroretinogram and photoreceptor phenotypes. These include the overexpression of the PITPd of *rdgB* by itself (Milligan et al., 1997; Yadav et al., 2016), which shines a light on the unclear function of the non-PITPd domains of this protein, which were mostly identified through bioinformatics. A separate study found that pharmacologically blocking calcium channels inhibited the light-dependent retinal degeneration (Sahly et al., 1992). This latter study suggests that the degeneration may be caused by a toxic increase of intracellular Ca^{2+} through voltage-gated Ca^{2+} channels.

In this thesis, mutation in the *Drosophila rdgB*^{9} gene was used for its efficacy and speed at developing retinal degeneration, making it an ideal model to study the molecular pathways involved in cellular degeneration. The aim of this work is attempt to clarify the molecular pathway involved in retinal degeneration induced by *rdgB*^{9}. In addition, this mutant presents a particular advantage to screen for proteins that may be modulators of pathways involved in cellular degeneration. The ability of these proteins to modulate cellular degeneration were further tested in a neurodegenerative model.

1.3. Neurodegeneration

1.3.1. Neurodegenerative diseases

Neurodegenerative diseases are devastating conditions that affect millions of lives globally. These diseases include Alzheimer's disease, Parkinson's disease, Huntington's disease, and Amyotrophic Lateral Sclerosis among others. A key feature from all of these diseases is the progressive process known as neurodegeneration, where the structural integrity of neurons and their functions deteriorate, leading to cell death. This process can affect various regions and key circuits of the brain causing the wide range of symptoms found in such diseases, which, unfortunately, are incurable with limited treatment available.

Protein misfolding and propagation has been one of the major focuses in this field of research. Indeed, many of these neurodegenerative diseases have been associated to

critical mutations of specific proteins causing misfolds and mis-localisation (Graeber & Moran, 2002; Soto & Lisbell, 2008). Such misfolded proteins exhibit an altered behaviour and tend to create aggregations, as seen in patients with Alzheimer's disease with amyloid-β aggregates in the brain (Haass & Selkoe, 2007). These protein aggregates can disrupt normal protein translation, and will usually activate cellular stress pathways, leading to degeneration of neurons. This work will focus on a model for Huntington's disease to study neurodegeneration and the molecular pathways involved in this disease.

1.3.2. Huntington's disease

1.3.2.1. Background

Huntington's disease (HD) was originally described in 1842 by the physician Charles Waters, but George Huntington described it in further detail in 1872 (Huntington, 1872). The prevalence of HD is between four and ten per 100,000 people in the western world. This neurodegenerative disease exhibits motor, cognitive and psychiatric symptoms. It can present itself at any age, but most commonly around the age of 40, with death occurring between 15 and 20 years after disease onset. HD is inherited in an autosomal dominant manner, caused by a polyglutamine repeat expansion (CAG) in the gene *huntingtin* (*Htt*) which was first discovered nearly 30 years ago (The Huntington's Disease Collaborative Research, 1993). Sporadic cases of HD can occur although these are rare and may be confounded with unknown family history (Davis et al., 1994). The genetic penetrance of this disease depends on CAG repeat length as well as the patient's age, with longer repeats being associated with earlier onset. A unique aspect of HD is that diagnosis can be made long before the onset of any clinical symptoms through predictive genetic tests (Macleod et al., 2013). Unfortunately, besides symptomatic management drugs such as tetrabenazine to reduce chorea, no treatment exists for HD (Frank, 2014).

1.3.2.2. Clinical effects

The symptoms of HD are well characterised. Typically, early cognitive and psychiatric symptoms go undetected, these are sometimes called "soft signs", and include cognitive decline, learning difficulties, personality changes, impulsive disorders, depression, suicidal ideation, and irritability (Walker, 2007). These symptoms usually worsen with

progression of the disease, as an example, gene carriers are 1.74 times more likely to report depression than non-carriers, and are at a significantly higher risk of suicide (Julien et al., 2007). Another example of an early sign of HD are sleep disturbances. In fact, nearly 90% of HD patients reported sleep problems, with 61.7% of them rating these as very or moderately important factors to the patient's overall problems (Taylor & Bramble, 1997).

Clinical diagnosis is conventionally defined by the onset of symptoms affecting motor skills including chorea, trouble walking, unsteadiness, and clumsiness (Fahn et al., 2011). Motor-skill decline usually occurs later in the progression of HD, and can deeply affect the quality of life of HD patients.

The effect of the mutated gene can be seen years before any symptoms. It has been reported that neuronal aggregates and neuronal dysfunction occur in pre-symptomatic carriers long before the onset of the clinical phenotype (Gómez-Tortosa et al., 2001). This suggests that the molecular and pathological processes of HD begin early in the life of a mutation carrier. These unseen cellular effects can sometimes lead to premature death, decades before the expected clinical onset (Gómez-Tortosa et al., 2001).

1.3.2.3. Causes

At a brain structure level, post-mortem studies of HD patients have shown neuronal loss in the basal-ganglia-thalamocortical circuitry, primarily in the striatum (Sotrel et al., 1991). Certain motor skill symptoms have been associated with more specific neuronal circuits. The exact mechanism behind this form of neurodegeneration and HD pathogenesis remains unclear, although the *Htt* gene has been thoroughly studied since its discovery.

1.3.2.3.1. Huntingtin, CAG repeats and protein aggregation

Huntingtin (*Htt*) and its CAG repeats are directly linked with the development of HD. Interestingly, *Htt* is expressed throughout the brain, in both affected and unaffected brain regions, not limiting itself to vulnerable neurons, demonstrating that other factors may be necessary for neurodegeneration (Gourfinkel-An et al., 1998). The function of the wild-type protein HTT is poorly understood. Studies have found

probable roles in endocytosis, intracellular trafficking and membrane recycling (Cattaneo et al., 2005).

The HD pathogenesis has been linked to expanded forms of HTT with CAG repeats in the 5' end of the protein. In wild-type alleles of this protein, up to 26 CAG repeats can be found. Between 27 and 35 repeats are known as intermediate cases which will not necessarily cause HD in individuals, but may cause issues in subsequent generations (Bates et al., 2015). Repeats of over 37 will lead to HD, with the number of repeats inversely proportional to the age of onset of the disease, over 70 repeats is usually associated with juvenile onset. The number of repeats has been associated with the speed of disease progression but not with its severity (Swami et al., 2009).

This polyglutamine expansion disrupts normal protein maturation and leads to severe misfolding with rich β-sheet structure. Similarly to α-synuclein in PD and amyloid-β in AD, the misfolding of HTT in HD leads to protein aggregation, which is considered a gain-of-function. *In vitro* findings suggest that the polyglutamine expansion enables HTT to aggregate into dimers, trimers and oligomers (Peskett et al., 2018; Scherzinger et al., 1999; Williamson et al., 2010). The aggregation process causes major cellular dysfunction by creating aggregates of diverse sizes. It is yet to be understood which aggregate forms lead to disease and whether large insoluble aggregates may reduce toxicity (Eisenberg & Jucker, 2012; Leitman et al., 2013). There is also a possibility that these HTT aggregates may recruit wild-type HTT or even promote wild-type HTT aggregate losing its wild-type function, which may contribute to HD pathogenesis (Busch et al., 2003). The expanded form of HTT may also undergo aberrant splicing, with the N-terminal fragment containing the polyglutamine expansion separated from the full-length protein. This fragment, known as exon-1, has been found in cellular aggregates (Peskett et al., 2018).

The cellular localisation of these aggregates vary between being cytoplasmic or nuclear. Neuronal intranuclear inclusions are considered a hallmark of HD (Sieradzan et al., 1999). Yet, their mechanism and relevance are unknown. Past studies have found that neurons are able to clear nuclear inclusions effectively when mutant HTT production is stopped *in vitro* (Martín-Aparicio et al., 2001), further suggesting that these aggregates may be a protective mechanism.

The exact pathways leading from protein aggregation to neurodegeneration and pathogenesis remain unclear. Unfolded proteins have been shown to lead to the protective cellular response known as ER unfolded protein response (UPR) and the integrated stress response (ISR), which will be further discussed in section 1.4. (Vidal et al., 2011). With prolonged expression of the expanded forms of HTT, the UPR pathway leading to proteolysis of the misfolded proteins may be overwhelmed. In addition to this, chronic activation of this pathway without resolving ER stress leads to protein translation arrest and finally initiation of apoptotic pathways. This has been particularly implicated in neurodegeneration (Taalab et al., 2018), and will be further explored in a later section. Importantly, in the case of HD and other polyglutamine diseases, the CAG repeat has an effect on the secondary structure of the mRNA, leading to hairpin formation. The longer the CAG repeat, the more stable the hairpins become compared to the wild-type mRNA (Sobczak & Krzyzosiak, 2004). This secondary structure may be linked to a possible increase in protein sequestration.

Overall, these protein aggregates are still a matter of debate in terms of their toxicity, and whether they are the cause or a consequence of neurodegeneration seen in HD and other polyglutamine disorders.

1.3.2.3.2. RNA-binding proteins

RNA-binding proteins (RBPs) are proteins that contain structural motifs that recognise and bind to single or double stranded RNA molecules. These proteins participate in the formation of ribonucleoprotein (RNP) complexes, and can be cytoplasmic or nuclear (De Graeve & Besse, 2018). They play an essential role in normal cellular functions, such as mRNA stabilisation, localisation, splicing and translation (Kelaini et al., 2021; Maziuk et al., 2017). As they have a wide range of cellular functions, dysregulation in the expression or function of RBPs has been suggested to underlie some forms of cancer as well as neurodegenerative diseases.

The expression of polyglutamine proteins in disorders such as HD leads to a higher propensity for protein aggregation in cells. It has been demonstrated that RBPs, containing intrinsically disordered regions (IDRs), are vulnerable to being recruited into these aggregates (McLaughlin et al., 1996). The sequestration of RBPs such as transcription factors, chaperons, and splicing factors will compromise basic cellular function. For example, in the context of myotonic dystrophy, that is caused by a CTG

trinucleotide expansion in the *DMPK* gene, it has been shown that an RNA splicing protein (MBNL1) exhibits a high binding affinity to RNA that has trinucleotide repeats (Kino et al., 2004), inducing dysregulated alternative splicing (Mykowska et al., 2011). This suggests that binding and sequestration of MBNL1 may be a mechanism contributing to RNA toxicity in polyglutamine disorders (Li et al., 2008). RNAs containing CAG repeats have been shown to sequester other RBPs involved in ribosome formation, transcription factors, and even in the RNA interference pathway (Nalavade et al., 2013).

Overall, past studies have shown that the sequestration of RBPs may play a key role in the development of neurodegeneration. More research is required to understand the importance of the role they play. Here, two particular RBPs have been studied: a splicing factor known as SF3B2, and an as-of-yet uncharacterised protein that contains RNA binding motifs: CG42458. Unpublished work from the Padinjat laboratory in the National Centre for Biological Sciences (India) has found these proteins, among others, to be possible modulators of the retinal degenerative phenotype caused by the *rdgB*^{9} mutation. I attempted to confirm this finding, as well as test whether they also had a modulatory effect in a *Drosophila* model of HD.

1.3.2.3.3. RNP granule markers – Ataxin-2 and Rasputin

A subset of RNA-binding proteins are also known to be key components of RNP granules. RNP granules, such as stress granules (SG) or processing-bodies (PB), are membrane-less dense aggregations of RBPs and RNA molecules. Their physiological function varies from RNA transport and regulation, to protection from various forms of stress (De Graeve & Besse, 2018). For example, SGs form through liquid to phase transitions under cellular stress conditions such as heat, oxidative stress, and ultraviolet radiation (Namkoong et al., 2018). While PBs assemble around enzymes required for RNA degradation, SGs assemble around components of the translational machinery (Stoecklin & Kedersha, 2013). The exact function of RNP granules remains largely unknown, although it is proposed to be a defensive mechanism to protect sensitive nucleic material from possibly damaging external factors. Past studies have shown that the pathological formation of SG, and RNP granules in general, are a hallmark of many neurodegenerative diseases and play a role in their pathogenesis (Bakthavachalu et al., 2018; Desai & Bandopadhyay, 2020; Li et al., 2013; Liu-

Yesucevitz et al., 2014). Many proteins have now been characterised as colocalising in RNP granules, these include Me31B, FMR1, Rox8, and Caprin. In this work, Ataxin-2 and Rasputin, two RBPs that are also known to be RNP components, were studied.

Ataxin-2

Ataxin-2 (ATX2) is a key RNP granule protein that has been shown to regulate mRNA translation, and is involved in the formation of SGs and PBs (Orr, 2012). ATX2 has important clinical significance as its mutant forms have been associated to spinocerebellar ataxia type-2 (SCA2) as well as amyotrophic lateral sclerosis (ALS). Like most RBPs, ATX2 contains IDRs. It has been recently shown that these IDRs are required for efficient RNP granule assembly and for translation-dependent long-term memory (Bakthavachalu et al., 2018). In addition, the specific deletion of ATX2 IDRs prevents the development of forms of neurodegeneration in *Drosophila* (Bakthavachalu et al., 2018). Interestingly, the C-terminal IDR domain of ATX2 may be partially required for protein aggregation and neurodegeneration in *Drosophila* HD models (Huelsmeier et al., 2021). This same paper also found that expanded-HTT aggregates do not sequester known SG markers. Importantly, another study on HD found that expression of different expanded forms of *Htt* transgenes in circadian clock neurons induced circadian arrhythmicity, expanded-HTT aggregates in the small ventral lateral neurons, and decreased their numbers. These results suggest a cytotoxic effect from the expression of these expanded forms of *Htt*. A notable finding from this paper was the alleviation of these effects by knocking-down *atx2* using RNAi constructs (Xu et al., 2019b).

Although the mechanism and role of SG markers in HD development remain unclear, these recent findings suggest a prominent role for ATX2 and a possible role for SG formation in the development of neurodegenerative diseases, including HD.

Rasputin/G3BP

Rasputin (Rin), the *Drosophila* ortholog for the mammalian family of Ras GTPase-activating protein-binding proteins (G3BP), is an RBP necessary for SG formation in human cells as well as *Drosophila* S2 cells (Aguilera-Gomez et al., 2017; Tourrière et al., 2003). The role of Rin in normal and stressed conditions is unclear, even though it is crucial for fly survival as *rin* mutations lead to severe defects in

oogenesis and growth defects (Baumgartner et al., 2013; Costa et al., 2013). In unstressed cells, Rin has been shown to be associated with polysomes, and has a role in stabilising and promoting the translation of mRNAs (Laver et al., 2020). Strikingly, the expression of a null mutant of G3BP1 in mice leads to severe neuronal cell death, with all other organs being healthy (Zekri et al., 2005). Even though G3BP1 is ubiquitously expressed in humans and mice, the genetic deletion of G3BP1 led to a disproportionate effect on neurons, suggesting an essential role for G3BP1 on neuronal function. Due to its central regulatory function over SG formation, and its importance in neuronal cell survival, it is likely that it plays a role in the mechanisms underlying the onset and progression of neurodegenerative diseases (Sidibé et al., 2021). G3BP1 may also play a role in the pathophysiology of HD. A recent paper found an increased G3BP1 granule number and density in the superior frontal cortex of HD human brains, as well as in a rodent model (Sanchez et al., 2021).

1.4. Integrated stress response

The integrated stress response (ISR) is a heavily conserved molecular pathway in most eukaryotic cells (Pakos-Zebrucka et al., 2016). It is activated in response to various stressful stimuli, and aims to restore cellular homeostasis.

1.4.1. ISR pathway

In mammals, there are four main kinases that can activate the ISR (Figure 1-7). When any of these four kinases are activated, they will phosphorylate the key regulator, eukaryotic translation initiation factor 2 subunit 1 (eIF2α) (Pakos-Zebrucka et al., 2016). These four proteins were originally found to be activated by different forms of stressful triggers, but recent studies have shown some possible redundancy (Hamanaka et al., 2005).

a. General Control Nonderepressible-2 (GCN2) can sense amino acid deprivation through the binding of uncharged tRNAs. This kinase was first discovered in *Saccharomyces cerevisiae*, and is the only eIF2α kinase in yeast (Hinnebusch, 1988). When activated, it can repress protein translation through the phosphorylation of eIF2α, but it will also allow the translation of specific mRNA, in particular GCN4. This protein will enable the expression of genes that play a role in the biosynthesis of amino acids.

b. Double-Stranded RNA-Activated Protein Kinase (PKR) can be ribosomal-associated or located in the nucleus. This kinase phosphorylates itself through dimerisation in the presence of dsRNA during viral infection (Lemaire et al., 2008). Activated PKR will phosphorylate eIF2α and lead to the inhibition of protein translation. Although its function in viral infection has been well characterised, PKR has a variety of additional functions and triggers. For example, oxidative stress, ER stress and stress granules have all been shown to stimulate PKR (Lee et al., 2007; Reineke & Lloyd, 2015; Shimazawa & Hara, 2006).

c. Protein Kinase R (PKR)-like ER Protein (PERK), with two other ER stress sensors (IRE1 and ATF6), is part of the UPR. It is an essential protein for detecting misfolded proteins and reactive oxygen species in the ER. It is a highly conserved transmembrane protein containing a luminal domain which detects misfolded proteins. Its primary function is to phosphorylate eIF2α. The activation of PERK has been shown to lead to the downregulation of overall protein synthesis, mainly through eIF2α phosphorylation (Harding et al., 2003; Rutkowski & Kaufman, 2007).

d. Haemin-Regulated Inhibitor (HRI) is mainly expressed in erythroid cells, where it plays a key role in their developmental process (Han et al., 2001). Similar to the other eIF2α kinases, its activation leads to its dimerisation and autophosphorylation. Other forms of stress may also be able to activate this kinase, such as arsenite-induced oxidative stress (McEwen et al., 2005).

The phosphorylation of eIF2α will inhibit Cap-dependent mRNA translation, leading to protein translation arrest, but will selectively translate mRNA required for the regulation of the ISR (Wek, 2018). A well-studied protein that is strongly translated during eIF2α phosphorylation is ATF4. In *Drosophila*, ATF4 is encoded by cryptocephal (*crc*) and is crucial for regulating the ISR as it will initiate the expression of an eIF2α phosphatase, Growth Arrest and DNA Damage-inducible protein (GADD34). This phosphatase plays a major role in the negative feedback loop to regulate the ISR (Novoa et al., 2001). Activation of the ISR will indirectly lead to a unique transcriptional response, upregulating genes coding for heat-shock proteins and other chaperones, as well as genes involved in amino acid transport, oxidative stress protection, and in the

UPR (Harding et al., 2003; Singh et al., 2022). One such upregulated gene is CHOP, which plays an important role in ER-stress induced apoptosis (Bevilacqua et al., 2010).

An additional consequence of the activation of the ISR is the formation of ribonucleoprotein granules. As there is reduced translation of mRNAs, there is an increase in naked mRNAs that can bind to RNA-binding proteins (RBPs) and form ribonucleoprotein (RNP) complexes which can then assemble into granules, such as SGs (Kedersha et al., 2002; Kedersha et al., 1999; McEwen et al., 2005; Tauber & Parker, 2019). These membrane-less granules contain stalled and silent mRNAs, ribosomal subunits, and RBPs. As previously mentioned, pathogenic formation of these RNP granules, including SGs, have been implicated in the development of various neurodegenerative diseases (Bond et al., 2020). Part of the work conducted for this thesis helped establish that SG assembly and the altered stress-induced gene expression are driven by distinct signalling processes (see Appendix 2)(Singh et al., 2022). Interestingly, recent papers have suggested that modulating the ISR, such as by using the small ISR inhibitor (ISRIB), may be a therapeutic approach to reduce SG assembly in neurodegenerative diseases (Bugallo et al., 2020; Rabouw et al., 2019; Sidrauski et al., 2015; Young-Baird et al., 2020).

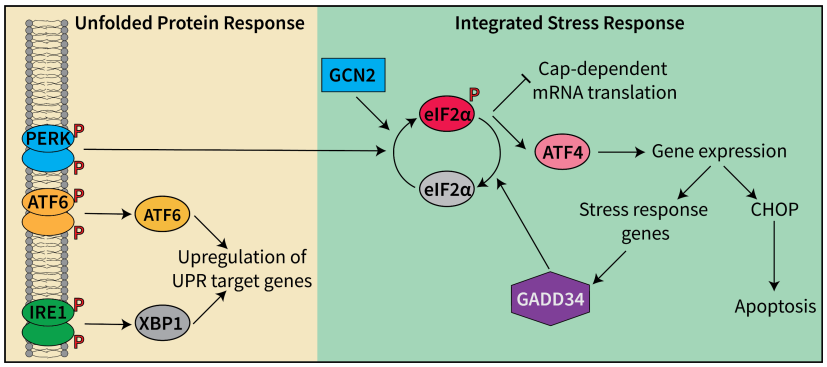

Figure 1-7 The unfolded protein response (UPR) and the integrated stress response (ISR) in Drosophila.

Unfolded proteins and ER stress will activate PERK, ATF6 and IRE1. ATF6 and IRE1 will indirectly lead to the upregulation of UPR target genes such as chaperones to facilitate removal of misfolded proteins. Activation of PERK through ER stress and activation of GCN2 through amino acid deprivation will phosphorylate eIF2α, the core of the ISR. Phosphorylated eIF2α leads to the inhibition of cap-dependent translation, while also selectively initiating the translation of mRNAs required in stress response, such as ATF4. ATF4 can bind to DNA targets to specifically express

genes involved in cellular adaptation to stress, including the phosphatase GADD34. This protein will dephosphorylate eIF2α to terminate the ISR.

In *Drosophila*, the ISR pathway is simplified as only two kinases have been identified: the Pancreatic eIF2α Kinase (PEK/PERK) and *Drosophila*-GCN2 (dGCN2). They are considered human orthologs for PERK and GCN2, respectively. Similarly to human PERK, *Drosophila* PERK encodes for an ER transmembrane kinase, responds to ER stress, and phosphorylates eIF2α. dGCN2 is a kinase that responds to amino acid deprivation by phosphorylating eIF2α.

1.4.2. ISR in diseases

1.4.2.1. Neurodegeneration

The UPR and the ISR have previously been heavily implicated in neurodegeneration, with a key role in the pathogenesis as well as a downstream consequence of neurodegeneration. The UPR is a cellular pathway involved in detecting unfolded or misfolded proteins and causing the upregulation of specific genes. PERK is part of the UPR, along with two other ER stress sensors known as IRE1 and ATF6. PERK is unique as it also plays a role in the ISR by phosphorylating eIF2α.

In post-mortem brain tissue from patients suffering from AD and PD, markers of the UPR have been found to be upregulated (Hoozemans et al., 2007; Hoozemans et al., 2012). In a study performed in post-mortem brain tissue of probable AD and other dementias, UPR activation in neurons at early stages of neurofibrillary degeneration was observed (Hoozemans et al., 2009). The UPR was shown to be upregulated in a rodent model for ALS using a mutant form of SOD1 (Nishitoh et al., 2008). In addition to this, Vaccaro *et al.* tested compounds that could inhibit the ISR in a TDP-43 model of ALS in *Caenorhabditis elegans*. They found that these compounds were able to suppress toxicity induced by the mutant form of TDP-43, indicating that they are possibly neuroprotective (Vaccaro et al., 2013).

Results have been more conflicted in the field of HD. One study found that a PERK activator significantly improved motor functions and delayed death onset in a rodent model of HD (Ganz et al., 2020), whereas another study reported reduced huntingtin toxicity by inhibiting PERK (Leitman et al., 2014). Interestingly, a study found that among the three major ER stress sensors, IRE1, and not PERK, is responsible for

modulating HTT aggregation during ER stress (Lee et al., 2012). Other studies have found that pathogenic expanded forms of HTT can induce ER stress before it aggregates into visible inclusions. This is further confirmed by the fact that ER stress is an early event in a pre-symptomatic HD rodent model, and that ER stress-related marker are increased in various *in vitro* models (Carnemolla et al., 2009; Duennwald & Lindquist, 2008; Leitman et al., 2014; Leitman et al., 2013).

Overall, these studies suggest that the ISR is likely implicated in the progression of neurodegeneration, although both activation and inhibition have been shown to be beneficial in HD models. This highlights the importance of understanding this pathway and its complexity as it may lead to new therapeutic targets. For example, the small molecule drug ISRIB, capable of reversing eIF2α phosphorylation, is currently being tested in clinical trials. It can reverse deleterious effects caused by traumatic brain injury in pre-clinical studies, and seems protective in other models of neurodegeneration (Bugallo et al., 2020; Frias et al., 2022; Young-Baird et al., 2020).

1.4.2.2. Retinal degeneration

The ISR has been of high interest in the field of retinal degeneration for many years. Being exposed to the environment and relatively isolated from the circulatory system, the eye is exposed to all potential stressors that can activate the ISR. It has been observed that the ISR is activated in ocular morbidities such as macular degeneration, diabetic retinopathy, and retinitis pigmentosa (Chu et al., 2021; Starr et al., 2018). Manipulating the ISR, either genetically or pharmacologically, has been shown to reduce disease phenotypes in rodent models of retinal degeneration (Athanasiou et al., 2017; Kang et al., 2012; Mendes et al., 2009; Starr et al., 2018). For example, a PERK inhibitor (PERKi) was tested for its potential ability to modulate retinal degeneration in a rat model (Athanasiou et al., 2017). They found reduced photoreceptor survivability and reduced visual function after treatment with PERKi. In cultured cells overexpressing the mutant *RHO-P23H*, PERKi led to increased aggregation of this opsin and the formation of inclusions. On the other hand, treatment with an inhibitor of eIF2α phosphatase, causing increased phosphorylation of eIF2α, led to improved photoreceptor survivability. These conflicting results suggest that PERK and eIF2α phosphorylation are part of the protective response limiting photoreceptor cell death in some forms of retinal degeneration.

A recent study in a mouse model for inherited retinal degeneration found persistent activation of the ISR through elevated expression of CHOP, ATF4, and phosphorylated eIF2α, and attenuation of cap-dependent protein translation (Starr et al., 2018). Another study found that activation of the UPR led to the dysfunction of the retinal pigment epithelium and increased the expression of an ER stress-responsive gene: vascular endothelial growth factor (Roybal et al., 2005). Overall, these studies suggest that the ISR is linked to the development of retinal degeneration, however, the exact role of the different pathways and proteins remain unclear. One of the remaining questions is whether ER stress in chronic conditions increases cellular toxicity or is protective. As these recent papers have suggested, both inhibiting PERK and increasing eIF2α phosphorylation seem to worsen the phenotype seen in these models of retinal degeneration.

In this work, the use of *Drosophila* permits the study of the ISR in both a retinal degeneration model and a neurodegenerative model. By genetically manipulating the expression of proteins involved in the ISR, this work will attempt to understand their role in retinal degeneration and neurodegeneration, elucidating possible overlapping pathways.

1.5. Aims and objectives

There is accumulating evidence that the ISR and RNP granule formation are involved in the development of neurodegeneration and retinal degeneration. The molecular mechanisms underlying the development of these pathologies remain unclear. Particularly, whether RNP granule components and RBPs are involved in the pathogenesis of retinal degeneration, similarly to neurodegenerative diseases like ALS and HD. Previous work from the Ramaswami laboratory has mainly focused on animal models of neurodegenerative diseases, namely: ALS, PD, and HD. Mutations of key proteins that are known to be associated to these pathologies can be expressed in specific cell lines in *Drosophila* to dissect the role of these proteins, and their domains, in neurodegeneration.

The aim of this work was first to elucidate the molecular pathway causing retinal degeneration in *rdgB* mutants in *Drosophila*. Currently, the exact mechanism underlying this form of retinal degeneration in *Drosophila* remains poorly understood. By modulating genes involved in the ISR, RNP granule formation, and in RNA

regulation, their possible roles in this form of cellular degeneration could be revealed, clarifying the pathways implicated in *rdgB* mutants, and in cellular degeneration in a larger perspective. For this purpose, RNAi constructs targeting the transcripts for these proteins have been used to downregulate their expression. The novel RNA-binding proteins tested here have only recently been identified as modulators of neurodegeneration, and have never been systematically studied in the context of retinal degeneration.

The second part of this work investigates the role of these same proteins in a neurodegenerative model. Previous work has established the implication of the ISR and of RNP granule assembly in the development of neurodegeneration in HD models. This work will test whether the novel RNA-binding proteins may also be modulators of a neurodegenerative phenotype caused by a *Htt* allele. For this purpose, an expanded form of the protein HTT was expressed in clock neurons, leading to a measurable dysfunction of the circadian rhythm, and to the degeneration of these neurons. Similar to the first part, RNAi constructs were used to downregulate the expression of these proteins of interest in this model of neurodegeneration.

In general, past literature has either focused on retinal degeneration or neurodegeneration. The unique approach in this project was to study both retinal degeneration and neurodegeneration in *Drosophila* using similar methods for genetic manipulation. The overall goal was to gain additional insights on potential overlapping molecular pathways involved in retinal degeneration and neurodegeneration.

The specific objectives were to:

1. Dissect the molecular pathway involved in retinal degeneration in *rdgB* *Drosophila* mutants
    a. Visually and molecularly test whether the ISR is activated in *rdgB* mutants;
    b. Assess the involvement of different ISR proteins in *rdgB* mutants by modulating their expression;
    c. Confirm the involvement of novel RNA-binding proteins previously identified in an unpublished genetic screen using RNAi;
    d. Assess the involvement of RNP granule components, and the specific cIDR domain in Ataxin-2 required for granule formation, in *rdgB* ^{9} mutants.
2. Study the molecular pathways that may be involved in neurodegeneration caused by the expression of an expanded form of Huntingtin (*Htt*Q138), elucidating overlapping molecular pathways with *rdgB*^{9} induced retinal degeneration.
    a. Assess the involvement of a specific ISR kinase, PERK, in neurodegeneration measured using a behavioural and cellular readout;
    b. Uncover whether the novel RNA-binding proteins CG42458 and SF3B2 are involved in this form of neurodegeneration using a behavioural and cellular readout;
    c. Confirm that Ataxin-2 mediates *Htt*Q138-induced neurodegeneration using a behavioural and cellular readout, as previously shown in literature;
    d. Test whether a key SG component, Rasputin, is involved in this model of neurodegeneration using a behavioural and cellular readout.

Chapter 2
Materials and Methods

2.1. Materials

2.1.1. *Drosophila* lines

Strains	Source	RRID	Notes
rdgB(9)Rh1GFP;; Rh1Gal4	NCBS	N/A	
tubulin(p)-ATF4.5'UTR>dsRed	Kang et al., 2015	N/A	
P[ry[+t7.2]=rh1-GAL4]3	BDSC	BDSC_8691	*Rh1-Gal4*
P[Pdf-GAL4.P0.5]2; P[Pdf-GAL4.P0.5]3	BDSC	BDSC_80939	*Pdf-Gal4*
rdgb(2); if/cyo; +/+	NCBS	N/A	
GMR-Gal4	BDSC	BDSC_1104	*GMR-Gal4*
P[TRiP.GL00030]attP2	BDSC	BDSC_35162	*perk* RNAi (TRiP)
P[5584]	VDRC	VDRC_16427	*perk* RNAi (VDRC)
P[TRiP.GL00267]attP2	BDSC	BDSC_35355	*gcn2* RNAi (TRiP)
P[103566]	VDRC	VDRC_103976	*gcn2* RNAi (VDRC)
P[TRiP.HMJ02071]attP40/CyO	BDSC	BDSC_42506	*CG42458* RNAi (TRiP)
P[113285]	VDRC	VDRC_108072	*CG42458* RNAi (VDRC)
P[TRiP.HMS00056]attP2	BDSC	BDSC_33651	*sf3b2* RNAi (TRiP)
P[101239]	VDRC	VDRC_105639	*sf3b2* RNAi (VDRC)
P[TRiP.HMS01392]attP2	BDSC	BDSC_36114	*atx2* RNAi (TRiP)
P[11562]	VDRC	VDRC_34955	*atx2* RNAi (VDRC)
P[14212]	VDRC	VDRC_29113	*rin* RNAi (VDRC)
M[w[+mC]=UAS-PPP1R15.M]ZH-51D/CyO	BDSC	BDSC_76250	UAS *gadd34*
+/+; UAS-mRFP-mHtt-Q138	Weiss et al., 2012	N/A	HTTQ138

Table 2-1 List of Drosophila strains used in this project, including their source, original identifier, and notes on the line.

BDSC: Bloomington Drosophila Stock Center, VDRC: Vienna Drosophila Resource Center, NCBS: National Centre for Biological Sciences (India), RRID: Research Resource Identifier, TRiP: Transgenic RNAi Project.

Antibodies and reagents	Source	Identifier
Rabbit anti-dsRed	Invitrogen	RRID: AB_560939
Mouse anti-CNX99A	DSHB	RRID: AB_2722011
Mouse anti-PDF	DSHB	RRID: AB_760350
Rabbit anti-TagRFP	Invitrogen	RRID: AB_10563941
Alexa Fluor® 488 goat anti-rabbit IgG	Invitrogen	RRID: AB_2534122
Alexa Fluor® 555 goat anti-mouse IgG	Invitrogen	RRID: AB_2535844
DAPI	Thermo Scientific	62247

Table 2-2 List of antibodies and reagents used in this project.

DSHB: Developmental Studies Hybridoma Bank

2.1.2. General laboratory chemicals and consumables

Chemicals and consumables	Source	Identifier
Chemicals		
Chloroform	HazMat Facility (TCD)	N/A
Ethanol (Rnase-free)	HazMat Facility (TCD)	N/A
GlycoBlue Coprecipitant	Thermo Scientific	AM9515
Isopropanol	HMF	N/A
Monarch RNA Cleanup Kit	New-England Biolabs	T2040L
qPCRBIO SyGreen Mix Lo-Rox	PCR Biosystems Ltd	PB20.11-01
RNaseOUT	Thermo Scientific	10777019
RNaseZap	Thermo Scientific	AM9780
Sodium phosphate dibasic heptahydrate	Sigma-Aldrich	237-707-0
Sodium phosphate monobasic dihydrate	Sigma-Aldrich	231-449-2
SuperScript III RT	Thermo Scientific	18080093
Trizol	Invitrogen	15596026
Tween®-20	Sigma-Aldrich	P9416
Vectashield Mounting Medium	Vector Laboratories	RRID: AB_2336789
Consumables		
MicroAmp Optical 96-well reaction plate	Applied Biosystems	N8010560
MicroAmp Optical Adhesive Film	Applied Biosystems	4311971

Table 2-3 List of chemicals and consumables used in this work.

2.1.3. Equipment

Equipment model	Manufacturer
General	
Biometra TAdvanced	Analytikjena
Microlite Microcentrifuge 3580	ThermoFisher Scientific
Centrifuge 5702	Eppendorf
DU®730 Spectrophotometer	Beckman Coulter®
NanoDrop2000	ThermoFisher Scientific
Fujifilm LAS-3000	FujiFilm
Microscopes	
Axioimager Z1 microscope	Carl Zeiss AG
AxioCam HRm	Carl Zeiss AG
Zeiss LSM880 Confocal	Carl Zeiss AG
Leica MZ75	Leica
RT-qPCR	
QuantStudio® 5	Applied Biosystems
Centrifuge 5810	Eppendorf
Circadian Rhythm	
DAM2 Drosophila Activity Monitor	TriKinetics Inc.

Table 2-4 List of equipment used in this work.

2.2. Methods

2.2.1. *Drosophila* stock maintenance and fly husbandry

All *Drosophila* stock lines were kept at room temperature, subject to a natural light cycle. Stock lines were "flipped" into a new vial every two weeks to ensure the flies had access to fresh food. Experimental fly lines were kept in an incubator at 25°C, in a 12/12 dark/light cycle. CO_2 was used to anesthetise flies on a semi-permeable pad whenever required, minimising the amount of time that the flies were anesthetised to avoid side-effects from CO_2. New external genetic lines were subjected to two weeks of quarantine to avoid mite infection.

2.2.2. Gal4/UAS system

The Gal4 transcription factor/Upstream Activating Sequence (Gal4/UAS) system is an essential genetic method used to study gene expression. This system is comprised of two components, the Gal4 sequence and the UAS sequence (Figure 2-1).The former will be preceded by a specific promoter targeting a cell line, meaning that in this cell population, the GAL4 protein will be expressed. On the other hand, the UAS sequence can be followed by a transgene of interest. When these two sequences are used in conjunction inside the same organism, the GAL4 protein can bind to the UAS sequence and this will lead to transcription of the sequence downstream. This means that by using this Gal4/UAS system, we are able to express various transgenes in specific cell lines. A wide range of Gal4 lines are available to use in *Drosophila*, ranging from promoters of neuron-specific proteins (embryonic lethal abnormal visual system, ELAV) to single neurons crucial in behaviour.

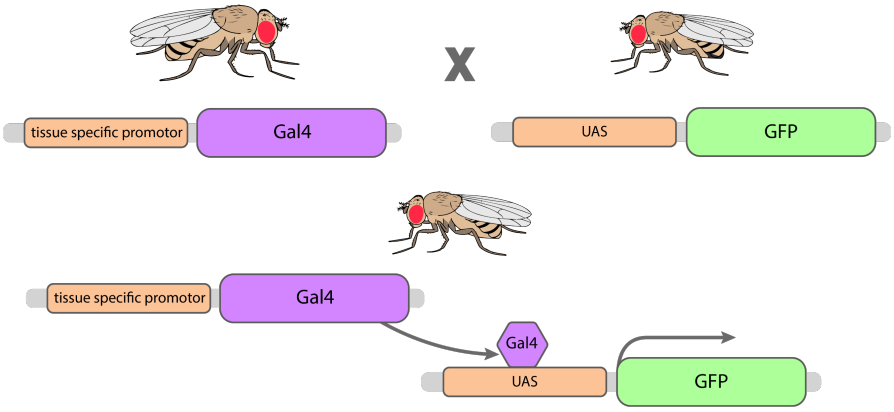

Figure 2-1 UAS/Gal4 system example with a UAS-GFP.

The F1 generation will express the Gal4 in a specific tissue as well as the UAS sequence associated to GFP, leading to the expression of the GFP protein in whichever specific tissue was chosen.

2.2.3. Retinal degeneration assessment

Each *Drosophila* compound eye is composed of roughly 800 units called ommatidia, composed of 8 photoreceptor cells (R1-R8) amongst other secondary cells. Each *Drosophila* photoreceptor cell contains a structure called the rhabdomere, an array of microvilli required for phototransduction. The rhabdomere analysis uses the fact that Rhodopsin-1 (Rh1) is primarily localised in the rhabdomeres of the outer photoreceptor cells (R1-R6). These rhabdomeres are organised in a stereotypic pattern and are easily visualised and quantified when paired with a GFP construct. In retinal degeneration models, the rhabdomeres begin to show features like disorganisation, morphological changes, or being absent. As conducted in previous studies (Campesan et al., 2011; Huang et al., 2015; Smalley et al., 2016; Yadav et al., 2018), the average number of rhabdomeres per ommatidium was calculated per fly.

A +/-;*Rh1GFP;Rh1Gal4* line was used as a control strain, the *rdgB*^{9}*,Rh1GFP/-;+/+; Rh1Gal4,UASDicer2* (RdgB^{9}) as the main retinal degenerative fly line to which various UAS-RNAi (RNAi) lines were crossed. The complete list of RNAi lines, their origin and insertion site details can be found in Table 2-5.

Line	Source	Insertion site	Vector	Reference
perk RNAi (TRiP)	BDSC	attP2	VALIUM22	35162
perk RNAi (VDRC)	VDRC	P-element (GD)	pUAST/pMF3	16427
gcn2 RNAi (TRiP)	BDSC	attP2	VALIUM22	35355
gcn2 RNAi (VDRC)	VDRC	30B3 (KK)	pKC26	103976
CG42458 RNAi (TRiP)	BDSC	attp40	VALIUM20	42506
CG42458 RNAi (VDRC)	VDRC	30B3 (KK)	pKC26	108072
sf3b2 RNAi (TRiP)	BDSC	attP2	VALIUM20	33651
sf3b2 RNAi (VDRC)	VDRC	30B3 (KK)	pKC26	105639
atx2 RNAi (TRiP)	BDSC	attP2	VALIUM20	36114
atx2 RNAi (VDRC)	VDRC	P-element (GD)	pUAST/pMF3	34955
rin RNAi (VDRC)	VDRC	P-element (GD)	pUAST/pMF3	29113

Table 2-5 Insertion sites of RNAi lines used in this project and vectors used when cloning constructs.

BDSC: Bloomington Drosophila Stock Center. VDRC: Vienna Drosophila Resource Center. TRiP: Transgenic RNAi Project.

This analysis was done at different time points (day 1, 3 and 5 after eclosure) to evaluate the speed of degeneration (Figure 2-2). At time points later than day 5, degenerating retinas in the RdgB9 line usually show no fluorescent rhabdomeres even with potential rescuing UAS-RNAi constructs. For each time point and each genotype, between 10 and 20 flies were used, and 15 ommatidia were analysed per fly on average. An Axioimager Z1 microscope equipped with an AxioCam HRm was used for this experiment. A 20x water immersion lens was used as the flies were immobilized in 2% agarose gel and submerged in water. Z-stacking was essential for capturing as many ommatidia as possible in this experiment due to the spherical nature of the *Drosophila* eye. For each retina 10 to 20 slices were acquired with a step of one micron. The images were randomised for the analysis, during which, the number of rhabdomeres for each visible ommatidium was counted. A two-way ANOVA was conducted followed by a *post-hoc* Dunnett's multiple comparison test.

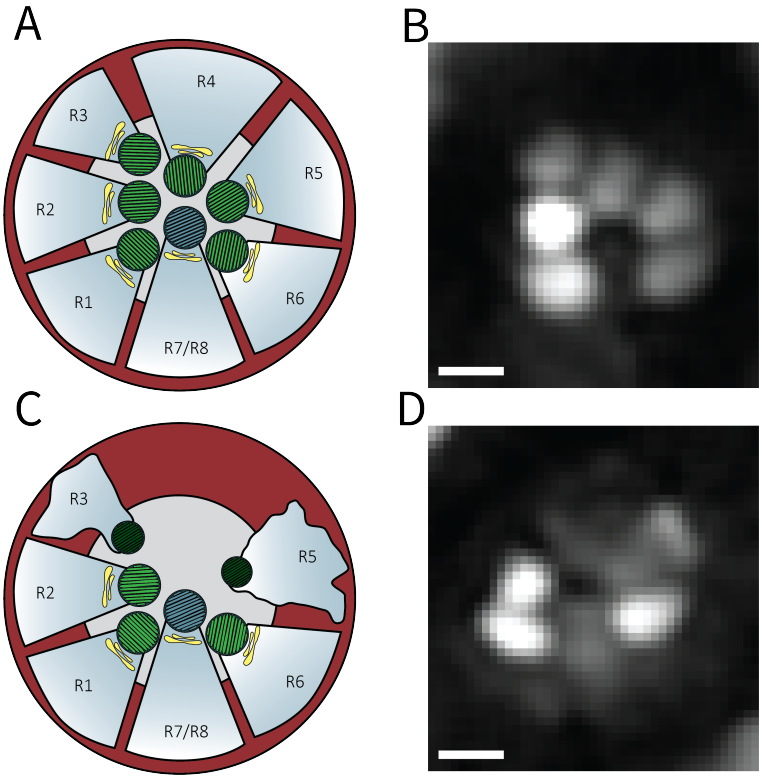

Figure 2-2 Retinal degeneration observed in* RdgB^{9} *flies.

(A) Diagram of a healthy ommatidium with all six RH1-expressing rhabdomeres in their stereotypical configuration. (B) Representative image of a healthy ommatidium with all six identifiable rhabdomeres expressing Rh1GFP. (C) Diagram of a degenerated ommatidium disorganised and missing rhabdomeres. (D) Representative image of a heavily degenerated ommatidium with only three identifiable rhabdomeres. White scale bar represents 4 µm.

2.2.4. Monitoring translational activation of ATF4

To monitor stress-induced translation of ATF4, an ATF4 reporter which places a dsRed gene under the control of the ATF4 5'UTR was used. This reporter was previously used to show the translational activation of ATF4 in response to ER stress, nutritional deprivation and protein misfolding (Kang et al., 2015). The *in vivo* ATF4 reporter $tubulin_p$-ATF4.5'UTR>dsRed was used in conjunction with both the *rdgB*^{9}*,Rh1GFP/-;; Rh1Gal4,UASDicer2* (hereafter referred to as RdgB^{9}) and the *rdgB*^{2}*/-; if/CyO* lines. Flies expressing this reporter were acquired from Dr. Min-Ji Kang's laboratory (Republic of Korea).

The hypomorphic *rdgB*^{2} mutant allele, which also leads to retinal degeneration similar to *rdgB*^{9}, was used instead of the *rdgB*^{9} allele as it is in a *white* null background (*w*-), leading to a decrease in autofluorescence. Male flies were used in this experiment as *rdgB* is located on the X chromosome, therefore female flies generated from an experimental cross also express a wild-type *rdgB* allele. Male pupae were collected and placed in an incubator at 25°C under normal light:dark (12:12h) cycle. For dark-rearing, the vials were wrapped in aluminium foil.

2.2.5. Immunohistochemistry

2.2.5.1. Dissected retinas – dsRed and CNX99A

Fourteen day-old male flies were first anesthetised before their heads were collected. The heads were transferred to a small petri dish containing PBS. Retinas were dissected using forceps and transferred to an ice-cold tube containing 4% PFA in PBS for fixation. Once all retinas were dissected and fixed, these were washed in 0.2% PBS-T three times for 10 min, and blocked in 10% FBS in 0.2% PBS-T for one hour at room temperature. Primary antibodies used were rabbit anti-dsRed (1:1000, Sigma-Aldrich), and mouse anti-CNX99A (1:1000, DSHB) in 10% FBS and 0.2% PBS-T. Retinas were probed overnight at 4°C. They were washed in 0.2% PBS-T three times for 10 min and stained with secondary antibodies at 1:1000 dilutions: Alexa Fluor®488 goat anti-rabbit and Alexa Fluor®555 goat anti-mouse, along with DAPI at 1:500 dilution, for three hours at room temperature. Retinas were washed three times with 0.2% PBS-T, and were mounted in Vectashield Mounting Medium (Vector Laboratories) on slides using coverslips (thickness no.1) as spacers. Confocal imaging was done using a Zeiss LSM880 confocal microscope.

2.2.5.2. Dissected brains – PDF and RFP

For PDF staining analysis, male brains were dissected promptly after the circadian rhythm experiments were complete (approximately ten days after eclosure). Between ten and fifteen brains were dissected in PBS, fixed in 4% PFA for 15 min, washed three times in 0.2% PBS-T for 15 min, and blocked for one hour at room temperature in 10% FBS and 0.2% PBS-T. Primary antibodies used were mouse anti-PDF (1:500, DSHB), rabbit anti-TagRFP (1:1000, Invitrogen) in 10% FBS and 0.2% PBS-T. Brains were probed overnight at 4°C. Brains were washed in 0.2% PBS-T three times for 15 min and stained with secondary antibodies at 1:1000 dilutions: Alexa Fluor®488 goat anti-mouse and Alexa Fluor®555 goat anti-rabbit, along with DAPI at 1:500 dilution, for three hours at room temperature. Preparations were mounted in Vectashield Mounting Medium (Vector Laboratories) on slides using coverslips. Confocal imaging was done using a Zeiss LSM880 confocal microscope.

2.2.5.3. Analysis of brain immunostainings

PDF and HTT (RFP) immunostainings were analysed from z-stack images collected on the Zeiss LSM880 confocal microscope. For both analyses, images were randomised and blinded. For PDF analysis, identifiable PDF-positive sLNv somas were counted and PDF intensity of sLNv somas was measured from their middle stack using ImageJ (https://imagej.net/). For the analysis of HTT aggregation, a rectangle (220 x 90 µm) was drawn between the medulla and protocerebrum to include all lLNv and sLNv somas. Using the 3D object counter plugin in ImageJ, HTT aggregates were identified and measured for volume using a constant threshold of 80 and a minimum size of 50 between all groups. Data was analysed using GraphPad Prism (https://www.graphpad.com/) with a one-way ANOVA followed by Tukey's *post-hoc* test.

2.2.6. RNA analysis

2.2.6.1. RNA extraction and purification

All RNA work was carried out on a dedicated RNA work bench. Prior to RNA work, all instruments and work surfaces were wiped down with RNaseZap™ (Thermo-Fisher Scientific).

For the assessment of stress-related genes in the retina of the $RdgB^9$ mutant line, retinal tissue from 40 seven-day-old flies was dissected in PBS. For RNAi validation, the GMR-Gal4 driver was used to validate the modulation of gene expression of specific genes in the developing eye in all cell types posterior to the morphogenetic furrow (Ellis et al., 1993). This Gal4 driver was used instead of Rh1-Gal4 due to the broader expression of GMR in the visual system, allowing for an improved signal-to-noise ratio analysis of gene expression levels. For this purpose, retinas from 40 three-day-old flies were dissected in PBS.

In both cases, retinas were resuspended and lysed in 500 µL of TRIzol® (Thermo-Fisher Scientific) using a small pestle and left at room temperature for five minutes. 100 µL of chloroform was added to the samples, these were vortexed and centrifuged for 30 min at 4°C at 13,500 RPM. The upper phase was transferred to a new RNase-free microtube and 600 µL of isopropanol and 1 µL of GlycoBlue™ Coprecipitant (AM9515, Thermo-Fischer). This was mixed by inverting the tubes and kept at -70°C for two hours. The samples were centrifuged for 30 min at 4°C at 13,500 RPM. The supernatant was removed, and the pellet was washed with 500 µL of 70% RNase-free ethanol. Pellets were left at room temperature for 15 to 20 minutes, and centrifuged once again for 30 min at 4°C at 13,500 RPM. The supernatant was removed and the pellet was resuspended in 20 µL of RNase-free water. These RNA samples were purified using the Monarch® RNA Cleanup Kit (New England Biolabs). Finally, RNA concentration was measured using a NanoDrop™ 2000 (Thermo-Fisher Scientific).

2.2.6.2. cDNA synthesis

20 µL of cDNA was synthesised from prepared RNA samples. The 5 µM oligo(dT)20, 10 mM dNTP mix, template RNA and RNase-free water were all added in a first step, after which, the mixture was heated to 65°C for 5 min and incubated on ice for 1 min. The remaining reagents, 5X First-Strand Buffer, 0.1M DTT, RNaseOUT™ (Thermo-Fisher Scientific) and SuperScript™III RT (Thermo-Fisher Scientific), were added to finalise the mixture. This was mixed by pipetting gently up and down, and incubated at 50°C for 60 min. The reaction was inactivated by heating the mixture to 70°C for 15 min. This was done using a custom program on a Biometra TAdvanced thermocycler (Analytikjena).

Reagents	Amount required for a 20 µL reaction
Oligo(dT)20 (5 µM)	1 µL
10mM dNTP mix	1 µL
5X First-Strand Buffer	4 µL
0.1M DTT	1 µL
RNaseOUT™ Recombinant RNase Inhibitor	1 µL
SuperScript™III RT	1 µL
Template RNA	10 pg-5 µg
Water	— µL
Total	**20 µL**

Table 2-6 Reaction mix for cDNA synthesis using SuperScript™ III RT from Thermo-Fisher Scientific.

Primer ID	Primer Sequence	Target Gene	Product Size (bp)
GT113	5'-TGATGCACCTTGTTTGGCTTC-3'	*atx2*	93
GT114	5'-TGTTGCTGCACCACCGGCAT-3'		
GT115	5'-AACGCCTCGTGCACCACCAA-3'	*gapdh*	149
GT116	5'-TCGCGCCACAGTTTGCCAGA-3'		
GT129	5'-AACTCAGGCCATAGTACCCG-3'	*atf4*	166
GT130	5'-CGCCTGTTTGTAAGCATCGA-3'		
GT133	5'-AGGCACCGATGGATGGATAG-3'	*ire1*	158
GT134	5'-GGGAGAGTATGTTGGCCTGT-3'		
GT135	5'-CCGCGACACCATGGAAATAG-3'	*cdk5*	175
GT136	5'-CTCGAAGACCAGGGTGAGTT-3'		
GT139	5'-GGCACGGTTTTCTTCGAACA-3'	*sod1*	220
GT140	5'-CCTCAATGTTGCCCAGATCG-3'		
GT141	5'-GATGCGGATAACCAGGTGAAC-3'	*sf3b2*	135
GT142	5'-CTGCCGTGCGAACTCAATCT-3'		
GT143	5'-TACTAGGTCCAGTGGTGC-3'	*perk*	64
GT144	5'-GCTTGTCCAGGTGGGAAGCTA-3'		
GT145	5'-TGTCCAACCAGACCAACTCG-3'	*cg42458*	195
GT146	5'-AGGCATTCCGAGCATCGAAT-3'		
GT147	5'-CCCTGGTGGAGAGTTTGATGC-3'	*gcn2*	65
GT148	5'-GTTACACTTGTCTACAAAGTCG-3'		
GT149	5'-CGAGCAATATCGGTTCGGG-3'	*gadd34*	78
GT150	5'-TGATGCACCTTGTTTGGCTTC-3'		

Table 2-7 Primer pairs used for quantitative polymerase chain reaction.

2.2.6.3. Real Time Quantitative Polymerase Chain Reaction

Real time quantitative polymerase chain reaction (RT-qPCR) is a commonly used method in laboratories to quantify and compare amounts of starting cDNA in different samples. Primer pairs were designed according to Mainland et al. (2017). Briefly, gene sequences were run through FlyPrimerBank (DRSC) which would consider the optimal primer sequence as well as their location in regards to RNAi constructs. Preference was given to primer pairs targeting the non-polyadenylated 5' end of the mRNA, as this was shown to ensure cleavage products would not be detected by qPCR. A list of primers used in this work can be found in Table 2-7.

In this work, a QuantStudio™ 5 qPCR machine (Applied Biosystems, UK) was used in conjunction with the qPCRBIO SyGreen Mix Lo-Rox (PCR Biosystems Ltd.) as the intercalating dye. Reactions were prepared in triplicate according to Table 2-8. The PCR plate (MicroAmp™ Optical 96-well reaction plate, Applied Biosystems, UK) was sealed with a MicroAmp ™ Optical Adhesive Film (Applied Biosystems, UK) to avoid evaporation, and centrifuged for 2 min at 100 RPM to spin down the reaction mixtures. The run method is represented in Figure 2-3.

Reagents	Volume required for a 10 µL reaction
qPCRBIO SyGreen Mix Lo-Rox	5 µL
Forward primer (10 µM)	0.4 µL
Reverse primer (10 µM)	0.4 µL
Template cDNA	<100 ng
PCR grade dH_2O	— µL
Total	**20 µL**

Table 2-8 Reaction mix for RT-qPCR reaction using qPCRBIO SyGreen Mix.

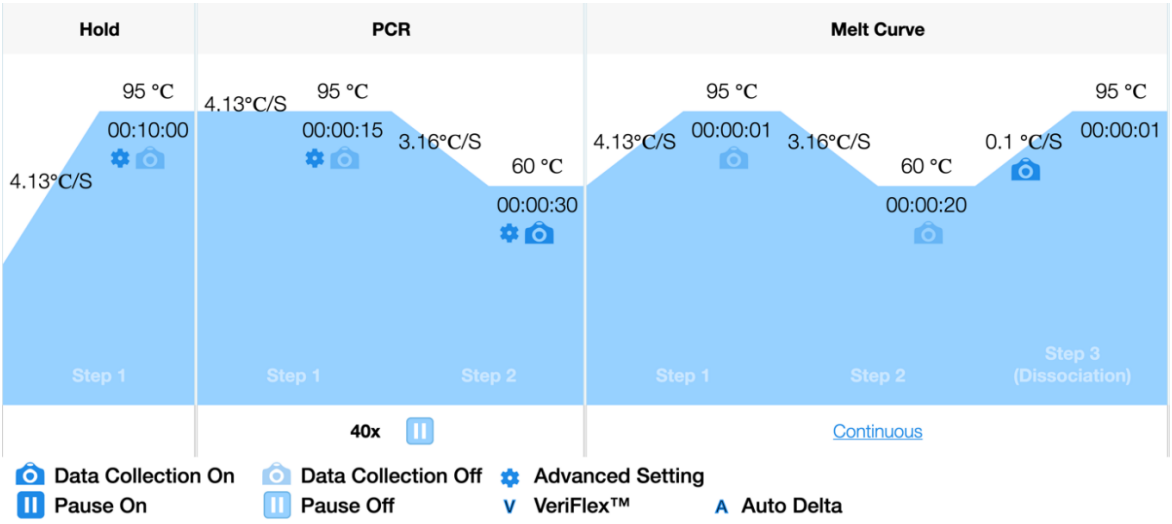

Figure 2-3 Run used for the Real-Time Quantitative Polymerase Chain Reactions (RT-qPCR).

Temperature is increased to and held at 95°C for 10 min for initial denaturation. The run cycles 40 times between a denaturation step at 95°C for 15 sec and an annealing and extension step at 60°C for 30 sec to promote primer binding and elongation. A melt curve is completed to detect non-specific PCR amplification.

2.2.6.4. RT-qPCR analysis

Data was collected from the machine and analysed using the dedicated software from Thermo-Fisher Scientific, Design and Analysis Software v1.5.2. The amplification plot and the melt curve were checked for any issues such as multiple peaks in the melt curve. Cycle threshold (Cq) values were extracted for housekeeping genes and the genes of interest. The comparative Cq method was used to quantify the difference in expression of genes of interest from an experimental sample compared to a control sample. For this purpose, the following formula was used: $\mathbf{2}^{-\Delta\Delta \boldsymbol{Cq}}$, where ΔΔCq is the difference between the ΔCq values of the experimental and the control sample. ΔCq is the difference in Cq values of the gene of interest compared to the Cq values of the reference gene. The formula transforms the ΔΔCq value into fold-difference values. For each reaction, triplicates were run, therefore the average Cq value was used for this calculation. Either a Student's t-test or a one-way ANOVA was conducted to detect significant differences between the ΔCq values, followed by a *post-hoc* Dunnett's multiple comparison test.

2.2.7. Circadian rhythm

2.2.7.1. Behavioural setup

Drosophila circadian rhythm can be inferred from their general locomotor activity. Therefore, to study their circadian rhythm, this project utilised *Drosophila* Activity Monitors (DAM)(Trikinetics, USA), as described in previous studies (Pfeiffenberger et al., 2010). DAMs can hold up to 32 individual flies in separate glass tubes (5 mm diameter, 100 mm length, Trikinetics) (Figure 2-4). Three-day-old male flies were anesthetised with CO2 and inserted into the tube containing about 10 mm of food inside one end (1% agar, 5% sucrose), and a foam plug in the other end. The DAMs detect whenever a fly crosses an infra-red beam, recording their locomotor activity. The number of crossings was binned per minute and the data was collected by a connected computer running the Trikinetics software. The flies were habituated to the tubes overnight inside of an incubator at 25°C, before initiating the experiment with a normal 12h:12h light/dark cycle for the first three days (the entrainment period), and constant darkness for the last four days (free-running period).

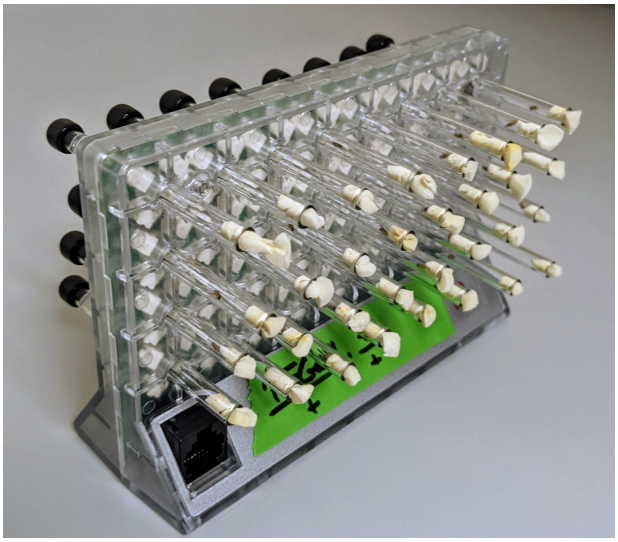

Figure 2-4 DAM2 Drosophila Activity Monitor.

A DAM apparatus loaded with 32 flies in individual tubes containing food, and sealed with a plastic cap and foam.

2.2.7.2. Circadian rhythm analysis

Using the Rethomics package on RStudio (Geissmann et al., 2019) (https://www.rstudio.com), activity plots for the entire experiment were produced to visualise general locomotor activity for each group. The SleepMat tool designed by the Allada laboratory (Sisobhan et al., 2022) was used to analyse the entrainment and the free-running periods using a Chi-square periodogram analysis. This analysis detects whether there are significant periods in the locomotor activity of individual flies, and reveals the power – significance (P-S) value for the strongest period of each fly. The P-S value was obtained by calculating the difference between the Chi-square power result and the period-adjusted significance threshold in these experiments. This value represents the power of rhythmicity, where the chi-square periodogram is capable of distinguishing a rhythmic pattern whenever the P-S value is superior to 0. When a significant period was detected, a period value between 14 and 34 hours was reported. The individual P-S values were gathered into GraphPad Prism (https://www.graphpad.com/) for each group and a one-way ANOVA was conducted with a Tukey's *post-hoc* multiple comparison test between experimental groups and between the experimental groups and their respective parental controls. A Fisher's exact test was used for analysing the percentage of rhythmic and arrhythmic flies between groups.

Chapter 3

Modulation of *rdgB*^{9}-Induced Retinal Degeneration

3.1. Introduction

The set of experiments in this chapter aims to shed light on the signalling pathway associated with retinal degeneration. In particular, the involvement of several components of the cellular stress response pathway and new RNA-binding proteins was investigated in a *Drosophila melanogaster* model of retinal degeneration. Primarily, the mutant allele *rdgB*^{9} is used in this chapter to induce retinal degeneration which can be observed with relative ease in young adult fly retinas. Although this RDGB protein was discovered over 40 years ago (Harris & Stark, 1977), how cellular degeneration occurs when it is mutated is still largely not understood. Determining what proteins are involved in the pathway leading to *rdgB*^{9}-induced retinal degeneration may help understand the cellular processes at play in cellular degeneration in a wider implication.

3.1.1. The *Drosophila* eye

The compound eyes of *Drosophila* are each composed of around 800 chiral hexagonal units known as ommatidia, which are commonly found in arthropods. *Drosophila* ommatidia contain eight microvillar photoreceptor cells, six are outer photoreceptors, and two are inner photoreceptors (Figure 1-2) (Hardie, 2001). The outer photoreceptors (R1-R6) run the entire length of the ommatidia, with the largest diameter at the surface, and express the photosensitive protein Rhodopsin-1 (Rh1) with a peak absorption wavelength of around 500nm. The two inner photoreceptors (R7 and R8) express other forms of Rhodopsin (Rh3-Rh6) that have varying peak absorption rates ranging from 350 to 550nm (Stavenga & Arikawa, 2008). As these are all microvillar photoreceptors, a unique characteristic of these cells is the extension known as rhabdomeres. Rhabdomeres are ordered arrays of densely packed microvilli, which contain the highest density of the rhodopsin proteins. The ommatidia also contain secondary support cells, including four non-neuronal cone cells, two primary pigment cells, six secondary pigment cells, and three tertiary pigment cells (Cagan & Ready, 1989). These support cells are essential for optimal image processing in the *Drosophila* visual system.

Phototransduction in microvillar photoreceptors functions differently to that in ciliary photoreceptors, present in chordates, including vertebrates (Figure 1-2). Once light reaches the rhodopsin protein, this changes its conformation leading to the activation

of the associated Gq protein. The α-subunit of the Gq protein activates phospholipase C (PLCβ) which catalyses the generation of inositol triphosphate (IP3) and diacylglycerol (DAG) from phosphatidylinositol-4,5-bisphosphate (PIP2). This enzymatic reaction somehow leads to the activation of TRP and TRP-like channels, causing a cytoplasmic Ca2+ influx (Hardie, 2008). The influx of calcium ions into the cell causes depolarisation, and the signal is transferred to downstream visual system components located in the optic lobe. As this molecular cascade requires PIP2, the recycling of this membrane component is crucial (Trivedi & Padinjat, 2007). This recycling of phosphoinositol taking place between the plasma membrane of the rhabdomere and the ER, has been well established and is illustrated in Figure 1-5. Many proteins involved in this cycle have been shown to lead to retinal degeneration when mutated (Wang & Montell, 2007).

Although the phototransduction pathway in ciliary photoreceptors differs significantly to microvillar phototransduction, there is evidence to suggest that signalling pathways implicated in initiation of retinal degeneration could be shared. This is particularly remarkable with the Rhodopsin protein (Rh1). Indeed, the same point mutations of *Rh1* lead to retinal degeneration in both *Drosophila* and vertebrate models (Galy et al., 2005; Xiong & Bellen, 2013).

3.1.2. Assessing retinal degeneration in the *Drosophila* retina

There is a large number of mutations in *Drosophila* that are known to lead to retinal degeneration. Many of these are point mutations of the key photo-sensitive protein Rhodopsin, such as Rh1-P37H, which have been linked to the human disease retinitis pigmentosa (Gorbatyuk et al., 2010). A selection of mutations that lead to retinal degeneration in *Drosophila* involve proteins that play a role in the recycling of PIP2 (Wang & Montell, 2007). One such protein, Retinal degeneration B (RDGB) is a phosphatidylinositol (PI) transfer protein (PITP) that transfers a PI molecule from the ER membrane to the rhabdomeric plasma membrane (Cockcroft et al., 2016; Yadav et al., 2018). This cycle occurs in the membrane contact site between the rhabdomeres and the ER extension known as the submicrovillar cisternae (SMC) (Figure 1-2). In the following experiments, the *rdgB*^{9} mutant allele was used. It corresponds to a hypomorphic allele of rdgB containing a single nonsense mutation (Gln147term) in its PITP domain which prevents RDGB from properly localising to this membrane contact

site, impairing phototransduction and leading to photoreceptor cell death (Harris & Stark, 1977; Paetkau et al., 1999; Vihtelic et al., 1991; Yadav et al., 2018). These effects can be assessed both morphologically, and functionally by monitoring the electrophysiological response of the retina (Paetkau et al., 1999).

Studying retinal degeneration in *Drosophila* is advantageous thanks to their similarity of cellular signalling pathways with mammalian cells, the speed of pathogenesis, and the vast library of genetic tools and strains that are readily available to researchers. In the context of this chapter, retinal degeneration will be morphologically assessed through the presence of an GFP reporter specifically expressed in Rh1 expressing photoreceptors, i.e. in the six outer photoreceptor cells. When these cells degenerate, the GFP signal decreases and the rhabdomeres become unidentifiable.

The pathway leading to retinal degeneration can be dissected by manipulating the expression of specific genes. Of particular interest in this project are genes involved in ER stress which have been shown to be implicated in different forms of neurodegenerative diseases and retinal degeneration (Athanasiou et al., 2017; Mendes et al., 2009; Vaccaro et al., 2013). The activation of the integrated stress response (ISR) leads to the initiation of the activating transcription factor (ATF4), which will promote the expression of stress response genes. In addition, other genes of interest in this project code for RNA-binding proteins (RBPs) that have a variety of cellular functions including stabilisation, splicing and translation of mRNA molecules, and contributing to the formation of ribonucleoprotein complexes (Gerstberger et al., 2014). Some RBPs have been shown to play a key role in the development of neurodegenerative diseases such as amyotrophic lateral sclerosis, and Huntington's disease (Hart & Gitler, 2012; Maziuk et al., 2017; McLaughlin et al., 1996). Moreover, many of these RBPs, such as Ataxin-2, have been found to be recruited in particles known as ribonucleoprotein (RNP) granules. Although these RNP granules have a functional role in healthy cells, such as in neurons (De Graeve & Besse, 2018), the pathological formation of these particles have been shown to be a hallmark of neurodegenerative diseases, ranging from FUS cytoplasmic inclusions in ALS and frontotemporal dementia (FTD), to P-bodies in Parkinson's disease (An et al., 2021; Desai & Bandopadhyay, 2020; Hallacli et al., 2022). However, it is still unclear how they may be linked to the pathogenesis of

these neurodegenerative diseases. It is even less clear how RBPs and RNP granules may be implicated in retinal degenerative diseases (Dash et al., 2016).

3.1.3. Aims

The main objective of this chapter is to understand the cellular mechanisms of retinal degeneration caused by mutations of *rdgB*. So far, the pathogenesis and the consequences of expressing mutant forms of this protein remain poorly understood. This work aims to understand whether the ISR is activated in this model of retinal degeneration, and to assess the involvement of proteins from this pathway, and other RNA-binding proteins, in the process underlying cellular degeneration.

3.2. Results

The main aim of this chapter is to understand the cellular mechanisms of retinal degeneration caused by mutations of *rdgB*. The following experiments were designed to evaluate the potential activation of the stress pathway in the RdgB^{9} retinal degeneration model and the role of the stress pathway components in the progression of this degeneration. Later, the role of novel RNA-binding proteins in this form of retinal degeneration was assessed. Finally, the role of specific RNA-binding proteins that are known to play a role in granule formation were also assessed in the context of the RdgB^{9} induced retinal degeneration.

3.2.1. *rdgB*^{9} mutation causes retinal degeneration

To confirm the retinal degeneration phenotype of the *rdgB*^{9} mutant allele, a retinal analysis with *rdgB*^{9}*, Rh1GFP/-; +/+; Rh1Gal4, UAS Dicer 2* male flies (RdgB^{9}) and *+/-; Rh1GFP; Rh1Gal4* male flies was conducted. The flies were screened for the number of missing rhabdomeres per ommatidia visualised by using a GFP reporter in Rh1-expressing outer photoreceptor cells (Rh1GFP). Absence of the GFP signal was interpreted as a missing rhabdomere, and therefore a degenerated photoreceptor cell. As a control, WT flies carrying just the Rh1GFP and Rh1Gal4 sequences were used. As the degeneration is light and age-dependent, the effect of the *rdgB*^{9} allele was assessed in 1-, 3-, and 5- day-old flies. The number of missing rhabdomeres was counted for each group and time point (Figure 3-1).

A two-way ANOVA was performed to analyse the effect of genotypes and the effect of aging on the number of missing rhabdomeres. This test revealed a significant effect from the genotypes ($F_{1, 247}$ = 75.71, p < 0.001), days ($F_{2,247}$ = 27.63, p < 0.001) and a significant effect from their interaction ($F_{2,247}$ = 25.96, p < 0.001). Specific comparisons were performed using Bonferroni's *post-hoc* tests.

One-day-old RdgB^{9} mutant flies exhibited no sign of degeneration, as indicated by a well-defined GFP signal in all outer photoreceptors similar to control flies (Figure 3-1, A). However, 3-day-old RdgB^{9} flies showed defective rhabdomere morphology, with a 12-fold increase in the number of missing rhabdomeres compared with control (p < 0.001, Bonferroni's *post-hoc* test). This degeneration progressed further as the flies aged, such that 5-day-old RdgB^{9} flies exhibited a nearly 50-fold increase in the number of missing rhabdomeres (p < 0.001, Bonferroni's *post-hoc* test).

These results indicate that the *rdgB*^{9} allele does lead to a quantifiable and significant retinal degeneration in the *Drosophila* fly from day 3, and that the Rh1GFP and the Rh1Gal4 transgenes alone do not lead to any form of retinal degeneration. For the next sections, day 1 data will not be included in the graphs for clarity purposes as there are no visible morphological differences in RdgB^{9} on day 1.

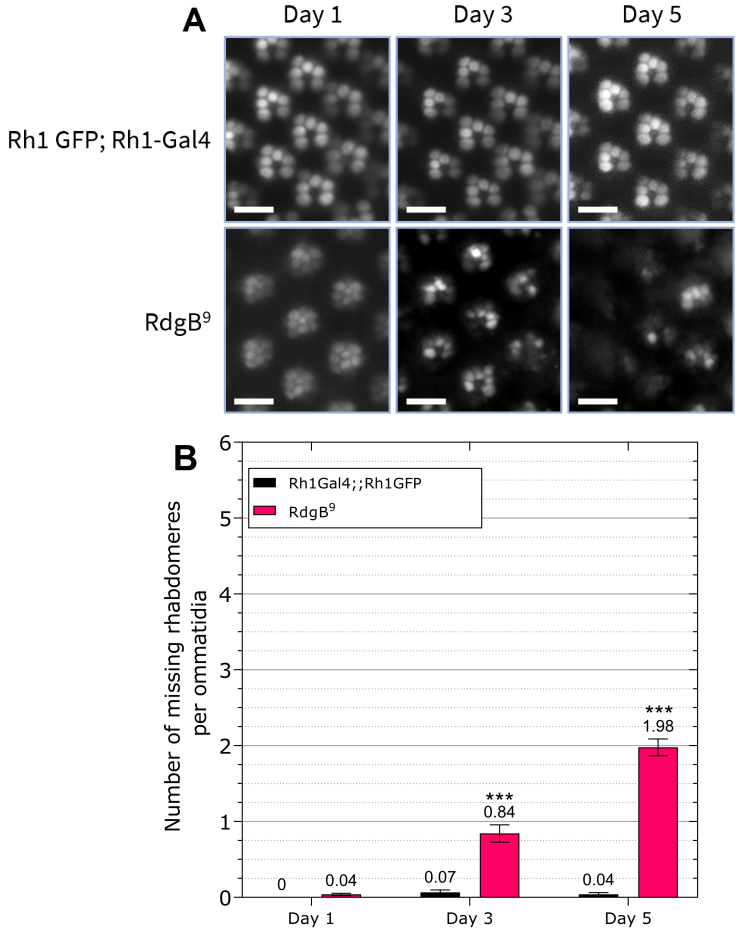

Figure 3-1 The rdgB*^{9} *mutation leads to a significant and quantifiable degeneration of photoreceptors compared to controls.

(A) Representative images of ommatidia from +/-;Rh1GFP;Rh1-Gal4 control male flies and rdgB^{9}*, Rh1GFP/-; +/+; Rh1Gal4, UAS Dicer 2 male flies (RdgB*^{9}*). White scale bar represents 10* μm*. (B) Drosophila retinas were analysed for the number of missing rhabdomeres per ommatidia. Data are presented as bar graphs representing the mean ± SEM (n = 18 – 78), ***p < 0.001 relative to control (two-way ANOVA with Bonferroni post-hoc test).*

3.2.2. Stress pathway activation in *rdgB* mutants

3.2.2.1. Assessment of ATF4 translational activation

When the ISR is activated, there is an increase in the translation of available ATF4 mRNA leading to downstream transcription of genes essential to cell survival after stress (Pitale et al., 2017). In the following experiments, an ATF4 reporter was used to assess the translational activation of ATF4, and therefore the activation of the ISR pathway as a whole. This was done by expressing a construct containing the fluorophore dsRed with the ATF4 5'UTR located upstream to its sequence, and driven ubiquitously by a tubulin promotor (tub$_{p}$-ATF4.5'UTR>dsRed). Whenever ATF4 is translated as a consequence of the ISR activation, this reporter will also be translated leading to the expression of dsRed. This reporter has been used and validated to show ISR activation in a previous study (Kang et al., 2015).

rdgB mutants lead to retinal degeneration through a molecular pathway that remains unclear. In this set of experiments, the involvement of the ISR in a line expressing the *rdgB*^{2} mutation was assessed. This mutant is white-eyed, an advantage over the *rdgB*^{9} mutation as it reduces autofluorescence caused by pigment cells.

Figure 3-2 depicts a representative image of a retinal dissection of a *rdgB*^{2}/-; tubulin$_{p}$-ATF4.5'UTR>dsRed/CyO; +/+ fly (hereafter referred to as RdgB^{2} x ATF4 reporter). The dsRed signal is amplified with an antibody targeting the fluorophore and seems to be mostly located at the base of the photoreceptors, as well as closer to the lens, possibly near the nucleus of the photoreceptors cells or in secondary structure cells. An antibody targeting CNX99A was used to mark the endoplasmic reticulum to locate the photoreceptor cells.

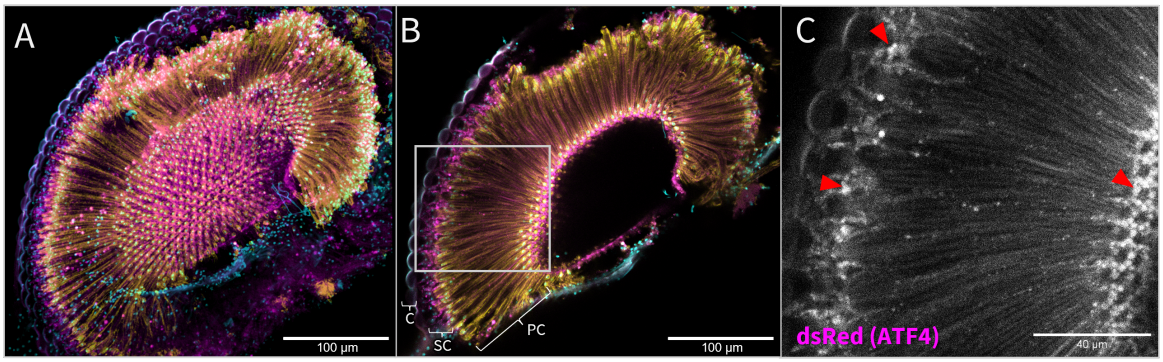

Figure 3-2 Representative images of the retina of a 10 day old rdgB^{2}/-; tubulin(p) ATF4.5'UTR > dsRed/CyO; +/+ fly with an ATF4 reporter staining. *The retina was dissected and prepared for staining using anti-dsRed (Rabbit 488 – Magenta), an antibody targeting ER membranes: anti-CNX99A (Mouse 555 – Yellow), and DAPI (Cyan). A: 3D projection of all stacks from the retina using the brightest point as a projection method. B: Single stack of a cross-section of the same retina. Labelled layers are the cornea (C), secondary cells (SC), and photoreceptor cells (PC). C: Magnified image from grey inset located in (B), red arrows show dsRed signal. Imaged using a Zeiss LSM 510-meta confocal microscope.*

After confirming the detection of ATF4 translational activation signal in *rdgB*^{2} mutants, the purpose was to investigate whether the activation of the ISR in these mutants is light-dependent. As such, RdgB^{2} x ATF reporter flies and control flies were either never exposed to light, or exposed to a normal 12/12hr light:dark cycle. If light triggers the ISR in RdgB^{2} flies, then it is expected to lead to an increase in dsRed signal in light-exposed flies as compared with dark-reared control and with light-reared control flies.

The results show no difference in the ATF4 reporter expression between light and dark-reared RdgB^{2} x ATF4 reporter flies (Figure 3-3, A and A'). There is a strong visual difference between the RdgB^{2} x ATF4 reporter flies and the ATF4 reporter control flies, both in the strength of the signal and its granularity (Figure 3-3, A, E, A' and E'). This suggests that light exposure without the *rdgB*^{2} mutation does not lead to ISR activation. Overall, these results are inconclusive due to inconsistencies in tissue preparation as a consequence of difficulties in dissecting the retinal tissue, which will be further discussed. Visual assessment of ATF4 activation may not be the optimal method to evaluate the activation of the stress pathway in these mutants. As such, the RT-qPCR method was used instead to investigate the upregulation of stress-related proteins in the RdgB^{9} model.

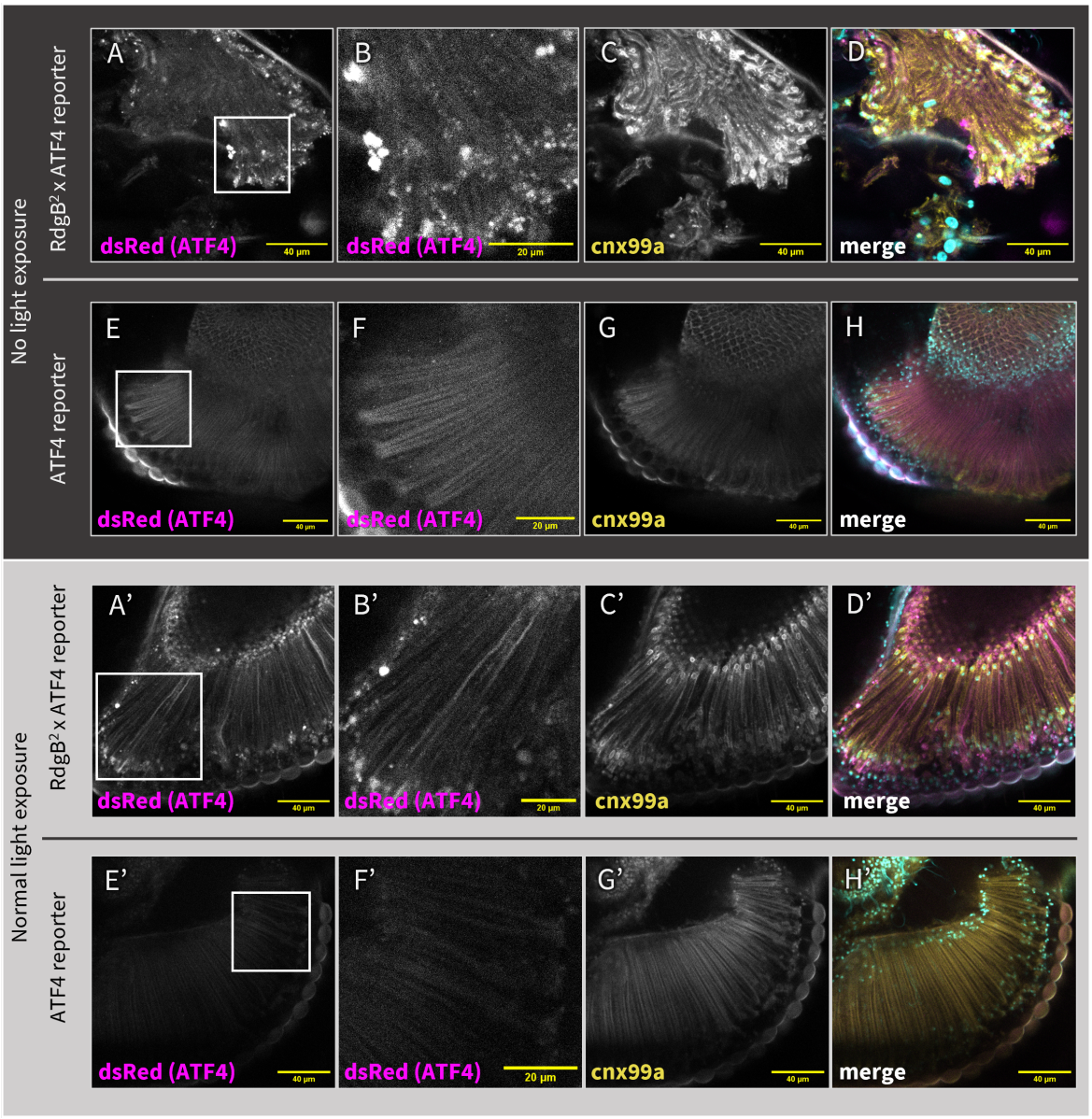

Figure 3-3 An ATF4 reporter was used to assess ISR activation depending on light exposure and the presence of the rdgB² mutation.

Five-day-old RdgB² x ATF4 reporter male flies (rdgB²/-;tubulin(p)-ATF4.5'UTR>dsRed/CyO;+/+) and control ATF4 reporter male flies (+/-;tubulin(p)-ATF4.5'UTR>dsRed/+;+/+) were used. One set of representative retina images per condition. Normal light exposure corresponds to a 12/12hr light:dark cycle. Retinas were dissected and stained using anti-dsRed (Rabbit 488 – Magenta), anti-CNX99A (Mouse 555 – Yellow), and DAPI (Cyan). (A-D) No light exposure RdgB² x ATF4 reporter flies. (E-H) No light exposure ATF4 reporter control flies. (A'-D') Normal light exposure RdgB² x ATF4 reporter flies. (E'-H') Normal light exposure ATF4 reporter control flies. (B, F, B', F') Magnification of the grey inset on the corresponding left images. Yellow bar represents 40 µm for all images except the magnified images (B, F, B' and F') which have a scale bar of 20 µm. Imaged using a Zeiss LSM880 confocal microscope.

3.2.2.2. Expression of stress-related genes

As assessing activation of the ISR by visualising ATF4 translation was not successful, an alternative method was used to test whether the activation of cellular stress pathways is involved in the degeneration process observed in the *rdgB*^{9}*, Rh1GFP/-; +/+; Rh1Gal4, UAS Dicer 2* (RdgB^{9}) line. A quantitative PCR was conducted to measure the RNA expression levels of various stress-related proteins. These stress-related proteins include ATF4, PERK and IRE1, which play a role in ER stress, CDK5, which is known to be upregulated during oxidative stress, and finally SOD1, which plays a role in oxidative stress response as well as SG dynamics.

RNA was extracted from retinas originating from RdgB^{9} mutant flies as well as from control unstressed Canton S (CS) flies for baseline Cq values. CS flies that had been heat-shocked for one hour at 37°C were also used in this experiment as a positive control, as excessive temperature has been shown to trigger changes in the expression levels of stress-responsive genes (Sørensen et al., 2005). The RNA from these groups was extracted and reverse-transcription followed by a quantitative PCR were completed. The results are represented as fold change based on the Cq values obtained (Figure 3-4).

The RdgB^{9} flies show a high variability in gene expression across the three replicates for all targets. This could be a result of background signal coming from neighbouring tissue, as the degeneration only affects the photoreceptors, a small subset of cells in the dissected tissue. The possible reasons for this variability will be further explored in the discussion.

For heat-shocked CS flies, results show an upregulation of *perk* in the heat-shocked CS group, with a fold-change of 2.87 compared to the CS group. Nevertheless, no changes in gene expression were observed in other cellular stress components. The low variability between replicates, compared to the RdgB^{9} group, suggests that the expression of these other genes are truly unaffected by heat-stress. A one-way ANOVA on ranks was used for individual target gene groups separately, comparing ΔCq values from the CS, heat-shocked CS, and RdgB^{9} groups. No significance was detected in any group: [ATF4]p = 0.4393, [PERK]p = 0.1679, [IRE1]p = 0.7214, [CDK5]p = 0.8286, and [SOD1]p = 0.5107.

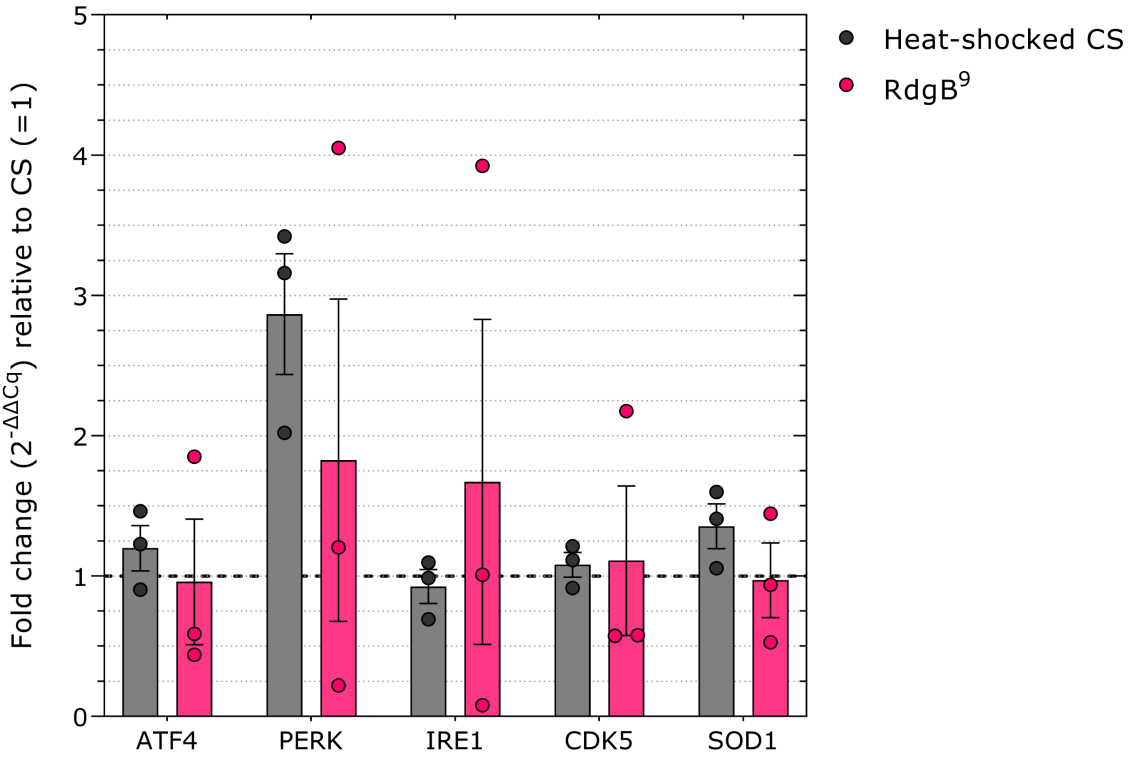

Figure 3-4 Expression of stress-related genes exhibited high variability across replicate experiments in RdgB^{9} flies.

Detected fold changes ($2^{-\Delta\Delta Cq}$) in the expression of stress-related genes are plotted compared to Canton S (CS) flies (dotted line, y = 1). Bar graph represents the mean value, error bars represent SEM values, and three replicates are represented as dots. ΔCq values were used for statistical tests. A one-way ANOVA on ranks test comparing the CS, heat-shocked CS and RdgB^{9} groups for each individual target gene revealed no significant differences for either target genes. RdgB^{9} corresponds to rdgB^{9}, Rh1GFP/-; +/+; Rh1Gal4, UAS Dicer 2.

3.2.3. Modulating the RdgB^{9} retinal degeneration phenotype

The previous results show that the rdgB9 mutation leads to a quantifiable retinal degeneration phenotype in the *Drosophila* eye. Therefore, I decided to investigate the possible involvement of seven genes in this form of retinal degeneration. Different genes from different pathways were tested by manipulating their expression levels: components of the ISR (3.2.3.1), novel RNA-binding proteins (3.2.3.2), and finally, proteins that play a role in ribonucleoprotein (RNP) -granule dynamics (3.2.3.3).

3.2.3.1. Requirement of the ISR in the RdgB^{9} model of retinal degeneration

The involvement of ISR components was assessed in the RdgB^{9} model of retinal degeneration. To do so, the expression levels of specific target genes were modulated via RNAi knockdown or overexpressed in RdgB^{9} mutant flies of different ages. Specifically, UAS-RNAi (RNAi) constructs targeting the transcripts for PERK and GCN2, kinase proteins that are implicated in the phosphorylation of eIF2α, and therefore activating the ISR, were used. In addition, the phosphatase protein GADD34, which has an antagonistic effect to the kinases, was overexpressed in photoreceptors using a UAS construct driven by Rh1-Gal4. This overexpression of a phosphatase was expected to have a similar effect as knocking-down the kinases. These constructs were combined with the RdgB^{9} line (*rdgB*^{9}*,Rh1GFP/-;+/+;Rh1Gal4,UASDicer2*) leading to the following genotypes:

- *rdgB*^{9}*, Rh1GFP/-; +/+; Rh1Gal4, UAS Dicer 2/UAS perk RNAi (TRiP)*
  (referred to as RdgB^{9} x UAS *perk* RNAi (TRiP));
- *rdgB*^{9}*, Rh1GFP/-; +/+; Rh1Gal4, UAS Dicer 2/UAS perk RNAi (VDRC)*
  (referred to as RdgB^{9} x UAS *perk* RNAi (VDRC));
- *rdgB*^{9}*, Rh1GFP/-; +/+; Rh1Gal4,UAS Dicer 2/UAS gcn2 RNAi (TRiP)*
  (referred to as RdgB^{9} x UAS *gcn2* RNAi (TRiP));
- *rdgB*^{9}*, Rh1GFP/-; UAS gcn2 RNAi (VDRC)/+; Rh1Gal4,UAS Dicer 2/+*
  (referred to as RdgB^{9} x UAS *gcn2* RNAi (VDRC));
- *rdgB*^{9}*, Rh1GFP/-; UAS gadd34/+; Rh1Gal4, UAS Dicer 2/+*
  (referred to as RdgB^{9} x UAS *gadd34*).

The effect of these genetic manipulations on retinal degeneration was investigated. The prediction was that if the ISR is activated in RdgB^{9} flies, then knocking-down the kinases PERK and GCN2, responsible for phosphorylating the ISR effector eIF2α, would alleviate the degenerative phenotype. Similarly, overexpressing the phosphatase GADD34 was predicted to have a comparable effect.

A two-way ANOVA was performed to analyse the effect of genotypes and the effect of aging on the number of missing rhabdomeres. This test revealed that there was a statistically significant effect from the genotypes ($F_{5, 543}$ = 12.860, p < 0.001), days ($F_{2,543}$ = 243.900, p < 0.001) and a significant interaction between the effects of genotypes and days ($F_{10, 543}$ = 2.627, p = 0.0040). Specific comparisons were performed using Dunnett's *post-hoc* tests.

As expected, no difference was detected in 1-day-old flies between any of the groups as degeneration is not yet visible at this point. In 3-day-old mutant flies in which *perk* was knocked down compared to RdgB^{9}, a 70% decrease in the number of missing rhabdomeres was observed, using both *perk* RNAi (TRiP) (p = 0.0033, Dunnett's *post-hoc* test) and *perk* RNAi (VDRC) (p = 0.0019, Dunnett's *post-hoc* test). Neither RdgB^{9} x *gcn2* RNAi (TRiP) or RdgB^{9} x *gcn2* RNAi (VDRC) showed alleviation or worsening of the degenerative phenotype as compared with the RdgB^{9} control group. Finally, RdgB^{9} x UAS *gadd34* worsened the degenerative phenotype with a 75% increase in missing rhabdomeres compared to the RdgB^{9} control on day 3 (p < 0.001, Dunnett's *post-hoc* test).

The analysis in 5-day-old flies revealed less striking rescues of the degenerative phenotype. RdgB^{9} x *perk* RNAi (TRiP) and RdgB^{9} x *perk* RNAi (VDRC) showed a significant (27%) and a non-significant (16%) decrease, respectively, in missing rhabdomeres compared to RdgB^{9} (*perk* RNAi (TRiP): p = 0.0193; *perk* RNAi (VDRC): p = 0.1798, Dunnett's *post-hoc* test). Neither RNAi constructs targeting *gcn2* led to a modulation of the degenerative phenotype on day 5 compared to RdgB^{9}. Finally, overexpressing *gadd34* on day 5 led to a non-significant (10%) increase in missing rhabdomeres compared to RdgB^{9}.

To validate these genetic constructs, their efficiency was tested using the RT-qPCR method. For this purpose, GMR-Gal4 was used to drive the UAS-RNAi and UAS-*gadd34*

constructs in all retinal cells, retinas were dissected and prepared for RNA analysis. GMR-Gal4 flies without the UAS-effector transgenes were used as control in the subsequent fold change calculations. Therefore, for all target genes, the fold change for GMR-Gal4 is equal to 1. Figure 3-5 (C) shows the fold change ($2^{-\Delta\Delta Cq}$) in the expression of the genes: *perk*, *gcn2* and g*add34*. *perk* RNAi (TRiP) leads to an 80.75% downregulation, whereas *perk* RNAi (VDRC) leads to a 66.55% downregulation in the expression of *perk*. *gcn2* RNAi (TRiP) and *gcn2* RNAi (VDRC) both lead to a non-significant decrease in the expression of *gcn2* of 12.35% and of 37.78%, respectively. Overexpression of *gadd34* by expressing UAS *gadd34* in GMR-positive cells leads to a 2854% upregulation in the expression of *gadd34*. The results of a Student's *t*-test conducted on ΔCq values for this experiment are reported in Table 3-1.

Gene of interest	*perk*				*gcn2*				*gadd34*	
GMR-Gal4	+	+	+	+	+	+	+	+	+	+
RNAi (TRiP/VDRC) or UAS construct	-	TRiP	-	VDRC	-	TRiP	-	VDRC	-	+
ΔCq values	5.050	7.537	6.396	7.988	9.582	9.773	4.742	5.454	3.764	-1.120
df	2		2		2		2		2	
t-value	6.128		3.687		0.182		0.129		312.100	
p-value	0.026		0.066		0.872		0.910		< 0.001	
Fold change	0.193		0.335		0.877		0.622		29.540	

Table 3-1 qPCR results for perk, gcn2, and gadd34 expression modulation.

Statistical report for ΔCq means comparisons between control and experimental samples using a Student's t-test. df: degrees of freedom. For all ΔCq values, two biological replicates were completed.

These results demonstrate that UAS *perk* RNAi (TRiP) and UAS *perk* RNAi (VDRC) are both efficient at knocking-down *perk* transcripts, with the first RNAi having a stronger and significant effect compared to the second RNAi. On the other hand, UAS *gcn2* RNAi (TRiP) and (VDRC) both seem to be inefficient in decreasing transcript levels of *gcn2*. Finally, the overexpression of *gadd34* is highly efficient and significant.

Overall, the results in this section suggest that components of the ISR are involved in the development of retinal degeneration in RdgB^{9} flies, specifically through the expression of the ER stress protein PERK. Considering the qPCR results, the lack of effect on the retinal degeneration from either *gcn2* RNAi constructs could be from inefficient knockdown.

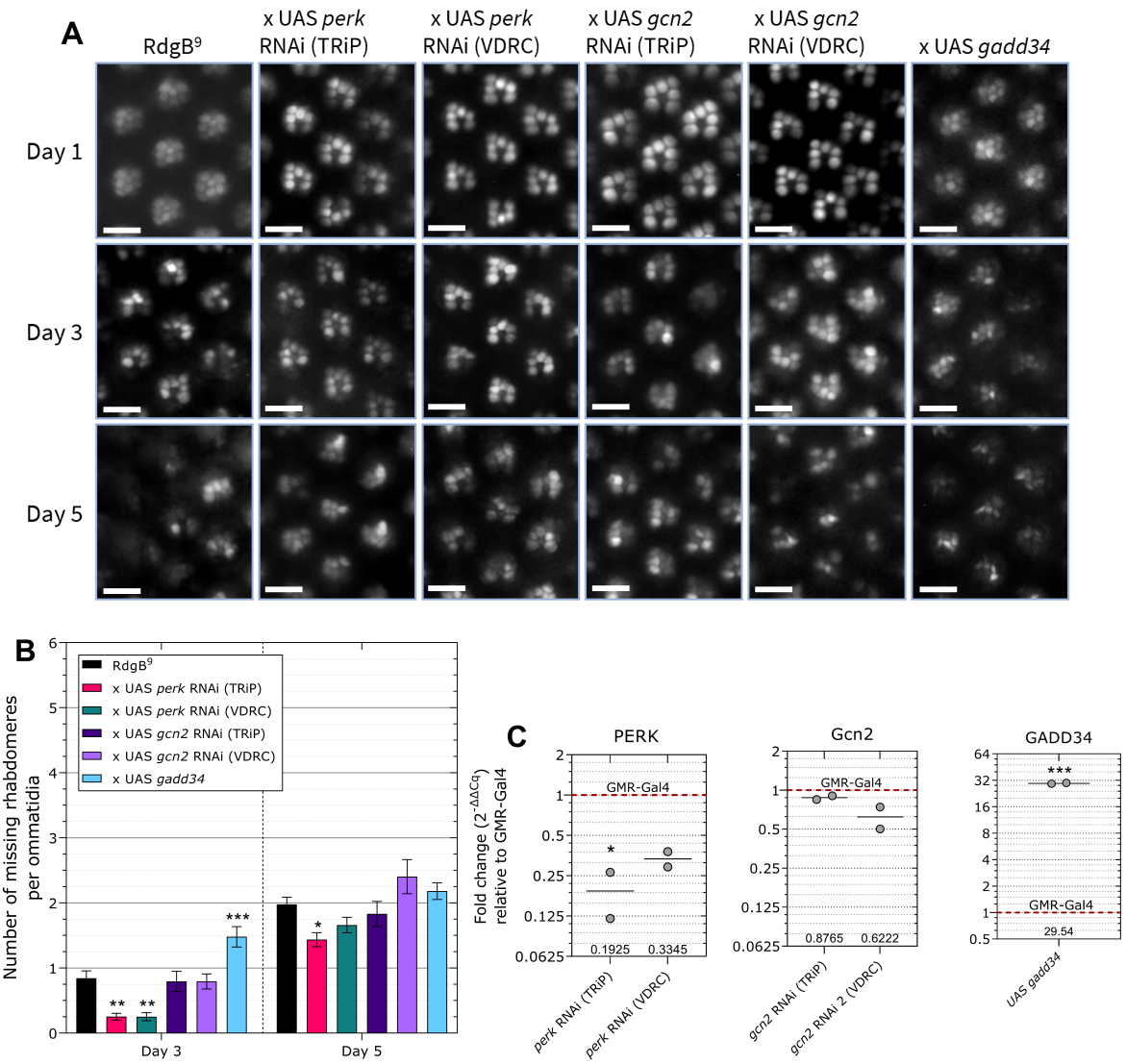

Figure 3-5 The ISR is involved in RdgB*^{9}*-related retinal degeneration through the kinase PERK.

(A) Representative images of ommatidia for each genotype and time point. The RdgB^{9} *line was crossed with various genetic constructs to modulate the expression levels of specific genes. White scale bar represents 10 µm. (B) Drosophila retinas were analysed for the number of missing rhabdomeres per ommatidia. Data from day 3 and day 5 are presented as bar graphs representing the mean ± SEM (n = 17 – 78), adjusted p-values: *p ≤ 0.05, **p ≤ 0.01, ***p ≤ 0.001 relative to RdgB*^{9} *(two-way ANOVA with Dunnett's post-hoc test). Day 1 data was omitted for clarity but included for statistical analysis. (C) Fold change in the expression of the genes perk, gcn2 and gadd34 after knockdown or overexpression in GMR-expressing cells compared to the GMR-Gal4 control tissue. Average of two biological replicates represented as a line and denoted above the x-axis. Adjusted p-values calculated from ΔCq values: *p = 0.0256, ***p < 0.001 relative to GMR-Gal4 (unpaired t-test). RdgB*^{9} *corresponds to rdgB*^{9}*,Rh1GFP/-;+/+;Rh1Gal4, UASDicer2. Full genotypes can be found in the results description.*

3.2.3.2. Requirement of novel RNA-binding proteins in the RdgB^{9} model of retinal degeneration

Having established a link between the ISR and *rdgB*^{9}-induced retinal degeneration, I attempted to identify other cellular elements that could play a role in this degenerative process. In a previous unpublished screen conducted by collaborators, novel RNA-binding proteins (RBP) have been identified as possible modulators of the RdgB^{9} phenotype. Based on other published screens conducted in neurodegenerative models, four of these proteins were selected to be more thoroughly tested in the RdgB^{9} degenerative model as they were identified as modifiers of neurodegenerative phenotypes: RPS27A, U2A, SF3B2, and CG42458 (Appocher et al., 2017; Chaplot et al., 2019; Lee et al., 2016). These four RBPs are poorly characterised, although, their sequences putatively suggest cellular roles. The extended gene sequences and protein alignments with the human orthologs of these four novel RBPs can be found in Appendix 3. RPS27A is a ribosomal protein that can bind to ubiquitin and is involved in protein degradation. U2A is involved in chromatin organisation. SF3B2 has a role in splicing, with the capacity to bind to the 12S RNA unit forming the key spliceosome component U2snRNP. Finally, CG42458 remains elusive, but is known to contain an RNA-binding sequence. Of these four, only SF3B2 and CG42458 were studied as the other RNAi lines did not produce enough progeny for setting up the required crosses. *rdgB*^{9}-induced retinal degeneration was assessed in flies of different ages expressing genetic constructs modulating the expression levels of *sf3b2* and *CG42458* genes. Two different RNAi constructs (TRiP/VDRC) for each target gene were combined with the RdgB^{9} line (*rdgB*^{9}*, Rh1GFP/-; +/+; Rh1Gal4, UAS Dicer 2*) leading to the following genotypes:

- *rdgB*^{9}*, Rh1GFP/-; +/+; Rh1Gal4, UAS Dicer 2/ UAS sf3b2 RNAi (TRiP)*
  (referred to as RdgB^{9} x *sf3b2* RNAi (TRiP));
- *rdgB*^{9}*, Rh1GFP/-; UAS sf3b2 RNAi (VDRC)/+; Rh1Gal4, UAS Dicer 2/+*
  (referred to as RdgB^{9} x *sf3b2* RNAi (VDRC));
- *rdgB*^{9}*, Rh1GFP/-; UAS CG42458 RNAi (TRiP)/+; Rh1Gal4, UAS Dicer 2/+*
  (referred to as RdgB^{9} x *CG42458* RNAi (TRiP));
- *rdgB*^{9}*, Rh1GFP/-; UAS CG42458 RNAi (VDRC)/+; Rh1Gal4, UAS Dicer 2/+*
  (referred to as RdgB^{9} x *CG42458* RNAi (VDRC)).

The effect of these genetic manipulations on retinal degeneration was investigated. The prediction was that if these RBPs play a role in the pathogenesis involved in *rdgB*^{9}-induced retinal degeneration, then modulating their genetic expression may affect the degenerative phenotype. As the role of RBPs in the development of degenerative diseases is still unclear, it is difficult to predict whether knocking-down the expression of these proteins will lead to a reduction or an increase in cellular toxicity caused by the *rdgB*^{9} mutation.

A two-way ANOVA was performed to analyse the effect of genotypes and the effect of aging on the number of missing rhabdomeres. This test revealed that there was a statistically significant effect from the genotypes ($F_{4, 439}$ = 16.900, p < 0.001), days ($F_{2,439}$ = 156.100, p < 0.001) and a significant interaction between the effects of genotypes and days ($F_{8, 439}$ = 4.374, p < 0.001). Specific comparisons were performed using Dunnett's *post-hoc* tests.

As expected, no difference was detected in 1-day-old flies between any of the groups as degeneration is not visible yet at this point. Day 1 data was excluded from Figure 3-6 for clarity. Knockdown of *CG42458* in RdgB^{9} flies had no significant impact on the degenerative phenotype, in both 3- and 5-day-old flies with either RNAi constructs. Interestingly, knockdown of *sf3b2* using the UAS *sf3b2* RNAi (TRiP) revealed a significant protective role with a 74% decrease in the number of missing rhabdomeres compared to RdgB^{9} (p = 0.001, Dunnett's *post-hoc* test). Conversely, knockdown of *sf3b2* using the UAS *sf3b2* RNAi (VDRC) line showed the opposite effect with a 56% increase in the number of missing rhabdomeres compared to RdgB^{9} (p = 0.0145, Dunnett's *post-hoc* test).

These effects were similarly observed on day 5. Knockdown of *CG42458* had no effect on the degenerative phenotype caused by the *rdgB*^{9} mutation. Knockdown of *sf3b2* still had contradictory effects between the two RNAi constructs. UAS *sf3b2* RNAi (TRiP) showed a significant 56% decrease in the number of missing rhabdomeres compared to the RdgB^{9} group (p < 0.001, Dunnett's *post-hoc* test), and UAS *sf3b2* RNAi (VDRC) again showed a significant increase of 37% in the number of missing rhabdomeres compared to RdgB^{9} (p = 0.0007, Dunnett's *post-hoc* test).

To validate these RNAi constructs, their efficiency was tested using the RT-qPCR method. For this purpose, GMR-Gal4 was used to drive these constructs in all retinal cells. Flies carrying only the GMR-Gal4 transgene were used as the control tissue in the subsequent fold change calculations. Figure 3-6 (C) shows that *CG42458* knockdown was much more efficient with the UAS *CG42458* RNAi (TRiP) construct than with the UAS *CG42458* RNAi (VDRC) construct, with a 73.89% and 24.07% downregulation compared with control, respectively. On the other hand, *sf3b2* knockdown was only moderately efficient, leading to a 30.08% and a 55.67% decrease in gene expression using UAS *sf3b2* RNAi (TRiP) and UAS *sf3b2* RNAi (VDRC), respectively. Nevertheless, these latter changes remained non-significant. The results of a Student's t-test conducted on ΔCq values for this experiment are reported in Table 3-2.

Gene of interest	*CG42458*				*sf3b2*			
GMR-Gal4	+	+	+	+	+	+	+	+
RNAi (TRiP/VDRC)	-	TRiP	-	VDRC	-	TRiP	-	VDRC
ΔCq values	7.168	7.622	7.098	9.123	5.278	5.820	6.067	7.266
df	2		2		2		2	
t-value	1.115		4.570		1.407		2.240	
p-value	0.3810		0.0447		0.2948		0.1544	
Fold change	0.7593		0.2611		0.6992		0.4433	

Table 3-2 qPCR results for CG42458 and sf3b2 expression modulation.

Statistical report for ΔCq means comparisons between control and experimental samples using a Student's t-test. df: degrees of freedom, t: t-statistic value, p: p-value. For all ΔCq values, two biological replicates were completed.

These results demonstrate that UAS *CG42458* RNAi (VDRC) is efficient at knocking-down *CG42458* transcripts. On the other hand, even though UAS *sf3b2* RNAi (VDRC) leads to a downregulation of more than 50%, neither UAS *sf3b2* RNAi (TRiP) or (VDRC) lead to a significant decrease in transcript levels of *sf3b2*.

Overall, the results in this section suggest a potential role for the RNA-binding and splicing protein SF3B2 in *rdgb*^{9}-induced retinal degeneration, but this needs to be confirmed with additional experiments in the future. The conflicting results between RNAi constructs targeting the same transcript raise questions regarding the efficiency of the RNAi constructs or possibly the involvement of the proteins. These possibilities will be further discussed in section (3.3.).

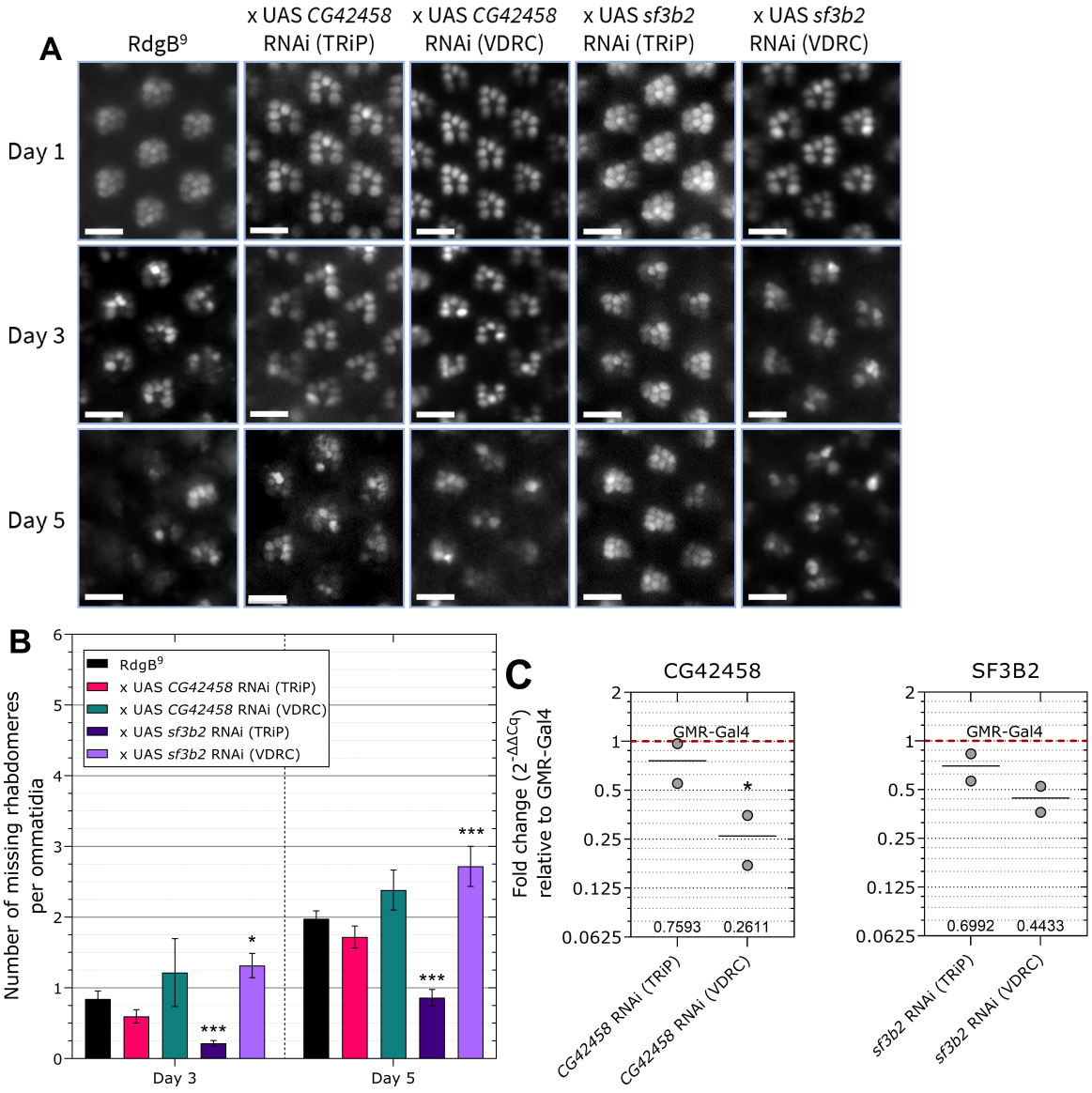

Figure 3-6 The involvement of novel RBPs in rdgB*^{9}*-induced retinal degeneration.

(A) Representative images of ommatidia for each genotype and time point. The RdgB^{9} *line was crossed with various genetic constructs to modulate the expression levels of specific genes. White scale bar represents 10 µm. (B) Drosophila retinas were analysed for the number of missing rhabdomeres per ommatidia. Data are presented as bar graphs representing the mean ± SEM (n = 10 – 78), *p ≤ 0.05, **p ≤ 0.01, ***p ≤ 0.001 relative to RdgB*^{9} *(two-way ANOVA with Dunnett's post-hoc test). Day 1 data was omitted for clarity but included for statistical analysis. (C) Fold change in the expression of the genes CG42458 and sf3b2 after knockdown in GMR-expressing cells compared to the GMR-Gal4 control. Average of two biological replicates represented as a line and denoted above the x-axis. Adjusted p-values calculated from ΔCq values: *p = 0.0447 relative to GMR-Gal4 (unpaired t-test). RdgB*^{9} *corresponds to rdgB*^{9}*, Rh1GFP/-; +/+; Rh1Gal4, UAS Dicer 2. Full genotypes can be found in the results description and in Chapter 2.*

3.2.3.3. Requirement of RNP granule assembly proteins in the RdgB^{9} model of retinal degeneration

Ribonucleoprotein (RNP) particles have been of high interest in recent literature for their role in the pathogenesis of several degenerative diseases such as amyotrophic lateral sclerosis (ALS) (Hart & Gitler, 2012; Li et al., 2013; Liu-Yesucevitz et al., 2014). RNP particles, or granules, are enriched in RNA molecules and regulatory proteins, such as RBPs, and play a key role in basic RNA metabolism (Banani et al., 2017). It has been established that mutations in multiple RNP particle components can lead to neurodegenerative diseases (Bakthavachalu et al., 2018; Gao et al., 2018; Shang & Huang, 2016), although the exact connection between the perturbation of RNP particles dynamics and pathogenesis is still unclear. Even less is known about their possible role in retinal degeneration (Dash et al., 2016; Lachke et al., 2011). Here, the hypothesis that the RBPs and RNP particle components Ataxin-2 (ATX2) and Rasputin (Rin) play a role in RdgB^{9} retinal degeneration was tested. These two RBPs have been shown to be important for the formation of RNP granules and are involved in the development of neurodegeneration, as discussed in section 1.3.2.3.

3.2.3.3.1. Knockdown of Ataxin-2 and Rin

In this section, RNAi constructs targeting the transcripts for the proteins Ataxin-2 and Rasputin (Rin) were used in the RdgB^{9} model of retinal degeneration. *rdgB*^{9}-induced retinal degeneration was assessed in flies of different ages expressing genetic constructs modulating the expression levels of *atx2* and *rin* genes. Two different RNAi constructs for *atx2* (TRiP/VDRC), and one RNAi construct for *rin* (VDRC) were combined with the RdgB^{9} line (*rdgB*^{9}*, Rh1GFP/-; +/+; Rh1Gal4, UAS Dicer 2*) leading to the following genotypes:

- *rdgB*^{9}*, Rh1GFP/-; +/+; Rh1Gal4, UAS Dicer 2/UAS atx2 RNAi (TRiP)*
  (referred to as RdgB^{9} x *atx2* RNAi (TRiP));
- *rdgB*^{9}*, Rh1GFP/-; UAS atx2 RNAi (VDRC)/+; Rh1Gal4,UAS Dicer 2/+*
  (referred to as RdgB^{9} x *atx2* RNAi (VDRC));
- *rdgB*^{9}*, Rh1GFP/-; UAS rin RNAi (VDRC)/+; Rh1Gal4, UAS Dicer 2/+*
  (referred to as RdgB^{9} x *rin* RNAi (VDRC)).

The effect of these genetic manipulations on retinal degeneration was investigated. The prediction was that if these RNP granule components play a role in the pathogenesis involved in *rdgB*^{9}-induced retinal degeneration, then modulating their genetic expression may affect the degenerative phenotype. As the role of RNPs in the context of retinal degeneration is still unknown, it is difficult to predict whether knocking-down the expression of these proteins will lead to a reduction or an increase in cellular toxicity caused by the *rdgB*^{9} mutation. Although, in a preliminary result from our collaborators in the Prof. Padinjat laboratory (NCBS, India), knockdown of *atx2* led to a rescue of the degenerative phenotype caused by the *rdgB*^{9} phenotype.

A two-way ANOVA was performed to analyse the effect of genotypes and the effect of aging on the number of missing rhabdomeres. This test revealed that there was a statistically significant effect from the genotypes ($F_{3, 380}$ = 5.385, p = 0.0012), days ($F_{2,380}$ = 105.2, $p < 0.001$) and a significant interaction between the effects of genotypes and days ($F_{6, 380}$ = 2.713, p = 0.0136). Specific comparisons were performed using Dunnett's *post-hoc* tests.

As expected, the retinal analysis revealed no difference in 1-day-old flies between any of the groups as degeneration is not yet visible at this point. Day 1 data was excluded from Figure 3-7 (B) for clarity. A significant reduction in degeneration was detected using UAS *atx2* RNAi (TRiP) but not UAS *atx2* RNAi (VDRC) with a 61% and a 12% decrease respectively in the number of missing rhabdomeres compared to the RdgB^{9} group in 3-day-old flies (UAS *atx2* RNAi (TRiP): p = 0.0145; UAS *atx2* RNAi (VDRC): p = 0.8943; Dunnett's *post-hoc* test). This protective effect from UAS *atx2* RNAi (TRiP) remained in 5-day-old flies, with a significant decrease (35%) in the number of missing rhabdomeres compared to RdgB^{9} (p = 0.0004, Dunnett's *post-hoc* test). Knockdown of *rin* on the other hand was only protective in 5-day-old flies, with a significant decrease (36%) in the number of missing rhabdomeres compared to RdgB^{9} (p = 0.0010, Dunnett's *post-hoc* test).

The efficiency of these constructs was tested using the RT-qPCR method, using GMR-Gal4 to drive each construct, similarly to previous experiments. Figure 3-7 (C) shows *atx2* knockdown had an efficiency of approximately 60%, with UAS *atx2* RNAi (TRiP) leading to a 59.63% downregulation and UAS *atx2* RNAi (VDRC) leading to a 63.89% downregulation. In addition, UAS *rin* RNAi (VDRC) led to a 55.42% decrease in the

expression of *rin*. The results of a Student's *t*-test conducted on ΔCq values for this experiment are reported in Table 3-3.

Gene of interest	*atx2*				*rin*	
GMR-Gal4	+	+	+	+	+	+
RNAi (TRiP/VDRC)	-	TRiP	-	VDRC	-	VDRC
ΔCq values	1.444	2.804	1.798	3.300	0.6610	1.887
df	2		2		2	
t-value	0.6927		5.689		2.921	
p-value	0.5601		0.0295		0.0999	
Fold change	0.4037		0.3611		0.4458	

Table 3-3 qPCR results for atx2 and rin expression modulation.

Statistical report for ΔCq means comparisons between control and experimental samples using a Student's t-test. df: degrees of freedom. For all ΔCq values, two biological replicates were completed.

These results demonstrate that UAS *atx2* RNAi (VDRC) leads to a stronger and significant decrease in the expression of *atx2* compared to UAS *atx2* RNAi (TRiP). On the other hand, *rin* RNAi leads to a decrease in transcripts levels of *rin*, but these changes remain non-significant.

Overall, these results support the idea that these RNP granule components may be involved in the molecular mechanism underlying the RdgB^{9} model of retinal degeneration.

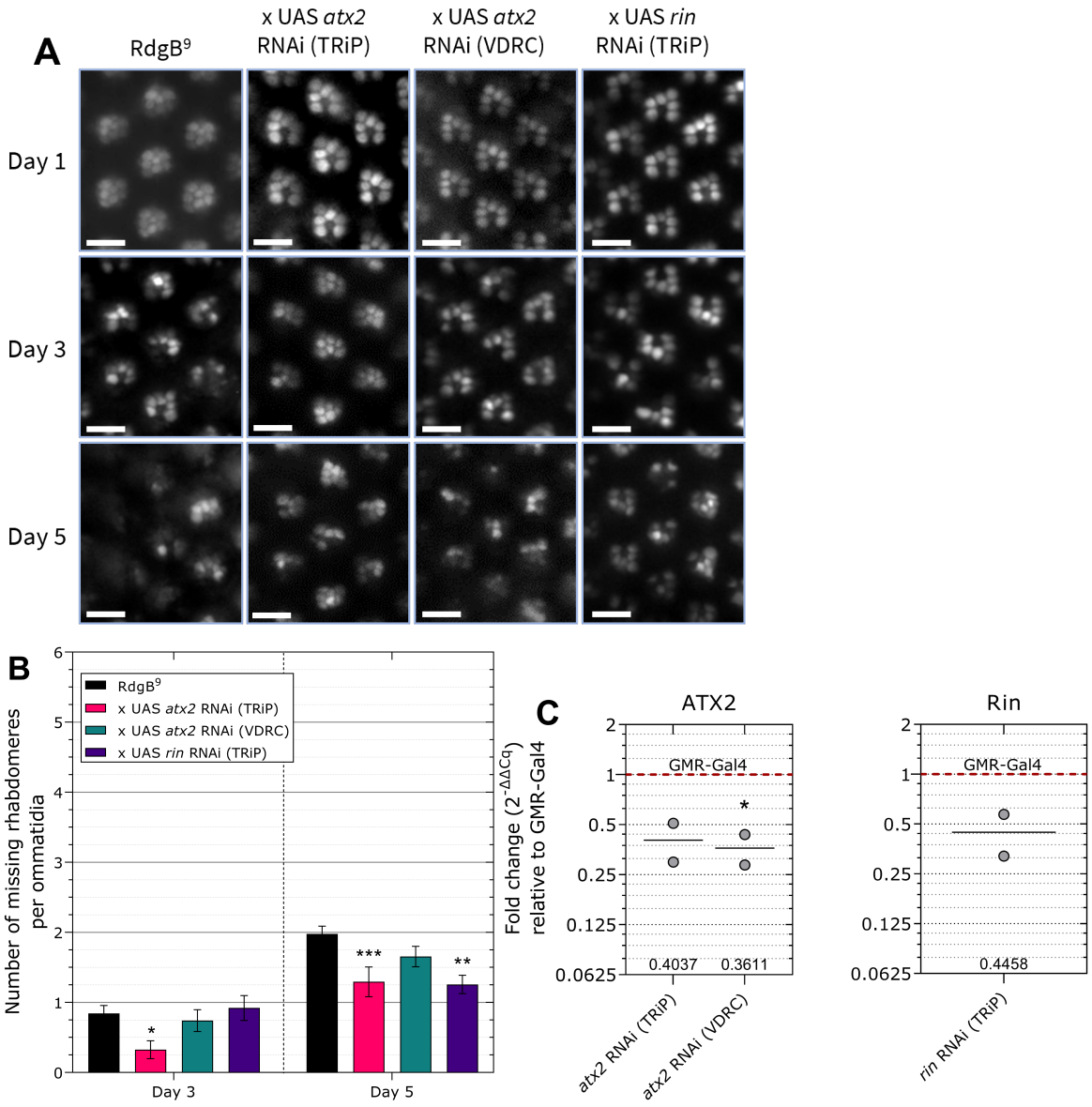

Figure 3-7 The RNP granule formation pathway may be involved in rdgB*^{9}*-induced retinal degeneration.

(A) Representative images of ommatidia for each genotype and time point. The RdgB^{9} *line was crossed with various genetic constructs to modulate the expression levels of specific genes. White scale bar represents 10 µm. (B) Drosophila retinas were analysed for the number of missing rhabdomeres per ommatidia. Data are presented as bar graphs representing the mean ± SEM (n = 10 – 78), *p ≤ 0.05, **p ≤ 0.01, ***p ≤ 0.001 relative to RdgB*^{9} *(two-way ANOVA with Dunnett's post-hoc test). Day 1 data was omitted for clarity but included for statistical analysis. (C) Fold change in the expression of the genes atx2 and rin after knockdown compared to GMR-Gal4. Average of two biological replicates represented as a line and denoted above the x-axis. Adjusted p-values calculated from ΔCq values: *p = 0.0295 relative to GMR-Gal4 (unpaired t-test). RdgB*^{9} *corresponds to rdgB*^{9}*, Rh1GFP/-; +/+; Rh1Gal4, UAS Dicer 2. Full genotypes can be found in the results description.*

3.2.3.3.2. Requirement of the intrinsically disordered region of Ataxin-2 in the RdgB^{9} *model of retinal degeneration*

The observation that *atx2* knockdown had a protective role in degeneration led me to further dissect the involvement of this protein and its function in the RdgB^{9} model for retinal degeneration. In previous work from our laboratory, the intrinsically disordered region located at the C-terminus (cIDR) of the ATX2 protein has been shown to be important for the formation of RNP granules, both *in vitro* and *in vivo* (Bakthavachalu et al., 2018). As such, I investigated whether removal of the cIDR domain of ATX2, thereby impeding the formation of RNP granules, could alleviate *rdgB*^{9}-induced retinal degeneration. For this purpose, using CRISPR/Cas9, a mutant *Drosophila* line was previously developed in our laboratory to replace the wild-type form of *atx2* with an allele of *atx2* lacking the cIDR. This engineered line was then crossed to the RdgB^{9} line (*rdgB*^{9}*, Rh1GFP/-; +/+; Rh1Gal4, UAS Dicer 2*) for this project, leading to the following genotype:

rdgB^{9}*,Rh1GFP/-; +/+; atx2*Δ*cIDR/atx2*Δ*cIDR* (referred to as RdgB^{9} x Atx2ΔcIDR).

The effect of this mutant form of *atx2* on retinal degeneration was investigated. The prediction was that if RNP granule formation plays a role in the pathogenesis involved in *rdgB*^{9}-induced retinal degeneration, then expressing this mutant form of *atx2*, which lacks the key domain for RNP granule formation, may affect the degenerative phenotype. This mutant had a protective effect in neurodegenerative models for amyotrophic lateral sclerosis and Huntington's disease in *Drosophila* (Bakthavachalu et al., 2018; Huelsmeier et al., 2021). Although the role of RNP granule formation in the development of retinal degeneration is still unclear, it was predicted that this mutant may have a protective effect against the cellular toxicity caused by the *rdgB*^{9} mutation.

A two-way ANOVA was performed to analyse the effect of genotypes and the effect of aging on the number of missing rhabdomeres. This test revealed that there was a significant effect from the genotypes ($F_{1, 231}$ = 17.89, p < 0.001), days ($F_{2, 231}$ = 97.62, p < 0.001) and an interaction effect between genotypes and days ($F_{2, 231}$ = 4.826, p = 0.0088). Specific comparisons were performed using Bonferroni's *post-hoc* tests.

As expected, the retinal analysis revealed no difference in 1-day-old flies between any of the groups as degeneration is not yet visible at this point. Day 1 data was excluded

from Figure 3-8 (B) for clarity. However, a trend towards increased degeneration was observed in 3-day-old RdgB^{9} mutant flies that also lacked the cIDR domain. This effect became significant in 5-day-old RdgB^{9} x Atx2ΔcIDR mutant flies with a 63% increase in the number of missing rhabdomeres compared to the RdgB^{9} control (p < 0.001, Bonferroni's *post-hoc* test).

These results suggest that, contrary to what was expected, removing the cIDR from *atx2* may facilitate retinal degeneration in this model, which indicates a possible role for *atx2* to suppress cellular degeneration caused by the *rdgB*^{9} mutation. These results, and their contradiction with results from the knockdown of *atx2* will be further discussed (3.3.3.1.3).

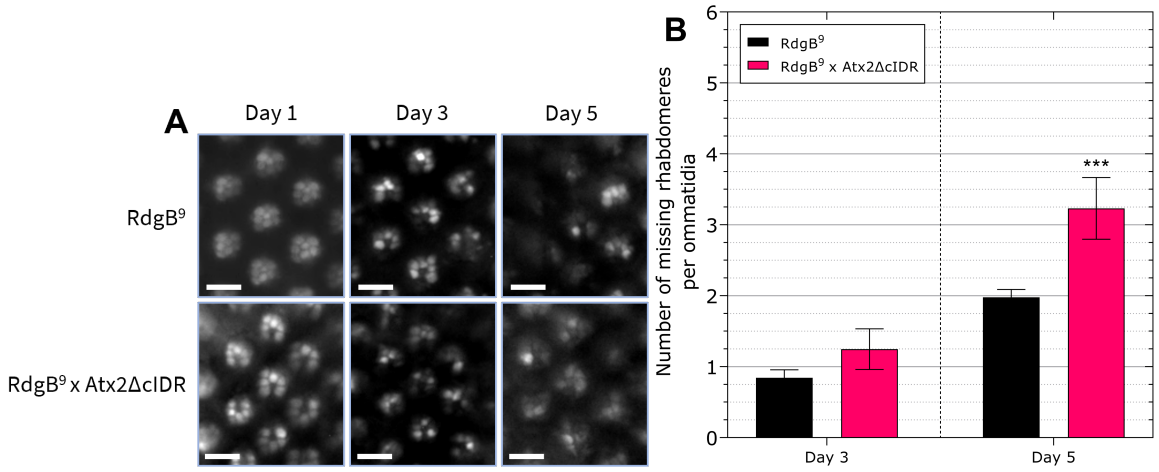

Figure 3-8 The intrinsically disordered region f ATX2 suppresses rdgB^{9}-induced retinal degeneration.

*(A) Representative images of ommatidia for each genotype and time point. The RdgB^{9} line was crossed with a mutant lacking the cIDR domain of ATX2. White scale bar represents 10 µm. (B) Drosophila retinas were analysed for the number of missing rhabdomeres per ommatidia. Data are presented as bar graphs representing the mean ± SEM (n = 12 – 78). ***p ≤ 0.001 relative to RdgB^{9} (two-way ANOVA with a post-hoc Bonferroni's multiple comparisons test). Day 1 data was omitted for clarity but included for statistical analysis. RdgB^{9} corresponds to rdgB^{9},Rh1GFP/-;+/+; Rh1Gal4,UAS Dicer 2. Full genotypes can be found in the results description.*

3.3. Discussion

The experiments in this chapter were designed to test whether specific pathways are involved in photoreceptor cell degeneration. The results portray ER stress as being a key event in the pathogenesis underlying *rdgB*^{9}-induced retinal degeneration. Although no conclusive observations could be drawn from assessing the activation of the ISR in *rdgB* mutants, it was observed here that the ER stress kinase PERK, a key component of the ISR, is required for *rdgB*^{9}-induced retinal degeneration. A possible explanation would be that the phosphatidylinositol cycle is dysfunctional because of the *rdgB* mutant allele (Cockcroft et al., 2016) leading to ER stress, activating PERK, phosphorylating eIF2α, and initiating the usual downstream events: general translational arrest (Wek, 2018), expression of specific stress response genes (Feder & Hofmann, 1999; Skopkova et al., 2017; Young-Baird et al., 2020), and induction of RNP granules (Kedersha et al., 2000; Namkoong et al., 2018). Usually, these cellular responses could be enough to handle an acute stress trigger (such as hypoxia, or calcium depletion) (Rutkowski & Kaufman, 2007). In the context of *rdgB* mutant alleles, and other genetic mutations causing ER stress, this becomes a prolonged activation of PERK. This could explain the short time-frame to effectively rescue the degenerative phenotype after knocking-down *perk* seen in this work (Figure 3-5, B). The consequences of prolonged PERK activation leads to pro-apoptotic signals through the activation of the CHOP pathway (Bevilacqua et al., 2010), which leads to retinal degeneration. This model will be further explored in 3.3.4.

In this section, I will first be discussing and interpreting the results and limitations from the stress pathway activation assessment (3.3.1.), then the genetic manipulations and their efficiency will be discussed (3.3.2.), and finally the results from modulating the RdgB^{9} phenotype will be discussed (3.3.3.).

3.3.1. Stress pathway activation in *rdgB* mutants

3.3.1.1. Main findings and limitations

The exact pathway underlying retinal degeneration in RdgB^{9} mutant *Drosophila* flies remains unknown. In an attempt to shine a light on the molecular mechanism underlying this form of retinal degeneration, I attempted to determine whether the ISR was activated in response to a mutated form of *rdgB*. A downstream consequence of ISR activation is the increased translation of the ATF4 protein which leads to transcriptional upregulation of various genes required for cellular response to stressful conditions. Although its multiple downstream effects have led to conflicting opinions on the therapeutic application of downregulating ATF4, it has been a focal point for therapeutic strategies. Indeed, it is often found upregulated in patients suffering from neurodegenerative diseases as well as forms of cancer (Pitale et al., 2017; Singleton & Harris, 2012; Wei et al., 2015).

Kang et al. (2015) designed a genetic reporter using the ATF4 open reading frame (ORF) to show ISR upregulation in various conditions of stress. They demonstrated ISR activation in response to protein misfolding in eye discs expressing mutant forms of *Rh1*, as well as in different tissues of *Drosophila* after larval starvation and nutritional deprivation. Using this ATF4 reporter to visually assess the stress response in *rdgB*^{2} mutant flies proved to be problematic. The dissection and the imaging process was difficult to complete in a consistent and repeatable fashion without tissue damage (Figure 3-3). Nevertheless, an interesting observation that can be made is that *rdgB*^{2} mutants (both normal and no light exposure) had an increased dsRed signal in the form of granules compared to the control group. This could suggest that this mutant is leading to increased ATF4 translation, and therefore ISR activation, but would require further experiments to validate this hypothesis.

Due to time constraints, the RT-qPCR technique was used as an alternative method to the ATF4 reporter to assess the activation of the ISR in *rdgB* mutants. This experiment tested the hypothesis that there is an increased transcription of stress-related genes with the expression of the *rdgB*^{9} allele. RNA was extracted from a negative control Canton S. group (CS), a positive control of CS flies that were heat-shocked for one hour, and the experimental RdgB^{9} group (*rdgB*^{9}*, Rh1GFP/-; +/+; Rh1Gal4, UAS Dicer 2)*. The tested genes were *perk*, *atf4*, *cdk5*, *ire1*, and *sod1*. The RNA samples taken from the

heat-shocked CS flies had a small amount of error and showed an upregulation of *perk* transcripts. Whereas the results from the RdgB^{9} group had a large amount of noise in the three replicates. This suggests that the sample acquisition, and not the RT-qPCR technique itself, is unsuited to answer the original hypothesis. By dissecting and using the entire retina, the RNA molecules originating from the degenerating photoreceptor cells could be diluted with RNA molecules coming from various secondary support cells, as well as other contaminating tissues. In which case, if there is any variation in the expression of the stress proteins studied in the photoreceptor cells, this would be overshadowed by mostly unaffected neighbouring tissue. Two additional limitations complicate the results from this experiment. First, the RT-qPCR method is dependent on consistent levels in the expression of reference genes. The variability in GAPDH expression in response to ISR activation was not tested in these experiments. However, past literature has found that GAPDH RNA levels remained stable in response to various forms of stress, including mild heat shock (Atwan, 2020). Second, the amplification efficiency is dependent on primer optimisation for each amplicon, with primer pairs not being equally efficient when using SyGreen. As this was not performed, it can not be determined whether the variation in fold change results from primer efficiency.

Overall, the increased transcription of *perk* in heat-shocked flies is an interesting finding in itself, and in agreement with previous literature showing upregulation of stress-related genes *in vivo* with *Drosophila*, and *in vitro* after West-Nile virus infection of neurons (Sørensen et al., 2005; van Marle et al., 2007), however, these results could not be used to conclude with any certainty that the ISR is activated in *rdgB* mutant *Drosophila* flies.

3.3.1.2. Further studies

The visual assessment of the ATF4 reporter requires more time and practice for the dissection and for protocol optimisation. The study design could also be elaborated to test how light exposure leads to retinal degeneration by subjecting different groups to different light conditions. This could clarify the time course of gene induction, and the consequences of different light conditions in ATF4 upregulation. Testing the possibility that the stress response is proportional to light strength could be possible by using a more detailed lighting system. This could be done with the recently described

Drosophila Interactive System for Controlled Optical (DISCO) allowing for precise light manipulation and behavioural output (Moulin et al., 2022). Kang et al. (2015) originally described this reporter *Drosophila*'s mutant larval eye discs. This is a different approach with a possibly simpler dissection that could be attempted in *rdgB* mutants. Although, cellular toxicity caused by *rdgB* mutants in larval eye imaginal discs may not be as obvious as it would be in adult retinas.

The single-cell RNA (scRNA) sequencing technique could be used instead of the RT-qPCR method. Use of scRNA sequencing has increased in research as it allows to sequence RNA molecules for every cell individually. This would allow us to specifically look at photoreceptor cells and whether there is an increased expression of the stress-related proteins. This technique was considered during this project, but due to time constraints it was deemed unfeasible as the protocol would have to first be optimised. In addition, the bioinformatic analysis would require a considerable amount of time and skill. The data obtained from this kind of experiment would be highly valuable to the understanding of the *rdgB*^{9}-induced retinal degeneration. In addition, instead of using CS flies as the reference sample, such as in the RT-qPCR conducted in this project, a light-deprived RdgB^{9} group would be a better control as it would have the same genetic background.

3.3.2. Efficiency of knockdown and overexpression

3.3.2.1. Main findings

RNA interference is a wide-spread technology used in *Drosophila* publications, and has become an essential genetic tool. As of 2021, the Transgenic RNAi Project (TRiP) had generated over 12,000 TRiP lines (Hu et al., 2021). Nearly half of the RNAi constructs used in this current work originated from this collection. The other RNAi constructs originated from the Vienna *Drosophila* Resource Center (VDRC) collection, which has over 12,000 RNAi lines. This latter RNAi collection includes three libraries that vary based on the insertion site of the RNAi construct: the GD, KK and shRNA collections.

The aim of this experiment was to validate the RNAi lines used in this project. GMR-Gal4 was used for this purpose to have a more widespread expression of the construct. Indeed, the RNAi constructs were expressed in a small subset of cells with Rh1Gal4 found in the RdgB^{9} line, as well as with PDFGal4 in the following chapter. The Glass

Multiple Receptor (GMR) sequence is an engineered transcription regulatory region that is expressed in the developing eye, although it has been shown to also be expressed in the developing wings, brain and other tissues (Li et al., 2012). The difference in Gal4 constructs used leads to various implications in interpreting the results as well as limitations that will be further discussed.

In this validation experiment, most RNAi constructs led to a decreased expression of their target RNA. Not all of these RNAi constructs led to a significant decrease according to individual Student's *t*-tests. Significance was reached with UAS *perk* RNAi (TRiP), UAS *CG42458* RNAi (VDRC), and UAS *atx2* RNAi (VDRC), with a 80.75%, 73.89%, and 63.89% mean decrease, respectively. Although they did not reach significance, four RNAi constructs did lead to a notably strong decreased expression of their target: UAS *perk* RNAi (VDRC), UAS *atx2* RNAi (TRiP), UAS *sf3b2* RNAi (VDRC) and UAS *rin* RNAi (VDRC) at a 66.55%, 59.63%, 55.67%, and 55.42% mean reduction, respectively. Overall, these results are not surprising as RNAi-mediated gene knockdown is never 100% efficient, with a considerable amount of variation from one line to another. This does however suggest that results from experiments involving these RNAi constructs have to be weighed with their knockdown levels.

In the context of the ISR, to modulate the core regulator eIF2α there are two viable options: (1) knocking-down the primary kinases (PERK and GCN2) that will phosphorylate eIF2α, or (2) overexpress the phosphatase *gadd34*. Both of these options will lead to a decrease in the phosphorylation of eIF2α, and consequentially a decrease in the downstream effect of the ISR. For this purpose, this work also attempted to overexpress *gadd34* by expressing this gene with an upstream UAS. This led to an increased expression of nearly 3000% with the GMR-Gal4 driver.

3.3.2.2. Limitations

Although RNAi technology is widely used in the *Drosophila* field of research, it comes with various limitations that can be controlled for.

First, some RNAi lines can lead to false-negative results simply due to inactive RNAi constructs, which is estimated to include between 15 and 40% of all RNAi lines (Heigwer et al., 2018). By checking the efficiency of these constructs we are confirming their activity or inactivity, thereby reducing the likelihood of a false-negative to arise.

Second, false-positive results can arise from off-target effects. These occur when the siRNA molecules target additional mRNAs, leading to unintended effects. Off-target effects have been shown to be a significant source of error in *Drosophila* RNAi screens (Kulkarni et al., 2006; Ma et al., 2006; Seinen et al., 2011). This was avoided by using two non-overlapping RNAi constructs targeting the same gene of interest. It is unlikely that these two RNAi constructs would have identical off-targets, meaning that any resulting phenotype that is shared between them is most likely related to reduced expression of the gene of interest (Heigwer et al., 2018). More importantly, the insertion sites that were used to create these RNAi libraries have been shown to have an impact on the RNAi validity. Indeed, approximately 25% of the VDRC KK RNAi lines have been shown to cause false-positive enhancement of a growth-regulatory pathway, depending on their insertion site, leading to organ malformations (Vissers et al., 2016). Three of the eleven RNAi constructs used in this work were from KK library, but these were in the correct insertion site, 30B3, therefore should not lead to any unexpected phenotype. Furthermore, according to the online tool UP-TORR designed by the Drosophila RNAi Screening Centre to analyse RNAi constructs, no off-target genes were predicted from the RNAi lines used in this work (Hu et al., 2013).

Third, the efficiency of these constructs was tested using a different Gal4 construct than in the next sets of experiments. Therefore, they may have a different knockdown or overexpression level when used in conjunction with Rh1Gal4 or PDFGal4. This is a limitation in most studies that include an RNAi validation experiment. Knockdown validation is usually done by immunostaining imaginal discs with antibodies targeting these proteins after expressing the constructs using a different Gal4 such as PtcGal4. Considering that some proteins studied in this thesis are uncharacterised, specific antibodies do not exist yet. Western- and northern-blots would not be effective for this tissue-specific RNAi knockdown for this particular case (Mainland et al., 2017). As suggested in the previous section, a scRNA-seq method could be used for this purpose as well, allowing to confirm knockdown levels specifically in photoreceptor cells or a subset of neurons.

Fourth, a limitation to consider in relation to the RT-qPCR method is the design of primer pair sets. Past literature has shown that primer design and RNA isolation method can influence detection of gene knockdown (Mainland et al., 2017). In this

work, the primer pairs were designed according to their recommendation of amplifying a region 5' of the RNAi cut site. However, the primer pair designs could be affecting the perceived efficiency of the knockdown by binding to cleaved mRNA fragments. This could result in an overestimation of the amount of functional mRNA. Once again, the scRNA sequencing method could be a solution to overcome this limitation as it bypasses the requirement for specific gene primer pairs.

Finally, in comparison to the retinal analysis experiment, this RNAi validation experiment did not include a UAS Dicer 2. The overexpression of Dicer 2, an enzyme that facilitates the activation of the RNA-induced silencing complex (RISC), means that the RNAi construct is more efficient (Tijsterman & Plasterk, 2004). This construct was included in the RdgB^{9} strain (*rdgB*^{9}*, Rh1GFP/-; +/+; Rh1Gal4, UAS Dicer 2*), meaning that the efficiency of these RNAi constructs is likely to be improved in the retinal analysis experiment.

3.3.3. Pathways involved in *rdgB*^{9}-induced retinal degeneration

3.3.3.1. Main findings

The main objective of this chapter was to dissect the molecular pathways involved in retinal degeneration in *rdgB* mutants. For this reason, genes from the ISR and genes coding for RNA binding proteins, some of which are known RNP granule markers, were knocked down using RNAi constructs, or overexpressed using UAS constructs. The efficiency of these genetic constructs was tested and addressed in the previous section.

3.3.3.1.1. Integrated stress response/unfolded protein response

Of particular interest in the ISR is the stress kinase PERK, also part of the unfolded protein response. PERK and its functions have been well characterised from past literature. In humans and other mammals PERK has been shown to activate after the ER chaperone BiP binds to misfolded proteins, thereby dissociating itself from PERK and other sensors. This dissociation between BiP and PERK leads to the dimerisation and phosphorylation of PERK, which will phosphorylate eIF2α and lead to general inhibition of protein translation and the activation of ATF4. Modulating PERK and its function is a therapeutic avenue that is currently being investigated for the treatment of various neurodegenerative diseases (Bugallo et al., 2020; Rabouw et al., 2019). More information about this cascade can be found in Chapter 1 (1.4).

The results here show that the ISR plays a role in *rdgB*^{9}-induced retinal degeneration specifically through PERK activation. Indeed, the two independent *perk* RNAi constructs led to a strong rescue of the RdgB^{9} phenotype on day 3. These two constructs also led to a strong knockdown effect assessed with RT-qPCR, suggesting that the observed phenotype is linked to the knockdown. On the other hand, the two *Gcn2* RNAi constructs did not rescue the degenerative phenotype. This latter result could be explained by the poor knockdown efficiency (*Gcn2* RNAi 1: 12.35%, *Gcn2* RNAi 2: 37.78%), but it may be that the protein GCN2 is not required for this form of degeneration. Finally, overexpressing the phosphatase *gadd34* led to a significant aggravation of the phenotype with an increase in the number of missing rhabdomeres (Figure 3-5).

Overall, these results demonstrate a significant role for the stress kinase PERK in this form of retinal degeneration, which may be in agreement with known functions of the ER, and ER stress specifically. Indeed, as shown in Yadav et al. (2018), wild-type RDGB localises with the ER bound protein VAP, which plays a key role in inhibiting the ER-associated degradation pathway (ERAD). Mutant forms of RDGB have been shown to mislocalise, which may lead to a higher availability of VAP causing a stronger inhibition of the ERAD pathway. This in turn could cause an increase in misfolded proteins in the cell, which is known to lead to ER stress and activate the UPR through PERK (McLaughlin et al., 2022). Manipulating upstream sensors such as the ER chaperone Hsc3, the *Drosophila* homolog to BiP, may be an interesting avenue to further dissect this pathway (Hyung & Steller, 2007). Alternatively, a mutant form of RDGB can compromise the phosphatidylinositol cycle (Cockcroft et al., 2016), which may indirectly cause ER stress considering that this cycle, and the ratio between PIP_3 and PIP_2, has regulatory roles in many other cellular functions, such as ion channels, pumps and lipid metabolism (Balla et al., 2009; Hamid et al., 2020).

In addition, Sahly et al. (1992) showed that retinal degeneration induced by the *rdgB*^{9} allele can be inhibited by applying calcium channel blockers. They suggested that these channels are critically affected in this form of retinal degeneration, leading to Ca^{2+} spikes before any morphological signs of degeneration. As toxic intracellular calcium is a common mechanism of cell death, and considering the role of the ER in regulating

intracellular calcium concentrations (Burdakov et al., 2005), the ER may be activating stress pathways due to a dysfunctional regulation of intracellular calcium.

If knocking-down *perk*, which is known to phosphorylate eIF2α, leads to an observed phenotypic difference, a similar result was expected when overexpressing *gadd34*, which is known to dephosphorylate eIF2α and restore protein translation. Surprisingly, this was not the case, with an overexpression of *gadd34* leading to a significant increase in degenerating rhabdomeres. This effect could be explained by two possible hypotheses: (1) the overexpression is too strong, causing eIF2α to never be activated which may lead to cellular toxicity; (2) the protein product GADD34 may be required for other pathways and the overexpression of it is causing dysregulation in these as well. In previous studies, knockdown of *gadd34* enhanced TDP-43 toxicity in *Drosophila* models of ALS (Kim et al., 2014), suggesting that modulating the expression of this gene can be an option for modulating eIF2α phosphorylation. More studies are required to understand the role of the protein GADD34 in this form of retinal degeneration.

3.3.3.1.2. Novel RNA-binding proteins

This work attempted to repeat and confirm results from a preliminary RNAi screen conducted by the Padinjat laboratory (NCBS, India) that found a wide selection of RNA-binding proteins to (RBPs) be modulating retinal degeneration. In this project, focus was given on two particular RBPs: CG42458 and SF3B2.

In the case of CG42458, a poorly characterised RBP, neither RNAi construct led to a significant difference in the retinal analysis. Only the UAS *CG42458* RNAi (VDRC) led to a significant knockdown, whereas the UAS *CG42458* RNAi (VDRC) only decreased the expression by about 25%. Overall, these are inconclusive results as the lack of difference for the first RNAi could be a result of poor knockdown efficiency, though they suggest that CG42458 is not required for retinal degeneration in this model.

Based on human studies, SF3B2 is a splicing factor when it binds to SF3BA and the 12S RNA unit to form the U2snRNP, a key component for the spliceosome and linked to the development of craniofacial microsomia (Timberlake et al., 2021). Interestingly, mislocalisation of spliceosome components has been shown to happen during neurodegeneration. A recent study found SF3B2 to be a genetic modifier of VAP(P58S)

aggregation *in vitro*, a commonly used model to study neurodegeneration (Chaplot et al., 2019). Interestingly, both RNAi constructs used here had a significant, but contradictory, effect on day 3 and day 5. The UAS *sf3b2* RNAi (TRiP) construct led to a significant rescue of the degenerative phenotype, whereas the UAS *sf3b2* RNAi (VDRC) enhanced the degenerative phenotype. Neither construct had a significant reduction in the expression of *sf3b2*, although the UAS *sf3b2* RNAi (VDRC) had a noteworthy decrease of 55.67%. The result for the TRiP construct suggests a possible off-target effect leading to the rescue of the degenerative phenotype. Whereas the result from the second RNAi could suggest that this splicing protein is required to alleviate retinal degeneration. Although, as neither of these RNAi constructs led to a significant knockdown, these are inconclusive results and require further work to establish whether or not these proteins are involved in *rdgB*^{9}-induced retinal degeneration.

Overall, these results suggest that CG42458 is not required in the pathway leading to *rdgB*^{9}-induced retinal degeneration. Interestingly, SF3B2, and therefore the spliceosome, may have a key role in the toxicity induced by this mutant allele.

3.3.3.1.3. RNP granule components

RNP granule components, such as Ataxin-2 (ATX2), are of particular interest due to their established involvement in the pathogenesis of neurodegenerative diseases (Alami et al., 2014; Bakthavachalu et al., 2018; Huelsmeier et al., 2021; Liu-Yesucevitz et al., 2014; Sanchez et al., 2021; Tourrière et al., 2003; Vance et al., 2009). Indeed, cellular stress can trigger the formation of RNP granules, such as stress-granules, which contain stalled mRNA molecules, RBPs and other translation factors. These granules seem to confer a protective effect to acute stress, although the mechanism behind this is poorly understood (Wolozin, 2012). Among the proteins that were identified in the RNAi screen conducted in the Prof. Padinjat laboratory, the RNA-binding and RNP granule protein Ataxin-2 was found to modulate retinal degeneration caused by the *rdgB*^{9} mutation. Therefore, I attempted to repeat this finding and test the idea that proteins involved in RNP granule formation are required in the *rdgB*^{9} model of retinal degeneration. For this purpose, RNAi constructs targeting *atx2* and a second RNP granule component *Rasputin* (*rin*), were used in conjunction with the *rdgB*^{9} mutation.

From the two RNAi constructs against *atx2*, only the UAS *atx2* RNAi (TRiP) construct led to a significant reduction in retinal degeneration. Surprisingly, only the UAS *atx2* RNAi (VDRC) construct against *atx2* led to a significant (64%) decrease in its expression, although the TRiP RNAi construct led to a notable knockdown of more than 50%. Unfortunately, only a single RNAi line is currently available that has previously been shown to affect *rin* expression. Consequently, any possible off-target effects from the RNAi construct cannot be excluded. Knockdown of *rin* led to a significant decrease in the measured degeneration on day 5. This construct led to a noteworthy but non-significant knockdown of nearly 60%. Considering the importance of this RBP in the formation of stress granules and mRNA stabilisation (Laver et al., 2020; Tourrière et al., 2003), and its involvement in neurodegeneration (Sanchez et al., 2021; S. Zhang et al., 2010) these novel results suggest that RNP granule formation, and specifically stress-granule formation, may be involved in *rdgB*^{9}-induced retinal degeneration, with more work required to show this conclusively.

To further test the hypothesis that RNP granule formation is required for *rdgB*^{9}-induced retinal degeneration, a mutant allele of *atx2* was homozygously introduced in flies with the *rdgB*^{9} background (*rdgB*^{9}*,Rh1GFP/-;+/+;atx2*Δ*cIDR)*. Indeed, this mutant form of *atx2* was generated in our laboratory, and lacks the cIDR domain which is required for efficient RNP granule formation and for pathogenesis in neurodegenerative models in *Drosophila* (Bakthavachalu et al., 2018). This led to unexpected results as the homozygous expression of *Atx2*Δ*cIDR* significantly increased the amount of degenerated rhabdomeres on day 5. These results are in contradiction with the previously presented results after knocking-down *atx2* and *rin*, but are also in contradiction with previous observations in neurodegenerative models. Indeed, the *Atx2*Δ*cIDR* mutation was shown to reduce degeneration induced by the expression of a C9ORF72-encoded GR50 dipeptide repeat or FUS in the *Drosophila* eye using the GM4-Gal4 driver (Bakthavachalu et al., 2018). Past clinical genetic studies have determined that hexanucleotide repeat expansions in the second intron of C9ORF72 can cause ALS in humans through the formation of SG-related RNP assemblies (DeJesus-Hernandez et al., 2011; Mizielinska et al., 2014).

The results presented here suggest that the cIDR, and therefore RNP granule formation, may actually be required to alleviate the cellular toxicity introduced by the *rdgB*^{9}

mutation. Overall, these results are difficult to consolidate with the RNAi work. An explanation could be found in the potential differences between short-term and long-term effects from stress-induced RNP granules. As previously mentioned, it is still unclear whether these kind of RNP granules offer some form of protection critical for cell survival and are a consequence of stress responses in a degenerating cell, or whether they are toxic to the cell and a cause of neurodegeneration. In the context of *rdgB*^{9}-induced retinal degeneration, RNP granule formation may protect sensitive RNA molecules until ER stress is resolved. As ER stress cannot be resolved due to a genetic mutation, the long-term effect of RNP granules becomes cytotoxic. Removing the cIDR domain from the *atx2* gene may be removing the ability of the cell to initiate RNP granule formation, therefore accelerating retinal degeneration. Whereas knocking-down RNP granule components, with varying degrees of efficiency, leads to a more cytoprotective modulation of RNP granule formation, leading to less degeneration. As this putative model is mostly based on previous findings in different cell types and degenerative models, more work is required to fully dissect the possible involvement of RNP granules in *rdgB*^{9}-induced retinal degeneration.

3.3.3.2. Limitations

The retinal analysis protocol that was used for this chapter was based on previous literature (Campesan et al., 2011; Huang et al., 2015; Smalley et al., 2016; Yadav et al., 2018). Although it is a useful method for assessing cell health and degeneration in *Drosophila*, it depends on human judgement. In this project, any possible bias was removed by randomising the image files, although the reliance on human judgement means that variation is introduced. This variation should be similarly present in all groups.

Additional controls are usually required when using an allele such as *Atx2*Δ*cIDR*, for example using a null *atx2* mutant, alleles with deletions of other regions, or using a heterozygote expression to see whether there is a causal relationship between the amount of mutant and wild-type *atx2* and the phenotype observed. These controls would be particularly interesting to confirm these preliminary results regarding the formation of RNP granules in retinal degeneration.

3.3.3.3. Further studies

The main objective from this chapter was to dissect the molecular pathway involved in retinal degeneration in *rdgB* mutants. The results obtained and described in this chapter show that the ISR is involved in this form of retinal degeneration, specifically through the stress kinase PERK. Nonetheless, further studies would be valuable to conclusively demonstrate the requirement of this protein, and possibly the involvement of RNA-binding proteins and RNP granule components. For this purpose, several experiments would be interesting to conduct.

First, research using RNAi technology usually have additional genotypes to show a causal relationship between modulating the expression of a gene and an observed phenotype. One essential experiment to conduct is to use hypomorphic or loss-of-function alleles of *perk*, and the other genes studied in this work. Introducing these alleles in the RdgB^{9} line should lead to comparable results to what has been observed with the RNAi constructs. Alternatively, overexpressing a wild-type *perk* allele with a UAS *perk* RNAi construct should revert the phenotype back to a degeneration similar to the RdgB^{9} line. This would demonstrate a direct causal link between knocking-down the expression of *perk* and an alleviated retinal degeneration. An additional method to determine the requirement of the ISR would be to feed RdgB^{9} flies either a PERK inhibitor or the ISR inhibitor (ISRIB) to reverse the effect of eIF2α. PERK inhibitors have previously been used in models of traumatic brain injury and spinal cord injury in mice (Saraswat Ohri et al., 2022; Sen et al., 2017). Although, its mechanism of action and effect been put into question (Krishnamoorthy et al., 2014). ISRIB has been reported to reverse deleterious effects caused by traumatic brain injury and other models of neurodegeneration (Bugallo et al., 2020; Frias et al., 2022; Young-Baird et al., 2020). However, feeding pharmacological compounds comes with limitations as well. Unlike the specific knockdown of *perk* in photoreceptor cells, adding a PERK inhibitor or ISRIB into fly food means that the ISR will be affected ubiquitously in the *Drosophila* body possibly causing confounding effects. In addition, the drug dosage may vary significantly between individual flies. Finally, considering the importance of the stress response in healthy photoreceptor cells due to light-induced oxidative damage (Zhang et al., 2014), a PERK inhibitor may have a stronger effect than partially knocking-down the expression of the protein, possibly leading to deleterious effects in photoreceptor

cells through an inappropriate stress response. However, the advantage of this method is the relative simplicity of the protocol, requiring little preparation and fewer genetic crosses.

Second, using the electrical response of photoreceptors through electroretinography (ERG) could help further understand the pathways involved in retinal degeneration in RdgB^{9} flies. Indeed, flies with the *rdgB*^{9} allele were originally described as having impaired responses to light, with an ERG phenotype that can be detected earlier than the morphological differences (Harris & Stark, 1977). The ERG technique may bring a more detailed understanding of the role of the proteins tested in this work and whether they are crucial for early or late stages of retinal degeneration.

Third, an interesting question to test is whether RdgB^{9} *Drosophila* flies have impaired vision. So far, there has not been any work done to establish whether this could be a usable behavioural readout from these mutants. If the *rdgB*^{9} mutation does lead to an observable behaviour phenotype, could this impaired vision be rescued using the RNAi constructs that were successful in rescuing photoreceptor degeneration? The *Drosophila* Interactive System for Controlled Optical (DISCO), a setup described in Moulin et al. (2022) measures various locomotive related parameters while exposing flies to highly controllable LED light. This could be used to measure light-based behaviours such as locomotor response of flies exposed to sudden darkness stimuli (Moulin et al., 2022).

Fourth, as previously mentioned, the RdgB^{9} model presents a particular advantage to screen for proteins that may be modulators of pathways involved in cellular degeneration. However, it would be of high interest to genetically test the implication of these same pathways in a different model for retinal degeneration. This could be achieved by using mutant forms of the Rhodopsin protein, such as Rh1P37H. This would help determine how generalisable the work with RdgB^{9} might be in the field of retinal degeneration.

Finally, based on the observed effects of knocking-down RNP granule components and homozygously expressing *Atx2*Δ*cIDR* in the RdgB^{9} model, it would be particularly interesting to develop experiments that could confirm these observations. For instance, an informative line of experiments would be to confirm the presence of RNP

granules in rhabdomeres of *rdgB* mutants. This could be completed by staining the retinas of wild type flies or flies expressing *rdgB* mutant alleles with antibodies targeting RNP-components such as Ataxin-2, Rin, Caprin, or Me31B. Based on the results presented here, *rdgB* mutants are predicted to have an increased number of granules, with possible morphological differences. Another promising experiment would be to compare the effect of heterozygous versus homozygous expression of the *Atx2*Δ*cIDR* allele in the RdgB^{9} line. If the hypothesis that this *atx2* allele increases cytotoxicity due to the lack of RNP granule formation, then a heterozygous mutant should exhibit reduced degeneration. In addition, reduced RNP granule formation could be visually assessed in the immunostaining preparations as described above.

3.3.4. Conclusion

The ISR has been implicated in the pathogenesis of many human diseases. RBPs have also been a focus in understanding the development of neurodegenerative diseases. The results presented in this chapter demonstrate that the ISR, and specifically the stress kinase PERK, play a significant role in the pathway leading to retinal degeneration in the RdgB9 model. In addition, these results possibly implicate specific RBPs and RNP granule components such as ATX2. I propose the following model in an attempt to consolidate these findings (Figure 3-9):

1. The mutated RDGB protein does not properly localise to the contact site between the rhabdomere and the ER (Yadav et al., 2018);
2. The phosphatidylinositol cycle is compromised, and light exposure exacerbates this due to the phototransduction being activated (Cockcroft et al., 2016);
3. The ER senses this malfunctioning cycle and downstream pathways, it activates ER stress. Preliminary data from this work indicates this (Figure 3-3);
4. PERK dimerises and phosphorylates eIF2α, initiating the ISR and inhibiting general protein translation (Wek, 2018). Knocking-down *perk* rescues the degenerative phenotype as shown in this work (Figure 3-5);
5. Translated ATF4 activates the transcription of stress response genes (Neill & Masson, 2023). RBPs that may be involved in RNA metabolism could be detrimental to the cell's health, as knocking them down rescues the degenerative phenotype (Figure 3-6 and Figure 3-7);
6. ISR activation also leads to the formation of cytoprotective RNP granules to protect RNA molecules from stress exposure (Namkoong et al., 2018). Removing the cIDR from ATX2 blocks this formation and increases toxicity (Figure 3-8);
7. Chronic activation of PERK and the ISR, as well as long-term RNP granule formation, leads to the induction of the CHOP pathway and promotes cell death (8) (Bevilacqua et al., 2010).

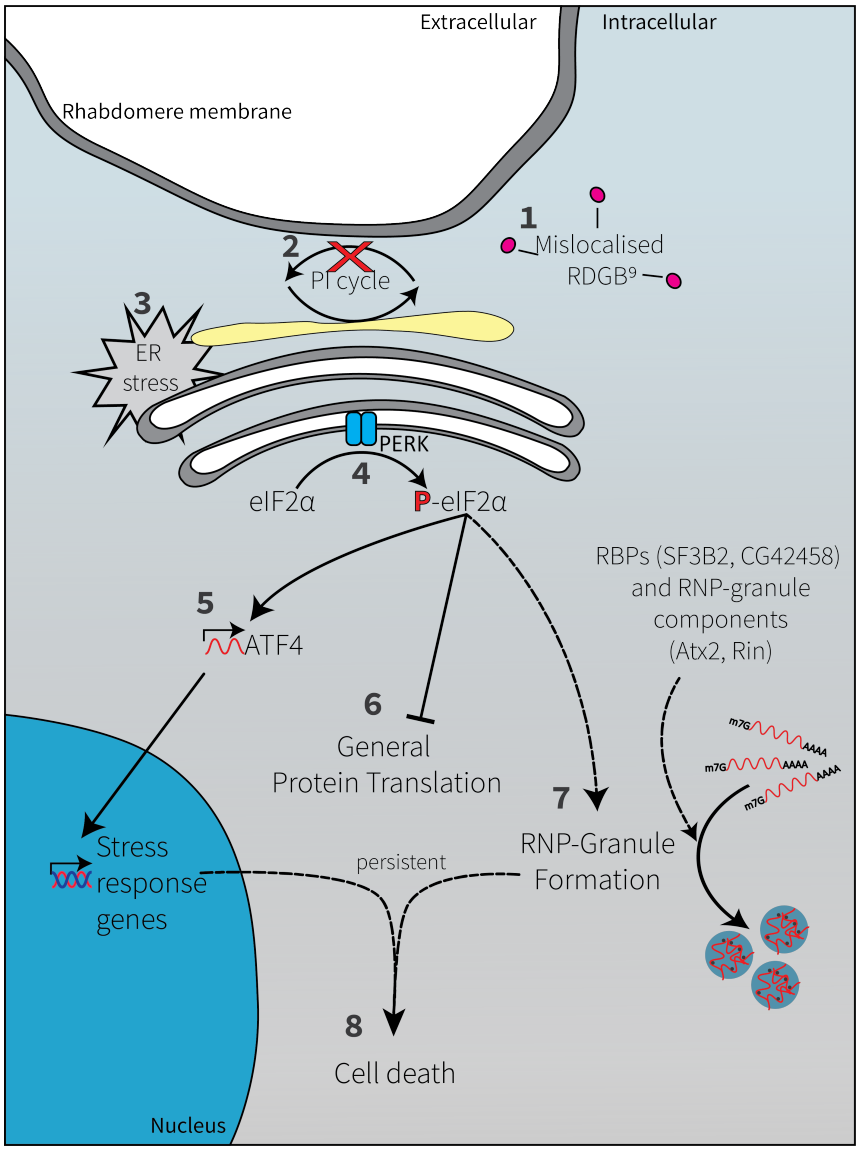

Figure 3-9 Model for mechanisms underlying rdgb⁹-induced retinal degeneration.

(1) RDGB⁹ mutant protein is mislocalised, leading to (2) the PI cycle being compromised. (3) This induces ER stress which (4) activates the ISR kinase PERK, phosphorylating eIF2α. eIF2α phosphorylation (5) induces the specific translation of ATF4 which will translocate to the nucleus and express stress response genes. eIF2α phosphorylation will also (6) inhibit general cap-dependent protein translation, and finally (7) induce the formation of RNP granules. The persistent formation of RNP granules and expression of stress response genes, such as CHOP, (8) leads to cell death.

Chapter 4

Modulation of Neurodegeneration Induced by an Expanded Form of HTT

4.1. Introduction

This chapter aims to assess the involvement of proteins involved in stress-response pathways in a *Drosophila* model of neurodegeneration. For this purpose, an expanded form of the human Huntingtin (*Htt*) gene was expressed in neurons controlling the circadian rhythm. Previous studies have shown that the expression of expanded forms of HTT in these neurons can lead to a dysfunctional circadian rhythm (Xu et al., 2019a). Therefore, a behavioural readout can be generated by analysing the activity pattern of *Drosophila* over time. This behavioural phenotype can be detected early in the process of neurodegeneration, even before cell death (Xu et al., 2019a). Eventually, the expression of expanded forms of *Htt* leads to cell death, which can be assessed through immunostaining. Using RNAi constructs to downregulate the expression of known components of the ISR, as well as RNA-binding proteins and RNP granule components, will help understand whether these pathways are required in this form of neurodegeneration.

4.1.1. Circadian rhythm

4.1.1.1. Functional background

All living beings have been shaped by exposure to their environment. This includes the rotation of the earth around its own axis leading to a 24-hour cycle involving a change in temperature and light exposure. From prokaryotes to plants and the largest mammals, all organisms have adapted to this 24h rhythm to their advantage. Circadian rhythms are daily, biological rhythms in behaviour or physiology with a period of approximately 24 h. According to Johnson et al. (2003), for a biological rhythm to be considered a circadian rhythm, three conditions need to be met: (1) endogenous (persistent in conditions of constant darkness), (2) entrainable (capable of being reset through exposure to external stimuli), and (3) temperature resistant (persistent across a range of physiological temperatures). Circadian rhythmicity is observable in sleeping and feeding patterns of animals, and in leaf movement or growth patterns in plants, to name a few.

In *Drosophila*, circadian rhythm was first observed in their eclosion rate (Pittendrigh, 1967). It can also be observed in their level of motor activity over the course of the day and in their sleeping behaviour (Konopka & Benzer, 1971; Peschel & Helfrich-Förster, 2011). Indeed, in a normal 12:12 hour light/dark (LD) cycle, two peaks of activity can

be observed in *Drosophila*, one at dawn and one at dusk, also known as morning and evening peaks. There is a slight anticipatory effect in *Drosophila*, with these peaks occurring slightly before the transitions. When placed in constant darkness (DD), *Drosophila* flies show a persistence of these rhythms, although the morning peak tends to decrease in amplitude (Dubowy & Sehgal, 2017). Through the work conducted in the laboratory of Seymour Benzer, the first genes implicated in the regulation of circadian rhythms were identified in *Drosophila* (Konopka & Benzer, 1971). Three mutant lines were generated, with dramatic alterations to the normal 24h circadian rhythm. These results, and later studies from various laboratories, were able to demonstrate the existence of molecular feedback loops, common to many species, that generate these circadian rhythms.

4.1.1.2. Genetic feedback loops

There are two major genetic feedback loops contributing to the endogenous circadian clock. These involve transcriptional control of various proteins that will then have an inhibitory effect on the same transcription factors that led to their expression. The first and most studied loop involves the genes *period* (*per*), *timeless* (*tim*), *clock* (*clk*) and *cycle* (*cyc*). After dark, PER and TIM are stable and reach their highest concentration. They enter the nucleus where they will bind to and inhibit the transcription factors CLK and CYC, leading to the inhibition of their own transcription. The concentration of *per* and *tim* mRNA and protein levels decrease slowly until dawn (Dubowy & Sehgal, 2017). In *Drosophila* specifically, there is an additional protein that plays a role in this feedback loop. The blue-light photopigment cryptochrome (CRY), expressed in a specific subset of clock neurons, will bind to TIM when activated by light, leading to the degradation of the protein TIM.

Although their functions are not completely understood, two homologues for *cry* exist in mammals: *cry1* and *cry2*. Previous reports have found both light-dependent (Kolarski et al., 2021; Lucas & Foster, 1999; Miyamoto & Sancar, 1998; Van Gelder et al., 2003; Vanderstraeten et al., 2020) and light-independent functions (Griffin et al., 1999; Lee et al., 2001; Okamura et al., 1999; Partch et al., 2006). It is now established that CRY proteins act like the protein TIM in *Drosophila*, and are components of the main negative feedback loop involving PER (Chaves et al., 2011; Lin & Todo, 2005). Their functions as possible photoreceptors and circadian rhythm modulators may be

dispensable and redundant with the role carried out by melanopsin-expressing retinal ganglion cells (Lin & Todo, 2005).

The second feedback loop, involving transcriptional control of the *Clk* gene, is not as well understood. Two other genes, a transcriptional activator *pdp1* and a repressor *vrille*, regulate the transcription of *Clk* maintaining a rhythmic expression. Studies suggest that these proteins may improve the precision of the first feedback loop (Cyran et al., 2003; Glossop et al., 2003).

4.1.1.3. Neuronal circuitry of the circadian clock

In *Drosophila*, around 150 neurons express the core clock components. This network of neurons is comparable to the mammalian superchiasmatic nucleus (SCN) which regulates behavioural circadian rhythms. The *Drosophila* clock network has two major clusters of neurons: the three groups of dorsal neurons (DN1-DN3), and the lateral neurons (LNs). The lateral neurons can be further subdivided into four groups: the small and large ventrolateral neurons (sLNvs and lLNvs), the dorsolateral neurons (LNds), and the lateral posterior neurons (LPNs) (Figure 4-1). This network of neurons in wild-type *Drosophila* flies, under normal conditions, will all express the core clock components in a nearly synchronised fashion (Roberts et al., 2015; Yoshii et al., 2009).

The output of this network is still being explored, but two groups of output neurons, receiving input from clock neurons, have been identified as being important for normal behavioural activity rhythms even though they do not express the molecular components mentioned previously. These are the neurons located in the *pars intercerebralis* that secrete the neuropeptide Diuretic Hormone 44, and the neurons located in the lateral horn that express the neuropeptide leucokinin; both of these neuropeptides are important for activity rhythms in constant darkness (Cavey et al., 2016; King et al., 2017).

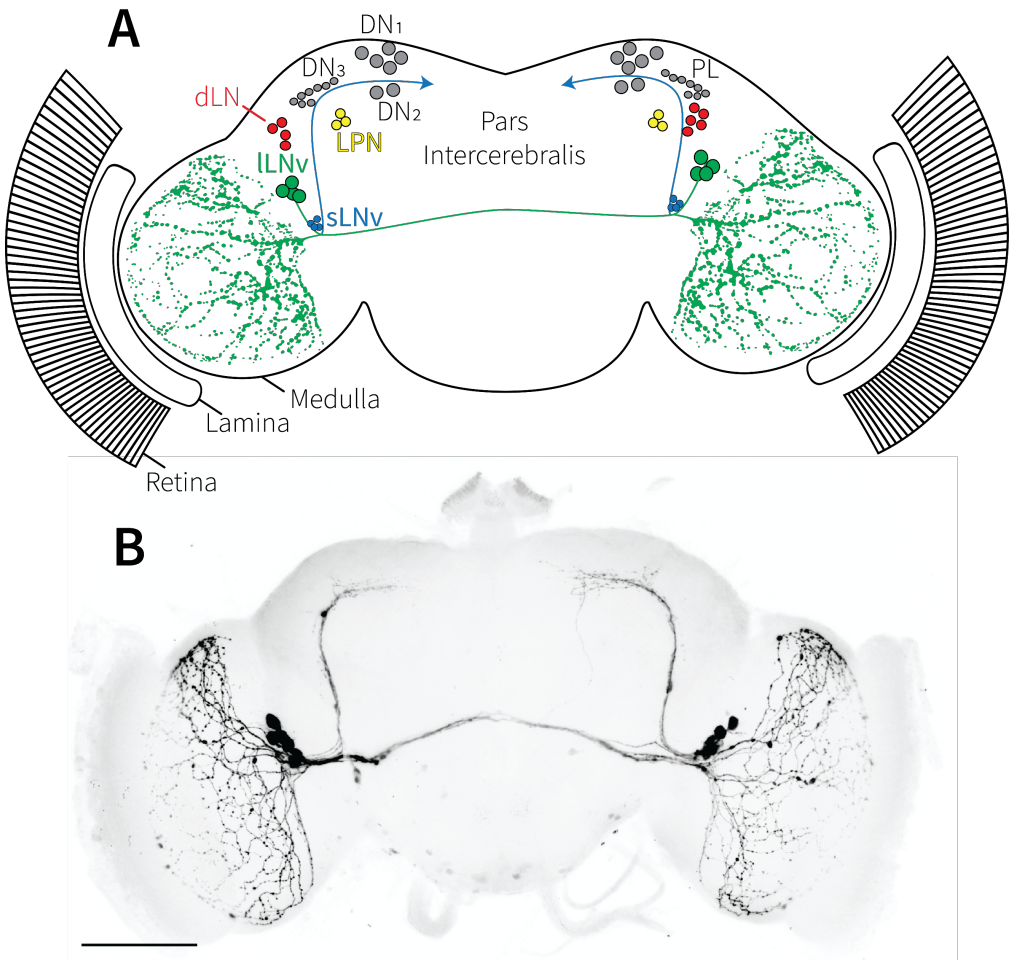

Figure 4-1 The neuronal circuitry of clock neurons in Drosophila.

(A) Schematic diagram of the neuronal circuitry of clock neurons. DN1-DN3: Dorsal neurons 1-3, dLN: dorsal lateral neurons, LPN: Lateral posterior neuron, lLNv: large ventral lateral neuron, sLNv: small ventral lateral neuron, PL: Pars lateralis. The well characterised arborisation of the ventral lateral neurons is shown in the medulla. These clock neurons send fibres into the dorsal protocerebrum including the neurosecretory centres in the pars intercerebralis, and pars lateralis, as well as into the accessory medulla. (B) Representative mosaic and z-stacked image of a PDFGal4/UAS-GFP; UAS-mRFP-HttQ138 Drosophila brain stained with a PDF antibody. Imaged using a Zeiss LSM880 confocal microscope, black bar represents 100 µm.

The synchrony of clock neurons arises predominantly through a mediating neuropeptide known as pigment dispersing factor (PDF). *Drosophila* flies expressing mutant forms of *pdf* or of its receptor *pdfr* exhibit strong phenotypes with an absent morning peak and an early evening peak under normal light conditions, and a shorter period that quickly diminishes under constant darkness, referred to as free-running, conditions (Lear et al., 2005; Mertens et al., 2005). This can be correlated to the fact that without PDF the molecular clock has been shown to run faster in groups of

neurons, and slower in other groups. In addition, individual cells tend to fall out of phase in PDF mutant flies (Yoshii et al., 2009; L. Zhang et al., 2010). Except for one PDF-negative LNv, all LNvs express this neuropeptide. Of particular importance to the behavioural output in *Drosophila* are the sLNvs, which have a molecular clock that persists for multiple days in complete darkness (Roberts et al., 2015). These PDF-positive sLNvs are known as the master pacemakers through the fact that they provide a signal to the rest of the clock circuit in the absence of light (Yao & Shafer, 2014). This ability is entirely dependent on PDF signalling, demonstrating the importance of this neuropeptide in maintaining this circadian rhythm. The exact downstream mechanism of PDF signalling is still unclear. Past studies have suggested that PDF may lead to an increase in cAMP production which may activate protein kinase A (PKA), stabilising PER and other clock proteins (Klose et al., 2016; Li et al., 2014). Another study proposed TIM as an additional downstream target of PDF firing, whereby PDF signalling stabilises TIM through the PKA pathway, and that PDF has an excitatory effect on target neurons, controlling neuronal output (Seluzicki et al., 2014).

In this chapter, PDF-expressing neurons were used to study the molecular pathways that are involved in neurodegeneration induced by the expression of an expanded form of the human Huntingtin gene (*Htt*). As these PDF-positive neurons degenerate, the activity peaks, and the circadian rhythm in general, will be particularly affected in the absence of light. The behavioural phenotype is expected to appear before cell death as toxicity will likely affect neuronal function. As the subset of cells expressing this toxic expanded form of *Htt* is so specific, the neurodegeneration does not affect the fly's general health, providing an additional advantage over manipulation of other cell types. This behavioural readout can then be used to investigate how modulating the expression of genes of interest may impact neurodegeneration.

4.1.2. Huntington's disease

4.1.2.1. General background

As described in Chapter 1, Huntington's disease (HD) is an inherited neurodegenerative disease that can present itself at any age. It is caused by a polyglutamine (CAG) repeat expansion in the gene *huntingtin* that codes for the 350 kDa protein HTT. The normal physiological function of this protein is not entirely understood, but recent studies demonstrate a role in axonal transport, and intracellular vesicular trafficking (Schulte & Littleton, 2011; Vitet et al., 2020). The symptoms of HD can be cognitive, psychiatric, and physical. The onset of physical symptoms that affect motor skills are usually the key symptoms that will lead to clinical diagnosis. Neuronal aggregates and neuronal dysfunction have been shown to occur long before the onset of the clinical phenotype (Gómez-Tortosa et al., 2001).

4.1.2.2. Sleep disorders

Although symptoms affecting motor skills are a hallmark of HD, cognitive symptoms can have a significant negative effect on the quality of life of HD patients. Among the cognitive symptoms, 90% of HD patients suffer circadian and sleep abnormalities (Goodman & Barker, 2010), including insomnia, increased sleep onset latency, REM sleep disorders, and excessive daytime sleepiness (Herzog-Krzywoszanska & Krzywoszanski, 2019). Sleep disorders can be found in both very early stages, and premorbid stages of HD progression (Goodman et al., 2011), which suggests that the mutant *Htt* allele can have a toxic cellular effect long before clinical diagnosis. These symptoms can be associated with the observations in post-mortem HD brains that the number of neurons in the SCN involved in regulating the circadian rhythm diminishes (Van Wamelen et al., 2013). These observations are replicated in transgenic *Drosophila* expressing a mutant form of *Htt* in PDF-expressing neurons which leads to a selective reduction in the number of sLNvs and a rapid loss of morning and evening peaks in the behavioural activity in constant darkness (Sheeba et al., 2010; Xu et al., 2019a). Although sleep and circadian rhythm disturbances in HD patients are well characterised, it remains unclear why this subset of neurons in *Drosophila* are particularly sensitive to the expanded forms of *Htt*. As previously mentioned, the molecular clock genes expressed in clock neurons are translationally and transcriptionally regulated. RNA-binding proteins likely play an important role in this,

of which, Ataxin-2 (ATX2) has been shown to interact with the polyA binding protein to promote PER translation (Zhang et al., 2013). Studies have also found that the HTT protein co-localises with components of neuronal granules and associates to mRNA in dendrites. The authors suggested that HTT may play a role in inhibiting RNA translation during transport in neuronal granules (Savas et al., 2010).

4.1.2.3. Molecular pathways in HD

The size of the polyglutamine tract in HTT is proportional to the speed of disease progression, but not necessarily with its severity (Swami et al., 2009). This expansion can disrupt normal protein maturation, and lead to protein misfolding with toxic neuronal aggregates. The exact pathway leading to cellular toxicity from these expanded forms of HTT is not well understood. Indeed, these aggregates may in fact be a cellular strategy to reduce toxicity (Eisenberg & Jucker, 2012). The unfolded protein response (UPR) and the integrated stress response (ISR) pathways are of high interest in the field of neurodegenerative diseases, including HD (Carnemolla et al., 2009; Leitman et al., 2013; Vidal et al., 2011). The UPR activates upon detection of misfolded proteins in the ER under normal conditions, which then initiates a cascade of events leading to the proteolysis of the misfolded proteins. With an endogenous expression of an expanded form of HTT, or any other genetic mutation that leads to protein misfolding, the UPR may be overwhelmed. In addition, chronic activation of ER stress leads to the activation of proapoptotic pathways (Taalab et al., 2018). HD, like other neurodegenerative diseases, is linked with pathological formation of ribonucleoprotein (RNP) aggregates or granules. These RNP granules encapsulate a large variety of different granules that occur under normal conditions such as neuronal RNP granules that play a role in axonal RNA transport (De Graeve & Besse, 2018). The dysfunction formation of RNP granules, such as stress granules (SG) and processing-bodies, has also been directly linked with many neurodegenerative conditions, for instance, different spinocerebellar ataxias and ALS (Bakthavachalu et al., 2018; Ramaswami et al., 2013). In HD specifically, previous literature suggests that the protein HTT may play a role in post-transcriptional processes and in mRNA translational repression during transport in neuronal granules (Savas et al., 2010; Savas et al., 2008). Recent work from the Ramaswami laboratory has found that the RNP granule assembly function of the ATX2 protein is required for neurodegeneration

induced by an expanded form of *Htt* (Huelsmeier et al., 2021). In addition, recent work from the Allada laboratory demonstrated that ATX2 mediates the toxicity of an expanded form of *Htt* in circadian clock neurons (Xu et al., 2019b).

Another family of RBPs that have also been studied in the context of HD are the Ras-GAP SH3 domain binding proteins (G3BP1 and G3BP2). The *Drosophila* ortholog for G3BP1 is Rasputin (Rin). Through their RNA-binding capacity, G3BPs are a necessary component for the formation of SGs (Aguilera-Gomez et al., 2017; Sidibé et al., 2021), but they have additional functions such as in axonal translation (Sahoo et al., 2018) and mRNA decay (Fischer et al., 2020). Interestingly, a recent study reported a possible role for G3BP1 and SG assembly in HD pathogenesis (Sanchez et al., 2021). Indeed, they found a significant increase in the density of G3BP1-positive granules in the cortex and hippocampus in both a rodent model for HD and in the superior frontal cortex of HD patients. In addition, another recent study found that the loss of G3BP1 hastens polyQ-expanded aggregation and toxicity in a *C. elegans* model of HD (Gutierrez-Garcia et al., 2023).

Taken together, it is still unclear what role protein aggregates and RNP granules play in the pathogenesis of HD. Disruption in sleep and circadian rhythms is a common feature in HD patients and in HD animal models. Despite it being a well characterised and a conserved trait of HD, the molecular mechanism linking mutant *Htt* alleles and disrupted circadian behaviour remains elusive. Considering that these symptoms typically appear in preliminary stages of HD, targeting involved pathways may be an interesting therapeutic approach to predict and possibly delay the onset of HD.

4.1.3. Aims

The main aim of this chapter is to understand the cellular mechanisms of neurodegeneration caused by the expression of a human expanded form of *Htt* in PDF-expressing neurons. The consequences of expanded glutamine tracts and how they lead to pathogenesis remain unclear. By using a behavioural readout as well as assessing cellular toxicity through PDF-stained sLNvs and HTT aggregation, this work aims to:

1. Study the involvement of the ISR and how it may modulate cellular toxicity.
2. Uncover the possible role of novel RBPs, elucidating the pathways involved in HD.
3. Confirm the finding that ATX2, an RNP granule component, is required for pathogenesis in this HD model.
4. Study the possible involvement of the *Drosophila* G3BP ortholog: Rasputin.

4.2. Results

The main aim of this chapter is to understand the cellular and molecular mechanisms of neurodegeneration caused by a polyglutamine expansion of the human *Htt* gene. Neurodegeneration was assessed through a behavioural readout on circadian rhythm parameters. The following experiments were designed to assess the role of an ER stress pathway component, of novel RNA-binding proteins, and of RNP granule components, in a polyglutamine expansion induced pathogenesis. In addition, experiments were designed to test whether defective circadian rhythm could be correlated with aggregation of the *Htt*Q138 protein or even cell death of master pacemaker neurons (sLNvs).

4.2.1. PERK mediates huntingtin toxicity in circadian rhythm neurons

Previous literature has implicated the ISR and the UPR in animal models of HD (Carnemolla et al., 2009) as well as in post-mortem HD brains (Leitman et al., 2013). As previously mentioned (4.1.2.3.), the unfolded protein response is activated in models of HD, most likely through the activation of the eIF2α kinase PERK. In order to investigate a possible role of PERK in a *Drosophila* model of HD, an RNAi construct was used to knockdown the transcript for *perk* in transgenic flies also overexpressing a CAG expanded form of human *Htt* specifically in PDF-expressing neurons. This could clearly establish a role for this protein and whether downregulating its expression may alleviate the neurodegenerative phenotype. The generated flies were used for analysis of their behavioural circadian rhythm and for assessment of cell death via immunohistochemistry.

4.2.1.1. Behaviour readout

Experimental flies were generated by crossing a PDFGal4 driver line with a line containing the *UAS-mRFP-HttQ138* construct, or a line containing both the UAS *perk* RNAi and the *UAS-mRFP-HttQ138* constructs. Control parental lines were also generated to have the PDFGal4 driver, and the UAS effectors by themselves. The generated genotypes were the following:

- *y[1], w*/-; PDFGal4/+; +/+* (referred to as PDFGal4);
- *+/-; +/+; UAS-mRFP-HttQ138/+* (referred to as Q138);
- *+/-; +/+; UAS perk RNAi (TRiP)/UAS-mRFP-HttQ138* (referred to as *perk* RNAi; Q138);
- *y[1], w*/-; PDFGal4/+; UAS-mRFP-HttQ138/+* (referred to as PDF>Q138);
- *+/-; PDFGal4/+; UAS perk RNAi (TRiP)/UAS-mRFP-HttQ138* (referred to as PDF> *perk* RNAi; Q138).

Newly eclosed male flies with the correct genotypes were collected over three days and then placed into the *Drosophila* Activity Monitors (DAMs) with access to food. The first three days were used to entrain the flies to a 12h:12h light:dark cycle, referred to as the entrainment period. The following four days were used to study their endogenous circadian rhythm in constant darkness, referred to as the free-running period. Once the seven days had elapsed, the experiment was concluded and the flies were collected for brain dissections.

4.2.1.1.1. Locomotor activity

First, to have an overall view of behaviour during the experiment, a general activity plot over the seven days was generated using the Rethomics framework package in R (Geissmann et al., 2019) (Figure 4-2). During the entrainment period, all genotypes appear to have a regular behavioural circadian rhythm, with distinct morning and evening peaks (yellow and black arrows, respectively). During the free-running period (black and grey background), these defined peaks remain identifiable in all control groups, although they appear to decrease in amplitude over time. Between control groups, there seems to be some variation in the amplitude of these activity peaks, which may be due to genetic background differences, this will be explored in the discussion section (4.3.1). Specifically the morning peaks, are promptly dampened in flies expressing *Htt*Q138 in PDF neurons over the course of the four days, with nearly no identifiable morning peaks on the sixth and seventh days. Finally, downregulation of *perk* seems to alleviate this phenotype, such that morning and evening peaks are moderately restored during the free-running period compared to the PDF>Q138 group.

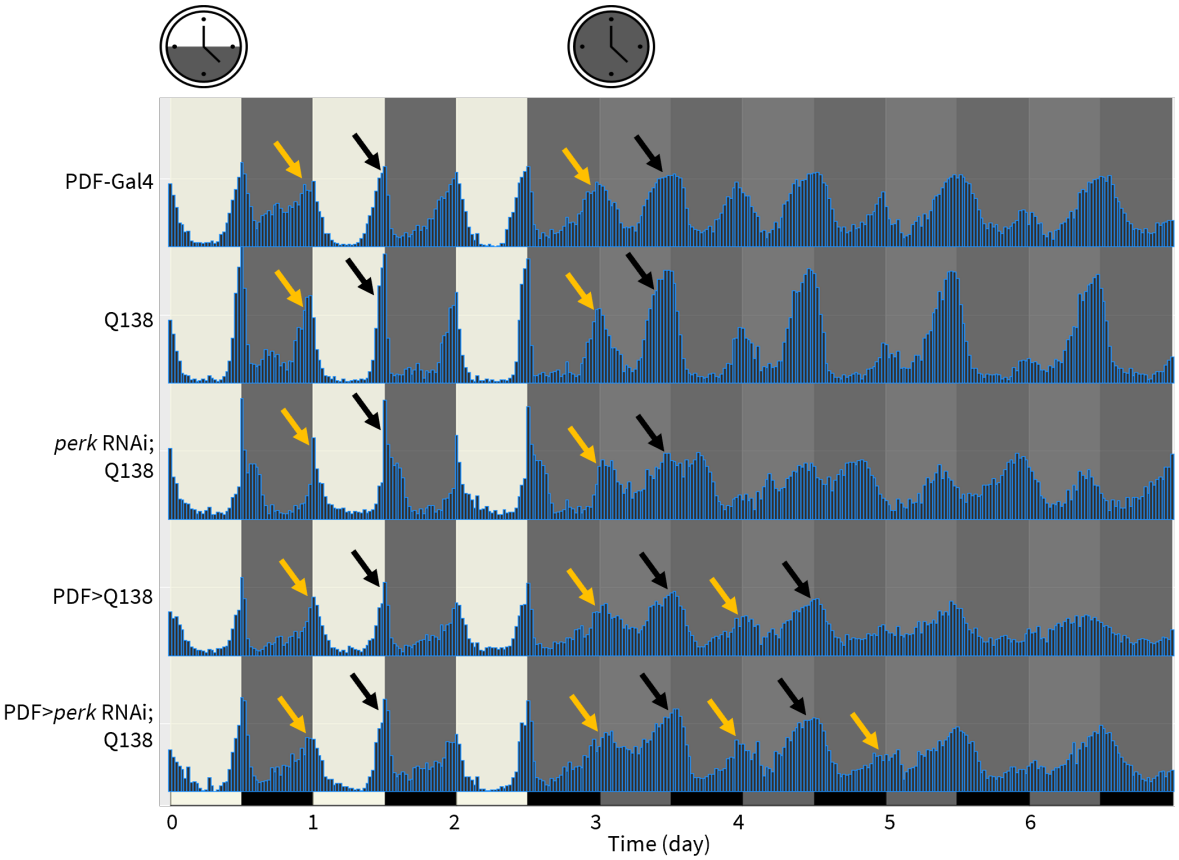

Figure 4-2 Activity plot showing PERK knockdown could rescue Huntingtin-mediated circadian rhythm dysfunction.

Activity plot of entire experiment, including the entrainment period (white and grey background) and the free-running period (grey and dark grey background). Activity is plotted as average of all flies in 30min bins. Yellow and black arrows indicate identifiable morning and evening peaks, respectively. Complete genotypes can be found in the results description.

4.2.1.1.2. PERK contributes to HttQ138-induced arrhythmicity

Next, the behavioural circadian rhythm of the previously mentioned flies was analysed in more detail using the SleepMat tool designed by the Allada laboratory (Sisobhan et al., 2022) in order to take a closer look at the broader range of circadian parameters. Three parameters were extracted from the raw data: (1) rhythmicity, as revealed by the mean power of rhythmicity according to a Chi Square distribution, and expressed as the difference between the Chi power and the significance threshold (Power – Significance; P-S), (2) the number of flies that had a significant rhythm, and (3) the mean period value of this significant rhythm. These parameters were measured during the entrainment period and during the free-running period. More details about the statistical analysis can be found in the methods description in Chapter 2 (2.2.7.2).

This detailed analysis revealed a significant difference in the power of rhythmicity between groups during the free-running period (one-way ANOVA: $F_{4, 119}$ = 18.10, p < 0.001) (Figure 4-3, B). Specifically, that flies expressing the expanded form of *Htt* in PDF-positive neurons (PDF>Q138) demonstrated a sharp decrease in the power of rhythmicity which was statistically different when compared to the parental groups PDFGal4 (p = 0.0288, Tukey's *post-hoc* test), and Q138 (p < 0.001, Tukey's *post-hoc* test). Knocking *perk* down in these flies (PDF>*perk* RNAi; Q138) led to a strong rescue by nearly doubling the power of rhythmicity (92% increase) compared to the PDF>Q138 group, although this difference remained non-significant (p = 0.0848, Tukey's *post-hoc* test). Nevertheless, the power of rhythmicity in this group was similar to the parental groups PDFGal4 (p = 0.9882, Tukey's *post-hoc* test) and *perk* RNAi; Q138 (p > 0.9999, Tukey's *post-hoc* test), suggesting that it did rescue the degenerative phenotype caused by the expanded form of *Htt* to parental control levels. As expected, no significant difference in rhythmicity between genotypes was detected during the entrainment period, (one-way ANOVA: $F_{4, 120}$ = 1.159, p = 0.3323), and no differences were found between groups (Figure 4-3, A).

Based on the values of the power of rhythmicity from individual flies, the percentage of flies that showed a significant rhythmicity and their peak period values were extracted for each group. Individual flies were considered rhythmic during the free-running period if they had a P-S value greater than half of their P-S value from the entrainment period. Most control flies were rhythmic during the entrainment period, specifically 95% of the flies in the PDFGal4 group, 88% in the Q138 group, and 81% in the *perk* RNAi; Q138 group (Figure 4-3, C). The experimental PDF>Q138 group did have a slight decrease in the percentage of rhythmic flies, with only 74% showing rhythmicity during the entrainment period, whereas 95% of flies from the PDF>*perk* RNAi; Q138 experimental group showed rhythmicity. No significant difference was detected using Fisher's exact tests between parental and experimental groups. In addition, all rhythmic flies had a mean period value of 24 hours, with the exception of the *perk* RNAi; Q138 control group that showed a shorter period of 23.75 hours.

However, when the lighting condition was switched to constant darkness, only 53% of the flies from the PDF>Q138 group showed rhythmicity, a significant reduction compared to both parental groups (PDFGal4 vs PDF>Q138: p = 0.01; Q138 vs

PDF>Q138: $p < 0.001$, Fisher's exact test) and with a mean period of 23.50 hours, further demonstrating the loss of a behavioural circadian rhythm caused by the expanded form of *Htt* (Figure 4-3, D). When *perk* was knocked down in the PDF>*perk* RNAi; Q138 group, the percentage of flies that were rhythmic increased back to 67%, although this difference remained non-significant compared to PDF>Q138 ($p = 0.21$, Fisher's exact test). These flies had a mean period of 24 hours, showing that not only has a significant periodicity been re-established in 10% of flies, it has also been rectified to the normal 24h period.

In the control groups, only 72% of the flies from the *perk* RNAi; Q138 control group showed a significant rhythmicity, while nearly all flies from the PDFGal4 and the Q138 control groups showed a significant rhythmicity (90% and 97%, respectively). Interestingly, the Q138 and *perk* RNAi; Q138 control groups had different periods of around 23.75 h and 25.50 h, respectively, when subjected to constant darkness.

Overall these results suggest that the neuronal toxicity induced by the expanded form of *Htt*, measured through circadian rhythm dysfunction, is mediated by the ISR and UPR component PERK. These results are in accordance with previous literature, and will be further discussed in the following sections (4.3.1.1).

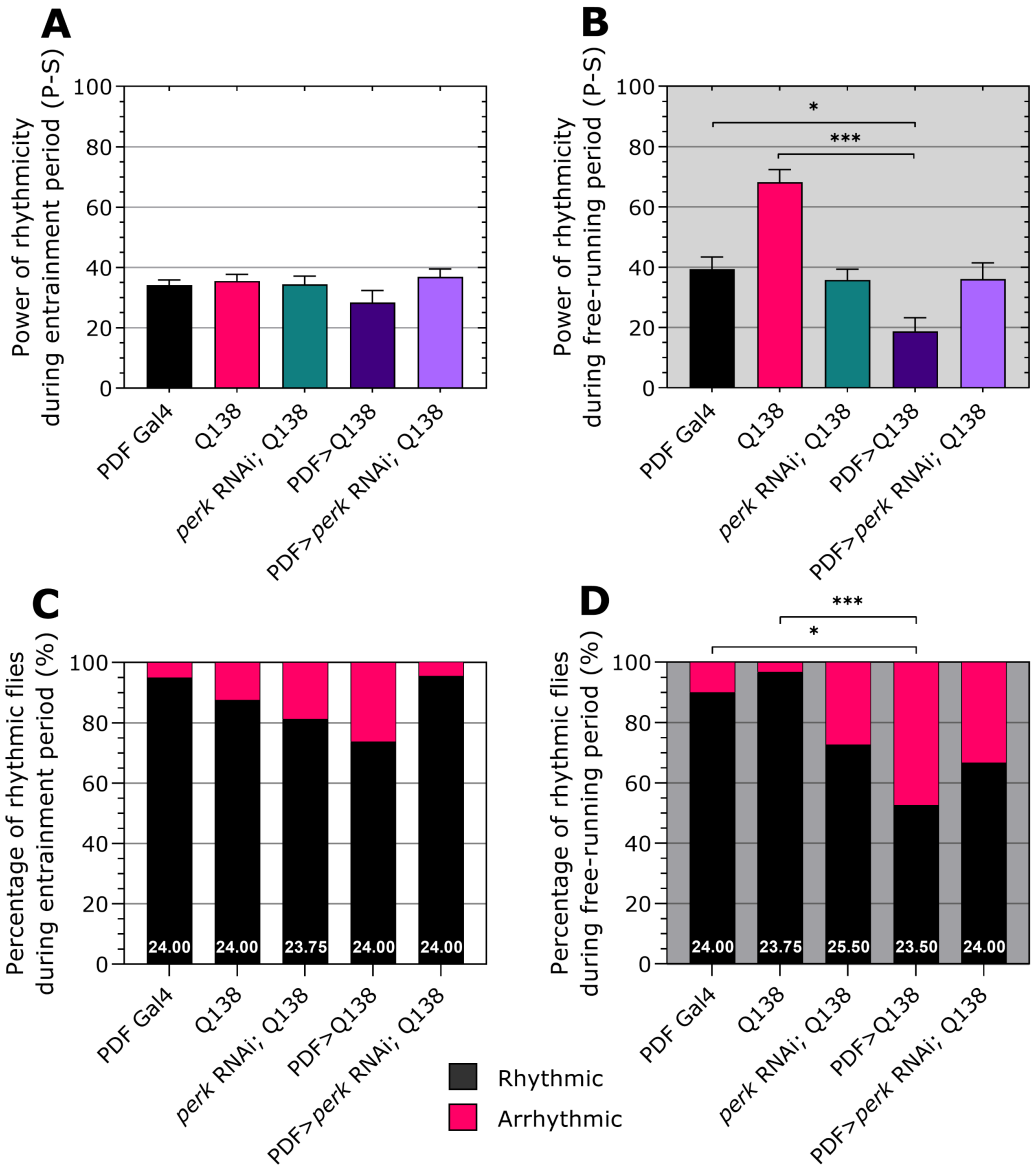

Figure 4-3 PERK is required for huntingtin-mediated arrhythmicity.

*Average power of rhythmicity during the entrainment period (A) and the free-running period (B) conditions. Power of rhythmicity corresponds to Power – Significance (P-S). Mean value calculated using individual fly values from SleepMat (Sisobhan et al., 2022). Data presented as mean ± SEM, *p = 0.0288, ***p < 0.001, Tukey's post-hoc test. (C) Percentage of rhythmic and arrhythmic flies during the entrainment period, and (D) the free-running period conditions. Flies were considered rhythmic if they had a P-S ≥ mean P-S during entrainment divided by two. Bonferroni adjusted p-values obtained from Fischer's exact test comparing parental crosses to experimental crosses, *p = 0.01, **p < 0.001. Annotated value inside the black rectangles correspond to the mean period of the rhythmic flies. Full genotypes can be found in the results description 4.2.1.1.*

4.2.1.2. Cellular toxicity

Immunostaining was conducted to assess whether the observed circadian rhythm dysfunction induced by the expanded form of *Htt* could be associated with cell death or HTT aggregation in the sLNvs, as reported in a previous study (Xu et al., 2019a). In addition, this experiment was to test whether the measured behavioural rescue from *perk* RNAi could be due to reduced sLNv cell death or HTT aggregation. Regardless of individual rhythmicity values, flies from the behavioural experiment were promptly dissected and their brains were stained for PDF and mRFP-*Htt*Q138.

4.2.1.2.1. PERK knockdown does not improve PDF neuron survivability

To investigate the occurrence of cell death by HTT expansion in the sLNvs population, a PDF staining was performed to detect and count PDF-expressing sLNvs per hemisphere and measure the PDF signal intensity in their somas (2.2.5.3).

A significant difference in the number of sLNv somas was detected between all groups (one-way ANOVA: $F_{2, 32}$ = 14.45, p < 0.001) (Figure 4-4, B). In line with the literature (Dubowy & Sehgal, 2017), the PDFGal4 group had an average of 3.27 sLNvs per hemisphere. This number significantly decreased to 1.17 sLNv per hemisphere in flies expressing *Htt*Q138 in PDF-expressing neurons (PDF>Q138) (p < 0.001, Tukey's *post-hoc* test). In transgenic flies expressing both *Htt*Q138 and the *perk* RNAi construct (PDF>*perk* RNAi; Q138), the number of sLNvs increased to 1.91 per hemisphere. These were not statistically different to PDF>Q138 (p = 0.14, Tukey's *post-hoc* test), and were statistically different to the PDFGal4 group (p = 0.005, Tukey's *post-hoc* test).

No difference was detected in the PDF intensity between groups (one-way ANOVA: $F_{2, 26}$ = 2.051, p = 0.15) (Figure 4-4, C). Expression of *Htt*Q138 in PDF neurons led to a non-significant 55% decrease in the intensity of the signal when compared to PDFGal4 (p = 0.16, Tukey's *post-hoc* test). Down-regulating *perk* increased the intensity of the signal by 82%, but this difference remained non-significant when compared to PDF>Q138 (p = 0.23, Tukey's *post-hoc* test).

Overall, it seems that downregulating expression of *perk* is not associated with a significant rescue in the number of sLNvs after expression of *Htt*Q138.

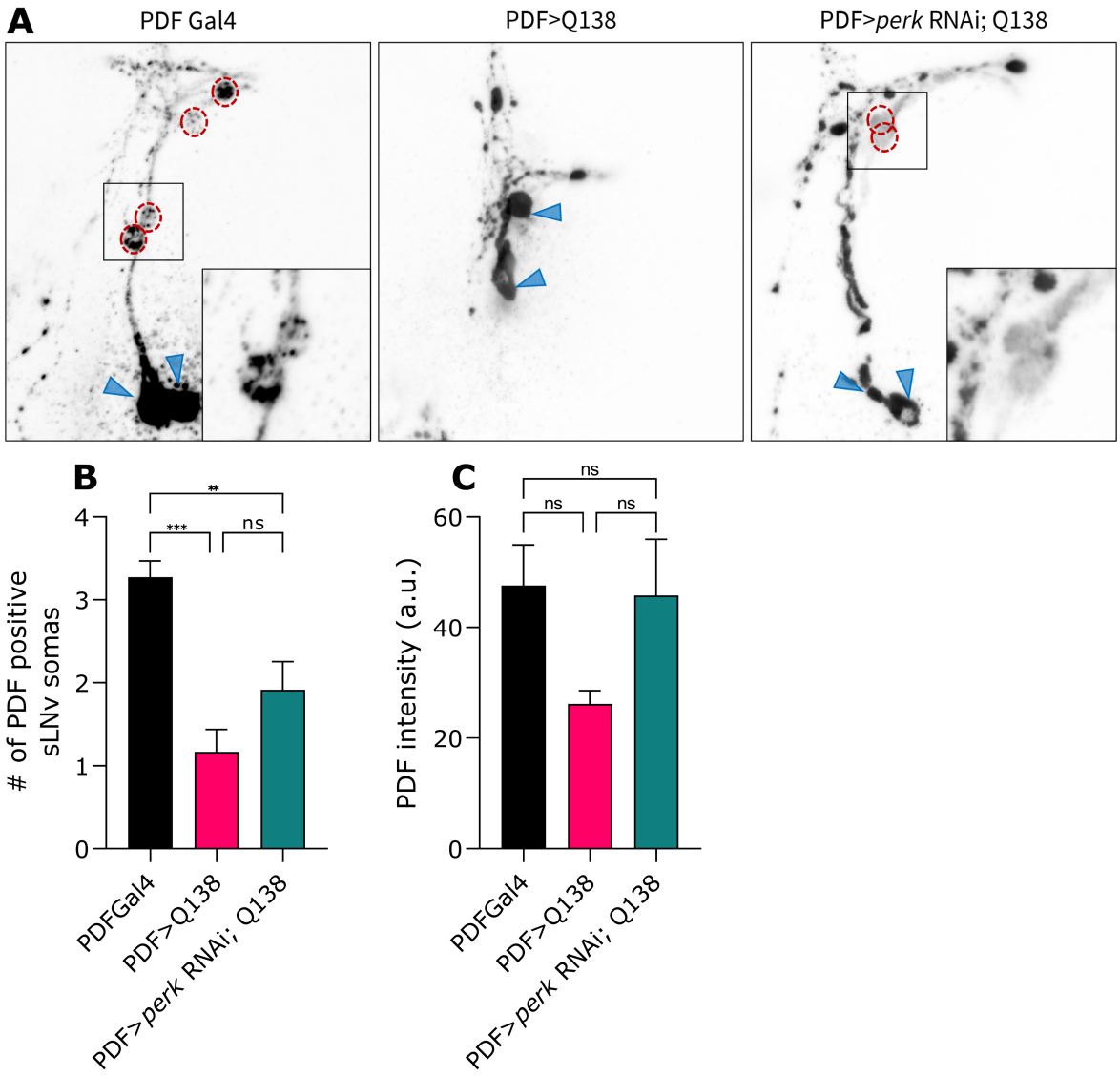

Figure 4-4 PERK knockdown is not sufficient to rescue HttQ138-induced cell death.

*(A) Representative images of brain sections from the groups PDFGal4, PDF>Q138, and PDF>perk RNAi; Q138, stained with a PDF antibody. sLNvs and lLNvs are labelled with red dotted circles and with blue arrows, respectively. Black scale bar represents 20 µm. sLNvs are magnified in the insets in the bottom right corner. Imaged using a Zeiss LSM880 confocal microscope. (B) Quantification of the number of identifiable somas in all three groups, data are presented as bar graphs representing the mean ± SEM, from left to right: PDFGal4 (n = 11), PDF>Q138 (n = 12), and PDF>perk RNAi; Q138 (n = 12), adjusted p-values: ** p = 0.005, *** p < 0.001, one-way ANOVA with Tukey's post-hoc test. (C) Quantification of PDF signal intensity from identifiable sLNv somas in all three groups, data are presented as bar graphs representing the mean ± SEM, from left to right PDFGal4 (n = 11), PDF>Q138 (n = 8), and PDF>perk RNAi; Q138 (n = 10), ns: non-significant, one-way ANOVA with Tukey's post-hoc test. Complete genotypes can be found in the results description 4.2.1.1.*

4.2.1.2.2. PERK knockdown has no effect on volume of Htt aggregates

The exact conformation of the HTTQ138 proteins and their cellular localisation could not be determined due to the protocol used. In other words, the detected signal could be from homogenous monomer cytoplasmic expression, or from different forms of protein aggregation. Nevertheless, the detected HTT signal will be referred to as aggregates for the purpose of clarity. Using the 3D Object Counter plugin in ImageJ, volume of the detected HTT aggregates was measured. Results and representative images are reported in Figure 4-5.

A significant difference in the volume of the HTT aggregates between the three groups was detected (one-way ANOVA: $F_{2, 30} = 11.86$, $p < 0.001$) (Figure 4-5, J). As expected, the expression of *Htt*Q138 led to a significant 15-fold increase in the volume of the HTT aggregates in comparison to the PDFGal4 control ($p < 0.001$, Tukey's *post-hoc* test). *Perk* knockdown had no significant effect on this observed phenotype, with a 9% increase in the volume of the HTT aggregates ($p = 0.87$, Tukey's *post-hoc* test).

Although there are limitations in the control groups used to analyse HTT aggregation, the analysis of the HTT staining in these three groups suggests that knocking-down the expression of *perk* has no effect on these HTT aggregates, which suggests that the observed behavioural effect may result from a different molecular or neuronal pathway.

Overall, the behavioural readout seems to suggest that PERK expression or activation could contribute to toxicity induced by the expression of an expanded form of *Htt*. Although, this may be independent from sLNv survivability and HTT aggregation. This is in accordance with previous literature suggesting a role for the ISR in the pathogenesis of various neurodegenerative diseases. These results and their limitations will be further discussed (4.3.1.1).

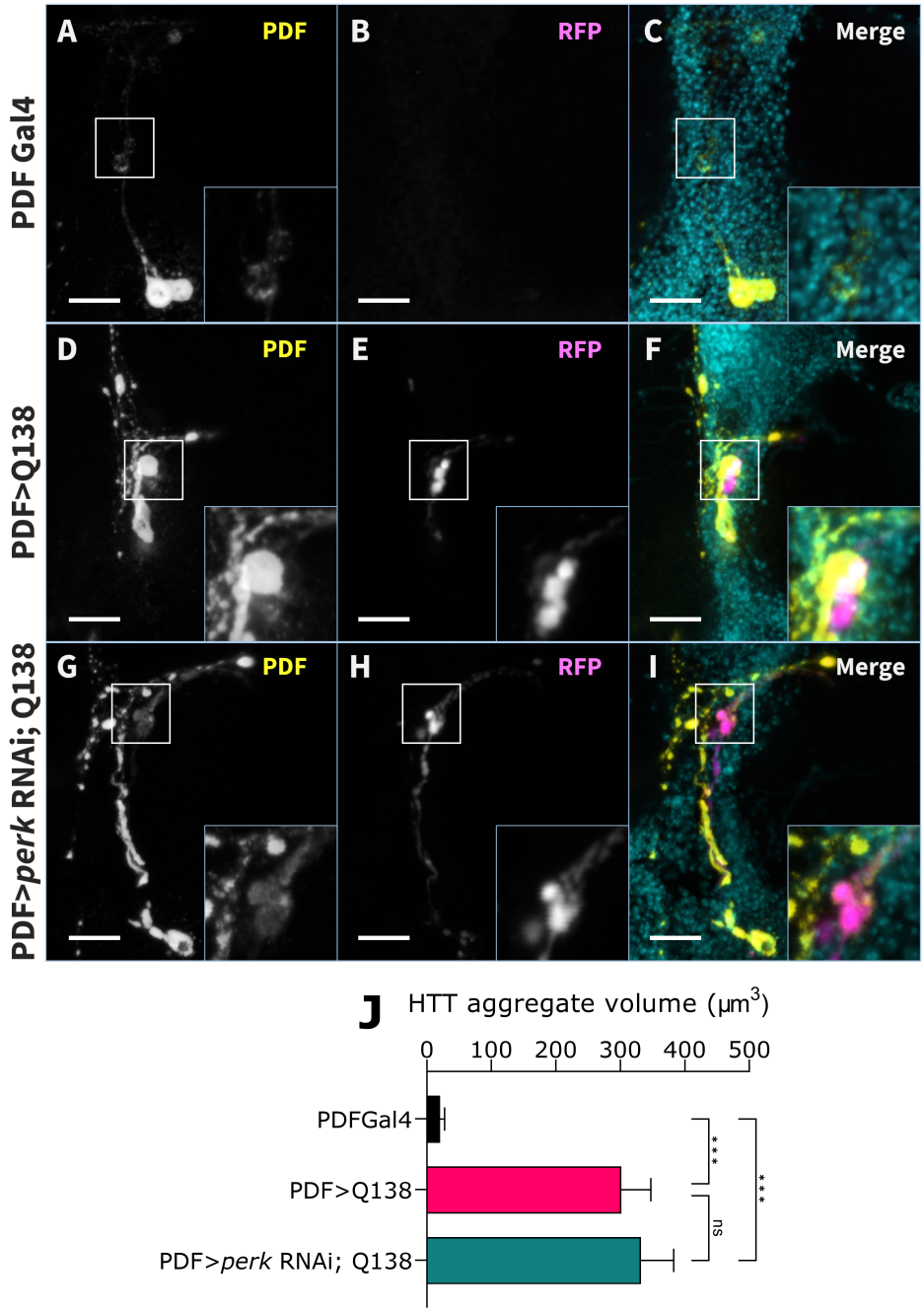

Figure 4-5 PERK does not modulate HttQ138 aggregate formation in the brain.

*Brains were dissected and stained using anti-PDF (anti-mouse 488 – yellow), anti-RFP (anti-rabbit 555 – magenta) and DAPI (cyan). Representative z-stacked images with corresponding insets in grey: (A – C) PDFGal4, (D – F) PDF>Q138, (G – I) PDF>perk RNAi; Q138. White scale bar represents 20 µm. (J) Staining analysis of HTT aggregate volume. Data are presented as bar graphs representing the mean ± SEM. N values: PDFGal4 = 8, PDF>Q138 = 13, and PDF>perk RNAi; Q138 = 12. ***p < 0.001 (one-way ANOVA with Tukey's post-hoc test), ns: non-significant. Full genotypes can be found in the results description 4.2.1.1.*

4.2.2. Novel RBPs may mediate huntingtin toxicity in circadian rhythm neurons

Past studies have demonstrated a role for RBPs in the pathogenesis of neurodegenerative diseases (Kino et al., 2004; Li et al., 2008; McLaughlin et al., 1996; Mykowska et al., 2011; Nalavade et al., 2013). More studies are required to fully understand the exact role that they play and the importance they have in different forms of neurodegenerative diseases. A particular advantage with using *Drosophila* as a model organism is the ease in conducting large genetic screens to identify novel components of pathways. As mentioned in Chapter 3, novel RBPs were identified in a recent screen in models for ALS (Appocher et al., 2017; Chaplot et al., 2019). As seen in Chapter 3, novel RBPs were tested in a retinal degenerative model, namely CG42458 and SF3B2. The latter seemed to play a role in the retinal degeneration induced by the *rdgB*^{9} mutation. In this chapter, the aim was to assess the implication of CG42458 and SF3B2 in this model for HD. In the interest to see whether these novel RBPs may have a role in the context of a neurodegenerative disease, RNAi constructs targeting the transcripts for SF3B2 and CG42458 were used in transgenic flies that also expressed a CAG expansion in the human *Htt* gene in PDF-expressing neurons.

Interestingly, the crosses involving expression of *sf3b2* RNAi (TRiP) in PDF-expressing neurons did not lead to any viable pupae, which may suggest a role for this protein in the developmental stages of these neurons. Due to this, the circadian rhythm experiments and subsequent immunostainings were not conducted for this RNAi line.

On the other hand, crosses involving expression of *CG42458* RNAi (VDRC) in PDF-expressing neurons did lead to viable flies and were used for the experiments. Although CG42458 remains elusive, it is known to have an RNA-binding sequence, and is predicted to have a role in RNA stabilisation and located in the cytosol.

4.2.2.1. Behaviour readout

As previously mentioned, experimental flies were generated by crossing a UAS *CG42458* RNAi line with either a PDFGal4 driver line or with a line containing both the PDFGal4 driver and the *UAS-mRFP-HttQ138* construct. Control parental lines were also generated to have the PDFGal4 driver, and the UAS effectors by themselves. The generated genotypes were the following:

- *y[1], w*/-; PDFGal4/+; +/Sb* (referred to as PDFGal4);
- *+/-; +/+; UAS-mRFP-HttQ138/+* (referred to as Q138);
- *+/-; UAS CG42458 RNAi (VDRC)/+; UAS-mRFP-HttQ138/Sb* (referred to as *CG42458* RNAi; Q138);
- *y[1], w*/-; PDFGal4/+; UAS-mRFP-HttQ138/Sb* (referred to as PDF>Q138);
- *+/-; PDFGal4/UAS CG42458 RNAi (VDRC); UAS-mRFP-HttQ138/Sb* (referred to as PDF>*CG42458* RNAi; Q138).

4.2.2.1.1. Locomotor activity

As previously described (4.2.1.1.), a behavioural experiment was conducted to measure general locomotor activity (Figure 4-6).

During the entrainment period (white and grey background), a regular behavioural circadian rhythm with defined morning and evening peaks (yellow and black arrows, respectively) can be seen in all genotypes. When the free-running period begins (black and dark-grey background), except for the *CG42458* RNAi; Q138 group, all control groups exhibit morning and evening peaks with a slight decrease in amplitude over time. The *CG42458* RNAi; Q138 group still shows morning and evening peaks, but there is a clear difference in their amplitude between the entrainment and free-running period.

In comparison, these peaks are promptly dampened in the PDF>Q138 group over the course of the four days, specifically with no identifiable morning peaks on the fifth and sixth days. Finally, the PDF>*CG42458* RNAi; Q138 group shows higher variability in the locomotor activity. The morning peaks do not seem restored but the evening peaks have increased in amplitude compared to the PDF>Q138 group.

Overall, *CG42458* knockdown does not seem to recover the dysfunctional circadian rhythm induced by the expression of *Htt*Q138.

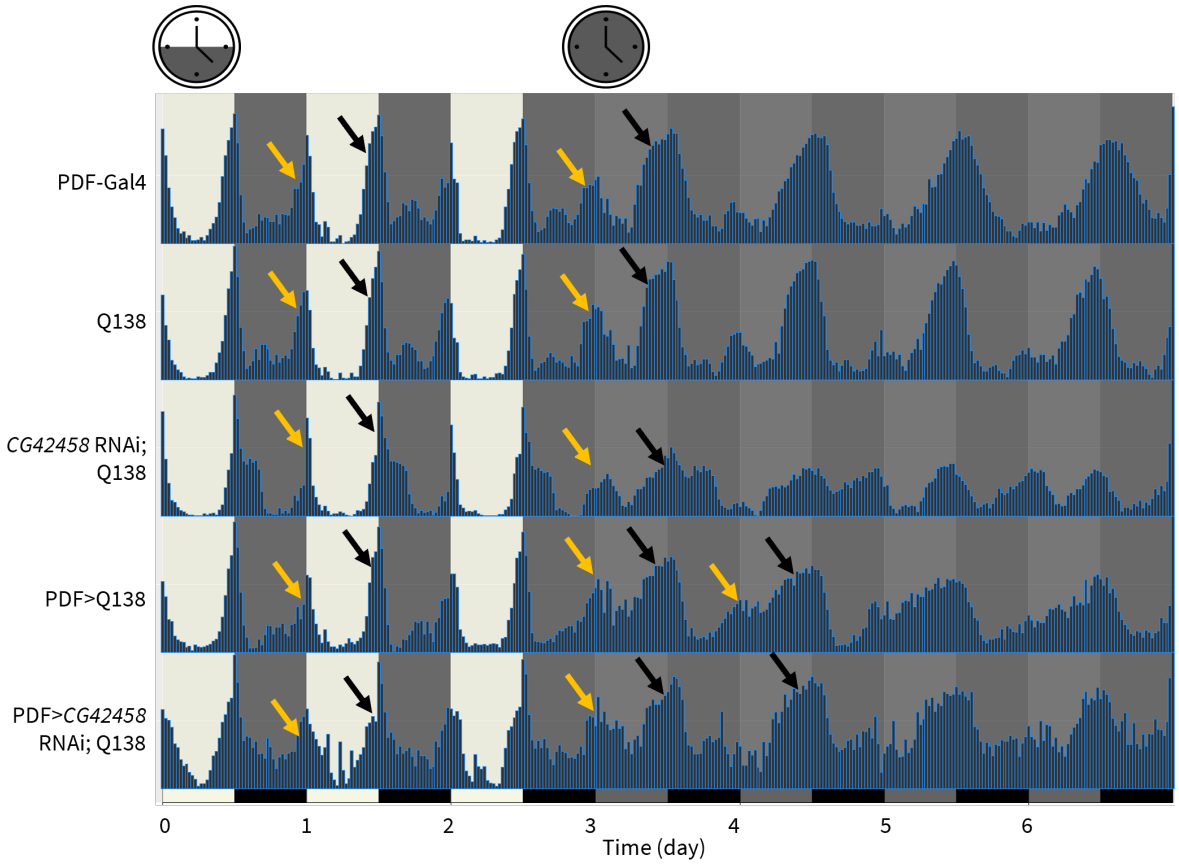

Figure 4-6 Activity plot showing that CG42458 knockdown does not seem to rescue Huntingtin-mediated circadian rhythm dysfunction.

Activity plot including the entrainment period (white and grey background) and the free-running period (grey and dark grey background). Activity is plotted as average of all flies in 30min bins. Yellow and black arrows indicate identifiable morning and evening peaks, respectively. Complete genotypes can be found in the results description 4.2.2.1.

4.2.2.1.2. CG42458 may be required for HttQ138-induced arrhythmicity

As previously described (4.2.1.1.): the mean power of rhythmicity (P-S), the number of flies that had a significant rhythm, and the mean period value of this significant behavioural rhythmicity, were extracted from the raw data.

During the free-running period, a significant difference in power of rhythmicity was detected between all groups (one-way ANOVA: $F_{4, 121} = 23.82$, $p < 0.001$) (Figure 4-7, B). Specifically, flies expressing the expanded form of *Htt* in PDF-positive neurons (PDF>Q138) demonstrated a sharp decrease in the rhythmicity which was statistically different when compared to the parental groups PDFGal4 ($p < 0.001$, Tukey's *post-hoc* test), and Q138 ($p < 0.001$, Tukey's *post-hoc* test). Knocking-down *CG42458* in these flies (PDF>*CG42458* RNAi; Q138) led to an 80% increase in the power of rhythmicity

compared to PDF>Q138, but this difference remained non-significant (p = 0.4158, Tukey's *post-hoc* test). The PDF>*CG42458* RNAi; Q138 group showed a power of rhythmicity value around 40% lower than its parental groups PDFGal4 (p = 0.12, Tukey's *post-hoc* test) and *CG42458* RNAi; Q138 (p = 0.06, Tukey's *post-hoc* test), suggesting that the observed increase brought the power of rhythmicity close to control levels. As expected, no differences were found between the groups during the entrainment period (one-way ANOVA: $F_{4, 123}$ = 10.78, p < 0.001), with the exception of the PDF>*CG42458* RNAi; Q138 group which had a significantly decreased power when compared to the *CG42458* RNAi; Q138 parental control group (p < 0.001, Tukey's *post-hoc* test) (Figure 4-7, A).

The percentage of rhythmic flies and their peak period values were extracted. Most control flies were rhythmic during the entrainment period, with 94% of the flies in the PDFGal4 group, 100% in the Q138 group, and 97% in the *CG42458* RNAi; Q138 group (Figure 4-7, C). The two experimental groups did have a slight decrease in the percentage of rhythmic flies, with 88% and 78% of flies showing rhythmicity in the PDF>Q138, and the PDF>*CG42458* RNAi; Q138 groups, respectively. No significant difference was detected using Fisher's exact tests between parental and experimental groups. All rhythmic flies had a mean period value of 24 hours.

However, when the lighting condition was switched to constant darkness, only 46% of the flies from the PDF>Q138 group showed rhythmicity, a significant decrease when compared to its parental groups (PDFGal4 vs PDF>Q138: p < 0.001; Q138 vs PDF>Q138: p < 0.001, Fisher's exact test) (Figure 4-7, D). PDF>Q138 exhibited a mean period of 23.75 h. When *CG42458* was knocked down in transgenic flies expressing *Htt*Q138, the percentage of rhythmic flies increased to 67%, a non-significant difference compared to the PDF>Q138 group (p = 0.44, Fisher's exact test). These flies had a mean period of 24.50 h, showing that *CG42458* knockdown did not re-establish power of rhythmicity levels similar the control groups, but it did rectify the period value close to a normal 24 h period.

In comparison, 94%, 97% and 84% of the flies had a significant rhythmicity in the PDFGal4, the Q138, and the *CG42458* RNAi; Q138 groups, respectively. The Q138 control group had a shorter period of 23.75 h, and the *CG42458* RNAi; Q138 group had a longer period value of 25.75 h.

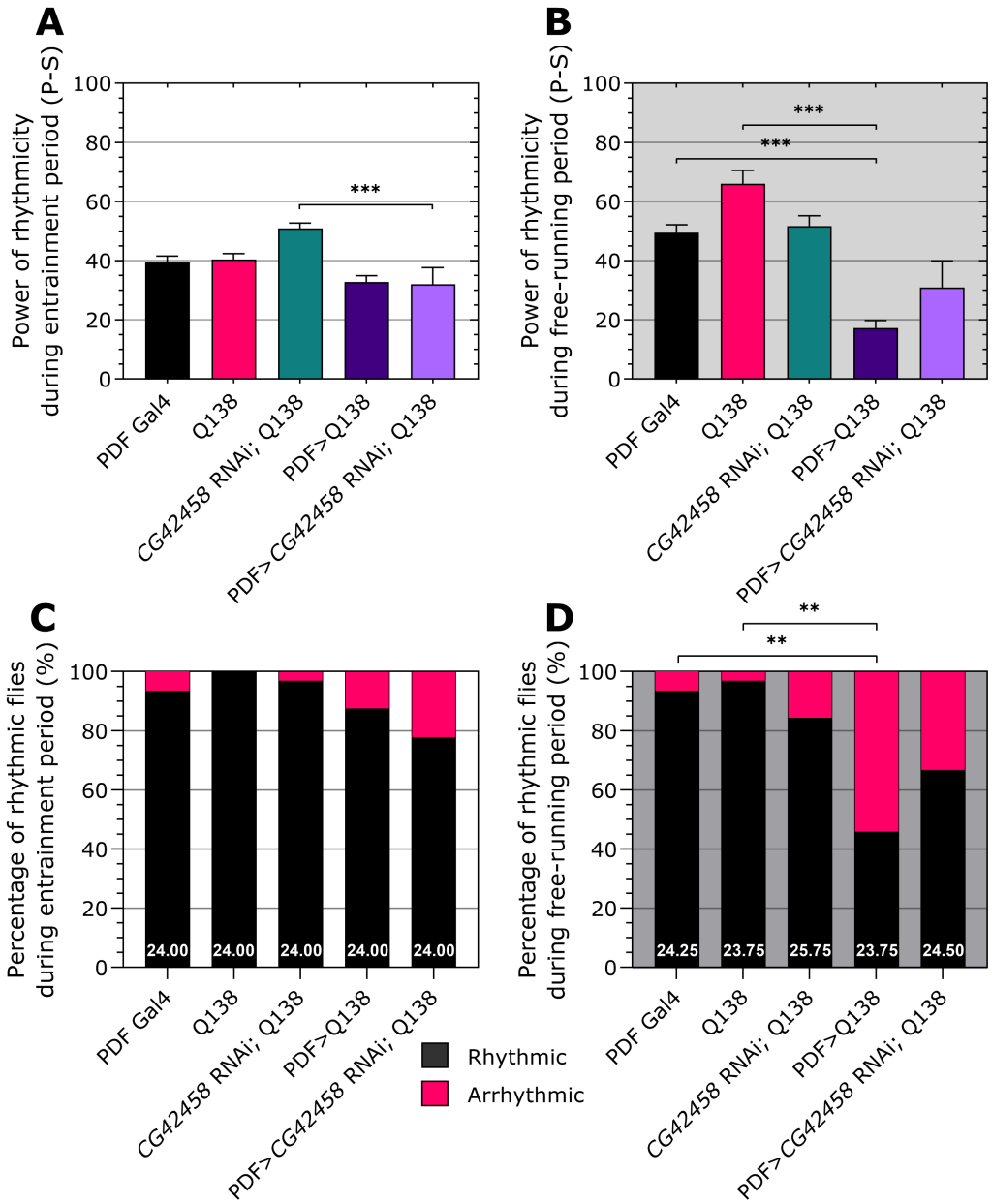

Figure 4-7 CG42458 may be required for Huntingtin-mediated arrhythmicity.

*Average power of rhythmicity during the entrainment period (A) and the free-running period (B) conditions. Power of rhythmicity corresponds to Power – Significance (P-S). Mean value calculated using individual fly values from SleepMat (Sisobhan et al., 2022). Data presented as mean ± SEM, ***p < 0.001, Tukey's multiple comparison post-hoc test. (C) Percentage of rhythmic and arrhythmic flies during the entrainment period, and (D) the free-running period conditions. Flies were considered rhythmic if they had a P-S ≥ mean P-S during entrainment divided by two. Bonferroni adjusted p-values obtained from Fischer's exact test comparing parental crosses to experimental crosses, **p < 0.001. Annotated value inside the black rectangles correspond to the mean period of rhythmic flies. Complete genotypes can be found in the results description 4.2.2.1.*

4.2.2.2. Cellular toxicity

Immunostaining was conducted to assess whether the observed circadian rhythm dysfunction induced by the expanded form of *Htt* could be associated with cell death or HTT aggregation in the sLNvs. Regardless of individual rhythmicity values, flies from the behavioural experiment were promptly dissected and their brains were stained for PDF and mRFP-*Htt*Q138.

4.2.2.2.1. CG42458 knockdown does not improve PDF neuron survivability

As previously described, a PDF staining was performed to detect and count the number of identifiable sLNvs per hemisphere and measured the mean PDF signal intensity in their somas (2.2.5.3).

Across the three groups, no significant difference in the number of sLNv somas (one-way ANOVA: $F_{2, 20} = 2.350$, $p = 0.1212$) (Figure 4-8, B). The PDFGal4 control group had an average of 2.93 sLNvs per hemisphere. This number decreased to 1.69 sLNv per hemisphere in flies expressing *Htt*Q138 in PDF-expressing neurons (PDF>Q138) ($p = 0.1118$, Tukey's *post-hoc* test). In transgenic flies expressing both *Htt*Q138 and the *CG42458* RNAi construct (PDF>*CG42458* RNAi; Q138), the number increased to 2.5 slNvs per hemisphere. This group was not statistically different to the PDF>Q138 ($p = 0.3431$, Tukey's *post-hoc* test), nor to the control PDFGal4 group ($p = 0.7484$, Tukey's *post-hoc* test).

PDF intensity did not differ significantly across the three groups (one-way ANOVA: $F_{2, 20} = 3.038$, $p = 0.0705$) (Figure 4-8, C). Expression of *Htt*Q138 in PDF-expressing neurons led to a non-significant 26% decrease in the intensity of the signal when compared to the PDFGal4 control group ($p = 0.6695$, Tukey's *post-hoc* test). Down-regulating *CG42458* increased the intensity of the signal by 98%, but this difference remained non-significant when compared to PDF>Q138 ($p = 0.0601$, Tukey's *post-hoc* test).

Overall, it seems that downregulating *CG42458* could rescue the circadian rhythm dysfunctional phenotype induced *Htt*Q138 expression, but does not rescue the decreased number of identifiable PDF-positive sLNvs.

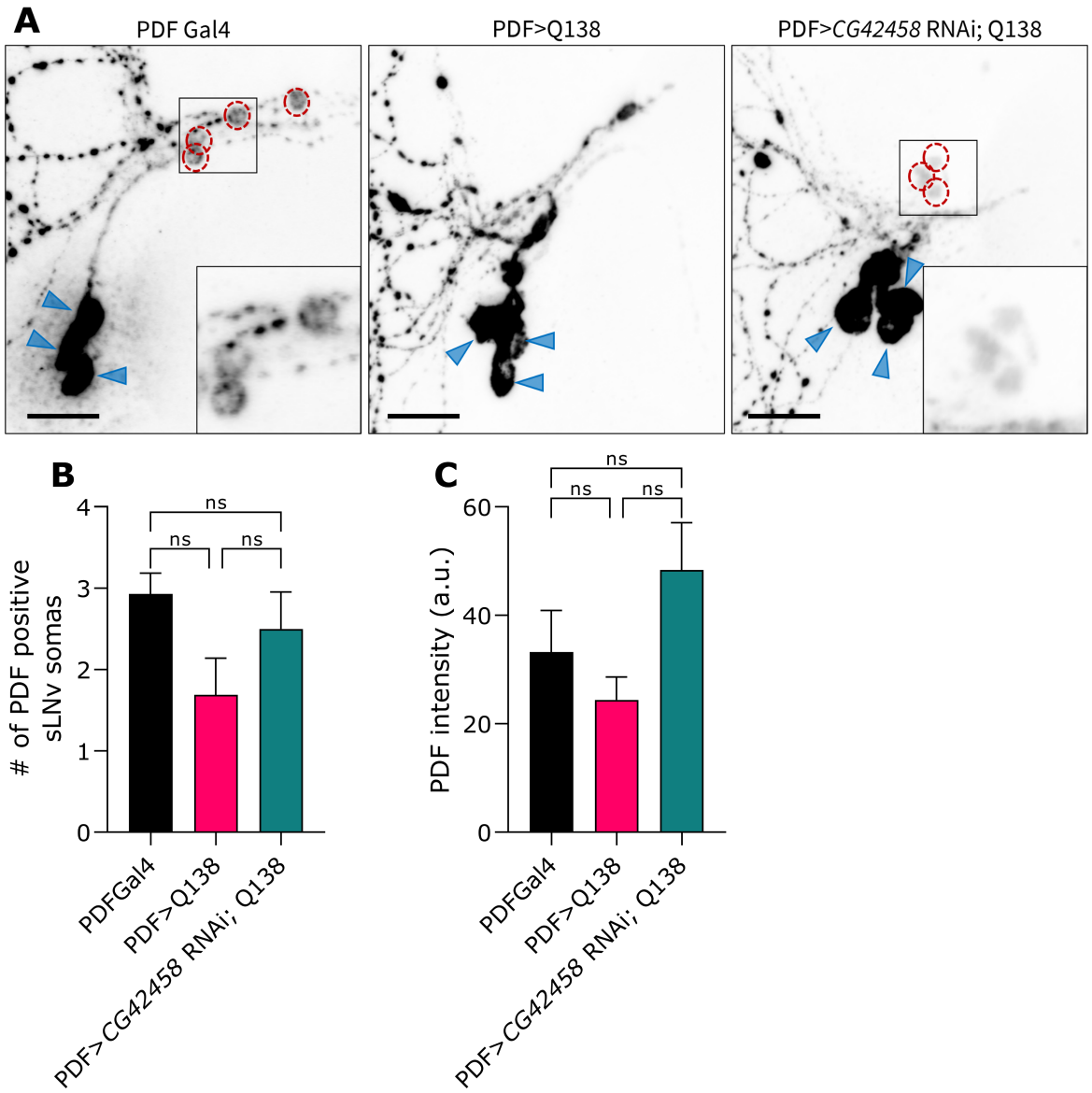

Figure 4-8 CG42458 does not modulate cell death induced by HttQ138.

(A) Representative images of brain sections from the groups PDFGal4, PDF>Q138, and PDF>CG42458 RNAi; Q138, stained with a PDF antibody. sLNvs and lLNvs are labelled with red dotted circles and with blue arrows, respectively. Black scale bar represents 20 µm. sLNvs are magnified in the insets in the bottom right corner. Imaged using a Zeiss LSM880 confocal microscope. (B) Quantification of the number of identifiable somas in all three groups, data are presented as bar graphs representing the mean ± SEM (n = 8). (C) Quantification of PDF signal intensity from identifiable sLNv somas in all three groups, data are presented as bar graphs representing the mean ± SEM (n = 8). Complete genotypes can be found in the results description 4.2.2.1.

4.2.2.2.2. CG42458 knockdown does not affect volume of Htt aggregates

As previously described (4.2.1.2.2), the volume of HTT aggregates was measured. Results and representative images are reported in Figure 4-9.

The volume of the HTT aggregates differed significantly between the three groups (one-way ANOVA: $F_{2, 15} = 3.686$, $p = 0.0499$) (Figure 4-9, J). As expected, the expression of *Htt*Q138 led to a 65-fold increase in the volume of the HTT aggregates in comparison to the PDFGal4 control, although this difference remained non-significant, possibly due to the low *n* value for the PDFGal4 group ($p = 0.2638$, Tukey's *post-hoc* test). *CG42458* knockdown had no significant effect on this observed phenotype, with a 60% increase in the volume of the HTT aggregates ($p = 0.2994$, Tukey's *post-hoc* test).

The analysis of the HTT staining in these three groups suggests that knocking-down the expression of *CG42458* has no effect on the volume of these HTT aggregates, similarly to the lack of effect on the circadian rhythm.

Overall, the behavioural readout seems to suggest that *CG42458* could mediate toxicity induced by the expression of an expanded form of *Htt*, however, *CG42458* downregulation had no effect on cell survivability or HTT aggregation. These results and their limitations, specifically in relation to the inadequate controls, will be further discussed in the discussion section (4.3).

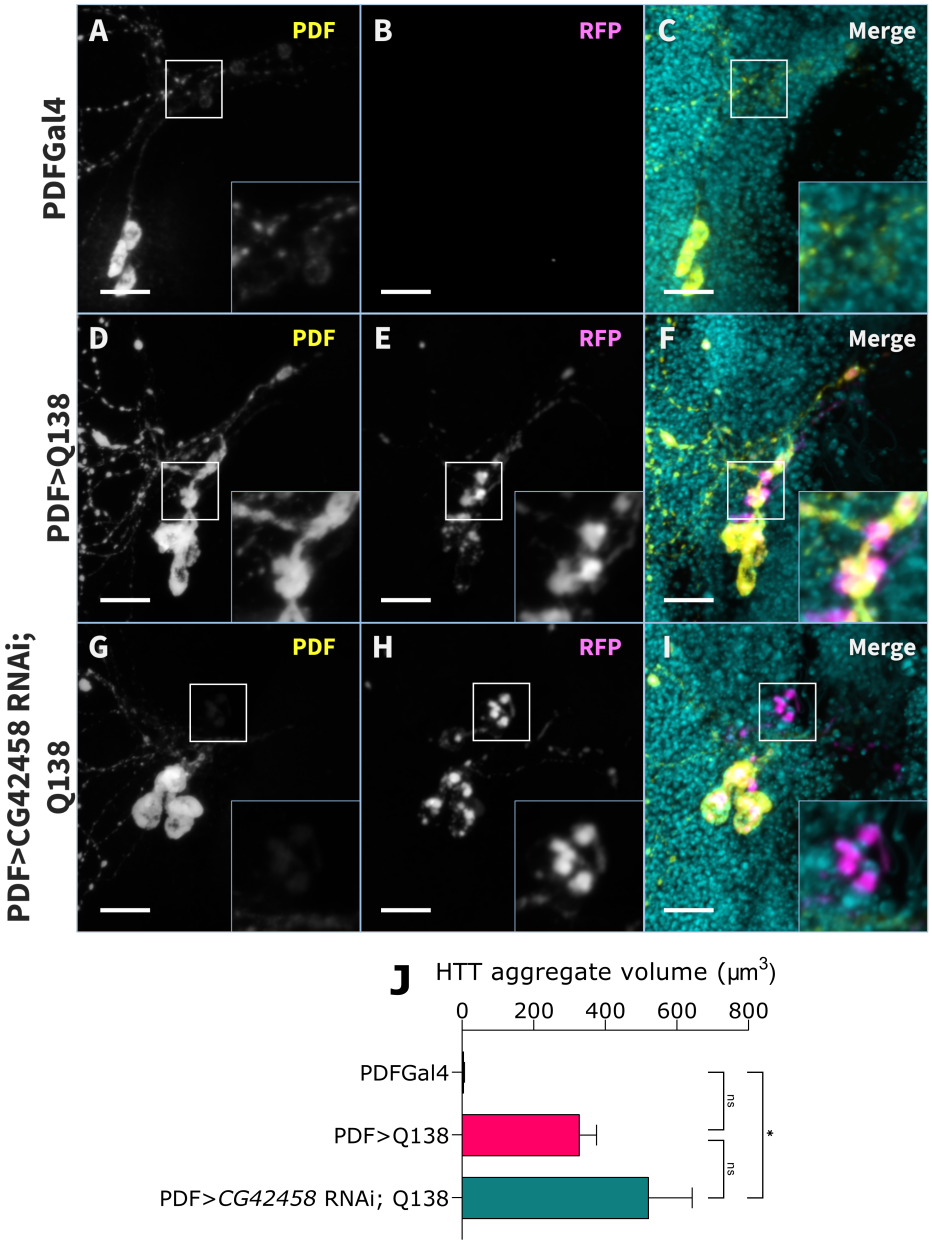

Figure 4-9 CG42458 does not modulate HttQ138 aggregate formation in the brain.

*Brains were dissected and stained using anti-PDF (anti-mouse 488 – yellow), anti-RFP (anti-rabbit 555 – magenta) and DAPI (cyan). Representative z-stacked images with corresponding insets in grey: (A – C) PDFGal4, (D – F) PDF>Q138, (G – I) PDF>CG42458 RNAi; Q138. White scale bar represents 20 µm. (J) Staining analysis of HTT aggregate volume. Data are presented as bar graphs representing the mean ± SEM. N values PDFGal4 = 2, PDF>Q138 = 8, and PDF>CG42458 RNAi; Q138 = 8. *p < 0.05, one-way ANOVA with Tukey's post-hoc test), ns: non-significant. Complete genotypes can be found in the results description 4.2.2.1.*

4.2.3. Ataxin-2 mediates huntingtin toxicity in circadian rhythm neurons

Recent work investigating the molecular mechanism leading to HD pathogenesis has uncovered a possible link with RBPs, and ribonucleoprotein (RNP) granule components. Wild-type HTT is not a known component of RNP granules, nor are the expanded HTT aggregates known to sequester RNP granule components. Despite this, recently published work has demonstrated that Ataxin-2 (ATX2), and its C-domain intrinsically disordered region (IDR), promotes HTT aggregation and neurodegeneration (Huelsmeier et al., 2021; Xu et al., 2019b). To confirm the role of this known RNP granule component, an RNAi construct was used to down-regulate *atx2* gene expression in transgenic flies that were expressing a CAG expanded form of human *Htt*, associated to a UAS effector and the mRFP fluorophore (*UAS-mRFP-HttQ138*). These constructs were expressed in PDF-positive neurons using a PDFGal4 driver. The generated flies were used for analysis of their behavioural circadian rhythm and for assessment of cell death via immunohistochemistry.

4.2.3.1. Behaviour readout

Experimental flies were generated by crossing a PDFGal4 driver line with a line containing the *UAS-mRFP-HttQ138* construct, or a line containing both the UAS *atx2* RNAi and the *UAS-mRFP-HttQ138* constructs. Control parental lines were also generated to have the PDFGal4 driver, and the UAS effectors by themselves. The generated genotypes were the following:

- *$y^{[1]}$, w*/-; PDFGal4/+; PDFGal4/+* (referred to as PDFGal4);
- *+/-; +/+; UAS-mRFP-HttQ138/+* (referred to as Q138);
- *+/-; UAS atx2 RNAi (VDRC)/+; UAS-mRFP-HttQ138* (referred to as *atx2* RNAi; Q138);
- *$y^{[1]}$, w*/-; PDFGal4/+; PDFGal4/UAS-mRFP-HttQ138* (referred to as PDF>Q138);
- *$y^{[1]}$, w*/-; PDFGal4/UAS atx2 RNAi (VDRC); PDFGal4/UAS-mRFP-HttQ138* (referred to as PDF>*atx2* RNAi; Q138).

4.2.3.1.1. Locomotor activity

The behavioural experiment was conducted identically to previous sections (4.2.1.1.) (Figure 4-10). All genotypes exhibited a regular behavioural circadian rhythm during the entrainment period (white and black background), with defined morning and evening activity peaks (yellow and black arrows, respectively). As reported in the two previous sections, during the free-running period begins (black and dark-grey background) both morning and evening activity peaks remain unaltered in control groups, whereas they are promptly dampened in the PDF>Q138 group. Importantly, *atx2* knockdown partially restored the peaks in *Htt*Q138-expressing flies when compared to the PDF>Q138 group. Although the morning peak does decrease over time, the evening peak remains nearly as robust as the control groups (black arrows).

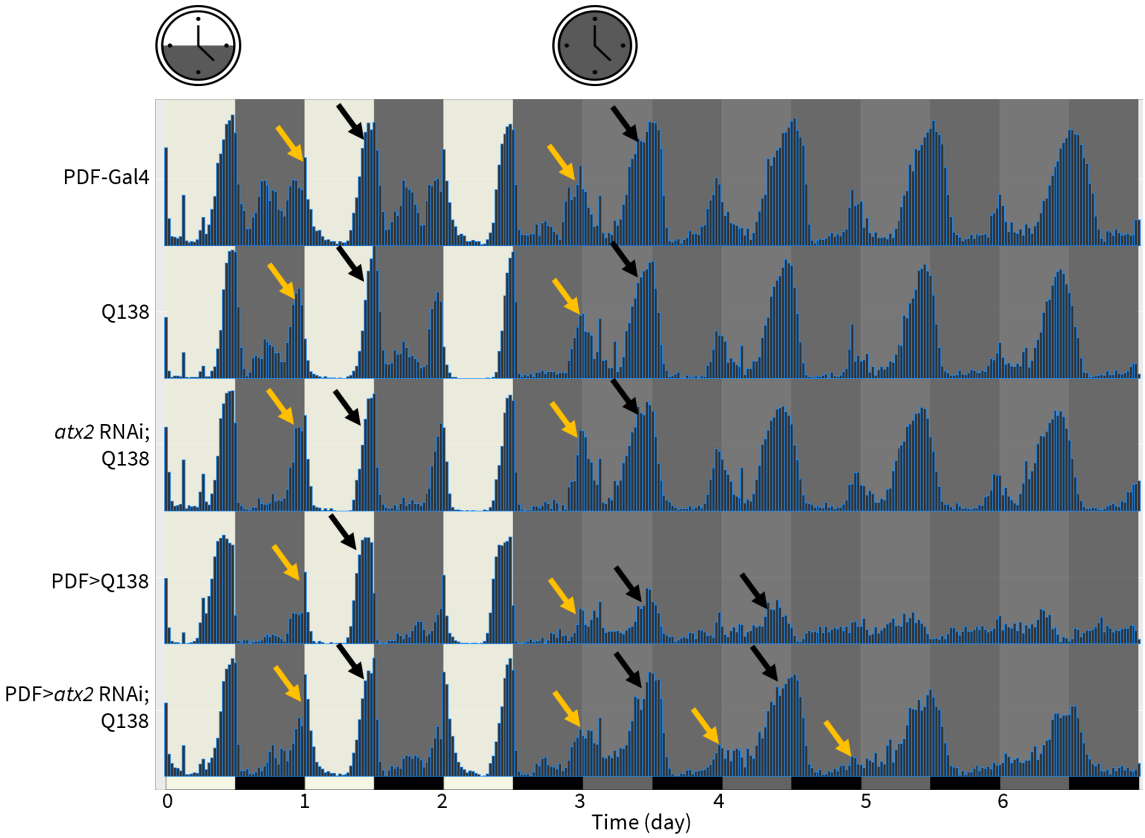

Figure 4-10 Activity plot showing that Ataxin-2 is required for Huntingtin-mediated circadian rhythm dysfunction.

Activity plot including the entrainment period (white and grey background) and the free-running period (grey and dark-grey background). Activity is plotted as average of all flies in 30min bins. Yellow and black arrows indicate identifiable morning and evening peaks, respectively. Complete genotypes can be found in the results description 4.2.3.1.14.2.3.1.

4.2.3.1.2. ATX2 is required for HttQ138-induced arrhythmicity

As described in previous sections, the mean power of rhythmicity (P-S), the number of flies that had a significant rhythm, and the mean period value of this significant behavioural rhythmicity, were extracted from the raw data.

During the free-running period, groups showed a significant difference in their power of rhythmicity (one-way ANOVA: $F_{4, 151} = 70.58$, $p < 0.001$) (Figure 4-11, B). Specifically, flies expressing the expanded form of *Htt* in PDF-positive neurons (PDF>Q138) demonstrated a sharp decrease in the rhythmicity which was statistically different when compared to the parental groups PDFGal4 ($p < 0.001$, Tukey's *post-hoc* test), and Q138 ($p < 0.001$, Tukey's *post-hoc* test). Knocking-down *atx2* in these flies (PDF>*atx2* RNAi; Q138) led to a significant rescue by increasing the power of rhythmicity eight-fold compared to the PDF>Q138 group ($p < 0.001$, Tukey's *post-hoc* test). Although the power of rhythmicity was increased in this group, it did not rescue to control levels ($p < 0.001$, vs PDFGal4 and *atx2* RNAi; Q138, Tukey's *post-hoc* test). As expected, no differences were found between the groups during the entrainment period, with the exception of the PDF>*atx2* RNAi; Q138 group which had a significantly decreased power when compared to the *atx2* RNAi; Q138 parental control group ($p = 0.0224$, Tukey's *post-hoc* test) (one-way ANOVA: $F_{4, 151} = 3.311$, $p = 0.0124$) (Figure 4-11, A).

During the free-running period, only 10% of the flies from the PDF>Q138 group showed rhythmicity, a significant decrease compared to its two parental groups (PDFGal4 vs PDF>Q138: $p < 0.001$; Q138 vs PDF>Q138: $p < 0.001$, Fisher's exact test) (Figure 4-11, D). PDF>Q138 also exhibited a mean period of 23 h, further demonstrating the loss of a circadian rhythm caused by *Htt*Q138. When *atx2* was knocked down in the PDF>*atx2* RNAi; Q138 group, the percentage of flies that were rhythmic increased back to 81.25%, a significant increase compared to PDF>Q138 ($p < 0.001$, Fisher's exact test). These flies had a mean period of 24.25 h, showing that not only has a significant periodicity been re-established in most flies, it has also been rectified to the normal 24 h period. As expected, control flies from the PDFGal4, the Q138, and from the Q138; *atx2* RNAi groups were all rhythmic. Interestingly, the Q138 and *atx2* RNAi; Q138 control groups had a slightly shorter period of around 23.75 h when subjected to constant darkness.

As expected, during the entrainment period, 94% of the flies in the PDFGal4 group, 97% in the Q138 group, and 100% in the *atx2* RNAi; Q138 group (Figure 4-11, C). The two experimental groups did have a slight decrease in the percentage of rhythmic flies which remained non-significant compared to the parental groups, with 77% and 81% of flies showing rhythmicity in the PDF>Q138, and the PDF>*atx2* RNAi; Q138 groups, respectively. All rhythmic flies had a mean period value of 24 hours.

Overall, these results demonstrate that the neuronal toxicity induced by the expanded form of *Htt*, measured through locomotor circadian rhythm, is mediated by the RNP granule component ATX2. These results are in accordance with previous literature (Huelsmeier et al., 2021; Xu et al., 2019b), and will be further discussed in the following sections.

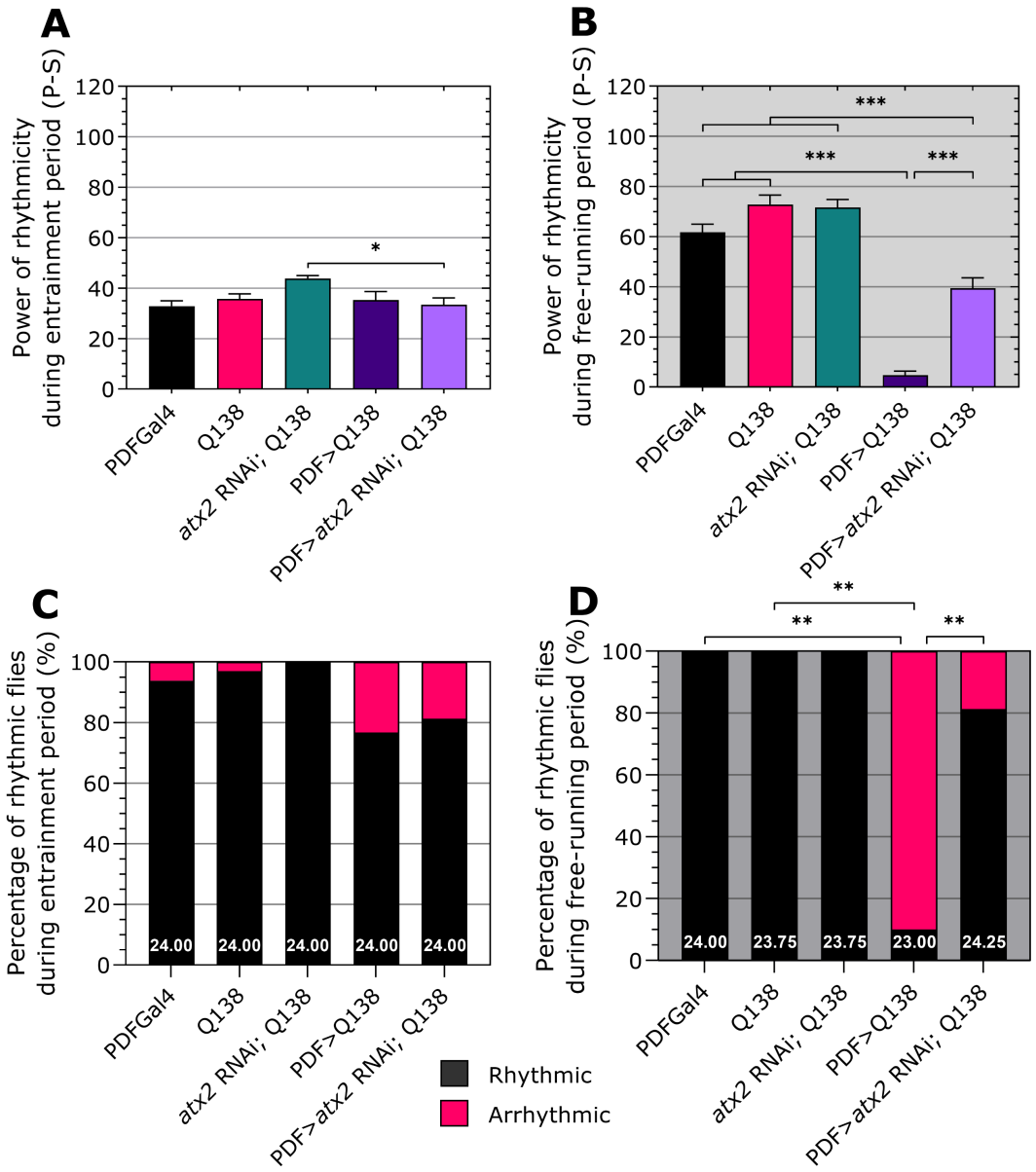

Figure 4-11 Ataxin-2 is required for HttQ138-mediated arrhythmicity.

*Average power of rhythmicity during the entrainment period (A) and the free-running period (B) conditions. Power of rhythmicity corresponds to Power – Significance (P-S). Mean value calculated using individual fly values from SleepMat (Sisobhan et al., 2022). Data presented as mean ± SEM, *p < 0.05, **p < 0.01, and ***p < 0.001, Tukey's multiple comparison post-hoc test. (C) Percentage of rhythmic and arrhythmic flies during the entrainment period, and (D) the free-running period conditions. Flies were considered rhythmic if they had a P-S ≥ mean P-S during entrainment divided by two. Bonferroni adjusted p-values obtained from Fischer's exact test comparing parental crosses to experimental crosses, **p < 0.001. Annotated value inside the black rectangles correspond to the mean period of the rhythmic flies. Complete genotypes can be found in the results description 4.2.3.1.*

4.2.3.2. Cellular toxicity

Knocking-down the expression of *atx2* led to a significant rescue of the circadian rhythm. As in previous sections, the number of identifiable sLNvs, their PDF intensity, and HTT aggregation, were assessed. Regardless of individual rhythmicity values, flies from the behavioural experiment were promptly dissected and the brains were stained for PDF and mRFP-*Htt*Q138.

4.2.3.2.1. Atx2 knockdown decreases survivability of sLNvs

The number of identifiable sLNvs per hemisphere were quantified using the PDF staining, and the mean PDF signal intensity in their somas was measured (2.2.5.3).

There was a significant difference between groups in the number of identifiable sLNvs (one-way ANOVA: $F_{2, 37}$ = 38.34, p < 0.001) (Figure 4-12, B). More specifically, the PDFGal4 control group had an average of 3.16 sLNvs per hemisphere. This number significantly decreased to 1.71 sLNvs per hemisphere in flies expressing *Htt*Q138 in PDF-expressing neurons (PDF>Q138) (p < 0.001, Tukey's *post-hoc* test). The number decreased to 0.15 slNvs per hemisphere in transgenic flies expressing both *Htt*Q138 and the *atx2* RNAi construct (PDF>*atx2* RNAi; Q138). This decrease was significantly different when compared to PDF>Q138 (p < 0.001, Tukey's *post-hoc* test) and to the control PDFGal4 group (p < 0.001, Tukey's *post-hoc* test).

When looking at the signal intensity of the somas, a similar trend was observed, even though differences were not statistically significant (one-way ANOVA: $F_{2, 24}$ = 3.254, p = 0.0562) (Figure 4-12, C). Expression of *Htt*Q138 in PDF-expressing neurons led to a non-significant 23% decrease in the intensity of the signal when compared to the PDFGal4 control group (p = 0.4570, Tukey's *post-hoc* test). Knocking-down *atx2* decreased the intensity of the signal by 86% in observable somas (n = 2), but this difference remained non-significant when compared to PDF>Q138 (p = 0.1819, Tukey's *post-hoc* test).

Overall, downregulation of *atx2* rescues the dysfunctional circadian rhythm induced by *Htt*Q138 expression, and surprisingly also decreases the number of identifiable PDF-positive sLNvs, suggesting an interesting role for ATX2 in this model of neurodegeneration.

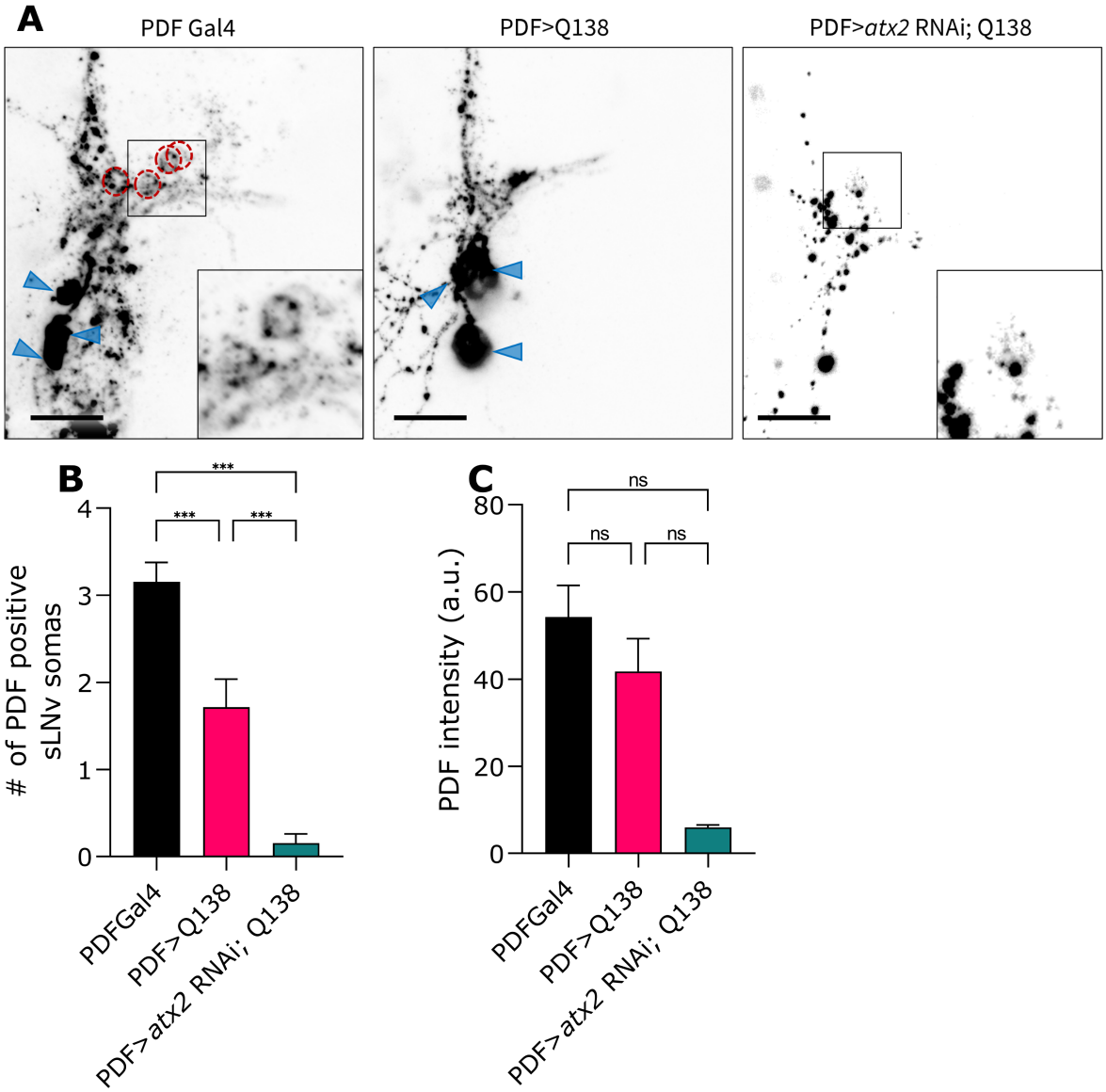

Figure 4-12 Ataxin-2 knockdown aggravates cell death induced by HttQ138.

*(A) Representative images of brain sections from the groups PDFGal4, PDF>Q138, and PDF>atx2 RNAi; Q138, stained with a PDF antibody. sLNvs and lLNvs are labelled with red dotted circles and with blue arrows, respectively. Black scale bar represents 20 µm. sLNvs are magnified in the insets in the bottom right corner. Imaged using a Zeiss LSM880 confocal microscope. (B) Quantification of the number of identifiable somas in all three groups, data are presented as bar graphs representing the mean ± SEM, from left to right PDFGal4 (n = 13), PDF>Q138 (n = 14), and PDF>atx2 RNAi; Q138 (n = 13). (C) Quantification of PDF signal intensity from identifiable sLNv somas in all three groups, data are presented as bar graphs representing the mean ± SEM, from left to right PDFGal4 (n = 13), PDF>Q138 (n = 12), and PDF>atx2 RNAi; Q138 (n = 2), ***p < 0.001, ns: non-significant. Complete genotypes can be found in the results description 4.2.3.1.*

4.2.3.2.2. Atx2 knockdown decreases volume of Htt aggregates

As previously described (4.2.1.2.2), volume of the HTT aggregates was measured. Results and representative images are reported in Figure 4-13.

A significant difference in the volume of the HTT aggregates between the three groups was detected (one-way ANOVA: $F_{2, 35} = 13.71$, $p < 0.001$) (Figure 4-13, J). As expected, the expression of *Htt*Q138 led to a significant 7-fold increase in the volume of the HTT aggregates in comparison to the PDFGal4 control ($p = 0.0002$, Tukey's *post-hoc* test). Knockdown of *atx2* led to a significant 80% decrease in the volume of the identifiable HTT aggregates ($p = 0.0003$, Tukey's *post-hoc* test).

As already mentioned, the analysis of HTT in this work is limited by the lack of appropriate controls. However, the results suggest that knocking-down the expression of *atx2* greatly affects the formation, or clearance, of these HTT aggregates. These results in conjunction with the behavioural results indicates a role for ATX2 in mediating the toxicity induced by the expression of an expanded form of *Htt*. Although the unexpected decrease in identifiable PDF-positive neurons after *atx2* knockdown differs with the rescued circadian rhythm. These results and their limitations will be further discussed (4.3.1.3).

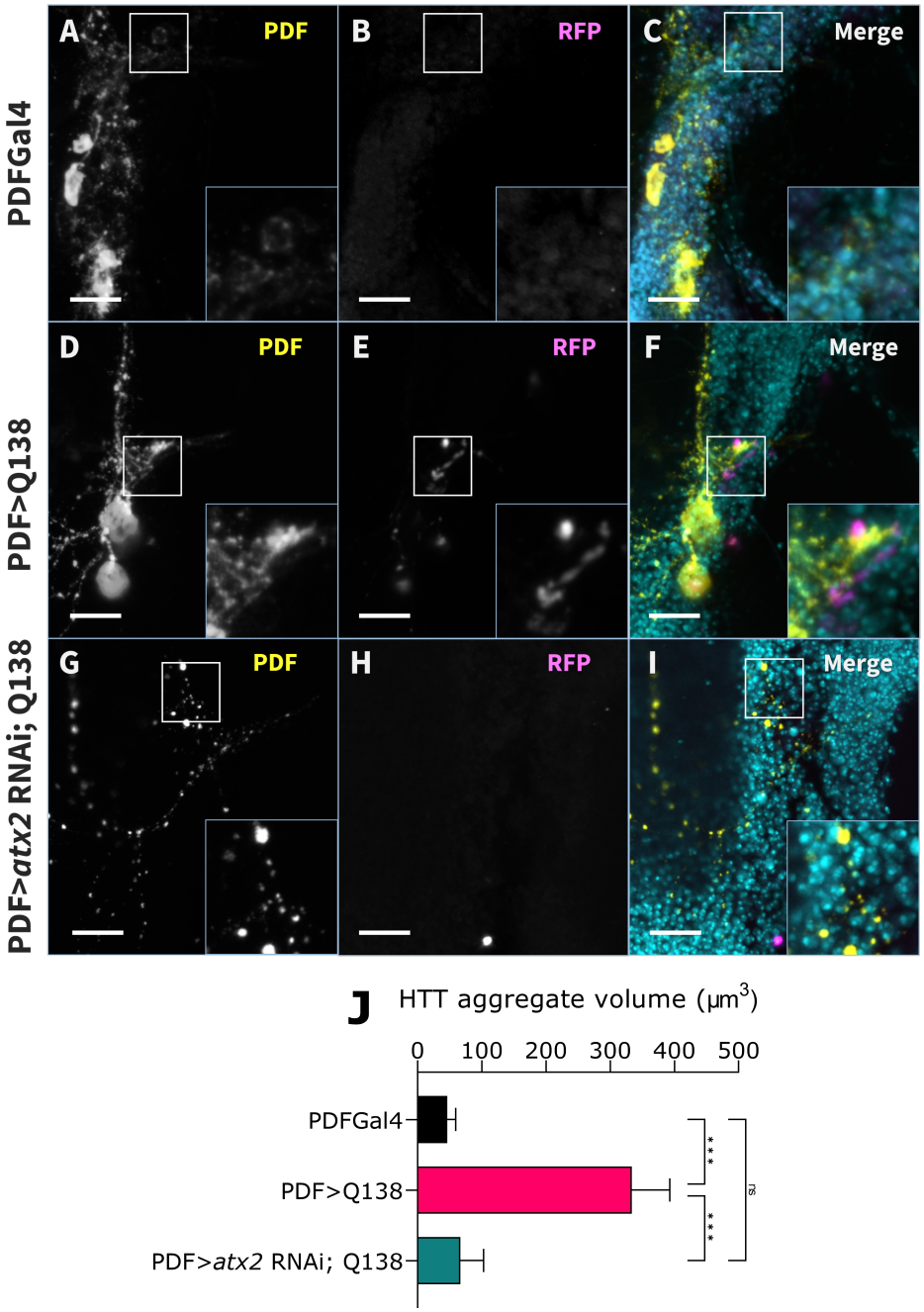

Figure 4-13 Ataxin-2 modulates HttQ138 aggregate formation in the brain.

*Brains were dissected and stained using anti-PDF (anti-mouse 488 – yellow), anti-RFP (anti-rabbit 555 – magenta) and DAPI (cyan). Representative z-stacked images with corresponding insets in grey: (A – C) PDFGal4, (D – F) PDF>Q138, (G – I) PDF>atx2 RNAi; Q138. White scale bar represents 20 µm. (J) Staining analysis of HTT aggregate volume. Data are presented as bar graphs representing the mean ± SEM. N values: PDFGal4 = 11, PDF>Q138 = 14, and PDF>atx2 RNAi; Q138 = 13. ***p < 0.001 (one-way ANOVA with Tukey's post-hoc test), ns: non-significant. Complete genotypes can be found in the results description 4.2.3.1.*

4.2.4. Rasputin may play a protective role against Huntingtin toxicity

Rasputin (Rin) is the *Drosophila* ortholog for the human G3BP protein family (G3BP1 and G3BP2). As previously mentioned, recent studies have reported a possible role for G3BP1 and SG assembly in HD pathogenesis (Sanchez et al., 2021), and more specifically a possible ameliorative role in HD-related protein aggregation (Gutierrez-Garcia et al., 2023). These findings taken together suggest an important role for G3BP in neurodegenerative diseases, and in particular HD. To study the role of this known SG component, an RNAi construct was used to down-regulate the expression of *rin* in transgenic flies that were expressing a CAG expanded form of human *Htt*, associated to a UAS effector and the mRFP fluorophore (*UAS-mRFP-HttQ138*). These constructs were expressed in PDF-positive neurons using a PDFGal4 driver. The generated flies were used for analysis of their behavioural circadian rhythm and for assessment of cell death via immunohistochemistry.

4.2.4.1. Behaviour readout

Experimental flies were generated by crossing a PDFGal4 driver line with a line containing the *UAS-mRFP-HttQ138* construct, or a line containing both the UAS *rin* RNAi and the *UAS-mRFP-HttQ138* constructs. Control parental lines were also generated to have the PDFGal4 driver, and the UAS effectors by themselves. The generated genotypes were the following:

- *$y^{[1]}$, w*/-; PDFGal4/+; +/+* (referred to as PDFGal4);
- *+/-; +/+; UAS-mRFP-HttQ138/+* (referred to as Q138);
- *+/-; UAS rin RNAi (VDRC)/+; UAS-mRFP-HttQ138* (referred to as *rin* RNAi; Q138);
- *$y^{[1]}$, w*/-; PDFGal4/+; UAS-mRFP-HttQ138/+* (referred to as PDF>Q138);
- *+/-; PDFGal4/UAS rin RNAi (VDRC); UAS-mRFP-HttQ138/+*
  (referred to as PDF>*rin* RNAi; Q138).

4.2.4.1.1. Locomotor activity

Locomotor activity was measured over several days and two different lighting conditions (Figure 4-14). As previously observed, all genotypes show a regular behavioural circadian rhythm during the entrainment period (white and grey background), with defined morning and evening peaks (yellow and black arrows, respectively). When the free-running period begins (black and dark-grey background), these defined peaks remain clearly identifiable in all control groups except for the *rin* RNAi; Q138 group, however their amplitude decreases over time. In comparison, the morning peaks are promptly dampened in the PDF>Q138 group over the course of the four days, with none being identifiable on the fifth and sixth days. Finally, in the PDF>*rin* RNAi; Q138 group, general locomotor activity is drastically dampened during the free-running period. Neither morning or evening peaks are identifiable from the second day in constant darkness condition. Overall, *rin* knockdown seems to worsen the dysfunctional circadian rhythm induced by the expression of *Htt*Q138.

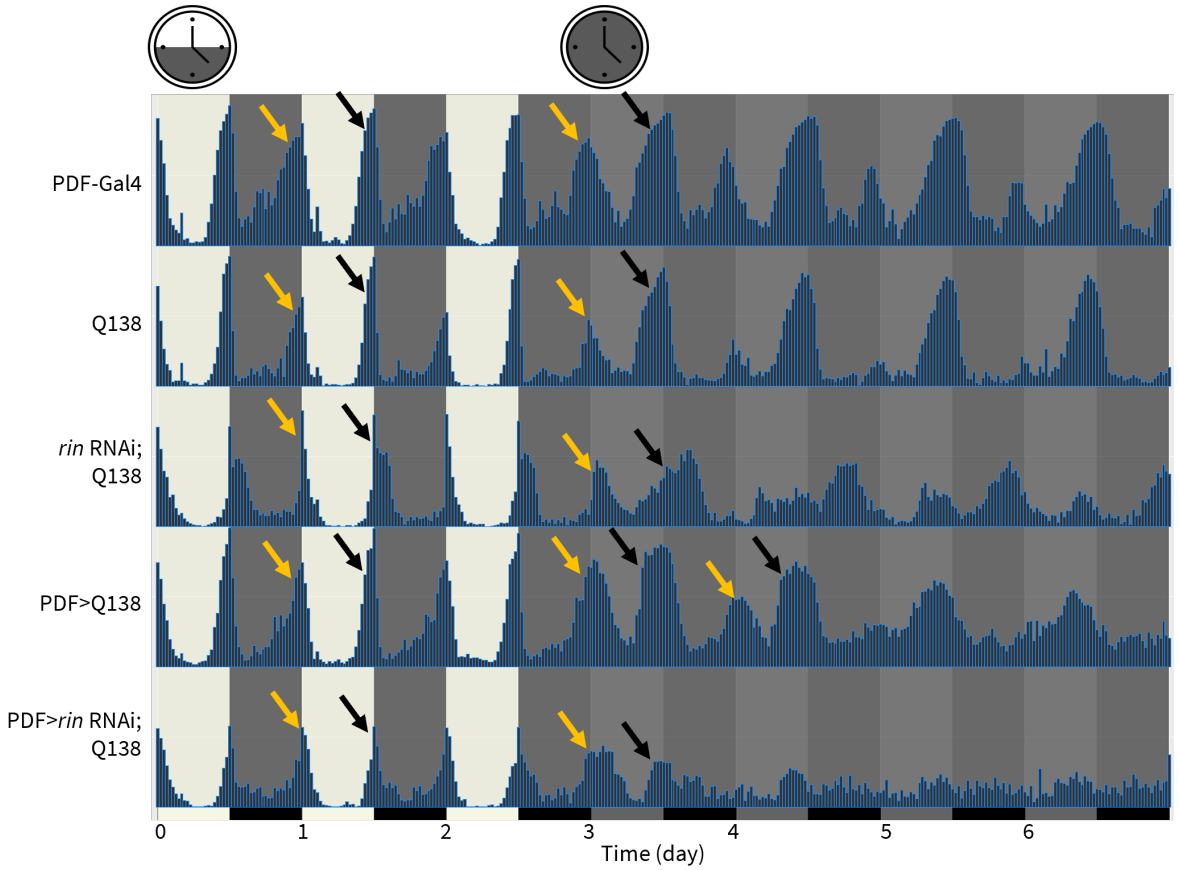

Figure 4-14 Activity plot showing that Rasputin may play a protective role against Huntingtin-mediated circadian rhythm dysfunction.

Activity plot including the entrainment period (white and grey background) and the free-running period (grey and dark-grey background). Activity is plotted as average of all flies in 30min bins. Yellow and black arrows indicate identifiable morning and evening peaks, respectively. Complete genotypes can be found in the results description 4.2.4.1.

4.2.4.1.2. Rin knockdown worsens HttQ138-induced arrhythmicity

The mean power of rhythmicity (P-S), the number of flies that had a significant rhythm, and the mean period value of this significant behavioural rhythmicity were extracted from the raw data (4.2.1.1.).

During the free-running period, groups exhibited a significant difference in the power of rhythmicity (one-way ANOVA: $F_{4, 135} = 44.27$, $p < 0.001$) (Figure 4-15, B). Specifically, flies expressing the expanded form of *Htt* in PDF neurons (PDF>Q138) demonstrated a sharp decrease in the rhythmicity which was statistically different when compared to the parental groups PDFGal4 ($p < 0.001$, Tukey's *post-hoc* test), and Q138 ($p < 0.001$, Tukey's *post-hoc* test). Knocking-down *rin* in these flies (PDF>*rin* RNAi; Q138) led to a significant 72% decrease in the power of rhythmicity compared to the PDF>Q138

group (p = 0.0312, Tukey's *post-hoc* test). The PDF>*rin* RNAi; Q138 group was also significantly different to its parental groups PDFGal4 ($p < 0.001$, Tukey's *post-hoc* test) and *rin* RNAi; Q138 ($p < 0.001$, Tukey's *post-hoc* test).

As expected, no differences were found between the groups during the entrainment period (one-way ANOVA: $F_{4, 136} = 5.054$, $p = 0.0008$), with the exception of the PDF>*rin* RNAi; Q138 group which had a significantly decreased power when compared to the *rin* RNAi; Q138 parental group (p = 0.0046, Tukey's *post-hoc* test) (Figure 4-15, A).

During the entrainment period, all groups showed high percentages of rhythmicity. Indeed, 97% of the flies in the PDFGal4 group, 87% in the Q138 group, 100% in the *rin* RNAi; Q138 group, 94% in the PDF>Q138 group, and 84% in the PDF>*rin* RNAi; Q138 group, showed rhythmicity. No significant difference was detected using Fisher's exact tests between parental and experimental groups. All rhythmic flies had a mean period value of 24 hours. (Figure 4-15, C)

In comparison, when the lighting condition was switched to constant darkness, only 58% of the flies from the PDF>Q138 group showed rhythmicity, a significant decrease when compared to its parental groups (PDFGal4 vs PDF>Q138: p = 0.002; Q138 vs PDF>Q138: p = 0.002, Fisher's exact test) (Figure 4-15, D). Interestingly, PDF>Q138 exhibited a mean period of 23 hours, further demonstrating the loss of a behavioural circadian rhythm caused by *Htt*Q138. When *rin* was knocked down in the PDF>*rin* RNAi; Q138 group, the percentage of flies that were rhythmic further decreased to 16%, a significant difference compared to the PDF>Q138 group (p = 0.004, Fisher's exact test). However, these flies had a mean period of 24 h, showing that *rin* knockdown aggravated the effect of *Htt*Q138 on the power of rhythmicity, but it rectified the period value to a normal 24h period. As expected, 94%, 93% and 89% of the control flies had a significant rhythmicity in the PDFGal4, the Q138, and the *rin* RNAi; Q138 groups, respectively. The *rin* RNAi; Q138 control group had a slightly shorter period value of 23.75 h.

Overall, the analysis of the circadian rhythm seems to confirm the observations made from the locomotor activity plot: knocking-down the expression of *rin* further deteriorates the dysfunctional circadian rhythm induced by *Htt*Q138 expression.

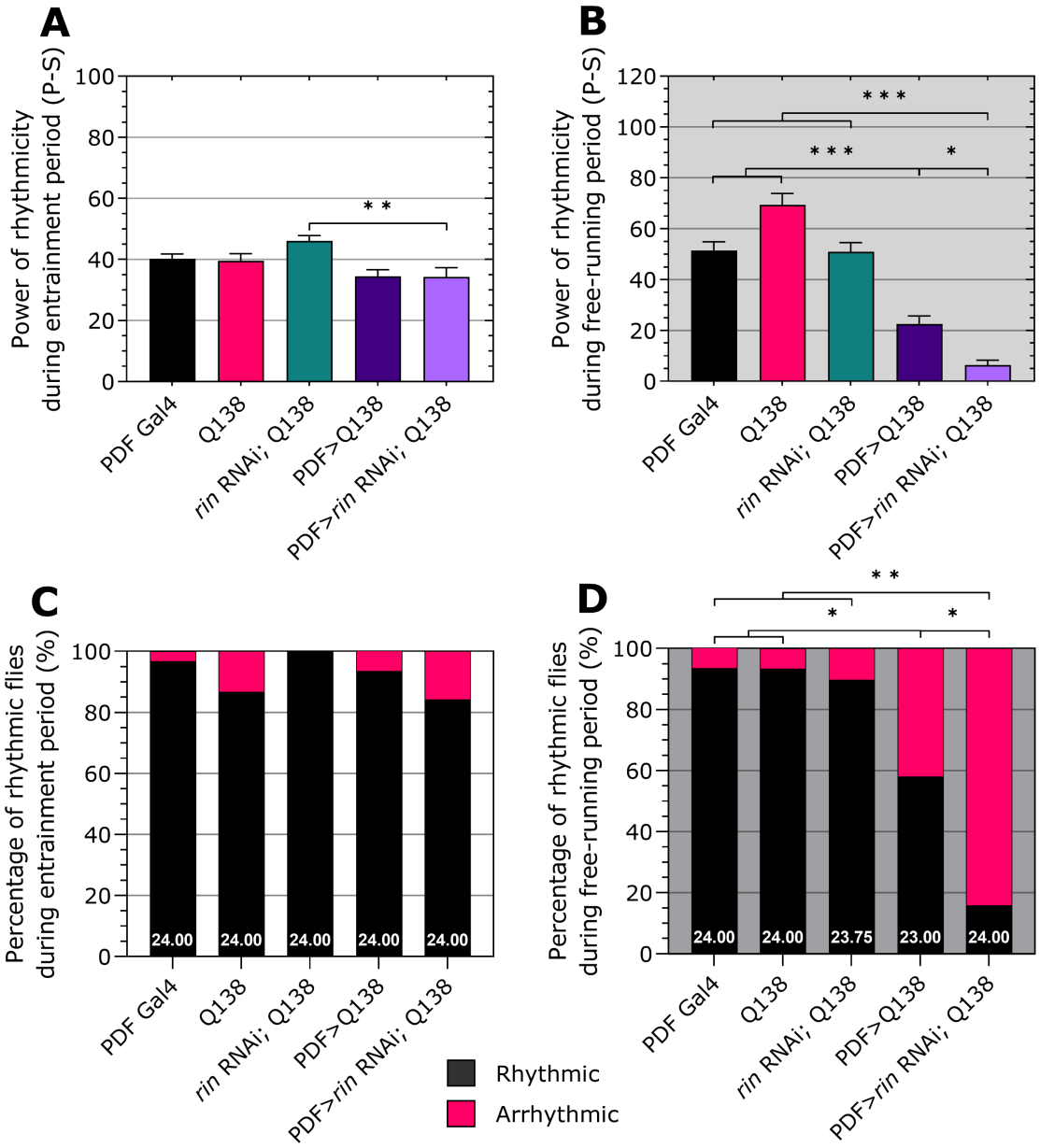

Figure 4-15 Rin knockdown aggravates HttQ138-induced arrhythmicity.

*Average power of rhythmicity during the entrainment period (A) and the free-running period (B) conditions. Power of rhythmicity corresponds to Power – Significance (P-S). Mean value calculated using individual fly values from SleepMat (Sisobhan et al., 2022). Data presented as mean ± SEM, *p < 0.05, **p < 0.01, and ***p < 0.001, Tukey's multiple comparison post-hoc test. (C) Percentage of rhythmic and arrhythmic flies during the entrainment period, and (D) the free-running period conditions. Flies were considered rhythmic if they had a P-S ≥ mean P-S during entrainment divided by two. Bonferroni adjusted p-values obtained from Fischer's exact test comparing parental crosses to experimental crosses,*p < 0.01,**p < 0.001. Annotated value inside the black rectangles correspond to the mean period of the rhythmic flies. Complete genotypes can be found in the results description 4.2.4.1.*

4.2.4.2. Cellular toxicity

Knocking-down the expression of *rin* led to a significant deterioration of the circadian rhythm. Immunostaining of the brains was done to test whether the observed rhythmicity deterioration with the *rin* RNAi construct is associated with an increased death of sLNvs, or of HTT aggregation. Regardless of individual rhythmicity values, flies from the behavioural experiment were promptly dissected and the brains were stained for PDF and mRFP-*Htt*Q138.

4.2.4.2.1. Rin knockdown does not affect PDF neurons survivability

The number of identifiable sLNvs per hemisphere were quantified using the PDF staining, and the mean PDF signal intensity in their somas was measured (2.2.5.3). Results are reported in Figure 4-16.

The number of identifiable sLNv somas differed significantly between groups (one-way ANOVA: $F_{2, 29}$ = 4.611, p = 0.02) (Figure 4-16, B). As expected, the PDFGal4 had an average of 3.1 sLNvs per hemisphere. This number significantly decreased to 1.64 sLNvs per hemisphere in flies expressing *Htt*Q138 in PDF-positive neurons (PDF>Q138) (p < 0.03, Tukey's *post-hoc* test). The number slightly increased to 1.73 sLNvs per hemisphere in transgenic flies expressing both *Htt*Q138 and the *rin* RNAi construct (PDF>*rin* RNAi; Q138). This decrease was not significantly different when compared to PDF>Q138 (p = 0.98, Tukey's *post-hoc* test) but significantly lower compared to the PDFGal4 group (p = 0.04, Tukey's *post-hoc* test).

Expression of *Htt*Q138 in PDF-expressing neurons led to a non-significant 31% decrease in the intensity of the signal when compared to the PDFGal4 group (p = 0.1059, Tukey's *post-hoc* test) (one-way ANOVA: $F_{2, 23}$ = 2.271, p = 0.1258) (Figure 4-16, C). Knocking-down *rin* slightly increased the intensity of the signal by 25% in observable somas, but this difference remained non-significant when compared to PDF>Q138 (p = 0.4958, Tukey's *post-hoc* test).

Overall, *rin* knockdown deteriorates the circadian rhythm phenotype in this model of neurodegeneration, but does not lead to a further decrease in the number of identifiable PDF-positive sLNvs or their PDF intensity.

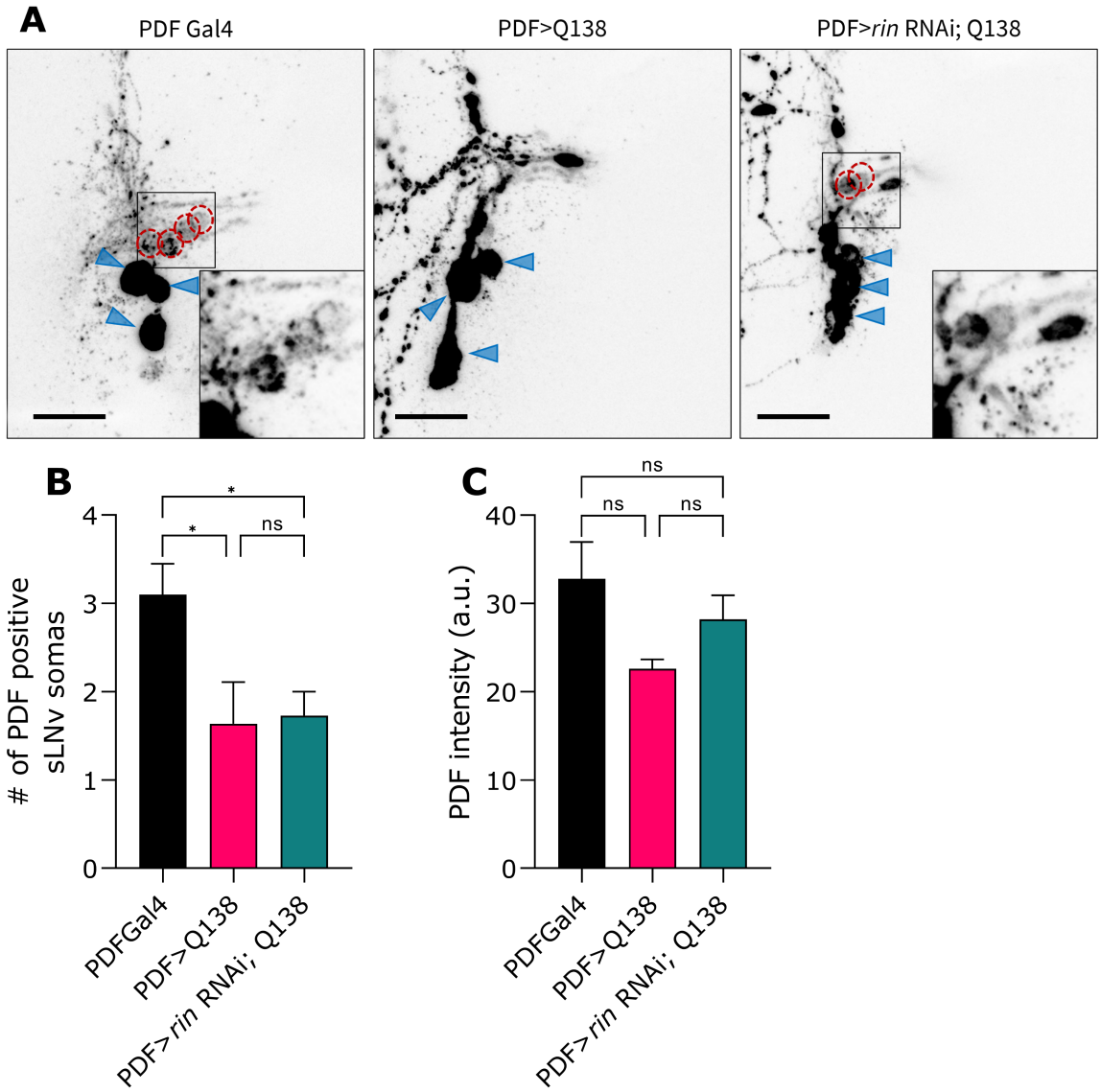

Figure 4-16 Rasputin knockdown does not affect cell death induced by HttQ138.

(A) Representative images of brain sections from the groups PDFGal4, PDF>Q138, and PDF>rin RNAi; Q138, stained with a PDF antibody. sLNvs and lLNvs are labelled with red dotted circles and with blue arrows, respectively. Black scale bar represents 20 µm. sLNvs are magnified in the insets in the bottom right corner. Imaged using a Zeiss LSM880 confocal microscope.

*(B) Quantification of the number of identifiable somas in all three groups, data are presented as bar graphs representing the mean ± SEM, from left to right PDFGal4 (n = 10), PDF>Q138 (n = 11), and PDF>rin RNAi; Q138 (n = 11). (C) Quantification of PDF signal intensity from identifiable sLNv somas in all three groups, data are presented as bar graphs representing the mean ± SEM, from left to right PDFGal4 (n = 10), PDF>Q138 (n = 7), and PDF>rin RNAi; Q138 (n = 9), *p < 0.05, ns: non-significant. Complete genotypes can be found in the results description 4.2.4.1.*

4.2.4.2.2. Rin knockdown increases the volume of Htt aggregates

As previously described (4.2.1.2.2), volume of the HTT aggregates was measured. Results and representative images are reported in Figure 4-17.

A significant difference in the volume of the HTT aggregates between the three groups was detected (one-way ANOVA: $F_{2,29} = 53.02$, $p < 0.001$) (Figure 4-17, J). The expression of *Htt*Q138 led to a significant 11-fold increase in the volume of the HTT aggregates in comparison to the PDFGal4 control ($p < 0.001$, Tukey's *post-hoc* test). Knockdown of *rin* led to a significant 55% increase in the volume of the identifiable HTT aggregates ($p = 0.001$, Tukey's *post-hoc* test).

The analysis of HTT aggregates suggest that knocking-down the expression of *rin* greatly increases the formation, or decreases the clearance, of these HTT aggregates.

These results in conjunction with the behavioural results indicates a protective role for Rin in this model of neurodegeneration. However, as previous reports have suggested that Rin is required for normal neuronal function, these results may simply be originating from neuronal toxicity due to a decreased Rin expression. These results and their limitations will be further discussed (4.3.1.3.2).

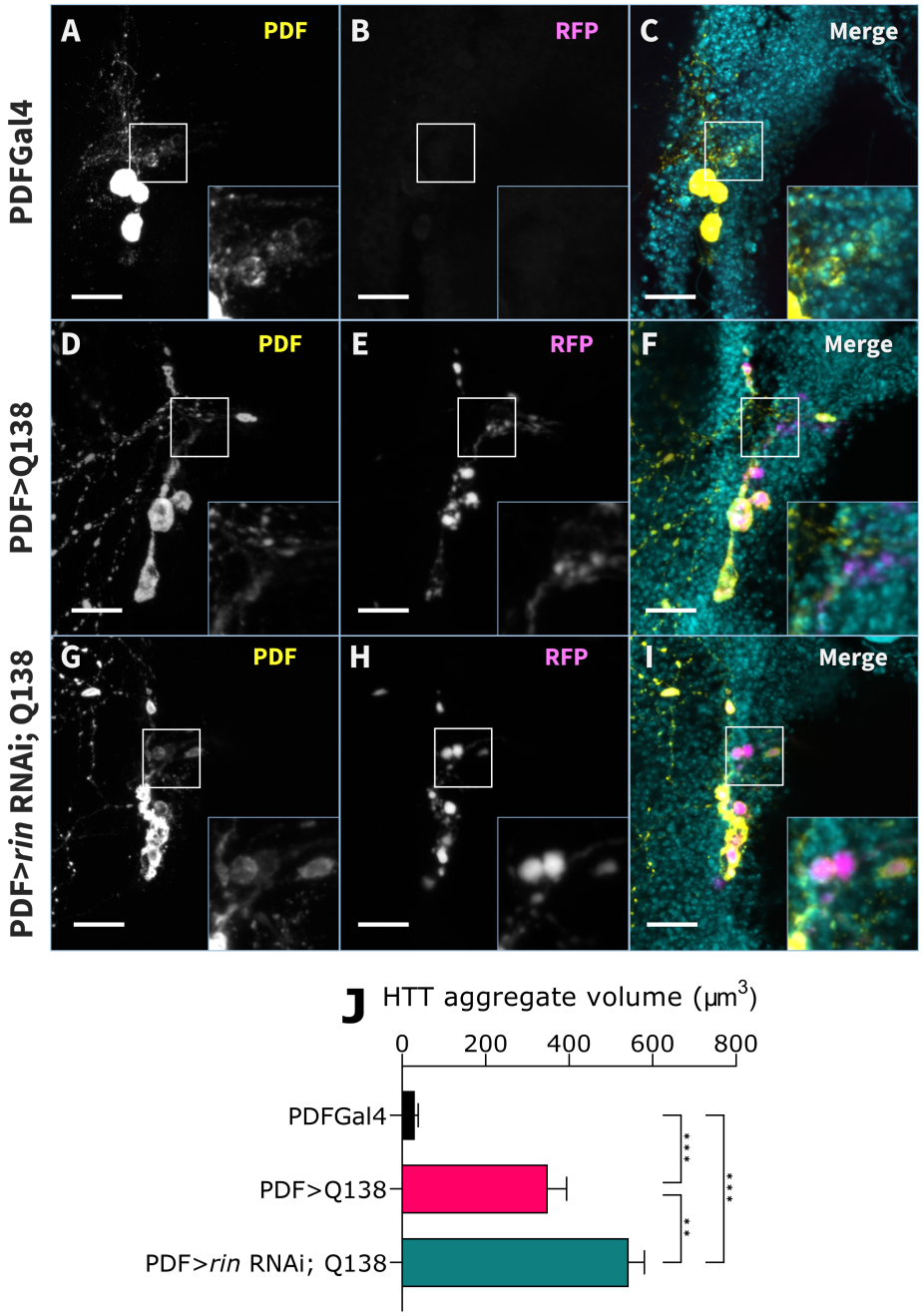

Figure 4-17 Rasputin modulates HttQ138 aggregate formation in the brain.

*Brains were dissected and stained using anti-PDF (anti-mouse 488 – yellow), anti-RFP (anti-rabbit 555 – magenta) and DAPI (cyan). Representative z-stacked images with corresponding insets in grey: (A – C) PDFGal4, (D – F) PDF>Q138, (G – I) PDF>rin RNAi; Q138. White scale bar represents 20 µm. (J) Staining analysis of HTT aggregate volume. Data are presented as bar graphs representing the mean ± SEM. N values from: PDFGal4 = 10, PDF>Q138 = 11, and PDF>rin RNAi; Q138 = 11. **p < 0.01 ***p < 0.001 (one-way ANOVA with Tukey's post-hoc test), ns: non-significant. Complete genotypes can be found in the results description 4.2.4.1.*

4.3. Discussion

The experiments in this chapter were designed to assess whether specific proteins are involved in a model of neurodegeneration induced by a polyglutamine expansion in the human *Htt* gene (*Htt*Q138). By knocking-down the expression of specific transcripts using RNAi constructs, we can ask whether these proteins can alleviate the phenotype resulting from the expression of an expanded form of HTT, and so, expand the role of these proteins from retinal to neuronal degeneration. Circadian rhythm parameters are sensitive and reveal changes at a systems level and were used to assess neurodegeneration in this work. Indeed, PDF-expressing neurons are crucial for clock neuron synchrony in constant darkness. When these neurons dysfunction, the circadian rhythm in free-running conditions is disturbed (Lear et al., 2005; Mertens et al., 2005; Yoshii et al., 2009; L. Zhang et al., 2010). Expressing *Htt*Q138, can lead to aggregate formation in neurons and cells (Huelsmeier et al., 2021; Landles et al., 2010; Peskett et al., 2018), which can then affect their normal function, such as in regulating circadian rhythm (Xu et al., 2019a).

In this work, circadian rhythm dysfunction was measured in every experiment where *Htt*Q138 was expressed in PDF-positive neurons. This clear neurodegenerative phenotype was then rescued by knocking-down the expression of *ataxin-2* (*atx2*), and to a lesser extent, *perk* and *CG42458*. Interestingly, the neurodegenerative phenotype was further exacerbated when *rin* was knocked down.

The role of *atx2* in mediating this form of neurodegeneration has already been established (Xu et al., 2019b), and the experiments presented here are in accordance with these finding. Although ER stress and the ISR have been implicated in different forms of neurodegenerative diseases, the involvement of *perk*, and the possibility of reducing neurodegenerative phenotypes by downregulating the ISR is still a matter of debate (Ganz et al., 2020; Leitman et al., 2014; Shacham et al., 2021; Vidal et al., 2011). Recent work has also established a potential protective role for Rin in a different HD model in *C. elegans* (Gutierrez-Garcia et al., 2023), which would be in agreement with the results reported in this thesis.

In addition to assessing circadian rhythm dysfunction, cell survivability and HTT aggregation were assessed after expression of the *Htt*Q138 transgene, with and without the different RNAi constructs. Although, the interpretation of these results

come with a set of limitations that will be further discussed, knocking-down *atx2* led to a striking reduction in identifiable sLNv somas and a strong reduction in *Htt* expression and aggregation. In contrast, knockdown of *rin* did not significantly affect the survivability of sLNvs, but did increase the volume of HTT aggregates. These are novel findings which will be further interpreted.

Overall, the results presented in this chapter suggest that the proteins PERK, ATX2, and Rin, play a role in the pathogenesis of this HD model.

4.3.1. Pathways involved in *Htt*Q138-induced neurodegeneration

RNAi constructs were used to knockdown the expression of various genes and to study the different pathways and proteins involved in the pathogenesis induced by *Htt*Q138 expression. Although RNAi technology is widely used to screen for novel proteins in the context of different pathologies, as previously mentioned in Chapter 3, this technology comes with various limitations including the efficiency of knockdown and off-target effects. Both of these limitations have been discussed in Chapter 3, with methods adopted to decrease their consequences in this thesis. In addition to these two limitations, RNAi constructs may also be detrimental to general health (Alic et al., 2012). In the retinal degeneration model used in Chapter 3, flies were studied at five-days-old maximum. In the model of neurodegeneration used in this chapter, flies were kept alive until around ten-days-old. Therefore the possibility of RNAi expression affecting health should be taken into account when interpreting these results.

Neurodegeneration was assessed at a systems level using the circadian rhythm parameters, and at a cellular level by analysing sLNv cell viability and HTT protein aggregation. A correlation between reduced sLNv viability and a dysfunctional circadian rhythm was not anticipated as this behavioural readout is sensitive and reduced power of rhythmicity may appear long before cell death. Additionally, previous work has established that the presence of a single sLNv is enough to induce a behavioural rhythm (Helfrich-Forster, 1998).

The identification of these neurons was dependent on PDF expression, which leads to two major limitations. First, PDF gene expression or mRNA translation may be inhibited for various reasons when *Htt*Q138 is expressed or when specific genes are being down-regulated, which could lead to an underestimation of the number of sLNv

somas. Second, not only have studies demonstrated that PDF levels oscillate in a circadian fashion, but sLNvs have also been shown to morphologically change and adapt their synaptic contacts and arborisation across the day (Gorostiza et al., 2014; Herrero et al., 2020; Park et al., 2000). In the context of this work, although attention was given to dissect brains at the same time of day, PDF staining is still limited to whether the sLNvs were consistently expressing PDF.

Finally, the occasional presence of mutations in the genes *stubble* (*Sb*), *white* (*w*), and *yellow* (*yw*), and the expression of two PDFGal4 drivers in the ATX2 experiment, mean that these experiments can not be compared between each other. These genetic background differences are a limitation to this work as these can affect sleep behaviour.

These neurodegenerative readouts were used to assess whether different proteins known to contribute to different pathways were involved in the pathogenesis underlying *Htt*Q138 neurodegeneration. Of particular interest, PERK, CG42458, ATX2 and Rin were studied.

4.3.1.1. Integrated stress response/unfolded protein response

Previous literature has shown that the ISR and the UPR are activated in models of ND, including HD, as well as in post-mortem analysis of ND patients (Carnemolla et al., 2009; Hoozemans et al., 2009; Leitman et al., 2014; Leitman et al., 2013; Nishitoh et al., 2008; Vaccaro et al., 2013). Whether the activation of these pathways is protective or contributes to neurotoxicity remains unclear (Ganz et al., 2020; Hoozemans et al., 2009; Shacham et al., 2021). Therefore, using an RNAi construct to downregulate the expression of PERK is of particular interest. As demonstrated in Chapter 3, decreasing the expression of this kinase in a retinal degenerative model led to a significant rescue of the phenotype (3.2.3.1), suggesting that this protein may contribute to the toxicity induced by the *rdgB*^{9} mutation. If knocking-down its expression in this neurodegenerative model also leads to a phenotypic rescue, it would demonstrate a clear overlapping pathway between these two forms of cellular degeneration. It would also establish that PERK activity is linked to increased cytotoxicity in this model of neurodegeneration.

The results from this experiment show that the ISR could play a role in this model of neurodegeneration through the kinase PERK. Indeed, downregulating *perk* led to a 92% increase in the power of rhythmicity compared to the neurodegenerative group (PDF>Q138), bringing rhythmicity back to parental control levels. In addition, *perk* knockdown did not significantly increase the percentage of rhythmic flies, but did increase the period value from 23.50 h to 24.00 h, suggesting that decreasing the expression of *perk* in transgenic flies expressing the cytotoxic *Htt*Q138 transgene improved rhythmicity and re-establishes the circadian period value back to control levels.

In this experiment, expression of *Htt*Q138 in PDF-expressing neurons did lead to a degeneration of sLNv neurons. Although a trend was observed in both the number of sLNv somas and the PDF intensity, knocking-down the expression of *perk* did not lead to a significant improvement of this phenotype. Finally, *perk* knockdown had no impact on *Htt*Q138 aggregate volume compared to the neurodegenerative group (PDF>Q138).

Overall these results suggest that PERK may contribute to pathogenesis in this HD model. By knocking down its expression, the power of rhythmicity is mildly rescued and the period value is restored to normal values. This behavioural rescue could be correlated to the observed trend that *perk* knockdown increases the number of identifiable sLNv somas and PDF intensity, even though *Htt*Q138 aggregation does not seem to be impacted. This indicates that a decreased expression of PERK, and therefore a decreased phosphorylation of eIF2α, may lead to decreased cellular toxicity, but may not improve *Htt*Q138 clearance. This is consistent with a study conducted by Lee et al., (2012) that found that only the activity of the UPR kinase IRE1 is required for HTT aggregation. Overexpressing a dominant-negative mutant of PERK failed to inhibit aggregation, suggesting that among the three major ER stress sensors (IRE1, PERK, and ATF6), only IRE1 modulates the cytotoxic aggregation of HTT (Lee et al., 2012).

More studies need to be conducted to understand how modulating the expression of *perk* may affect a neurodegenerative phenotype as seen in this work without improving the toxic aggregation of HTT. Future experiments could aim to use different RNAi constructs targeting different ISR or UPR components, such as GCN2 or IRE1, to assess whether other proteins of these pathways are involved in this model of cellular degeneration. Additionally, using a null mutant of *perk*, feeding the flies a PERK

inhibitor, or the ISR inhibitor (ISRIB), may be useful to confirm the behavioural effect observed here.

4.3.1.2. Novel RNA-binding protein

As previously mentioned, RNA metabolism and homeostasis seems to be a crucial function that is affected in HD, with various RNA-binding proteins (RBPs) shown to be involved in the pathogenesis of HD (Kino et al., 2004; Li et al., 2008; McLaughlin et al., 1996; Mykowska et al., 2011; Nalavade et al., 2013). The wild-type HTT protein has been shown to associate with RBPs, and specifically RNP granule components (Savas et al., 2010). In an attempt to identify novel RBPs that may also be involved in the pathogenesis of HD, two proteins were selected for these experiments, namely SF3B2 and CG42458. Both of these RBPs have previously been found in large genetic screens to modulate neurodegenerative phenotypes (Appocher et al., 2017; Chaplot et al., 2019; Lee et al., 2016). SF3B2 has a role in RNA splicing, with the capacity to bind to the 12S RNA unit forming the key spliceosome component U2snRNP. Although the physiological function of CG42458 has not been identified, predicted functions inferred from its sequence include RNA stabilisation, RNA-binding, and is predicted to be located in the cytosol.

The RNAi lines used in this experiment were selected based on the results from Chapter 3; specifically whether they led to a significant knockdown of their target transcript. Interestingly, using the *sf3b2* RNAi (TRiP) line for this experiment proved to be difficult as it led to an unviable first filial generation. This suggests that this protein is particularly important in PDF-expressing neurons and for brain development, or that PDF is expressed in different tissues at different time-points during development. A previous study using *in situ* hybridisation found that *sf3b2* was heavily expressed in the early stages of embryonic development, in the primordium of the embryonic central brain (Hammonds et al., 2013). Future experiments could employ conditional expression of the RNAi construct to study the role of SF3B2 in this model of neurodegeneration. This could be achieved by using a thermosensitive Gal80 to inhibit Gal4, preventing gene expression unless the flies are placed at the appropriate temperature.

The *CG42458* RNAi (VDRC) line led to a normal first filial generation, and the experiment was conducted as planned. However, due to the original *CG42458* RNAi line

and time constraints, a mutation in the stubble (S*b*) gene was present in all groups in this experiment, which should be taken into account when interpreting these results. The presence of this marker may account for behavioural variability. Unexpectedly, the parental control group expressing the *Htt*Q138 and *CG42458* RNAi constructs led to a decreased amplitude in locomotion, as seen in the activity plot (Figure 4-6), which may suggest a leaky expression of the RNAi construct. As expected, the expression of *Htt*Q138 in PDF-expressing neurons led to a significant decrease in the power of rhythmicity. Transgenic flies that were also expressing the *CG42458* RNAi construct showed a slight increase in the power of rhythmicity, but this difference remained non-significant compared to flies expressing only the *Htt*Q138 transgene. The percentage of rhythmic flies also remained unchanged with *CG42458* knockdown. In terms of cellular toxicity, this experiment did not find a significant difference in the number of identifiable sLNvs or PDF intensity between groups. Finally, *CG42458* knockdown did not lead to any significant difference in the volume of the identifiable HTT aggregates, although a trend to increase their volume was observed.

Overall, these results show that this protein does not seem involved in the pathogenesis of this neurodegenerative model. The observed trend in rescuing the decreased power of rhythmicity in flies expressing *Htt*Q138 justifies additional experiments to validate the observations from this experiment with appropriate controls.

4.3.1.3. RNP granule components

RNP granules, including stress granules (SGs), have been extensively studied in recent years in the context of neurodegenerative diseases. A dysfunction in their formation has been implicated in the development of various neurodegenerative diseases, including ALS, FTD and HD (Wolozin & Ivanov, 2019). Specific proteins have been identified as key components of RNP granules, some of which are required for granule formation in specific conditions. Their role in the development of neurodegenerative diseases remain unclear, although recent studies suggest that the dysfunctional formation of RNP granules contributes to HD pathogenesis (Huelsmeier et al., 2021; Savas et al., 2010; Savas et al., 2008; Xu et al., 2019b). ATX2 in particular has attracted attention as a possible therapeutic target for diseases such as SCA2, ALS and FTD. Indeed, knocking-down *atx2*, or removing its intrinsically disordered region (IDR),

reduces SG formation and improves neurodegenerative phenotypes (Bakthavachalu et al., 2018). In addition, knocking-down *atx2* has also been associated to improved circadian rhythm in a neurodegenerative model of HD (Xu et al., 2019b). These observations taken together make ATX2 an interesting target to study in this model of neurodegeneration.

The SG component G3BP1, or Rin in *Drosophila*, has been shown to be necessary for stress-granule formation (Aguilera-Gomez et al., 2017; Laver et al., 2020), and has been observed in higher density in the brains of HD patients and HD rodent models (Sanchez et al., 2021). In addition, G3BP1 has been reported to have a possible ameliorative role in a *C. elegans* model for HD, with a function in suppressing protein aggregation (Gutierrez-Garcia et al., 2023).

The experiments in this section were designed to confirm the effect observed when knocking-down *atx2* in this model, as reported by Xu et al. (2019b), as well as assess a key SG component, Rin, in this model of neurodegeneration.

4.3.1.3.1. Ataxin-2

In the experiment using the *atx2* RNAi (VDRC) construct, a striking difference was observed in transgenic flies expressing the *Htt*Q138 transgene in PDF-expressing neurons both in the activity plot, as well as in the rhythmicity analysis. Indeed, PDF>Q138 had a power of rhythmicity of around 4.68 whereas the power of rhythmicity of the parental flies was around 67.24. Knocking-down *atx2* led to a strong rescue of the power of rhythmicity with an eight-fold increase compared to the PDF>Q138 group. Knockdown of *atx2* also rescued the percentage of rhythmic flies from 10% in the PDF>Q138 group to 80%. These results demonstrate that ATX2 mediates neurodegeneration induced by *Htt*Q138 when expressed in PDF-expressing neurons, in agreement with previous findings (Xu et al., 2019b). The striking effect of *Htt*Q138 on the circadian rhythm observed in this experiment, compared to previous experiments, may be originating from the presence of two PDFGal4 drivers. Indeed, two PDFGal4 drivers were consistently used across the groups that required a Gal4 driver, namely the control group PDFGal4, and the two experimental groups PDF>Q138 and PDF>*atx2* RNAi; Q138.

In terms of identifiable sLNv somas and their PDF intensity, expression of *Htt*Q138 led to a strong decrease in both the number of somas and their PDF intensity. Surprisingly, knocking-down *atx2* exacerbated this phenotype with nearly no identifiable sLNv somas. This unexpected result is interesting as it is paired with a strong behavioural rescue. As previously mentioned, sLNv identification was dependent on PDF staining, and therefore on PDF expression. As whole-cell labelling was not employed in this experiment, it can not be determined whether the sLNvs have undergone cell death or have halted PDF expression. Adding to this uncertainty, knocking-down *atx2*, with a known function in mRNA translation, may affect translational mechanisms and consequently PDF expression. In either case, whether there is a decreased expression of PDF or a degeneration of the sLNvs, *atx2* RNAi was associated with an improved circadian rhythm. This finding is not far-removed from the observations made by Xu et al., where they had not observed a significant increase in the number of identifiable sLNv somas in transgenic flies expressing an expanded form of *Htt* and an *atx2* RNAi construct (Xu et al., 2019b). An interesting finding that is comparable to this previous study is the decrease in the volume of HTT aggregates in transgenic flies with both the *Htt*Q138 and *atx2* RNAi transgene. Indeed, PDF>*atx2* RNAi; Q138 flies had smaller HTT aggregates compared to the PDF>*Htt*Q138 group. This last set of results suggests that knocking-down *atx2* affects *Htt*Q138 aggregation, either through decreased expression or through the increased clearance of *Htt*Q138. Considering the known role of ATX2 in RNA regulation (Ostrowski et al., 2017), the former explanation seems more likely, although more studies are required to determine the cause of this observation.

Future experiments should aim to confirm the results seen in this work. This can be done using different *atx2* RNAi constructs or *atx2* null mutants. During this project, a mutant form of *atx2* that lacked the cIDR was tested in this circadian rhythm experiment. Unfortunately, these flies did not exhibit normal sleep behaviour, possibly due to the expression of dsRed in the retina. Special attention will have to be given to these transgenic lines to guarantee that these do not affect sleep functions by themselves.

4.3.1.3.2. Rasputin

In the experiment using the *rin* RNAi (VDRC) construct, a significant difference was observed in transgenic flies expressing *Htt*Q138 in PDF neurons both in the activity plot, as well as in the rhythmicity analysis. Indeed, PDF>Q138 had a power of rhythmicity of around 22.54 whereas the power of rhythmicity of the parental flies was around 60. Knocking-down the expression of *rin* led to a further deterioration of the power of rhythmicity with a 70% decrease compared to the PDF>Q138 group. *Rin* knockdown also decreased the percentage of rhythmic flies from 58% in the PDF>Q138 group to 16%. These results demonstrate that reducing the expression of *rin* hastens neurodegeneration induced by *Htt*Q138 when expressed in PDF neurons. This could suggest a protective role for this SG-related protein, which would be in agreement with a previous study that had also reported an ameliorative role for Rin in a HD model (Gutierrez-Garcia et al., 2023). However, considering previous literature has established the requirement of G3BP1 for normal neuronal function (Baumgartner et al., 2013; Costa et al., 2013; Zekri et al., 2005), knocking-down *rin* may be affecting sLNvs regardless of *Htt*Q138 expression. To clarify this possibility, it would be of interest to repeat this experiment with an additional group of flies only expressing the PDFGal4 driver and the *rin* RNAi construct.

In terms of cell survivability and HTT aggregation, decreasing the expression of *rin* led to interesting results when paralleled with the behavioural experiments. Indeed, *rin* knockdown did not affect the number of identifiable sLNvs, or their intensity, compared to the PDF>Q138 group. However, reducing the expression of *rin* did affect the volume of the HTT aggregates in the brain. This suggests that there is either an increased expression of *Htt*Q138, or a reduced clearance of this toxic protein when *rin* is knocked-down. This finding is in accordance with a recent report that observed a G3BP1/HTT interaction, and an increase in total levels of a mutant HTT protein after G3BP1 knockdown (Gutierrez-Garcia et al., 2023). Overall, these findings suggest a vital role for Rin in preventing *Htt*Q138 aggregation. However, additional experiments are required to confirm these results and test whether the observations made in this thesis result from a possible decrease in SG formation due to *rin* knockdown.

4.3.2. Further studies

The circadian rhythm is a powerful readout to study the cellular processes involved in neurodegeneration. The experiments in this thesis demonstrated that the ISR and RNP granule formation contribute to *Htt*Q138-induced cytotoxicity. As already mentioned in this section, further experiments will definitively establish the role that these proteins play in HD, and in neurodegeneration in a wider sense.

Suitable genetic controls should have been identified and prioritised, specifically for the behavioural experiments. Indeed, several limitations appeared during the process of conducting these experiments.

1. A group expressing a mock RNAi construct and the *Htt*Q138 transgene would determine whether the activation of the RNAi pathway is contributing to the observed phenotypes. In addition, this group would ensure that the phenotypic rescue is not a result of the presence of two UAS constructs instead of one. A preliminary and separate experiment was conducted during this thesis to test whether flies expressing a UAS-GFP construct with the *Htt*Q138 transgene (PDF>GFP; Q138) showed improved rhythmicity compared to a PDF>Q138 group (see Appendix 1) due to the presence of two UAS constructs. The PDF>GFP; Q138 flies surprisingly showed a further reduction in the power of rhythmicity. The observed reduction in rhythmicity could be due to the overexpression of the GFP protein in this population of neurons. Future experiments should incorporate a group expressing a mock RNAi instead in each iteration to confirm these results.

2. The genetic background of each group needs to be identical. Indeed, in the experiments presented here, due to time constraints, parental lines introduced differences in the *white* and *yellow* genes, as well as the presence of a mutation in the phenotypic gene *stubble* (*Sb*). Genetic backgrounds have been shown to significantly affect sleep behaviour (Zimmerman et al., 2012), consequently, future experiments should employ adequate genetic controls with consistent genetic backgrounds.

3. Different polyglutamine expansion lengths of *Htt* could have been used to study dynamics of aggregation, and the consequences on circadian rhythm. In addition, the use of a short expansion, such as *Htt*Q25, with the presence of a tagged fluorophore

would be a more suitable control when comparing *Htt* expression and aggregation, instead of PDFGal4 by itself as carried out in this thesis.

4. Although this would require recombination steps and several weeks to establish, a line expressing a UAS GFP construct along with the PDFGal4 construct would lead to an endogenous and constant expression of this fluorophore by PDF-expressing neurons. This is required to determine whether the cells are actually degenerating when expressing *Htt*Q138 or have simply halted PDF expression.

In conjunction with these genetic controls, future experiments should aim to use null mutants of proteins involved in the ISR, the UPR, and in RNP granule formation. This would confirm the findings from this thesis. In addition, to further elucidate the pathway involved in this form of degeneration, future experiments could genetically manipulate proteins that are known to interact with RNP granules and ATX2 specifically, such as Imp, Me31B or Caprin.

An additional analytical component that could be implemented in future circadian rhythm experiments would be to correlate the number of identifiable sLNvs and PDF with the power of rhythmicity of individual flies. This could be done by either separating the flies that exhibited a strong circadian rhythm from the flies that did not before proceeding with the dissection, or by keeping all dissected brain separate and indexed to their original monitor and tube number.

It would be of interest to test whether the modulation of the expression of these proteins could affect anticipatory behaviour as well. Wild-type flies exhibit an anticipatory increase in activity before dawn and dusk (Tataroglu & Emery, 2014). This circadian hallmark may also be affected by the genetic manipulations performed in these experiments. As can be observed in the locomotor activity plots in these experiments, the different transgenic groups had variable anticipation profiles during the entrainment period. These deserve a more detailed analysis.

Finally, considering the remarkable results obtained in the behavioural and cellular readout when reducing the expression of *rin*, it would be valuable for future experiments to test the effect of *rin* knockdown or overexpression on neurons without the presence of a mutant *Htt* gene, and to assess whether SG formation is impacted in these neurons.

4.3.3. Conclusion

The central aim of this chapter was to determine whether the same proteins that contributed to the *rdgB*^{9}-induced retinal degeneration would also contribute to this model of HD, induced by an expanded form of the HTT protein. A dysfunctional circadian rhythm was the primary readout of neurodegeneration of key clock-regulating neurons. This approach to studying neurodegeneration adds a valuable translational component to the results, as sleep defects are a common marker in neurodegenerative diseases. Overall, the results presented in this chapter demonstrate that PERK, a key component of both the ISR and the UPR, and RNP granule components contribute to the cytotoxicity induced by an expanded form of the HTT protein. The exact role that the ISR, the UPR, or the formation of RNP granules may play in the development of neurodegeneration still remains to be elucidated. These results suggest that downregulating the expression of PERK and ATX2 may impact and slow the progression of HD pathogenesis, whereas Rin may have a protective role against toxic protein aggregation, and could contribute to delay disease progression.

Chapter 5
General Discussion and Future Directions

5.1. General discussion

Global life expectancy and, consequently, the number of people with neurodegenerative diseases have been increasing. According to the World Health Organisation, 55.2 million people were living with dementia in 2019, and this number is projected to increase to 139 million by 2050 if the prevalence and incidence remain the same (W.H.O., 2021). This only accounts for one form of neurodegeneration, which demonstrates the extent of the global societal cost of neurodegenerative diseases. Understanding the molecular mechanisms underlying the pathogenesis of these diseases is crucial to the discovery of potential therapeutic targets. Many of these neurodegenerative diseases have specific cellular events in common, namely the activation of pathways related to ER stress such as the unfolded protein response (UPR) and the integrated stress response (ISR). However, the role of these pathways in the pathogenesis of neurodegenerative diseases remains unclear.

Even though retinal degeneration can be similarly caused by misfolded proteins and was shown to involve the activation of similar cellular pathways, the study of this form of cellular degeneration is usually not performed under the same perspective as neurodegenerative diseases. Previous studies have implicated the UPR and the ISR in models of neurodegenerative diseases (Ganz et al., 2020; Hoozemans et al., 2007; Hoozemans et al., 2012; Hoozemans et al., 2009; Lee et al., 2012; Leitman et al., 2014; Nishitoh et al., 2008; Vaccaro et al., 2013), and in models of retinal degeneration (Athanasiou et al., 2017; Chu et al., 2021; Kang et al., 2012; Mendes et al., 2009; Starr et al., 2018). Interestingly, the role of RNP granules and RNA homeostasis has been established in neurodegenerative diseases such as amyotrophic lateral sclerosis (ALS) and Huntington's disease (HD), while RNA-binding proteins (RBP) and stress granules (SG) have also recently been shown to be involved in models of retinal degeneration (Dash et al., 2016; Shakhmantsir et al., 2019; Yamoah et al., 2023).

Overall, there is accumulating evidence that the UPR, the ISR, and RNA homeostasis are involved in the development of neurodegenerative as well as retinal degenerative diseases. My project aimed to determine the extent to which these cellular pathways contribute to degeneration in two models of degeneration: retinal and neuronal, using *Drosophila* as the model organism. The RdgB^{9} model of retinal degeneration offers a unique and rapid form of degeneration that can be observed with ease at the cellular

and molecular level. Expression of an expanded form of human *Htt* in a specific subset of clock neurons allowed me to investigate neurodegeneration at both behavioural and cellular levels. To investigate the involvement of the aforementioned cellular pathways in both models of degeneration, I employed RNA interference technology to modulate the expression of specific genes that are known to be involved in the UPR and the ISR (*perk*, *gcn2*, and *gadd34*), in post-transcriptional control of RNAs (*sf3b2* and *CG42458*), or in the formation of RNP granules (*atx2* and *rin*). Identifying the required proteins for the development of cellular degeneration can be accomplished by modulating the expression of these genes and by looking at both cellular and behavioural outputs. This unique approach of using an identical genetic tool allows us to draw parallels between retinal and neuronal degeneration.

5.1.1. Pathways involved in the RdgB^{9} model of retinal degeneration

The primary aim of this section was to elucidate the pathways involved in *rdgB^{9}*-induced retinal degeneration. The *rdgB^{9}* allele and its morphological and physiological consequences on the *Drosophila* retina was originally described in 1977 (Harris & Stark, 1977). Although this allele is commonly used for genetic screens to assess modulators of retinal degeneration, the exact molecular and cellular pathways leading to the observed phenotype remain unclear. In this thesis, retinal degeneration in *rdgB^{9}* mutant flies, also expressing transgenic UAS constructs modulating the expression of the genes of interest, was assessed by visualising and counting the number of identifiable photoreceptors in one-, three-, and five-day-old flies.

The *rdgB^{9}* mutation led to a significant decrease in the number of identifiable photoreceptors in three- and five-day-old flies. Although the tools and experimental design used in this work were not able to establish whether the ISR and the UPR were upregulated in these mutant flies, a significant rescue in the number of photoreceptors was observed after knocking-down the expression of *perk*, while modulation of GCN2 had no effect. This demonstrates that the ISR is involved in the degeneration of photoreceptors in this model of retinal degeneration, specifically through the kinase PERK, and not GCN2. The specificity of the ISR kinase strongly suggests that the *rdgB^{9}* mutation induces ER stress, activating PERK.

In addition, a significant rescue was observed when knocking-down the expression of *sf3b2*, *atx2*, and *rin*, although these rescues were only seen with one of the two

independent RNAi constructs used. Nevertheless, these results suggest that RBPs, and more specifically, RNP granule components, are involved in the development of retinal degeneration in this model. These findings align with recent evidence of RBP-containing granules in the retina of a mouse model of retinal degeneration (Yamoah et al., 2023).

Overall, this is the first study to clearly demonstrate that the ER stress response, specifically involving PERK and downstream RNP granule components, is indeed required for the progression of retinal degeneration in the RdgB^{9} model. Taken together, these results support further work to unravel the mechanism underlying ER stress and RBPs, in this model of retinal degeneration.

5.1.2. Pathways involved in the *Htt*Q138 model of neurodegeneration

It has been well established that expression of a polyglutamine expanded form of Huntingtin (*Htt*) can lead to toxic oligomeric conformations and aggregate formation in cells, causing neurodegenerative phenotypes in different models of HD (DiFiglia et al., 1997; Imarisio et al., 2008; Schaffar et al., 2004). Nevertheless, the mechanism connecting these toxic aggregates to cell death is unknown, and it is still uncertain whether aggregates or HTT oligomers are the cytotoxic agent. Previous studies have reported that the UPR and the ISR are involved in neurodegeneration induced by *Htt* glutamate expansion, although, conflicting results show that both upregulation and downregulation can rescue the neurodegenerative phenotypes (Ganz et al., 2020; Leitman et al., 2014). This demonstrates the current knowledge gap in terms of how these pathways contribute to the pathogenesis of HD. Similarly, more work is required to understand how RBPs, and RNA homeostasis in general, contribute to the development of HD. Recent studies have demonstrated, in two different models of HD in *Drosophila*, that ATX2 mediates cytotoxicity induced by expanded forms of HTT (Huelsmeier et al., 2021; Xu et al., 2019b), suggesting an important role for RBPs in the pathogenesis of HD.

The primary aim of the work conducted in this section was to assess whether proteins involved in the ISR, RNA metabolism, and RNP granule formation, were involved in the observed neurodegenerative phenotype. Expression of expanded forms of *Htt* have been used to generate valid HD models in *Drosophila*, and induce motor deficits, HTT

accumulation, neurodegeneration, and dysfunctional circadian rhythms (Agrawal et al., 2005; Jackson et al., 1998; Lee et al., 2004; Wolfgang et al., 2005; Xu et al., 2019a). In this work, an expanded form of human *Htt* (*Htt*Q138) was expressed in PDF-positive neurons, which has previously been demonstrated to lead to a dysfunctional circadian rhythm (Xu et al., 2019a; Xu et al., 2019b). A PDFGal4 driver was used to drive expression of this transgene specifically in the LNv neuronal population which have a master pacemaker function over all clock neurons. *Htt*Q138 toxicity can then be assessed through circadian behaviour, sLNv cell death, and HTT aggregation. This is a particularly interesting model to study HD as disruption of circadian rhythms is a common symptom in HD patients and animal models (Loh et al., 2013; Morton et al., 2005), thereby offering a valuable translational element.

The results consistently showed that the expression of *Htt*Q138 in PDF-expressing neurons led to a weak and inconsistent circadian rhythm. This is in agreement with the demonstrated role of LNvs in the maintenance of circadian rhythm in constant darkness (Roberts et al., 2015; Stoleru et al., 2004; Yao & Shafer, 2014). For example, in a *period*^{0} mutant background, exclusively expressing *period* in LNvs leads to a robust rescue of circadian rhythms in constant darkness (Grima et al., 2004).

Expression of *Htt*Q138 in PDF neurons also led to sLNv degeneration in all experiments as revealed by PDF staining, in accordance with a previous study (Xu et al., 2019a). However, as mentioned in Chapter 4, visual identification of sLNv somas was limited by whether the neurons were consistently expressing PDF. Downregulation of some genes involved in RNA regulation, such as *atx2*, may affect the expression of PDF, and therefore proper quantification of sLNv somas. This is a major limitation that will be further discussed (5.2).

In addition, expression and aggregation of *Htt*Q138 in PDF-expressing neurons was consistently found in all experiments, although, the quaternary structure and subcellular localisation of the HTTQ138 proteins could not be determined due to the magnification used. Indeed, the detected signal could be from homogenous monomer cytoplasmic expression, or from different forms of protein aggregation.

5.1.2.1. Ataxin-2 mediates HTT toxicity

Downregulating *atx2* by RNAi in the background of *Htt*Q138 expression in PDF neurons strongly rescued the circadian rhythm, in terms of both power of rhythmicity and percentage of rhythmic flies. However, knocking-down the expression of *atx2* was associated to a significant increase in the number of degenerating sLNvs. As the presence of a single sLNv is enough to induce a behavioural rhythm (Helfrich-Forster, 1998), it is possible that mutant flies expressing both the *Htt*Q138 transgene and the *atx2* RNAi construct have fewer sLNvs but that the cytotoxic effect of *Htt*Q138 has been resolved, hence the improved circadian rhythm.

In terms of HTT aggregation, *atx2* knockdown led to a highly significant decrease in the volume of the HTT aggregates. This observation is likely to be associated with the observed behavioural rescue. More precisely, knockdown of *atx2* improves clearance of *Htt*Q138 and consequently cell health, which is an observation in line with previous reports from our laboratory (Huelsmeier et al., 2021). These observations are still consistent with a previous report suggesting that *atx2* loss-of-function reduced HTT aggregation and improved free-running rhythmicity (Xu et al., 2019b). Overall, these results indicate and emphasise the significant role of ATX2 in HTT-mediated cytotoxicity, possibly through its RNA-binding and translational functions and are in agreement with previous reports (Huelsmeier et al., 2021; Xu et al., 2019b). Considering these results, the role of ATX2 in mediating cellular toxicity seems to overlap between retinal and neuronal degeneration, this will be discussed in section 5.1.3.

5.1.2.2. Rasputin: a protective role against HTT toxicity?

In contrast, downregulation of the key SG component *rasputin* led to remarkable results in these experiments. *Rin* knockdown, in transgenic flies expressing *Htt*Q138 in PDF neurons, significantly aggravated the behavioural phenotype induced by *Htt*Q138, further reducing the power of rhythmicity and the percentage of rhythmic flies. However, *rin* knockdown did not affect the number of identifiable sLNvs in the background of *Htt*Q138 expression but did significantly increase the size of the HTT aggregates. This observation is consistent with the behavioural phenotype described.

These observations demonstrate an interesting role for Rin in this model of HD. Indeed, two possible hypotheses arise that could explain this protective function for Rin against the cytotoxicity induced by *Htt*Q138. The first explanation is dependent on the SG-related function of Rin, where the formation of SGs, as seen in post-mortem brains of HD patients (Sanchez et al., 2021), may slow disease progression in HD. However, in a previous study from our laboratory, expanded HTT aggregates did not sequester known SG markers, including Rin (Huelsmeier et al., 2021). Critically, this SG-dependent hypothesis is contradicted by the strong circadian rhythm rescue when *atx2* was downregulated. The second explanation is independent of SG formation, whereby the downregulation of Rin is affecting neuronal development and function, as previously described (Baumgartner et al., 2013; Costa et al., 2013; Zekri et al., 2005). This latter hypothesis is consistent with the *atx2* knockdown observation, and that HTT aggregates do not sequester Rin (Huelsmeier et al., 2021).

Overall, these results are in agreement with previous studies suggesting an important role for G3BP1, the mammalian homolog for Rin, in HD (Gutierrez-Garcia et al., 2023; Sanchez et al., 2021). Specifically, these results hint at a possible protective function as knockdown of its expression hastened toxicity and neurodegeneration. As the mechanism of action for the protective effect of Rin is unclear and may not necessarily be SG-dependent, it would be useful to assess how exactly Rin may contribute to delaying disease progression. Optimising the staining and imaging methods for SG visualisation could determine whether the effect observed here is dependent, or not, on the SG formation function of Rin. Additionally, expressing the *rin* RNAi construct in PDF neurons without the *Htt*Q138 transgene would clarify the effect of *rin* knockdown in healthy neurons.

5.1.2.3. PERK and CG42458 are not essential to HTT toxicity

Knocking-down the expression of *perk* and a novel RBP, *CG42458*, in transgenic flies expressing *Htt*Q138 in PDF-expressing neurons partially rescued the power of rhythmicity. Neither downregulating *perk* nor *CG42458* was associated to a significant increase in the number of sLNv somas, although an upwards trend was detected. Finally, neither of these proteins seem to be involved with HTT aggregate formation, as knockdown of these genes did not lead to a significant difference in HTT aggregate volume.

These results hint at a possible role of ER stress and PERK, and CG42458, in the development of HD, but require further experiments to fully establish. The involvement of the ISR would support previous studies demonstrating that the ISR contributes to the pathogenesis of HD (Carnemolla et al., 2009; Duennwald & Lindquist, 2008; Leitman et al., 2014; Leitman et al., 2013).

5.1.3. Overlapping mechanisms in cellular degeneration

The principal objective of this thesis was to use similar genetic tools to clarify and compare the cellular pathways involved in the pathogenesis of retinal degeneration and neurodegeneration. RNAi constructs were used in two different models of cellular degeneration to modulate genes involved in the ER stress response, in post-transcriptional regulation of RNA molecules, and in RNP granule formation. Of these genes, only those playing a role in RNP granule formation showed a significant modulation of the degenerative phenotype observed in the two different models. However, ER stress through the activation of PERK, may also have an effect in the two models of cellular degeneration used in this work.

5.1.3.1. Integrated stress response

The ISR and the UPR pathways are found in all eukaryotic cells and will activate to restore cellular homeostasis after a stressful stimulus. Therefore, the observed results in the model of retinal degeneration when *perk* was knocked-down were foreseeable. However, these observations are still noteworthy. They demonstrate for the first time that *rdgB*^{9}-induced retinal degeneration is mediated by the ER stress sensor PERK, and that reducing the expression of this protein is a viable method to rescue the degenerative phenotype.

The results hint at the possibility that decreasing the expression of *perk* could reduce cytotoxicity induced by an expanded form of *Htt*. As previously mentioned, the implication of the ISR and of the UPR in neurodegenerative diseases such as HD has been well reported in previous studies (Carnemolla et al., 2009; Duennwald & Lindquist, 2008; Leitman et al., 2014; Leitman et al., 2013). Nevertheless, whether the activation of these pathways is protective or harmful to the cell remains a matter of debate (Ganz et al., 2020; Leitman et al., 2014; Shacham et al., 2021). Given the results reported here, it seems that the UPR could contribute to cytotoxicity and decreasing its activity by modulating expression of *perk* could reduce neurodegenerative phenotypes.

This builds on the hypothesis that inhibiting the UPR may be a compelling therapeutic approach for retinal degeneration and neurodegeneration. However, studies have reported pharmacological effects of PERK inhibition on pancreatic function, advocating for caution in the development of PERK inhibitors for therapeutic purposes (Atkins et al., 2013; Harding et al., 2012). More experimental work is necessary to determine the exact role of the ISR and of the UPR in retinal degeneration and in neurodegeneration, and which stages of these pathways could be targeted for therapeutic intervention.

5.1.3.2. RNP granule formation

RNP granules can be observed in a healthy cell serving normal physiological functions. These assemblies form membrane-less organelles known as RNP granules, containing a high concentration of RNA molecules and factors required for their translation and regulation, enabling higher translational efficiency and control (De Graeve & Besse, 2018). However, subtypes of RNP granules are predominantly found in unhealthy or diseased cells. Various neurodegenerative diseases, including ALS, SCA2, FTD and HD, have been linked with a dysfunctional formation of RNP granules, specifically SGs and PBs (An et al., 2021; Desai & Bandopadhyay, 2020; Li et al., 2013; Ramaswami et al., 2013). These diseases can be associated to specific mutations in key RBPs, including TDP-43, FUS, TIA1, and HTT (Asadi et al., 2021). Previously reported data have linked Ataxin-2 to various neurodegenerative diseases, including the eponymous spinocerebellar ataxia-2 (Koyano et al., 1999; Paul et al., 2018; Scoles et al., 2017), ALS (Bakthavachalu et al., 2018; Elden et al., 2010; Hart & Gitler, 2012), FTD (van Blitterswijk et al., 2014), and more recently HD (Huelsmeier et al., 2021; Xu et al., 2019b). The exact role of these proteins and of RNP granules in the development of

neurodegeneration remains unclear and an exciting field of research. Additionally, a recent study observed SGs containing RBPs such as TIA1, FUS and TDP43, in a mouse model of retinitis pigmentosa (Yamoah et al., 2023). This latest observation highlights the existence of similar cellular processes in retinal degeneration.

In this work, the results involving RNAi constructs in the RdgB^{9} model for retinal degeneration suggest that ATX2 and Rin mediate the degeneration of photoreceptor cells. However, the interpretation is made more complex by the fact that only one RNAi construct led to a significant decrease in the degenerative phenotype, and that expressing an *atx2* mutant lacking a domain required for granule formation led to an increase in degenerated photoreceptor cells. Interestingly, *atx2* knockdown in the *Htt*Q138 model for HD resulted in the strongest decrease in *Htt*-mediated toxicity, as seen in the circadian rhythm, which was associated with a decreased PDF-positive sLNv somas and a decreased aggregation of HTT in the brain. These results taken together suggest a novel role for ATX2 in mediating retinal degeneration and strengthens the established role of this RNP granule component in the development of neurodegeneration.

On the contrary, downregulating *rin* recovered the degenerative phenotype in the model for retinal degeneration, leading to fewer degenerated photoreceptor cells, but aggravated neurodegeneration induced by expression of *Htt*Q138 in PDF-positive neurons. As mentioned earlier, these results could originate from the different SG-dependent or independent functions that Rin may have. However, these opposite effects highlight how specific pathways, such as RNP granule formation, behave differently in neurodegeneration compared to retinal degeneration.

During this thesis, experiments were also conducted to clarify the interdependency between the stress-induced transcriptional changes and SG formation (Appendix 2). For this purpose, S2 cells that were knocked-down for *rin* and were stressed using sodium arsenite, were assessed for SG formation and translational arrest. Although there was a decrease in SG formation, translational arrest still occurred, demonstrating that these two cellular processes are driven by distinctive pathways (Singh et al., 2022).

5.2. Future directions

In consideration of the experiments presented in this thesis, specific experiments and controls should be carried out to confirm the reported results:

1. To confirm the role of ER stress in the RdgB^{9} model of retinal degeneration, future experiments should modulate the ISR and the UPR. This can be done by feeding RdgB^{9} flies ISRIB or a PERK inhibitor, by using a null *perk* mutant, or by expressing RNAi targets against the other UPR proteins such as IRE1.

2. To confirm the results reported in Chapter 4 it would be important to repeat the circadian rhythm experiments with the proposed genetic controls and additional experimental groups.

3. Expressing GFP in PDF-expressing neurons along with the *Htt*Q138 transgene would clarify whether sLNvs are degenerated or have stopped PDF expression. In the context of *atx2* knockdown, it would determine whether the decrease in HTT aggregation is originating from sLNv degeneration or from increased HTTQ138 clearance.

4. Overexpressing *rin* in PDF-positive neurons, with and without the *Htt*Q138 transgene, could determine how Rin may have a protective role against HTT toxicity. In addition, optimising the protocol used may determine whether SG formation is affected in these neurons. Overall, these experiments could clarify how Rin, and the formation of SG, are involved in HD.

Finally, the following lines of experiments would allow us to gain a broader view of the mechanisms underlying these results, and define their larger implications:

1. In addition to ER stress and the ISR, a recent study has reported TDP-43 containing stress granules in a mouse model for retinal degeneration (Yamoah et al., 2023). Considering that ATX2 and Rin seem to contribute to the degenerative phenotype observed in RdgB^{9} flies, and the importance of RNP granules in neurodegeneration, understanding the role of this process in retinal degeneration is of prime importance to identify possible therapeutic avenues. Future experiments could assess whether the *Drosophila* models for retinal degeneration lead to the formation of

RNP granules in the retina, and whether the formation could be modulated by inhibiting the ISR or expressing different forms of ATX2.

2. Upregulation of stress-response genes in *rdgB*^{9} mutant flies was not observed in the RT-qPCR experiment. Assessing how gene expression is modulated in response to the *rdgB*^{9} mutation, as well as the *Htt*Q138 mutant, using single-cell RNA sequencing could reconstruct molecular pathways and understand the transcriptional dynamics in these degenerating cells.

3. This thesis exclusively used mutations in the *rdgB* gene to induce retinal degeneration. It would be of interest to assess how the ISR, the novel RBPs, and RNP granule components affect a different retinal degeneration model in *Drosophila*, such as by expressing the Rh1P37H mutation in photoreceptors. If similar pathways are involved this would demonstrate the validity of using the *rdgB*^{9} mutation as a translational model for human retinal degeneration.

4. The role of ER stress, and its contribution to cytotoxicity in neurodegenerative models, is still unclear. In this thesis, knocking-down *perk* led to a clear rescue in the retinal degeneration model, but not in the neurodegeneration model. Downregulating *perk* in flies driving an expanded form of *Htt* in motor neurons using D42-Gal4, or in the entire eye using GMR-Gal4, and observing neurodegeneration through a climbing assay or through eye degeneration, respectively, would clarify the suggested role of PERK in this thesis.

5. Work should be undertaken to understand how SF3B2, CG42458, and the RNP granule components contribute to cell degeneration. By either inducing oxidative stress in *Drosophila* S2 cells or expressing different toxic forms of HTT, we could assess how knocking-down these RBPs affects translational arrest and RNP granule formation. These experiments would clarify the relationship and interdependency of these two pathways.

5.3. Concluding remarks

Past work to understand the mechanisms of cellular degeneration has either focused on retinal degeneration or neurodegeneration. These studies have revealed that the ISR and RBPs contribute to their pathogenesis, although the exact players and roles remain elusive. The overarching aim of this thesis was to understand the role of the ISR, of RNP granule formation, and of novel RBPs in two different models for cellular degeneration using similar genetic tools, gaining additional insights on potential overlapping molecular pathways in *Drosophila melanogaster*. The first results chapter demonstrated that proteins involved in the ISR, in RNP granule formation and in RNA regulation contributed to the degenerative phenotype observed in the retinas of *rdgB* mutants. The second results chapter confirmed crucial, but different, roles for the RNP granule components Ataxin-2 and Rasputin in the *Htt*Q138 neurodegenerative model. In addition, the results hinted at the possibility that the ISR contributes to the development of neurodegeneration in HD, whereas the novel RBP that modulated the $rdgB^{9}$ retinal degeneration did not seem to be involved in this model of neurodegeneration. Overall, this work demonstrated that modulating the ISR and RNP granule components can reduce the degenerative phenotype in models for both neurodegeneration and retinal degeneration (Figure 4-18). Future work should focus on confirming the results observed in this thesis, and clarify why the activity of the ISR and the RNP granule components worsens the phenotypes induced in these models of cellular degeneration.

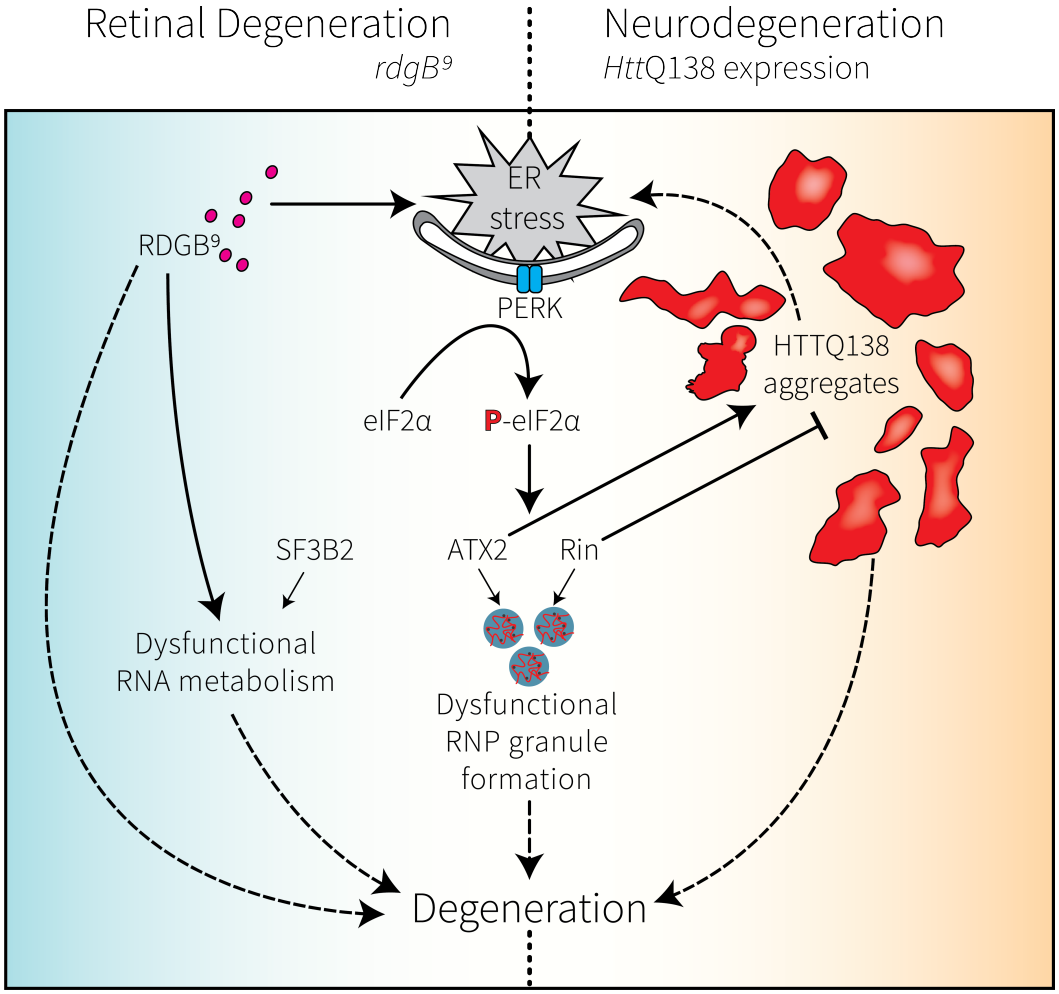

Figure 4-18 Molecular pathways involved in retinal degeneration and neurodegeneration. *rdgB⁹-induced retinal degeneration leads to ER stress, PERK activation, and eIF2α phosphorylation. HTT aggregates activate ER stress, leading to similar downstream events, but may also lead to neurodegeneration through separate pathways. Phosphorylated eIF2α participates in dysfunctional RNP granule formation in these models, which could contribute to cytotoxicity and cellular degeneration. Both models of degeneration require ATX2, as downregulating its expression rescues retinal and neuronal degenerative phenotypes. RIN is likely involved but may have different roles in these degenerative models as observed when downregulated, possibly due to its SG-independent functions. rdgB⁹ may also lead to dysfunctional RNA metabolism as demonstrated with downregulation of the spliceosome component SF3B2, which could contribute to retinal degeneration. rdgB⁹ may involve other pathways that lead to retinal degeneration.*

Bibliography

Agrawal, N., Pallos, J., Slepko, N., Apostol, B. L., Bodai, L., Chang, L. W., Chiang, A. S., Thompson, L. M., & Marsh, J. L. (2005). Identification of combinatorial drug regimens for treatment of Huntington's disease using Drosophila. *Proc Natl Acad Sci U S A*, *102*(10), 3777-3781. https://doi.org/10.1073/pnas.0500055102

Aguilera-Gomez, A., Zacharogianni, M., van Oorschot, M. M., Genau, H., Grond, R., Veenendaal, T., Sinsimer, K. S., Gavis, E. A., Behrends, C., & Rabouille, C. (2017). Phospho-Rasputin Stabilization by Sec16 Is Required for Stress Granule Formation upon Amino Acid Starvation. *Cell Reports*, *20*(4), 935-948. https://doi.org/10.1016/j.celrep.2017.06.042

Alami, N. H., Smith, R. B., Carrasco, M. A., Williams, L. A., Winborn, C. S., Han, S. S. W., Kiskinis, E., Winborn, B., Freibaum, B. D., Kanagaraj, A., Clare, A. J., Badders, N. M., Bilican, B., Chaum, E., Chandran, S., Shaw, C. E., Eggan, K. C., Maniatis, T., & Taylor, J. P. (2014). Axonal Transport of TDP-43 mRNA Granules Is Impaired by ALS-Causing Mutations. *Neuron*, *81*(3), 536-543. https://doi.org/10.1016/j.neuron.2013.12.018

Alic, N., Hoddinott, M. P., Foley, A., Slack, C., Piper, M. D. W., & Partridge, L. (2012). Detrimental Effects of RNAi: A Cautionary Note on Its Use in Drosophila Ageing Studies. *PLOS ONE*, *7*(9). https://doi.org/10.1371/journal.pone.0045367

An, H., de Meritens, C. R., & Shelkovnikova, T. A. (2021). Connecting the “dots”: RNP granule network in health and disease. In *Biochimica et Biophysica Acta - Molecular Cell Research* (Vol. 1868): Elsevier B.V.

Appocher, C., Mohagheghi, F., Cappelli, S., Stuani, C., Romano, M., Feiguin, F., & Buratti, E. (2017). Major hnRNP proteins act as general TDP-43 functional modifiers both in Drosophila and human neuronal cells. *Nucleic Acids Research*, *45*(13), 8026-8045. https://doi.org/10.1093/nar/gkx477

Arshavsky, V. Y., & Burns, M. E. (2014). Current understanding of signal amplification in phototransduction. *Cell Logist*, *4*, e29390. https://doi.org/10.4161/cl.29390

Asadi, M. R., Sadat Moslehian, M., Sabaie, H., Jalaiei, A., Ghafouri-Fard, S., Taheri, M., & Rezazadeh, M. (2021). Stress Granules and Neurodegenerative Disorders: A Scoping Review. *Front Aging Neurosci*, *13*, 650740. https://doi.org/10.3389/fnagi.2021.650740

Athanasiou, D., Aguila, M., Bellingham, J., Kanuga, N., Adamson, P., & Cheethamc, M. E. (2017). The role of the ER stress-response protein PERK in rhodopsin retinitis pigmentosa. *Human Molecular Genetics*, *26*(24), 4896-4905. https://doi.org/10.1093/hmg/ddx370

Atkins, C., Liu, Q., Minthorn, E., Zhang, S. Y., Figueroa, D. J., Moss, K., Stanley, T. B., Sanders, B., Goetz, A., Gaul, N., Choudhry, A. E., Alsaid, H., Jucker, B. M., Axten, J. M., & Kumar, R. (2013). Characterization of a novel PERK kinase inhibitor with antitumor and antiangiogenic activity. *Cancer Res*, *73*(6), 1993-2002. https://doi.org/10.1158/0008-5472.CAN-12-3109

Atwan, Z. W. (2020). GAPDH spike RNA as an alternative for housekeeping genes in relative gene expression assay using real-time PCR. *Bulletin of the National Research Centre*, *44*(1), 32. https://doi.org/10.1186/s42269-020-00284-1

Bakthavachalu, B., Huelsmeier, J., Sudhakaran, I. P., Hillebrand, J., Singh, A., Petrauskas, A., Thiagarajan, D., Sankaranarayanan, M., Mizoue, L., Anderson, E. N., Pandey, U. B., Ross, E., VijayRaghavan, K., Parker, R., & Ramaswami, M. (2018). RNP-Granule Assembly via Ataxin-2 Disordered Domains Is Required for Long-Term Memory and Neurodegeneration. *Neuron*. https://doi.org/10.1016/j.neuron.2018.04.032

Balla, T., Szentpetery, Z., & Kim, Y. J. (2009). Phosphoinositide signaling: new tools and insights. In *Physiology* (Vol. 24, pp. 231-244).

Banani, S. F., Lee, H. O., Hyman, A. A., & Rosen, M. K. (2017). Biomolecular condensates: Organizers of cellular biochemistry. In *Nature Reviews Molecular Cell Biology* (Vol. 18, pp. 285-298): Nature Publishing Group.

Bates, G. P., Dorsey, R., Gusella, J. F., Hayden, M. R., Kay, C., Leavitt, B. R., Nance, M., Ross, C. A., Scahill, R. I., Wetzel, R., Wild, E. J., & Tabrizi, S. J. (2015). Huntington disease. *Nat Rev Dis Primers*, *1*, 15005. https://doi.org/10.1038/nrdp.2015.5

Baumgartner, R., Stocker, H., & Hafen, E. (2013). The RNA-binding proteins FMR1, rasputin and caprin act together with the UBA protein lingerer to restrict tissue growth in Drosophila melanogaster. *PLoS Genet*, *9*(7), e1003598. https://doi.org/10.1371/journal.pgen.1003598

Berger, W., Kloeckener-Gruissem, B., & Neidhardt, J. (2010). The molecular basis of human retinal and vitreoretinal diseases. *Prog Retin Eye Res*, *29*(5), 335-375. https://doi.org/10.1016/j.preteyeres.2010.03.004

Berson, E. L., Rosner, B., Sandberg, M. A., & Dryja, T. P. (1991). Ocular Findings in Patients With Autosomal Dominant Retinitis Pigmentosa and a Rhodopsin Gene Defect (Pro-23-His). *Arch Ophthalmol*, *109*(1), 92-101. https://jamanetwork.com/

Bevilacqua, E., Wang, X., Majumder, M., Gaccioli, F., Yuan, C. L., Wang, C., Zhu, X., Jordan, L. E., Scheuner, D., Kaufman, R. J., Koromilas, A. E., Snider, M. D., Holcik, M., & Hatzoglou, M. (2010). eIF2α phosphorylation tips the balance to apoptosis during osmotic stress. *Journal of Biological Chemistry*, *285*(22), 17098-17111. https://doi.org/10.1074/jbc.M110.109439

Bond, S., Lopez-Lloreda, C., Gannon, P. J., Akay-Espinoza, C., & Jordan-Sciutto, K. L. (2020). The integrated stress response and phosphorylated eukaryotic initiation factor 2α in neurodegeneration. In *Journal of Neuropathology and Experimental Neurology* (Vol. 79, pp. 123-143): Oxford University Press.

Bugallo, R., Marlin, E., Baltanás, A., Toledo, E., Ferrero, R., Vinueza-Gavilanes, R., Larrea, L., Arrasate, M., & Aragón, T. (2020). Fine tuning of the unfolded protein response by ISRIB improves neuronal survival in a model of amyotrophic lateral sclerosis. *Cell Death and Disease*, *11*(5). https://doi.org/10.1038/s41419-020-2601-2

Burdakov, D., Petersen, O. H., & Verkhratsky, A. (2005). Intraluminal calcium as a primary regulator of endoplasmic reticulum function. *Cell Calcium*, *38*(3-4 SPEC. ISS.), 303-310. https://doi.org/10.1016/j.ceca.2005.06.010

Busch, A., Engemann, S., Lurz, R., Okazawa, H., Lehrach, H., & Wanker, E. E. (2003). Mutant huntingtin promotes the fibrillogenesis of wild-type huntingtin: A potential mechanism for loss of huntingtin function in Huntington's disease. *Journal of Biological Chemistry*, *278*(42), 41452-41461. https://doi.org/10.1074/jbc.M303354200

Cagan, R. L., & Ready, D. F. (1989). *The Emergence of Order in the Drosophila Pupal Retina* (Developmental Biology, Issue.

Campesan, S., Green, E. W., Breda, C., Sathyasaikumar, K. V., Muchowski, P. J., Schwarcz, R., Kyriacou, C. P., & Giorgini, F. (2011). The kynurenine pathway modulates neurodegeneration in a drosophila model of Huntington's disease. *Current Biology*, *21*(11), 961-966. https://doi.org/10.1016/j.cub.2011.04.028

Carnemolla, A., Fossale, E., Agostoni, E., Michelazzi, S., Calligaris, R., De Maso, L., Del Sal, G., MacDonald, M. E., & Persichetti, F. (2009). Rrs1 is involved in endoplasmic reticulum stress response in huntington disease. *Journal of Biological Chemistry*, *284*(27), 18167-18173. https://doi.org/10.1074/jbc.M109.018325

Cattaneo, E., Zuccato, C., & Tartari, M. (2005). Normal huntingtin function: An alternative approach to Huntington's disease. In *Nature Reviews Neuroscience* (Vol. 6, pp. 919-930).

Cavey, M., Collins, B., Bertet, C., & Blau, J. (2016). Circadian rhythms in neuronal activity propagate through output circuits. *Nat Neurosci*, *19*(4), 587-595. https://doi.org/10.1038/nn.4263

Chang, J. T., Milligan, S., Li, Y., Chew, C. E., Wiggs, J., Copeland, N. G., Jenkins, N. A., Campochiaro, P. A., Hyde, D. R., & Zack, D. J. (1997). *Mammalian Homolog of Drosophila retinal degeneration B Rescues the Mutant Fly Phenotype*.

Chaplot, K., Pimpale, L., Ramalingam, B., Deivasigamani, S., Kamat, S. S., & Ratnaparkhi, G. S. (2019). SOD1 activity threshold and TOR signalling modulate VAP(P58S) aggregation via reactive oxygen species-induced proteasomal degradation in a Drosophila model of amyotrophic lateral sclerosis. *DMM Disease Models and Mechanisms*. https://doi.org/10.1242/dmm.033803

Chaves, I., Pokorny, R., Byrdin, M., Hoang, N., Ritz, T., Brettel, K., Essen, L. O., van der Horst, G. T., Batschauer, A., & Ahmad, M. (2011). The cryptochromes: blue light photoreceptors in plants and animals. *Annu Rev Plant Biol*, *62*, 335-364. https://doi.org/10.1146/annurev-arplant-042110-103759

Chu, H. S., Peterson, C., Jun, A., & Foster, J. (2021). Targeting the integrated stress response in ophthalmology. In *Current Eye Research* (Vol. 46, pp. 1075-1088): Taylor and Francis Ltd.

Cockcroft, S., Garner, K., Yadav, S., Gomez-Espinoza, E., & Raghu, P. (2016). RdgBα reciprocally transfers PA and PI at ER-PM contact sites to maintain PI(4,5)P2 homoeostasis during phospholipase C signalling in Drosophila photoreceptors. *Biochemical Society Transactions*, *44*, 286-292. https://doi.org/10.1042/BST20150228

Cockcroft, S., & Raghu, P. (2018). Phospholipid transport protein function at organelle contact sites. *Curr Opin Cell Biol*, *53*, 52-60. https://doi.org/10.1016/j.ceb.2018.04.011

Colley, N. J., Cassill, J. A., Baker, E. K., & Zuker, C. S. (1995). Defective intracellular transport is the molecular basis of rhodopsin- dependent dominant retinal degeneration. *Proceedings of the National Academy of Sciences of the United States of America*, *92*(7), 3070-3074. https://doi.org/10.1073/pnas.92.7.3070

Costa, A., Pazman, C., Sinsimer, K. S., Wong, L. C., McLeod, I., Yates, J., 3rd, Haynes, S., & Schedl, P. (2013). Rasputin functions as a positive regulator of orb in Drosophila oogenesis. *PLOS ONE*, *8*(9), e72864. https://doi.org/10.1371/journal.pone.0072864

Cyran, S. A., Buchsbaum, A. M., Reddy, K. L., Lin, M.-C., Glossop, N. R. J., Hardin, P. E., Young, M. W., & Storti, R. V. (2003). *vrille, Pdp1, and dClock Form a Second Feedback Loop in the Drosophila Circadian Clock gives an approximately 24 hr (circadian) rhythm in RNA and protein levels of some clock components, and these rhythms continue even in a constant environment. The first description of a molecular clock feedback and Justin Blau 1, * loop involved rhythmic transcription of Drosophila pe* (Cell, Issue.

Daiger, S. P., Bowne, S. J., & Sullivan, L. S. (2014). Genes and Mutations Causing Autosomal Dominant Retinitis Pigmentosa. *Cold Spring Harb Perspect Med*, *5*(10). https://doi.org/10.1101/cshperspect.a017129

Dash, S., Siddam, A. D., Barnum, C. E., Janga, S. C., & Lachke, S. A. (2016). RNA-binding proteins in eye development and disease: implication of conserved RNA granule components. In *Wiley Interdisciplinary Reviews: RNA* (Vol. 7, pp. 527-557): Blackwell Publishing Ltd.

Davis, M. B., Bateman, D., Quinn, N. P., Marsden, C. D., & Harding, A. E. (1994). Mutation analysis in patients with possible but apparently sporadic Huntington's disease. *The Lancet*, *344*(1), 714-716. https://doi.org/https://doi.org/10.1016/S0140-6736(94)92208-X

De Graeve, F., & Besse, F. (2018). Neuronal RNP granules: from physiological to pathological assemblies. *Biological Chemistry*. https://doi.org/10.1515/hsz-2011-xxxx

DeJesus-Hernandez, M., Mackenzie, I. R., Boeve, B. F., Boxer, A. L., Baker, M., Rutherford, N. J., Nicholson, A. M., Finch, N. A., Flynn, H., Adamson, J., Kouri, N., Wojtas, A., Sengdy, P., Hsiung, G. Y., Karydas, A., Seeley, W. W., Josephs, K. A., Coppola, G., Geschwind, D. H., . . . Rademakers, R. (2011). Expanded GGGGCC hexanucleotide repeat in noncoding region of C9ORF72 causes chromosome 9p-linked FTD and ALS. *Neuron*, *72*(2), 245-256. https://doi.org/10.1016/j.neuron.2011.09.011

Desai, P., & Bandopadhyay, R. (2020). Pathophysiological implications of RNP granules in frontotemporal dementia and ALS. In *Neurochemistry International* (Vol. 140): Elsevier Ltd.

DiFiglia, M., Sapp, E., Chase, K. O., Davies, S. W., Bates, G. P., Vonsattel, J. P., & Aronin, N. (1997). Aggregation of huntingtin in neuronal intranuclear inclusions and dystrophic neurites in brain. *Science*, *277*(5334), 1990-1993. https://doi.org/10.1126/science.277.5334.1990

Dryja, T. P., McGee, T., Reichel, E., Hahn, L. B., Cowley, G., Yandell, D. W., Sandberg, M. A., & Berson, E. L. (1990). *LETTERS TO NATURE A point mutation of the rhodopsin gene in one form of retinitis pigmentosa*.

Dubowy, C., & Sehgal, A. (2017). Circadian rhythms and sleep in Drosophila melanogaster. *Genetics*, *205*(4), 1373-1397. https://doi.org/10.1534/genetics.115.185157

Duennwald, M. L., & Lindquist, S. (2008). Impaired ERAD and ER stress are early and specific events in polyglutamine toxicity. *Genes Dev*, *22*(23), 3308-3319. https://doi.org/10.1101/gad.1673408

Eisenberg, D., & Jucker, M. (2012). The amyloid state of proteins in human diseases. In *Cell* (Vol. 148, pp. 1188-1203): Elsevier B.V.

Elden, A. C., Kim, H. J., Hart, M. P., Chen-Plotkin, A. S., Johnson, B. S., Fang, X., Armakola, M., Geser, F., Greene, R., Lu, M. M., Padmanabhan, A., Clay-Falcone, D., McCluskey, L., Elman, L., Juhr, D., Gruber, P. J., Rub, U., Auburger, G., Trojanowski, J. Q., . . . Gitler, A. D. (2010). Ataxin-2 intermediate-length polyglutamine expansions are associated with increased risk for ALS. *Nature*, *466*(7310), 1069-1075. https://doi.org/10.1038/nature09320

Ellis, M. C., O'Neill, E. M., & Rubin, G. M. (1993). Expression of Drosophila glass protein and evidence for negative regulation of its activity in non-neuronal cells by another DNA-binding protein. *Development*, *119*(3), 855-865. https://doi.org/10.1242/dev.119.3.855

Fahn, S., Jankovic, J., & Hallett, M. (2011). Huntington disease. In *Principles and Practice of Movement Disorders* (pp. 311-334). Elsevier. https://doi.org/10.1016/B978-1-4377-2369-4.00014-7

Fain, G. L., Hardie, R., & Laughlin, S. B. (2010). Phototransduction and the Evolution of Photoreceptors. *Current Biology*, *20*(3), R114-R124. https://doi.org/10.1016/j.cub.2009.12.006

Fan, B., Sun, Y. J., Liu, S. Y., Che, L., & Li, G. Y. (2017). Neuroprotective strategy in retinal degeneration: Suppressing ER stress-induced cell death via inhibition of the mTOR signal. *International Journal of Molecular Sciences*, *18*(1). https://doi.org/10.3390/ijms18010201

Fanelli, F., & Seeber, M. (2010). Structural insights into retinitis pigmentosa from unfolding simulations of rhodopsin mutants. *FASEB Journal*, *24*(9), 3196-3209. https://doi.org/10.1096/fj.09-151084

Farber, D., Heckenlively, J. R., Sparkes, R., & Bateman, J. (1991). *Conferences and Reviews Molecular Genetics of Retinitis Pigmentosa*.

Feder, M. E., & Hofmann, G. E. (1999). *HEAT-SHOCK PROTEINS, MOLECULAR CHAPERONES, AND THE STRESS RESPONSE: Evolutionary and Ecological Physiology* (Annu. Rev. Physiol, Issue. www.annualreviews.org

Fischer, J. W., Busa, V. F., Shao, Y., & Leung, A. K. L. (2020). Structure-Mediated RNA Decay by UPF1 and G3BP1. *Mol Cell*, *78*(1), 70-84 e76. https://doi.org/10.1016/j.molcel.2020.01.021

Fitzgibbon, J., & Hunt, D. (1995). Drosophila Visual Transduction, a Model System For Human Eye Disease? In *Degenerative Diseases of the Retina* (pp. 255-261). Springer US. https://doi.org/10.1007/978-1-4615-1897-6_29

Frank, S. (2014). Treatment of Huntington's Disease. In *Neurotherapeutics* (Vol. 11, pp. 153-160).

Frias, E. S., Hoseini, M. S., Krukowski, K., Paladini, M. S., Grue, K., Ureta, G., Rienecker, K. D. A., Walter, P., Stryker, M. P., Rosi, S., Borlongan, C., & Trachtenberg, J. (2022). Aberrant cortical spine dynamics after concussive injury are reversed by integrated stress response inhibition. *PNAS*. https://doi.org/10.1073/pnas

Galy, A., Roux, M. J., Sahel, J. A., Léveillard, T., & Giangrande, A. (2005). Rhodopsin maturation defects induce photoreceptor death by apoptosis: A fly model for RhodopsinPro23His human retinitis pigmentosa. *Human Molecular Genetics*, *14*(17), 2547-2557. https://doi.org/10.1093/hmg/ddi258

Ganz, J., Shacham, T., Kramer, M., Shenkman, M., Eiger, H., Weinberg, N., Iancovici, O., Roy, S., Simhaev, L., Da'adoosh, B., Engel, H., Perets, N., Barhum, Y., Portnoy, M., Offen, D., & Lederkremer, G. Z. (2020). A novel specific PERK activator reduces toxicity and extends survival in Huntington's disease models. *Sci Rep*, *10*(1), 6875. https://doi.org/10.1038/s41598-020-63899-4

Gao, J., Wang, L., Huntley, M. L., Perry, G., & Wang, X. (2018). Pathomechanisms of TDP-43 in neurodegeneration. In *Journal of Neurochemistry* (Vol. 146, pp. 7-20): Blackwell Publishing Ltd.

Gaspar, P., Almudi, I., Nunes, M. D. S., & McGregor, A. P. (2019). Human eye conditions: insights from the fly eye. In *Human Genetics* (Vol. 138, pp. 973-991): Springer Verlag.

Geissmann, Q., Garcia Rodriguez, L., Beckwith, E. J., & Gilestro, G. F. (2019). Rethomics: An R framework to analyse high-throughput behavioural data. *PLOS ONE*, *14*(1), e0209331. https://doi.org/10.1371/journal.pone.0209331

Gerstberger, S., Hafner, M., Ascano, M., & Tuschl, T. (2014). Evolutionary conservation and expression of human RNA-Binding proteins and their role in human genetic disease. *Advances in Experimental Medicine and Biology*, *825*. https://doi.org/10.1007/978-1-4939-1221-6_1

Glossop, N., Houl, J., Zheng, H., Ng, F., Dudek, S., & Hardin, P. (2003). VRILLE Feeds Back to Control Circadian Transcription of Clock in the Drosophila Circadian Oscillator. *Neuron*, *37*, 249-261.

Gómez-Tortosa, E., Macdonald, M. E., Friend, J. C., Taylor, S. A. M., Weiler, L. J., Cupples, L. A., Srinidhi, J., Gusella, J. F., Bird, E. D., Vonsattel, J.-P., & Myers, R. H. (2001). *Quantitative Neuropathological Changes in Presymptomatic Huntington's Disease* (Ann Neurol, Issue.

Goodman, A. O. G., & Barker, R. A. (2010). How vital is sleep in Huntington's disease? In *Journal of Neurology* (Vol. 257, pp. 882-897).

Goodman, A. O. G., Rogers, L., Pilsworth, S., McAllister, C. J., Shneerson, J. M., Morton, A. J., & Barker, R. A. (2011). Asymptomatic sleep abnormalities are a common early feature in patients with Huntington's disease. *Current Neurology and Neuroscience Reports*, *11*(2), 211-217. https://doi.org/10.1007/s11910-010-0163-x

Gorbatyuk, M. S., Knox, T., LaVail, M. M., Gorbatyuk, O. S., Noorwez, S. M., Hauswirth, W. W., Lin, J. H., Muzyczka, N., & Lewin, A. S. (2010). Restoration of visual function in P23H rhodopsin transgenic rats by gene delivery of BiP/Grp78. *Proceedings of the National Academy of Sciences of the United States of America*, *107*(13), 5961-5966. https://doi.org/10.1073/pnas.0911991107

Gorostiza, E. A., Depetris-Chauvin, A., Frenkel, L., Pirez, N., & Ceriani, M. F. (2014). Circadian pacemaker neurons change synaptic contacts across the day. *Curr Biol*, *24*(18), 2161-2167. https://doi.org/10.1016/j.cub.2014.07.063

Gourfinkel-An, I., Cancel, G., Duyckaerts, C., Faucheux, B., Hauw, J. J., Trottier, Y., Brice, A., Agid, Y., & Hirsch, E. C. (1998). Neuronal distribution of intranuclear inclusions in Huntington's disease with adult onset. *Neuroreport*, *9*(8), 1823-1826. https://doi.org/10.1097/00001756-199806010-00028

Graeber, M. B., & Moran, L. B. (2002). Mechanisms of Cell Death in Neurodegenerative Diseases: Fashion, Fiction, and Facts. *Brain Pathol*, *12*, 385-390. https://doi.org/10.1111/j.1750-3639.2002.tb00452.x.

Griciuc, A., Aron, L., & Ueffing, M. (2011). ER stress in retinal degeneration: A target for rational therapy? *Trends in Molecular Medicine*, *17*(8), 442-451. https://doi.org/10.1016/j.molmed.2011.04.002

Griffin, E. A., Jr., Staknis, D., & Weitz, C. J. (1999). Light-independent role of CRY1 and CRY2 in the mammalian circadian clock. *Science*, *286*(5440), 768-771. https://doi.org/10.1126/science.286.5440.768

Grima, B., Ché, E., Xia, R., & Ois Rouyer, F. (2004). Morning and evening peaks of activity rely on different clock neurons of the Drosophila brain. *Nature*. https://doi.org/10.1038/nature02935

Gutierrez-Garcia, R., Koyuncu, S., Hommen, F., Bilican, S., Lee, H. J., Fatima, A., & Vilchez, D. (2023). G3BP1-dependent mechanism suppressing protein aggregation in Huntington's models and its demise upon stress granule assembly. *Hum Mol Genet*. https://doi.org/10.1093/hmg/ddac304

Haass, C., & Selkoe, D. J. (2007). Soluble protein oligomers in neurodegeneration: Lessons from the Alzheimer's amyloid β-peptide. In *Nature Reviews Molecular Cell Biology* (Vol. 8, pp. 101-112).

Hallacli, E., Kayatekin, C., Nazeen, S., Wang, X. H., Sheinkopf, Z., Sathyakumar, S., Sarkar, S., Jiang, X., Dong, X., Di Maio, R., Wang, W., Keeney, M. T., Felsky, D., Sandoe, J., Vahdatshoar, A., Udeshi, N. D., Mani, D. R., Carr, S. A., Lindquist, S., . . . Khurana, V. (2022). The Parkinson's disease protein alpha-synuclein is a modulator of processing bodies and mRNA stability. *Cell*, *185*(12), 2035-2056.e2033. https://doi.org/10.1016/j.cell.2022.05.008

Hamanaka, R. B., Bennett, B. S., Cullinan, S. B., & Diehl, J. A. (2005). PERK and GCN2 contribute to eIF2α phosphorylation and cell cycle arrest after activation of the unfolded protein response pathway. *Molecular Biology of the Cell*, *16*(12), 5493-5501. https://doi.org/10.1091/mbc.E05-03-0268

Hamid, S. M., Citir, M., Terzi, E. M., Cimen, I., Yildirim, Z., Dogan, A. E., Kocaturk, B., Onat, U. I., Arditi, M., Weber, C., Traynor-Kaplan, A., Schultz, C., & Erbay, E. (2020). Inositol-requiring enzyme-1 regulates phosphoinositide signaling lipids and macrophage growth. *EMBO reports*, *21*(12). https://doi.org/10.15252/embr.202051462

Hammonds, A. S., Bristow, C. A., Fisher, W. W., Weiszmann, R., Wu, S., Hartenstein, V., Kellis, M., Yu, B., Frise, E., & Celniker, S. E. (2013). Spatial expression of transcription factors in Drosophila embryonic organ development. *Genome Biol*, *14*(12), R140. https://doi.org/10.1186/gb-2013-14-12-r140

Han, A.-P., Yu, C., Lu, L., Fujiwara, Y., Browne, C., Chin, G., Fleming, M., Leboulch, P., Orkin, S. H., & Chen, J.-J. (2001). Heme-regulated eIF2akinase (HRI) is required for translational regulation and survival of erythroid precursors in iron deficiency. *European Molecular Biology Organisation*, *20*(23), 6909-6918.

Hardie, R. C. (2001). Phototransduction in Drosophila melanogaster. *Journal of Experimental Biology*, *204*(20), 3403-3409.

Hardie, R. C. (2008). Phototransduction in Microvillar Photoreceptors of Drosophila and Other Invertebrates. *1*(January 2008), 77-130.

Hardie, R. C., Martin, F., Cochrane, G. W., Juusola, M., Georgiev, P., & Raghu, P. (2002). Molecular basis of amplification in Drosophila phototransduction: roles for G protein, phospholipase C, and diacylglycerol kinase. *Neuron*, *36*(4), 689-701. https://doi.org/10.1016/s0896-6273(02)01048-6

Harding, H. P., Zhang, Y., Zeng, H., Novoa, I., Lu, P. D., Calfon, M., Sadri, N., Yun, C., Popko, B., Paules, R., Stojdl, D. F., Bell, J. C., Hettmann, T., Leiden, J. M., & Ron, D. (2003). *An Integrated Stress Response Regulates Amino AcidMetabolism and Resistance to Oxidative Stress* (Molecular Cell, Issue. http://www.molecule.org/

Harding, H. P., Zyryanova, A. F., & Ron, D. (2012). Uncoupling proteostasis and development in vitro with a small molecule inhibitor of the pancreatic endoplasmic reticulum kinase, PERK. *J Biol Chem*, *287*(53), 44338-44344. https://doi.org/10.1074/jbc.M112.428987

Harris, W. A., & Stark, W. S. (1977). Hereditary retinal degeneration in Drosophila melanogaster: A mutant defect associated with the phototransduction process. *Journal of General Physiology*, *69*(3), 261-291. https://doi.org/10.1085/jgp.69.3.261

Hart, M. P., & Gitler, A. D. (2012). ALS-associated ataxin 2 polyQ expansions enhance stress-induced caspase 3 activation and increase TDP-43 pathological modifications. *Journal of Neuroscience*, *32*(27), 9133-9142. https://doi.org/10.1523/JNEUROSCI.0996-12.2012

Heigwer, F., Port, F., & Boutros, M. (2018). Rna interference (RNAi) screening in Drosophila. *Genetics*, *208*(3), 853-874. https://doi.org/10.1534/genetics.117.300077

Helfrich-Forster, C. (1998). Robust circadian rhythmicity of Drosophila melanogaster requires the presence of lateral neurons: a brain-behavioral study of disconnected mutants. *J Comp Physiol A*, *182*(4), 435-453. https://doi.org/10.1007/s003590050192

Henderson, S. R., Reuss, H., & Hardie, R. C. (2000). Single photon responses in Drosophila photoreceptors and their regulation by Ca2+. *Journal of Physiology*, *524*(1), 179-194. https://doi.org/10.1111/j.1469-7793.2000.00179.x

Herrero, A., Yoshii, T., Ispizua, J. I., Colque, C., Veenstra, J. A., Muraro, N. I., & Ceriani, M. F. (2020). Coupling Neuropeptide Levels to Structural Plasticity in Drosophila Clock Neurons. *Curr Biol*, *30*(16), 3154-3166 e3154. https://doi.org/10.1016/j.cub.2020.06.009

Herzog-Krzywoszanska, R., & Krzywoszanski, L. (2019). Sleep disorders in Huntington's disease. In *Frontiers in Psychiatry* (Vol. 10): Frontiers Media S.A.

Hinnebusch, A. G. (1988). *Mechanisms of Gene Regulation in the General Control of Amino Acid Biosynthesis in Saccharomyces cerevisiae* (MICROBIOLOGICAL REVIEWS, Issue.

Hoozemans, J. J., van Haastert, E. S., Eikelenboom, P., de Vos, R. A., Rozemuller, J. M., & Scheper, W. (2007). Activation of the unfolded protein response in Parkinson's disease. *Biochem Biophys Res Commun*, *354*(3), 707-711. https://doi.org/10.1016/j.bbrc.2007.01.043

Hoozemans, J. J., van Haastert, E. S., Nijholt, D. A., Rozemuller, A. J., & Scheper, W. (2012). Activation of the unfolded protein response is an early event in Alzheimer's and Parkinson's disease. *Neurodegener Dis*, *10*(1-4), 212-215. https://doi.org/10.1159/000334536

Hoozemans, J. J. M., Van Haastert, E. S., Nijholt, D. A. T., Rozemuller, A. J. M., Eikelenboom, P., & Scheper, W. (2009). The unfolded protein response is activated in pretangle neurons in alzheimer's disease hippocampus. *American Journal of Pathology*, *174*(4), 1241-1251. https://doi.org/10.2353/ajpath.2009.080814

Hotta, Y., & Benzer, S. (1970). Genetic dissection of the Drosophila nervous system by means of mosaics. *Proc Natl Acad Sci U S A*, *67*(3), 1156-1163. https://doi.org/10.1073/pnas.67.3.1156

Hu, Y., Comjean, A., Rodiger, J., Liu, Y., Gao, Y., Chung, V., Zirin, J., Perrimon, N., & Mohr, S. E. (2021). FlyRNAi.org-the database of the Drosophila RNAi screening center and transgenic RNAi project: 2021 update. *Nucleic Acids Research*, *49*(D1), D908-D915. https://doi.org/10.1093/nar/gkaa936

Hu, Y., Flockhart, I., Vinayagam, A., Bergwitz, C., Berger, B., Perrimon, N., & Mohr, S. E. (2011). An integrative approach to ortholog prediction for disease-focused and other functional studies. *BMC Bioinformatics*, *12*, 357. https://doi.org/10.1186/1471-2105-12-357

Hu, Y., Roesel, C., Flockhart, I., Perkins, L., Perrimon, N., & Mohr, S. E. (2013). UP-TORR: online tool for accurate and Up-to-Date annotation of RNAi Reagents. *Genetics*, *195*(1), 37-45. https://doi.org/10.1534/genetics.113.151340

Huang, Y., Xie, J., & Wang, T. (2015). A fluorescence-based genetic screen to study retinal degeneration in drosophila. *PLOS ONE*, *10*(12). https://doi.org/10.1371/journal.pone.0144925

Huelsmeier, J., Walker, E., Bakthavachalu, B., & Ramaswami, M. (2021). A C-terminal ataxin-2 disordered region promotes Huntingtin protein aggregation and neurodegeneration in Drosophila models of Huntington's disease. *G3: Genes, Genomes, Genetics*, *11*(12). https://doi.org/10.1093/g3journal/jkab355

Huntington, G. (1872). On Chorea. *Medical and Surgical Reporter of Philadelphia*, 1872-1872.

Hyung, D. R., & Steller, H. (2007). Unfolded protein response in Drosophila: Why another model can make it fly. In *Cell Cycle* (Vol. 6, pp. 830-835): Taylor and Francis Inc.

Imarisio, S., Carmichael, J., Korolchuk, V., Chen, C. W., Saiki, S., Rose, C., Krishna, G., Davies, J. E., Ttofi, E., Underwood, B. R., & Rubinsztein, D. C. (2008). Huntington's disease: from pathology and genetics to potential therapies. *Biochem J*, *412*(2), 191-209. https://doi.org/10.1042/BJ20071619

Jackson, G. R., Salecker, I., Dong, X., Yao, X., Arnheim, N., Faber, P. W., MacDonald, M. E., & Zipursky, S. L. (1998). Polyglutamine-expanded human huntingtin transgenes induce degeneration of Drosophila photoreceptor neurons. *Neuron*, *21*(3), 633-642. https://doi.org/10.1016/S0896-6273(00)80573-5

Johnson, C., Elliott, J., Foster, R., Honma, K.-I., & Kronauer, R. (2003). Fundamental Properties of Circadian Rhythms. In *Chronobiology: Biological Timekeeping* (pp. 67-106). Sinauer Associates, Inc. Publishers.

Julien, C. L., Thompson, J. C., Wild, S., Yardumian, P., Snowden, J. S., Turner, G., & Craufurd, D. (2007). Psychiatric disorders in preclinical Huntington's disease. *Journal of Neurology, Neurosurgery and Psychiatry*, *78*(9), 939-943. https://doi.org/10.1136/jnnp.2006.103309

Kang, K., Ryoo, H. D., Park, J.-E., Yoon, J.-H., & Kang, M.-J. (2015). A Drosophila Reporter for the Translational Activation of ATF4 Marks Stressed Cells during Development. *PLOS ONE*, *10*(5), e0126795-e0126795. https://doi.org/10.1371/journal.pone.0126795

Kang, M. J., Chung, J., & Ryoo, H. D. (2012). CDK5 and MEKK1 mediate pro-apoptotic signalling following endoplasmic reticulum stress in an autosomal dominant retinitis pigmentosa model. *Nature Cell Biology*, *14*(4), 409-415. https://doi.org/10.1038/ncb2447

Kedersha, N., Chen, S., Gilks, N., Li, W., Miller, I. J., Stahl, J., & Anderson, P. (2002). Evidence That Ternary Complex (eIF2-GTP-tRNA i Met)-Deficient Preinitiation Complexes Are Core Constituents of Mammalian Stress Granules. *Molecular Biology of the Cell*, *13*, 195-210. https://doi.org/10.1091/mbc.01

Kedersha, N., Cho, M. R., Li, W., Yacono, P. W., Chen, S., Gilks, N., Golan, D. E., & Anderson, P. (2000). *Dynamic Shuttling of TIA-1 Accompanies the Recruitment of mRNA to Mammalian Stress Granules 7* (The Journal of Cell Biology, Issue. http://www.jcb.org/cgi/content/full/151/6/1257

Kedersha, N. L., Gupta, M., Li, W., Miller, I., & Anderson, P. (1999). *RNA-binding Proteins TIA-1 and TIAR Link the Phosphorylation of eIF-2 to the Assembly of Mammalian Stress Granules* (00219525/99/12/1). (The Journal of Cell Biology, Issue. http://www.jcb.org

Kelaini, S., Chan, C., Cornelius, V. A., & Margariti, A. (2021). RNA-Binding Proteins Hold Key Roles in Function, Dysfunction, and Disease. *Biology (Basel)*, *10*(5). https://doi.org/10.3390/biology10050366

Khan, N. W., Falsini, B., Kondo, M., & Robson, A. G. (2017). Inherited Retinal Degeneration: Genetics, Disease Characterization, and Outcome Measures. In *Journal of Ophthalmology* (Vol. 2017): Hindawi Limited.

Kim, H. J., Raphael, A. R., Ladow, E. S., McGurk, L., Weber, R. A., Trojanowski, J. Q., Lee, V. M. Y., Finkbeiner, S., Gitler, A. D., & Bonini, N. M. (2014). Therapeutic modulation of eIF2α phosphorylation rescues TDP-43 toxicity in amyotrophic lateral sclerosis disease models. *Nature Genetics*, *46*(2), 152-160. https://doi.org/10.1038/ng.2853

King, A. N., Barber, A. F., Smith, A. E., Dreyer, A. P., Sitaraman, D., Nitabach, M. N., Cavanaugh, D. J., & Sehgal, A. (2017). A Peptidergic Circuit Links the Circadian Clock to Locomotor Activity. *Curr Biol*, *27*(13), 1915-1927 e1915. https://doi.org/10.1016/j.cub.2017.05.089

Kino, Y., Daisuke, M., Oma, Y., Takeshita, Y., Sasagawa, N., & Ishuira, S. (2004). Muscleblind protein, MBNL1/EXP, binds specifically to CHHG repeats. *Human Molecular Genetics*, *13*(5), 495-507. https://doi.org/10.1093/hmg/ddh056

Klose, M., Duvall, L. B., Li, W., Liang, X., Ren, C., Steinbach, J. H., & Taghert, P. H. (2016). Functional PDF Signaling in the Drosophila Circadian Neural Circuit Is Gated by Ral A-Dependent Modulation. *Neuron*, *90*(4), 781-794. https://doi.org/10.1016/j.neuron.2016.04.002

Kolarski, D., Miller, S., Oshima, T., Nagai, Y., Aoki, Y., Kobauri, P., Srivastava, A., Sugiyama, A., Amaike, K., Sato, A., Tama, F., Szymanski, W., Feringa, B. L., Itami, K., & Hirota, T. (2021). Photopharmacological Manipulation of Mammalian CRY1 for Regulation of the Circadian Clock. *J Am Chem Soc*, *143*(4), 2078-2087. https://doi.org/10.1021/jacs.0c12280

Konopka, R. J., & Benzer, S. (1971). *Clock Mutants of Drosophila melanogaster (eclosion/circadian/rhythms/X chromosome)*.

Koyanagi, M., Kubokawa, K., Tsukamoto, H., Shichida, Y., & Terakita, A. (2005). Cephalochordate melanopsin: Evolutionary linkage between invertebrate visual cells and vertebrate photosensitive retinal ganglion cells. *Current Biology*, *15*(11), 1065-1069. https://doi.org/10.1016/j.cub.2005.04.063

Koyano, S., Uchihara, T., Fujigasaki, H., Nakamura, A., Yagishita, S., & Iwabuchi, K. (1999). Neuronal intranuclear inclusions in spinocerebellar ataxia type 2: triple-labeling immunofluorescent study. *Neurosci Lett*, *273*(2), 117-120. https://doi.org/10.1016/s0304-3940(99)00656-4

Krishnamoorthy, J., Rajesh, K., Mirzajani, F., Kesoglidou, P., Papadakis, A. I., & Koromilas, A. E. (2014). Evidence for eIF2α phosphorylation-independent effects of GSK2656157, a novel catalytic inhibitor of PERK with clinical implications. *Cell Cycle*, *13*(5), 801-806. https://doi.org/10.4161/cc.27726

Kulkarni, M. M., Booker, M., Silver, S. J., Friedman, A., Hong, P., Perrimon, N., & Mathey-Prevot, B. (2006). Evidence of off-target effects associated with long dsRNAs in Drosophila melanogaster cell-based assays. *Nature Methods*, *3*(10), 833-838. https://doi.org/10.1038/nmeth935

Kurada, P., & O'Tousa, J. E. (1995). Retinal degeneration caused by dominant rhodopsin mutations in Drosophila. *Neuron*, *14*(3), 571-579. https://doi.org/10.1016/0896-6273(95)90313-5

Lachke, S. A., Alkuraya, F. S., Kneeland, S. C., Ohn, T., Aboukhalil, A., Howell, G. R., Saadi, I., Cavallesco, R., Yue, Y., Tsai, A. C., Nair, K. S., Cosma, M. I., Smith, R. S., Hodges, E., Alfadhli, S. M., Al-Hajeri, A., Shamseldin, H. E., Behbehani, A., Hannon, G. J., . . . Maas, R. L. (2011). Mutations in the RNA granule component TDRD7 cause cataract and glaucoma. *Science*, *331*(6024), 1571-1576. https://doi.org/10.1126/science.1195970

Landles, C., Sathasivam, K., Weiss, A., Woodman, B., Moffitt, H., Finkbeiner, S., Sun, B., Gafni, J., Ellerby, L. M., Trottier, Y., Richards, W. G., Osmand, A., Paganetti, P., & Bates, G. P. (2010). Proteolysis of mutant huntingtin produces an exon 1 fragment that accumulates as an aggregated protein in neuronal nuclei in Huntington disease. *J Biol Chem*, *285*(12), 8808-8823. https://doi.org/10.1074/jbc.M109.075028

Laver, J. D., Ly, J., Winn, A. K., Karaiskakis, A., Lin, S., Nie, K., Benic, G., Jaberi-Lashkari, N., Cao, W. X., Khademi, A., Westwood, J. T., Sidhu, S. S., Morris, Q., Angers, S., Smibert, C. A., & Lipshitz, H. D. (2020). The RNA-Binding Protein Rasputin/G3BP Enhances the Stability and Translation of Its Target mRNAs. *Cell Reports*, *30*(10), 3353-3367.e3357. https://doi.org/10.1016/j.celrep.2020.02.066

Lear, B. C., Merrill, C. E., Lin, J. M., Schroeder, A., Zhang, L., & Allada, R. (2005). A G Protein-coupled receptor, groom-of-PDF, is required for PDF neuron action in circadian behavior. *Neuron*, *48*(2), 221-227. https://doi.org/10.1016/j.neuron.2005.09.008

Lee, C., Etchegaray, J. P., Cagampang, F. R., Loudon, A. S., & Reppert, S. M. (2001). Posttranslational mechanisms regulate the mammalian circadian clock. *Cell*, *107*(7), 855-867. https://doi.org/10.1016/s0092-8674(01)00610-9

Lee, E. S., Yoon, C. H., Kim, Y. S., & Bae, Y. S. (2007). The double-strand RNA-dependent protein kinase PKR plays a significant role in a sustained ER stress-induced apoptosis. *FEBS Letters*, *581*(22), 4325-4332. https://doi.org/10.1016/j.febslet.2007.08.001

Lee, H., Noh, J. Y., Oh, Y., Kim, Y., Chang, J. W., Chung, C. W., Lee, S. T., Kim, M., Ryu, H., & Jung, Y. K. (2012). IRE1 plays an essential role in ER stress-mediated aggregation of mutant huntingtin via the inhibition of autophagy flux. *Hum Mol Genet*, *21*(1), 101-114. https://doi.org/10.1093/hmg/ddr445

Lee, K. H., Zhang, P., Kim, H. J., Mitrea, D. M., Sarkar, M., Freibaum, B. D., Cika, J., Coughlin, M., Messing, J., Molliex, A., Maxwell, B. A., Kim, N. C., Temirov, J., Moore, J., Kolaitis, R. M., Shaw, T. I., Bai, B., Peng, J., Kriwacki, R. W., & Taylor, J. P. (2016). C9orf72 Dipeptide Repeats Impair the Assembly, Dynamics, and Function of Membrane-Less Organelles. *Cell*. https://doi.org/10.1016/j.cell.2016.10.002

Lee, W. C., Yoshihara, M., & Littleton, J. T. (2004). Cytoplasmic aggregates trap polyglutamine-containing proteins and block axonal transport in a Drosophila model of Huntington's disease. *Proc Natl Acad Sci U S A*, *101*(9), 3224-3229. https://doi.org/10.1073/pnas.0400243101

Leitman, J., Barak, B., Benyair, R., Shenkman, M., Ashery, U., Hartl, F. U., & Lederkremer, G. Z. (2014). ER stress-induced eIF2-alpha phosphorylation underlies sensitivity of striatal neurons to pathogenic huntingtin. *PLOS ONE*, *9*(3), e90803. https://doi.org/10.1371/journal.pone.0090803

Leitman, J., Ulrich Hartl, F., & Lederkremer, G. Z. (2013). Soluble forms of polyQ-expanded huntingtin rather than large aggregates cause endoplasmic reticulum stress. *Nature Communications*, *4*. https://doi.org/10.1038/ncomms3753

Lemaire, P. A., Anderson, E., Lary, J., & Cole, J. L. (2008). Mechanism of PKR Activation by dsRNA. *Journal of Molecular Biology*, *381*(2), 351-360. https://doi.org/10.1016/j.jmb.2008.05.056

Leung, N. Y., & Montell, C. (2017). Unconventional Roles of Opsins. *Annual Review of Cell and Developmental Biology*. https://doi.org/10.1146/annurev-cellbio-100616

Li, L. B., Yu, Z., Teng, X., & Bonini, N. M. (2008). RNA toxicity is a component of ataxin-3 degeneration in Drosophila. *Nature*, *453*(7198), 1107-1111. https://doi.org/10.1038/nature06909

Li, W. Z., Li, S. L., Zheng, H. Y., Zhang, S. P., & Xue, L. (2012). A broad expression profile of the GMR-GAL4 driver in Drosophila melanogaster. *Genetics and molecular research : GMR*, *11*(3), 1997-2002. https://doi.org/10.4238/2012.August.6.4

Li, Y., Guo, F., Shen, J., & Rosbash, M. (2014). PDF and cAMP enhance per stability in Drosophila clock neurons. *Proceedings of the National Academy of Sciences of the United States of America*, *111*(13). https://doi.org/10.1073/pnas.1402562111

Li, Y. R., King, O. D., Shorter, J., & Gitler, A. D. (2013). Stress granules as crucibles of ALS pathogenesis. In *Journal of Cell Biology* (Vol. 201, pp. 361-372).

Lin, C., & Todo, T. (2005). The cryptochromes. *Genome Biol*, *6*(5), 220. https://doi.org/10.1186/gb-2005-6-5-220

Liu-Yesucevitz, L. Q., Lin, A. Y., Ebata, A., Boon, J. Y., Reid, W., Xu, Y. F., Kobrin, K., Murphy, G. J., Petrucelli, L., & Wolozin, B. (2014). ALS-linked mutations enlarge TDP-43-enriched neuronal RNA granules in the dendritic arbor. *Journal of Neuroscience*, *34*(12), 4167-4174. https://doi.org/10.1523/JNEUROSCI.2350-13.2014

Loh, D. H., Kudo, T., Truong, D., Wu, Y., & Colwell, C. S. (2013). The Q175 mouse model of Huntington's disease shows gene dosage- and age-related decline in circadian rhythms of activity and sleep. *PLOS ONE*, *8*(7), e69993. https://doi.org/10.1371/journal.pone.0069993

Lucas, R. J., & Foster, R. G. (1999). Photoentrainment in mammals: a role for cryptochrome? *J Biol Rhythms*, *14*(1), 4-10. https://doi.org/10.1177/074873099129000380

Ma, Y., Creanga, A., Lum, L., & Beachy, P. A. (2006). Prevalence of off-target effects in Drosophila RNA interference screens. *Nature*, *443*(7109), 359-363. https://doi.org/10.1038/nature05179

Macleod, R., Tibben, A., Frontali, M., Evers-Kiebooms, G., Jones, A., Martinez-Descales, A., Roos, R., Bijlsma, E., Blinkenberg, E., Bombard, Y., Borry, P., Craufurd, D., Davis, M., De Die-Smulders, C., Downing, C., Dürr, A., Garcia Barcina, M., Glew, R., Heiberg, A., . . . Vetter,

L. (2013). Recommendations for the predictive genetic test in Huntington's disease. *Clinical Genetics*, *83*(3), 221-231. https://doi.org/10.1111/j.1399-0004.2012.01900.x

Mainland, R. L., Lyons, T. A., Ruth, M. M., & Kramer, J. M. (2017). Optimal RNA isolation method and primer design to detect gene knockdown by qPCR when validating Drosophila transgenic RNAi lines. *BMC Research Notes*, *10*(1). https://doi.org/10.1186/s13104-017-2959-0

Martín-Aparicio, E., Yamamoto, A., Lix Herná Ndez, F., Hen, R., Avila, J. S., & Lucas, J. J. (2001). *Proteasomal-Dependent Aggregate Reversal and Absence of Cell Death in a Conditional Mouse Model of Huntington's Disease*.

Maziuk, B., Ballance, H. I., & Wolozin, B. (2017). Dysregulation of RNA binding protein aggregation in neurodegenerative disorders. *Frontiers in Molecular Neuroscience*, *10*(April), 1-9. https://doi.org/10.3389/FNMOL.2017.00089

McEwen, E., Kedersha, N., Song, B., Scheuner, D., Gilks, N., Han, A., Chen, J. J., Anderson, P., & Kaufman, R. J. (2005). Heme-regulated inhibitor kinase-mediated phosphorylation of eukaryotic translation initiation factor 2 inhibits translation, induces stress granule formation, and mediates survival upon arsenite exposure. *Journal of Biological Chemistry*, *280*(17), 16925-16933. https://doi.org/10.1074/jbc.M412882200

McLaughlin, B. A., Spencer, C., & Eberwine, J. (1996). *CAG Trinucleotide RNA Repeats Interact with RNA-Binding Proteins* (Am. J. Hum. Genet, Issue.

McLaughlin, T., Medina, A., Perkins, J., Yera, M., Wang, J. J., & Zhang, S. X. (2022). Cellular stress signaling and the unfolded protein response in retinal degeneration: mechanisms and therapeutic implications. In *Molecular Neurodegeneration* (Vol. 17): BioMed Central Ltd.

Mendes, C. S., Levet, C., Chatelain, G., Dourlen, P., Fouillet, A., Dichtel-Danjoy, M. L., Gambis, A., Ryoo, H. D., Steller, H., & Mollereau, B. (2009). ER stress protects from retinal degeneration. *EMBO Journal*, *28*(9), 1296-1307. https://doi.org/10.1038/emboj.2009.76

Mendes, H. F., Van Der Spuy, J., Chapple, J. P., & Cheetham, M. E. (2005). Mechanisms of cell death in rhodopsin retinitis pigmentosa: Implications for therapy. *Trends in Molecular Medicine*, *11*(4), 177-185. https://doi.org/10.1016/j.molmed.2005.02.007

Mertens, I., Vandingenen, A., Johnson, E. C., Shafer, O. T., Li, W., Trigg, J. S., De Loof, A., Schoofs, L., & Taghert, P. H. (2005). PDF receptor signaling in Drosophila contributes to both circadian and geotactic behaviors. *Neuron*, *48*(2), 213-219. https://doi.org/10.1016/j.neuron.2005.09.009

Milligan, S. C., Alb, J. G., Elagina, R. B., Bankaitis, V. A., Hyde, D. R., Milligan, S. C., & Alb, J. G. (1997). *The Phosphatidylinositol Transfer Protein Domain of Drosophila Retinal Degeneration B Protein Is Essential for Photoreceptor Cell Survival and Recovery from Light Stimulation* (00219525/97/10/3). (The Journal of Cell Biology, Issue. http://www.jcb.org

Miyamoto, Y., & Sancar, A. (1998). Vitamin B2-based blue-light photoreceptors in the retinohypothalamic tract as the photoactive pigments for setting the circadian clock in mammals. *Proc Natl Acad Sci U S A*, *95*(11), 6097-6102. https://doi.org/10.1073/pnas.95.11.6097

Mizielinska, S., Gronke, S., Niccoli, T., Ridler, C. E., Clayton, E. L., Devoy, A., Moens, T., Norona, F. E., Woollacott, I. O. C., Pietrzyk, J., Cleverley, K., Nicoll, A. J., Pickering-Brown, S., Dols, J., Cabecinha, M., Hendrich, O., Fratta, P., Fisher, E. M. C., Partridge, L., & Isaacs, A. M. (2014). C9orf72 repeat expansions cause neurodegeneration in Drosophila through arginine-rich proteins. *Science*, *345*(6201), 1192-1194. https://doi.org/10.1126/science.1256800

Morton, A. J., Wood, N. I., Hastings, M. H., Hurelbrink, C., Barker, R. A., & Maywood, E. S. (2005). Disintegration of the sleep-wake cycle and circadian timing in Huntington's disease. *J Neurosci*, *25*(1), 157-163. https://doi.org/10.1523/JNEUROSCI.3842-04.2005

Moulin, T. C., Dey, S., Dashi, G., Li, L., Sridhar, V., Safa, T., Berkins, S., Williams, M. J., & Schiöth, H. B. (2022). A simple high-throughput method for automated detection of Drosophila melanogaster light-dependent behaviours. *BMC Biology*, *20*(1). https://doi.org/10.1186/s12915-022-01476-z

Mykowska, A., Sobczak, K., Wojciechowska, M., Kozlowski, P., & Krzyzosiak, W. J. (2011). CAG repeats mimic CUG repeats in the misregulation of alternative splicing. *Nucleic Acids Research*, *39*(20), 8938-8951. https://doi.org/10.1093/nar/gkr608

Nalavade, R., Griesche, N., Ryan, D. P., Hildebrand, S., & Krauß, S. (2013). Mechanisms of RNA-induced toxicity in CAG repeat disorders. *Cell Death and Disease*, *4*(8), e752-711. https://doi.org/10.1038/cddis.2013.276

Namkoong, S., Ho, A., Woo, Y. M., Kwak, H., & Lee, J. H. (2018). Systematic Characterization of Stress-Induced RNA Granulation. *Molecular Cell*, *70*(1), 175-187.e178. https://doi.org/10.1016/j.molcel.2018.02.025

Nasir-Ahmad, S., Lee, S. C. S., Martin, P. R., & Grünert, U. (2019). Melanopsin-expressing ganglion cells in human retina: Morphology, distribution, and synaptic connections. *Journal of Comparative Neurology*, *527*(1), 312-327. https://doi.org/10.1002/cne.24176

Neill, G., & Masson, G. R. (2023). A stay of execution: ATF4 regulation and potential outcomes for the integrated stress response. *Front Mol Neurosci*, *16*, 1112253. https://doi.org/10.3389/fnmol.2023.1112253

Nishitoh, H., Kadowaki, H., Nagai, A., Maruyama, T., Yokota, T., Fukutomi, H., Noguchi, T., Matsuzawa, A., Takeda, K., & Ichijo, H. (2008). ALS-linked mutant SOD1 induces ER stress- and ASK1-dependent motor neuron death by targeting Derlin-1. *Genes Dev*, *22*(11), 1451-1464. https://doi.org/10.1101/gad.1640108

Novoa, I., Zeng, H., Harding, H. P., Ron, D., Neibert, D. W., Hollander, M. C., Luethy, J. D., Papathanasiou, M., Fragoli, J., Holbrook, N. J., & Hoffman-Lieberman, B. (2001). *Feedback Inhibition of the Unfolded Protein Response by GADD34-mediated Dephosphorylation of eIF2* (The Journal of Cell Biology, Issue. http://www.jcb.org/cgi/content/full/153/5/1011

O'Tousa, J. E., Baehr, W., Martin, R. L., Hirsh, J., Pak, W. L., & Applebury, M. L. (1995). The Drosophila ninaE Gene Encodes an Opsin. *Cell*, *40*, 839-850.

Ocaka, L., Spalluto, C., Wilson, D. I., Hunt, D. M., & Halford, S. (2005). Chromosomal localization, genomic organization and evolution of the genes encoding human phosphatidylinositol transfer protein membrane-associated (PITPNM) 1, 2 and 3. *Cytogenetic and Genome Research*, *108*(4), 293-302. https://doi.org/10.1159/000081519

Okamura, H., Miyake, S., Sumi, Y., Yamaguchi, S., Yasui, A., Muijtjens, M., Hoeijmakers, J. H., & van der Horst, G. T. (1999). Photic induction of mPer1 and mPer2 in cry-deficient mice lacking a biological clock. *Science*, *286*(5449), 2531-2534. https://doi.org/10.1126/science.286.5449.2531

Orr, H. T. (2012). Cell biology of spinocerebellar ataxia. In *Journal of Cell Biology* (Vol. 197, pp. 167-177).

Ostrowski, L. A., Hall, A. C., & Mekhail, K. (2017). Ataxin-2: From RNA Control to Human Health and Disease. *Genes (Basel)*, *8*(6). https://doi.org/10.3390/genes8060157

Paetkau, D. W., Elagin, V. A., Sendi, L. M., & Hyde, D. R. (1999). Isolation and characterization of Drosophila retinal degeneration B suppressors. *Genetics*, *151*(2), 713-724.

Pak, W. L. (1995). Drosophila in vision research: The Friedenwald lecture. *Investigative Ophthalmology and Visual Science*, *36*(12), 2340-2357.

Pakos-Zebrucka, K., Koryga, I., Mnich, K., Ljujic, M., Samali, A., & Gorman, A. M. (2016). The integrated stress response. *EMBO reports*, *17*(10), 1374-1395. https://doi.org/10.15252/embr.201642195

Park, J. H., Helfrich-Forster, C., Lee, G., Liu, L., Rosbash, M., & Hall, J. C. (2000). Differential regulation of circadian pacemaker output by separate clock genes in Drosophila. *Proc Natl Acad Sci U S A*, *97*(7), 3608-3613. https://doi.org/10.1073/pnas.97.7.3608

Partch, C. L., Shields, K. F., Thompson, C. L., Selby, C. P., & Sancar, A. (2006). Posttranslational regulation of the mammalian circadian clock by cryptochrome and protein phosphatase 5. *Proc Natl Acad Sci U S A*, *103*(27), 10467-10472. https://doi.org/10.1073/pnas.0604138103

Paul, S., Dansithong, W., Figueroa, K. P., Scoles, D. R., & Pulst, S. M. (2018). Staufen1 links RNA stress granules and autophagy in a model of neurodegeneration. *Nat Commun*, *9*(1), 3648. https://doi.org/10.1038/s41467-018-06041-3

Penfold, P. L., Madigan, M. C., Gillies, M. C., & Provis, J. M. (2001). Immunological and Aetiological Aspects of Macular Degeneration. *Progress in Retinal and Eye Research*, *20*, 385-414.

Peschel, N., & Helfrich-Förster, C. (2011). Setting the clock - By nature: Circadian rhythm in the fruitfly Drosophila melanogaster. In *FEBS Letters* (Vol. 585, pp. 1435-1442): Elsevier B.V.

Peskett, T. R., Rau, F., O'Driscoll, J., Patani, R., Lowe, A. R., & Saibil, H. R. (2018). A Liquid to Solid Phase Transition Underlying Pathological Huntingtin Exon1 Aggregation. *Molecular Cell*, *70*(4), 588-601.e586. https://doi.org/10.1016/j.molcel.2018.04.007

Pfeiffenberger, C., Lear, B. C., Keegan, K. P., & Allada, R. (2010). Locomotor activity level monitoring using the Drosophila Activity Monitoring (DAM) System. *Cold Spring Harb Protoc*, *2010*(11), pdb prot5518. https://doi.org/10.1101/pdb.prot5518

Pitale, P. M., Gorbatyuk, O., & Gorbatyuk, M. (2017). Neurodegeneration: Keeping ATF4 on a tight leash. *Frontiers in Cellular Neuroscience*, *11*(December), 1-8. https://doi.org/10.3389/fncel.2017.00410

Pittendrigh, C. S. (1967). *CIRCA DIAN SYSTEMS, I. THE DRIVING OSCILLATION AND ITS ASSA Y IN DROSOPHILA PSEUDOOBSCURA**.

Rabouw, H. H., Langereis, M. A., Anand, A. A., Visser, L. J., de Groot, R. J., Walter, P., & van Kuppeveld, F. J. M. (2019). Small molecule ISRIB suppresses the integrated stress response within a defined window of activation. *Proceedings of the National Academy of Sciences*, *116*(6), 2097-2102. https://doi.org/10.1073/pnas.1815767116

Ramaswami, M., Taylor, J. P., & Parker, R. (2013). Altered ribostasis: RNA-protein granules in degenerative disorders. In *Cell* (Vol. 154): Elsevier B.V.

Reineke, L. C., & Lloyd, R. E. (2015). The Stress Granule Protein G3BP1 Recruits Protein Kinase R To Promote Multiple Innate Immune Antiviral Responses. *Journal of Virology*, *89*(5), 2575-2589. https://doi.org/10.1128/jvi.02791-14

Roberts, L., Leise, T. L., Noguchi, T., Galschiodt, A. M., Houl, J. H., Welsh, D. K., & Holmes, T. C. (2015). Light evokes rapid circadian network oscillator desynchrony followed by gradual phase retuning of synchrony. *Current Biology*, *25*(7), 858-867. https://doi.org/10.1016/j.cub.2015.01.056

Roybal, C. N., Marmorstein, L. Y., Vander Jagt, D. L., & Abcouwer, S. F. (2005). Aberrant accumulation of fibulin-3 in the endoplasmic reticulum leads to activation of the unfolded protein response and VEGF expression. *Investigative Ophthalmology and Visual Science*, *46*(11), 3973-3979. https://doi.org/10.1167/iovs.05-0070

Rutkowski, D. T., & Kaufman, R. J. (2007). That which does not kill me makes me stronger: adapting to chronic ER stress. In *Trends in Biochemical Sciences* (Vol. 32, pp. 469-476).

Sahly, I., Bar Nachum, S., Toby, E. S., Rom, A., Peretz, A., Kleimant, J., Bykt, T., Selingerti, Z., & Minke, B. (1992). *Calcium channel blockers inhibit retinal degeneration in the retinal-degeneration-B mutant of Drosophila (neuronal ceIl death/lght-Induced degenerathn/Ca2+ spoes/excessve psphorylatlon)* (Neurobiology, Issue. https://www.pnas.org

Sahoo, P. K., Lee, S. J., Jaiswal, P. B., Alber, S., Kar, A. N., Miller-Randolph, S., Taylor, E. E., Smith, T., Singh, B., Ho, T. S., Urisman, A., Chand, S., Pena, E. A., Burlingame, A. L., Woolf, C. J., Fainzilber, M., English, A. W., & Twiss, J. L. (2018). Axonal G3BP1 stress granule protein limits axonal mRNA translation and nerve regeneration. *Nat Commun*, *9*(1), 3358. https://doi.org/10.1038/s41467-018-05647-x

Saliba, R. S., Munro, P. M. G., Luthert, P. J., & Cheetham, M. E. (2002). The cellular fate of mutant rhodopsin: Quality control, degradation and aggresome formation. *Journal of Cell Science*, *115*(14), 2907-2918.

Sanchez, I. I., Nguyen, T. B., England, W. E., Lim, R. G., Vu, A. Q., Miramontes, R., Byrne, L. M., Markmiller, S., Lau, A. L., Orellana, I., Curtis, M. A., Maxwell Faull, R. L., Yeo, G. W., Fowler, C. D., Reidling, J. C., Wild, E. J., Spitale, R. C., & Thompson, L. M. (2021). Huntington's disease mice and human brain tissue exhibit increased G3BP1 granules and TDP43 mislocalization. *Journal of Clinical Investigation*, *131*(12). https://doi.org/10.1172/JCI140723

Saraswat Ohri, S., Andres, K., Howard, R. M., Brown, B. L., Forston, M. D., Hetman, M., & Whittemore, S. R. (2022). Acute pharmacological inhibition of PERK signaling after spinal cord injury spares oligodendrocytes and improves locomotor recovery. *Journal of Neurotrauma*. https://doi.org/10.1089/neu.2022.0177

Savas, J. N., Ma, B., Deinhardt, K., Culver, B. P., Restituito, S., Wu, L., Belasco, J. G., Chao, M. V., & Tanese, N. (2010). A role for Huntington disease protein in dendritic RNA granules. *Journal of Biological Chemistry*, *285*(17), 13142-13153. https://doi.org/10.1074/jbc.M110.114561

Savas, J. N., Makusky, A., Ottosen, S., Baillat, D., Then, F., Krainc, D., Shiekhattar, R., Markey, S. P., & Tanese, N. (2008). *Huntington's disease protein contributes to RNA-mediated gene silencing through association with Argonaute and P bodies microRNA poly-glutamine RNA interference post-transcriptional gene silencing neuronal RNA granule*. www.pnas.org/cgi/content/full/

Schaffar, G., Breuer, P., Boteva, R., Behrends, C., Tzvetkov, N., Strippel, N., Sakahira, H., Siegers, K., Hayer-Hartl, M., & Hartl, F. U. (2004). Cellular toxicity of polyglutamine expansion proteins: mechanism of transcription factor deactivation. *Mol Cell*, *15*(1), 95-105. https://doi.org/10.1016/j.molcel.2004.06.029

Scherzinger, E., Sittler, A., Schweiger, K., Heiser, V., Lurz, R., Hasenbank, R., Bates, G. P., Lehrach, H., & Wanker, E. E. (1999). *Self-assembly of polyglutamine-containing huntingtin fragments into amyloid-like fibrils: Implications for Huntington's disease pathology (huntingtinglutamine repeataggregation)* (Medical Sciences Communicated by Max F. Perutz, Medical Research Council, Issue. www.pnas.org.

Schulte, J., & Littleton, J. T. (2011). The biological function of the Huntingtin protein and its relevance to Huntington's Disease pathology. *Curr Trends Neurol*, *5*, 65-78. https://www.ncbi.nlm.nih.gov/pubmed/22180703

Scoles, D. R., Meera, P., Schneider, M. D., Paul, S., Dansithong, W., Figueroa, K. P., Hung, G., Rigo, F., Bennett, C. F., Otis, T. S., & Pulst, S. M. (2017). Antisense oligonucleotide therapy for spinocerebellar ataxia type 2. *Nature*, *544*(7650), 362-366. https://doi.org/10.1038/nature22044

Seinen, E., Burgerhof, J. G. M., Jansen, R. C., & Sibon, O. C. M. (2011). RNAi-induced off-target effects in Drosophila melanogaster: Frequencies and solutions. *Briefings in Functional Genomics*, *10*(4), 206-214. https://doi.org/10.1093/bfgp/elr017

Seluzicki, A., Flourakis, M., Kula-Eversole, E., Zhang, L., Kilman, V., & Allada, R. (2014). Dual PDF Signaling Pathways Reset Clocks Via TIMELESS and Acutely Excite Target Neurons to Control Circadian Behavior. *PLoS Biology*, *12*(3). https://doi.org/10.1371/journal.pbio.1001810

Sen, T., Gupta, R., Kaiser, H., & Sen, N. (2017). Activation of PERK elicits memory impairment through inactivation of CREB and downregulation of PSD95 after traumatic brain injury. *Journal of Neuroscience*, *37*(24), 5900-5911. https://doi.org/10.1523/JNEUROSCI.2343-16.2017

Senthilan, P. R., & Helfrich-Förster, C. (2016). Rhodopsin 7-The unusual Rhodopsin in Drosophila. *PeerJ*, *2016*(9). https://doi.org/10.7717/peerj.2427

Shacham, T., Patel, C., & Lederkremer, G. Z. (2021). PERK Pathway and Neurodegenerative Disease: To Inhibit or to Activate? *Biomolecules*, *11*(3). https://doi.org/10.3390/biom11030354

Shakhmantsir, I., Dooley, S. J., Kishore, S., Chen, D., Pierce, E., Bennett, J., & Sehgal, A. (2019). RNA Splicing Factor Mutations That Cause Retinitis Pigmentosa Result in Circadian Dysregulation. *Journal of Biological Rhythms*, 1-12. https://doi.org/10.1177/0748730419887876

Shang, Y., & Huang, E. J. (2016). Mechanisms of FUS mutations in familial amyotrophic lateral sclerosis. In *Brain Research* (Vol. 1647, pp. 65-78): Elsevier B.V.

Sheeba, V., Fogle, K. J., & Holmes, T. C. (2010). Persistence of morning anticipation behavior and high amplitude morning startle response following functional loss of small ventral lateral neurons in drosophila. *PLOS ONE*, *5*(7). https://doi.org/10.1371/journal.pone.0011628

Shichida, Y., & Matsuyama, T. (2009). Evolution of opsins and phototransduction. In *Philosophical Transactions of the Royal Society B: Biological Sciences* (Vol. 364, pp. 2881-2895): Royal Society.

Shieh, B. H. (2011). Molecular genetics of retinal degeneration a drosophila perspective. *Fly*, *5*(4), 356-368. https://doi.org/10.4161/fly.5.4.17809

Shimazawa, M., & Hara, H. (2006). Inhibitor of double stranded RNA-dependent protein kinase protects against cell damage induced by ER stress. *Neuroscience Letters*, *409*(3), 192-195. https://doi.org/10.1016/j.neulet.2006.09.074

Sidibé, H., Dubinski, A., & Vande Velde, C. (2021). The multi-functional RNA-binding protein G3BP1 and its potential implication in neurodegenerative disease. In *Journal of Neurochemistry* (Vol. 157, pp. 944-962): John Wiley and Sons Inc.

Sidrauski, C., McGeachy, A. M., Ingolia, N. T., & Walter, P. (2015). The small molecule ISRIB reverses the effects of eIF2α phosphorylation on translation and stress granule assembly. *eLife*. https://doi.org/10.7554/eLife.05033.001

Sieradzan, K. A., Mechan, A. O., Jones, L., Wanker, E. E., Nukina, N., & Mann, D. M. A. (1999). *Huntington's Disease Intranuclear Inclusions Contain Truncated, Ubiquitinated Huntingtin Protein*. http://www.idealibrary.com

Singh, A., Kandi, A. R., Jayaprakashappa, D., Thuery, G., Purohit, D. J., Huelsmeier, J., Singh, R., Pothapragada, S. S., Ramaswami, M., & Bakthavachalu, B. (2022). The transcriptional response to oxidative stress is independent of stress-granule formation. *Mol Biol Cell*, *33*(3), ar25. https://doi.org/10.1091/mbc.E21-08-0418

Singleton, D. C., & Harris, A. L. (2012). Targeting the ATF4 pathway in cancer therapy. In *Expert Opinion on Therapeutic Targets* (Vol. 16, pp. 1189-1202).

Sisobhan, S., Rosensweig, C., Lear, B. C., & Allada, R. (2022). SleepMat: a new behavioral analysis software program for sleep and circadian rhythms. *Sleep*, *45*(12). https://doi.org/10.1093/sleep/zsac195

Skopkova, M., Hennig, F., Shin, B. S., Turner, C. E., Stanikova, D., Brennerova, K., Stanik, J., Fischer, U., Henden, L., Müller, U., Steinberger, D., Leshinsky-Silver, E., Bottani, A., Kurdiova, T., Ukropec, J., Nyitrayova, O., Kolnikova, M., Klimes, I., Borck, G., . . . Kalscheuer, V. M. (2017). EIF2S3 Mutations Associated with Severe X-Linked Intellectual Disability Syndrome MEHMO. *Human Mutation*, *38*(4), 409-425. https://doi.org/10.1002/humu.23170

Smalley, J. L., Breda, C., Mason, R. P., Kooner, G., Luthi-Carter, R., Gant, T. W., & Giorgini, F. (2016). Connectivity mapping uncovers small molecules that modulate neurodegeneration in Huntington's disease models. *Journal of Molecular Medicine*, *94*(2), 235-245. https://doi.org/10.1007/s00109-015-1344-5

Sobczak, K., & Krzyzosiak, W. J. (2004). Patterns of CAG repeat interruptions in SCA1 and SCA2 genes in relation to repeat instability. *Hum Mutat*, *24*(3), 236-247. https://doi.org/10.1002/humu.20075

Sørensen, J. G., Nielsen, M. M., Kruhøffer, M., Justesen, J., & Loeschcke, V. (2005). *Full genome gene expression analysis of the heat stress response in Drosophila melanogaster* (Cell Stress & Chaperones, Issue. http://mit.biology.au.dk/aces

Soto, C., & Lisbell, E. (2008). *Protein Misfolding and Neurodegeneration* (Arch Neurol, Issue. https://jamanetwork.com/

Sotrel, A., Paskevich, P. A., Kiely, D. K., Bird, E. D., Williams, R. S., & Myers, R. H. (1991). Morphometric analysis of the prefrontal cortex in Huntington's disease. *Neurology*, *41*(7), 1117-1117. https://doi.org/10.1212/WNL.41.7.1117

Starr, C. R., Pitale, P. M., & Gorbatyuk, M. (2018). Translational attenuation and retinal degeneration in mice with an active integrated stress response. *Cell Death and Disease*, *9*(5), 1-9. https://doi.org/10.1038/s41419-018-0513-1

Stavenga, D. G., & Arikawa, K. (2008). One rhodopsin per photoreceptor: Iro-C genes break the rule. In *PLoS Biology* (Vol. 6, pp. 675-677).

Stoecklin, G., & Kedersha, N. (2013). Relationship of GW/P-bodies with stress granules. *Adv Exp Med Biol*, *768*, 197-211. https://doi.org/10.1007/978-1-4614-5107-5_12

Stoleru, D., Peng, Y., Agosto, J., & Rosbash, M. (2004). Coupled oscillators control morning and evening locomotor behaviour of Drosophila. *Nature*, *431*(7010), 862-868. https://doi.org/10.1038/nature02926

Sullivan, L. S., Bowne, S. J., Birch, D. G., Hughbanks-Wheaton, D., Heckenlively, J. R., Lewis, R. A., Garcia, C. A., Ruiz, R. S., Blanton, S. H., Northrup, H., Gire, A. I., Seaman, R., Duzkale, H., Spellicy, C. J., Zhu, J., Shankar, S. P., & Daiger, S. P. (2006). Prevalence of disease-causing mutations in families with autosomal dominant retinitis pigmentosa: a screen of known genes in 200 families. *Invest Ophthalmol Vis Sci*, *47*(7), 3052-3064. https://doi.org/10.1167/iovs.05-1443

Swami, M., Hendricks, A. E., Gillis, T., Massood, T., Mysore, J., Myers, R. H., & Wheeler, V. C. (2009). Somatic expansion of the Huntington's disease CAG repeat in the brain is associated with an earlier age of disease onset. *Human Molecular Genetics*, *18*(16), 3039-3047. https://doi.org/10.1093/hmg/ddp242

Taalab, Y. M., Ibrahim, N., Maher, A., Hassan, M., Mohamed, W., Moustafa, A. A., Salama, M., Johar, D., & Bernstein, L. (2018). Mechanisms of disordered neurodegenerative function: concepts and facts about the different roles of the protein kinase RNA-like endoplasmic reticulum kinase (PERK). *Rev Neurosci*, *29*(4), 387-415. https://doi.org/10.1515/revneuro-2017-0071

Tanackovic, G., Ransijn, A., Thibault, P., Abou Elela, S., Klinck, R., Berson, E. L., Chabot, B., & Rivolta, C. (2011). PRPF mutations are associated with generalized defects in spliceosome formation and pre-mRNA splicing in patients with retinitis pigmentosa. *Hum Mol Genet*, *20*(11), 2116-2130. https://doi.org/10.1093/hmg/ddr094

Tataroglu, O., & Emery, P. (2014). Studying circadian rhythms in Drosophila melanogaster. *Methods*, *68*(1), 140-150. https://doi.org/10.1016/j.ymeth.2014.01.001

Tauber, D., & Parker, R. (2019). 15-Deoxy-Δ12,14-prostaglandin J2 promotes phosphorylation of eukaryotic initiation factor 2α and activates the integrated stress response. *Journal of Biological Chemistry*, *294*(16), 6344-6352. https://doi.org/10.1074/jbc.RA118.007138

Taylor, N., & Bramble, D. (1997). Sleep disturbance and Huntingdon's disease. In *The British journal of psychiatry : the journal of mental science* (Vol. 171, pp. 393-393).

The Huntington's Disease Collaborative Research, G. (1993). A Novel Gene Containing a Trinucleotide Repeat That Is Expanded and Unstable on Huntington's Diseases Chromosomes. *Cell*, *72*, 971-983.

Tijsterman, M., & Plasterk, R. (2004). Dicers at RISC: The Mechanism of RNAi. *Cell*, *117*(1), 1-3.

Timberlake, A. T., Griffin, C., Heike, C. L., Hing, A. V., Cunningham, M. L., Chitayat, D., Davis, M. R., Doust, S. J., Drake, A. F., Duenas-Roque, M. M., Goldblatt, J., Gustafson, J. A., Hurtado-Villa, P., Johns, A., Karp, N., Laing, N. G., Magee, L., Mullegama, S. V., Pachajoa, H., . . . Luquetti, D. V. (2021). Haploinsufficiency of SF3B2 causes craniofacial microsomia. *Nature Communications*, *12*(1). https://doi.org/10.1038/s41467-021-24852-9

Tourrière, H., Chebli, K., Zekri, L., Courselaud, B., Blanchard, J. M., Bertrand, E., & Tazi, J. (2003). The RasGAP-associated endoribonuclease G3BP assembles stress granules. *Journal of Cell Biology*, *160*(6), 823-831. https://doi.org/10.1083/jcb.200212128

Trivedi, D., & Padinjat, R. (2007). RdgB proteins: Functions in lipid homeostasis and signal transduction. *Biochimica et Biophysica Acta - Molecular and Cell Biology of Lipids*, *1771*(6), 692-699. https://doi.org/10.1016/j.bbalip.2007.04.014

Tuson, M., Marfany, G., & Gonzalez-Duarte, R. (2004). Mutation of CERKL, a novel human ceramide kinase gene, causes autosomal recessive retinitis pigmentosa (RP26). *Am J Hum Genet*, *74*(1), 128-138. https://doi.org/10.1086/381055

Vaccaro, A., Patten, S. A., Aggad, D., Julien, C., Maios, C., Kabashi, E., Drapeau, P., & Parker, J. A. (2013). Pharmacological reduction of ER stress protects against TDP-43 neuronal toxicity in vivo. *Neurobiology of Disease*, *55*, 64-75. https://doi.org/10.1016/j.nbd.2013.03.015

van Blitterswijk, M., Mullen, B., Heckman, M. G., Baker, M. C., DeJesus-Hernandez, M., Brown, P. H., Murray, M. E., Hsiung, G. Y., Stewart, H., Karydas, A. M., Finger, E., Kertesz, A., Bigio, E. H., Weintraub, S., Mesulam, M., Hatanpaa, K. J., White, C. L., 3rd, Neumann, M., Strong, M. J., . . . Rademakers, R. (2014). Ataxin-2 as potential disease modifier in C9ORF72 expansion carriers. *Neurobiol Aging*, *35*(10), 2421 e2413-2427. https://doi.org/10.1016/j.neurobiolaging.2014.04.016

Van Gelder, R. N., Wee, R., Lee, J. A., & Tu, D. C. (2003). Reduced pupillary light responses in mice lacking cryptochromes. *Science*, *299*(5604), 222. https://doi.org/10.1126/science.1079536

van Marle, G., Antony, J., Ostermann, H., Dunham, C., Hunt, T., Halliday, W., Maingat, F., Urbanowski, M. D., Hobman, T., Peeling, J., & Power, C. (2007). West Nile Virus-Induced Neuroinflammation: Glial Infection and Capsid Protein-Mediated Neurovirulence. *Journal of Virology*, *81*(20), 10933-10949. https://doi.org/10.1128/jvi.02422-06

Van Wamelen, D. J., Aziz, N. A., Anink, J. J., Van Steenhoven, R., Angeloni, D., Fraschini, F., Jockers, R., Roos, R. A. C., & Swaab, D. F. (2013). Suprachiasmatic nucleus neuropeptide expression in patients with Huntington's disease. *Sleep*, *36*(1), 117-125. https://doi.org/10.5665/sleep.2314

Vance, C., Rogelj, B., Hortobágyi, T., De Vos, K. J., Nishimura, A. L., Sreedharan, J., Hu, X., Smith, B., Ruddy, D., Wright, P., Ganesalingam, J., Williams, K. L., Tripathi, V., Al-Saraj, S., Al-Chalabi, A., Leigh, P. N., Blair, I. P., Nicholson, G., De Belleroche, J., . . . Shaw, C. E. (2009). Mutations in FUS, an RNA processing protein, cause familial amyotrophic lateral sclerosis type 6. *Science*, *323*(5918), 1208-1211. https://doi.org/10.1126/science.1165942

Vanderstraeten, J., Gailly, P., & Malkemper, E. P. (2020). Light entrainment of retinal biorhythms: cryptochrome 2 as candidate photoreceptor in mammals. *Cell Mol Life Sci*, *77*(5), 875-884. https://doi.org/10.1007/s00018-020-03463-5

Vidal, R., Caballero, B., Couve, A., & Hetz, C. (2011). *Converging Pathways in the Occurrence of Endoplasmic Reticulum (ER) Stress in Huntington's Disease* (Current Molecular Medicine, Issue.

Vihtelic, T. S., Hyde, D. R., & O'Tousa, J. E. (1991). Isolation and characterization of the drosophila retinal degeneration B (rdgB) gene. *Genetics*, *127*(4), 761-768.

Vissers, J. H. A., Manning, S. A., Kulkarni, A., & Harvey, K. F. (2016). A Drosophila RNAi library modulates Hippo pathway-dependent tissue growth. *Nature Communications*, *7*. https://doi.org/10.1038/ncomms10368

Vitet, H., Brandt, V., & Saudou, F. (2020). Traffic signaling: new functions of huntingtin and axonal transport in neurological disease. *Curr Opin Neurobiol*, *63*, 122-130. https://doi.org/10.1016/j.conb.2020.04.001

W.H.O. (2021). *Global status report on the public health response to dementia: Web Annex Methodology for producing global dementia cost estimates*. World Health Organization. https://le.userservices.exlibrisgroup.com/view/uresolver/44UOLE_INST/openurl?u.ignore_date_coverage=true&rft.mms_id=991010037052602746

Walker, F. O. (2007). Huntington's disease. *The Lancet*, *369*, 218-228. https://doi.org/https://doi.org/10.1016/S0140-6736(07)60111-1

Walker, M. T., Rupp, A., Elsaesser, R., Guler, A. D., Sheng, W., Weng, S., Berson, D. M., Hattar, S., & Montell, C. (2015). RdgB2 is required for dim-light input into intrinsically photosensitive retinal ganglion cells. *Mol Biol Cell*, *26*(20), 3671-3678. https://doi.org/10.1091/mbc.E15-05-0288

Wang, T., & Montell, C. (2007). Phototransduction and retinal degeneration in Drosophila. In *Pflugers Archiv European Journal of Physiology* (Vol. 454, pp. 821-847).

Wassle, H., & Boycott, B. B. (1991). *Functional Architecture of the Mammalian Retina* (PHYSIOLOGICAL REVIEWS, Issue. www.physiology.org/journal/physrev

Wei, N., Zhu, L. Q., & Liu, D. (2015). ATF4: a Novel Potential Therapeutic Target for Alzheimer's Disease. In *Molecular Neurobiology* (Vol. 52, pp. 1765-1770): Humana Press Inc.

Wek, R. C. (2018). Role of eIF2α kinases in translational control and adaptation to cellular stress. *Cold Spring Harbor Perspectives in Biology*, *10*(7). https://doi.org/10.1101/cshperspect.a032870

Wert, K. J., Lin, J. H., & Tsang, S. H. (2014). General pathophysiology in retinal degeneration. In *Cell-Based Therapy for Retinal Degenerative Disease* (Vol. 53, pp. 33-43). S. Karger AG. https://doi.org/10.1159/000357294

Williamson, T. E., Vitalis, A., Crick, S. L., & Pappu, R. V. (2010). Modulation of Polyglutamine Conformations and Dimer Formation by the N-Terminus of Huntingtin. *Journal of Molecular Biology*, *396*(5), 1295-1309. https://doi.org/10.1016/j.jmb.2009.12.017

Wolfgang, W. J., Miller, T. W., Webster, J. M., Huston, J. S., Thompson, L. M., Marsh, J. L., & Messer, A. (2005). Suppression of Huntington's disease pathology in Drosophila by human single-chain Fv antibodies. *Proc Natl Acad Sci U S A*, *102*(32), 11563-11568. https://doi.org/10.1073/pnas.0505321102

Wolozin, B. (2012). Regulated protein aggregation: Stress granules and neurodegeneration. *Molecular Neurodegeneration*, *7*(1), 1-12. https://doi.org/10.1186/1750-1326-7-56

Wolozin, B., & Ivanov, P. (2019). Stress granules and neurodegeneration. *Nat Rev Neurosci*, *20*(11), 649-666. https://doi.org/10.1038/s41583-019-0222-5

Xiang, C., Wang, Y., Zhang, H., & Han, F. (2016). The role of endoplasmic reticulum stress in neurodegenerative disease. *Apoptosis*, *0*(0), 0-0. https://doi.org/10.1007/s10495-016-1296-4

Xiong, B., & Bellen, H. J. (2013). Rhodopsin homeostasis and retinal degeneration: Lessons from the fly. *Trends in Neurosciences*, *36*(11), 652-660. https://doi.org/10.1016/j.tins.2013.08.003

Xu, F., Kula-Eversole, E., Iwanaszko, M., Hutchison, A. L., Dinner, A., & Allada, R. (2019a). Circadian Clocks Function in Concert with Heat Shock Organizing Protein to Modulate Mutant Huntingtin Aggregation and Toxicity. *Cell Reports*, *27*(1), 59-70.e54. https://doi.org/10.1016/j.celrep.2019.03.015

Xu, F., Kula-Eversole, E., Iwanaszko, M., Lim, C., & Allada, R. (2019b). Ataxin2 functions via CrebA to mediate Huntingtin toxicity in circadian clock neurons. *PLOS Genetics*, *15*(10). https://doi.org/10.1371/journal.pgen.1008356

Yadav, S., Cockcroft, S., & Raghu, P. (2016). The Drosophila photoreceptor as a model system for studying signalling at membrane contact sites. *Biochemical Society Transactions*, *44*(2), 447-451. https://doi.org/10.1042/BST20150256

Yadav, S., Thakur, R., Georgiev, P., Deivasigamani, S., Krishnan, H., Ratnaparkhi, G., & Raghu, P. (2018). RDGBα localization and function at membrane contact sites is regulated by FFAT-VAP interactions. *Journal of Cell Science*, *131*(1). https://doi.org/10.1242/jcs.207985

Yamoah, A., Tripathi, P., Guo, H., Scheve, L., Walter, P., Johnen, S., Muller, F., Weis, J., & Goswami, A. (2023). Early Alterations of RNA Binding Protein (RBP) Homeostasis and ER Stress-Mediated Autophagy Contributes to Progressive Retinal Degeneration in the rd10 Mouse Model of Retinitis Pigmentosa (RP). *Cells*, *12*(7). https://doi.org/10.3390/cells12071094

Yao, Z., & Shafer, O. T. (2014). The Drosophila Circadian Clock Is a Variably Coupled Network of Multiple Peptidergic Units. *Science*, *343*(6178), 1513-1516. https://doi.org/10.1126/science.1246514

Yoshii, T., Vanin, S., Costa, R., & Helfrich-FÖrster, C. (2009). Synergic entrainment of drosophila?s circadian clock by light and temperature. *Journal of Biological Rhythms*, *24*(6), 452-464. https://doi.org/10.1177/0748730409348551

Young-Baird, S. K., Lourenço, M. B., Elder, M. K., Klann, E., Liebau, S., & Dever, T. E. (2020). Suppression of MEHMO Syndrome Mutation in eIF2 by Small Molecule ISRIB. *Molecular Cell*, *77*(4), 875-886.e877. https://doi.org/10.1016/j.molcel.2019.11.008

Zekri, L., Chebli, K., Tourrière, H., Nielsen, F. C., Hansen, T. V. O., Rami, A., & Tazi, J. (2005). Control of Fetal Growth and Neonatal Survival by the RasGAP-Associated Endoribonuclease G3BP. *Molecular and Cellular Biology*, *25*(19), 8703-8716. https://doi.org/10.1128/mcb.25.19.8703-8716.2005

Zhang, L., Chung, B. Y., Lear, B. C., Kilman, V. L., Liu, Y., Mahesh, G., Meissner, R. A., Hardin, P. E., & Allada, R. (2010). DN1p Circadian Neurons Coordinate Acute Light and PDF Inputs to Produce Robust Daily Behavior in Drosophila. *Current Biology*, *20*(7), 591-599. https://doi.org/10.1016/j.cub.2010.02.056

Zhang, S., Binari, R., Zhou, R., & Perrimon, N. (2010). A genomewide RNA interference screen for modifiers of aggregates formation by mutant huntingtin in drosophila. *Genetics*, *184*(4), 1165-1179. https://doi.org/10.1534/genetics.109.112516

Zhang, S. X., Sanders, E., Fliesler, S. J., & Wang, J. J. (2014). Endoplasmic reticulum stress and the unfolded protein responses in retinal degeneration. *Exp Eye Res*, *125*, 30-40. https://doi.org/10.1016/j.exer.2014.04.015

Zhang, Y., Ling, J., Yuan, C., Dubruille, R., & Emery, P. (2013). A role for Drosophila ATX2 in activation of PER translation and circadian behavior. *Science*, *340*(6134), 879-882. https://doi.org/10.1126/science.1234746

Zimmerman, J. E., Chan, M. T., Jackson, N., Maislin, G., & Pack, A. I. (2012). Genetic background has a major impact on differences in sleep resulting from environmental influences in Drosophila. *Sleep*, *35*(4), 545-557. https://doi.org/10.5665/sleep.1744

Appendices

Appendix 1. Presence of two UAS constructs does not lead to a reduction in the power of rhythmicity

To test the hypothesis that the presence of two UAS constructs is what led to the phenotypic rescue observed in the power of rhythmicity when expressing *perk* RNAi or *atx2* RNAi in conjunction with the toxic expression of *Htt*Q138, a separate circadian rhythm experiment was conducted with a group of flies expressing the PDFGal4 driver, the *UAS-mRFP-HttQ138* construct, and a UAS-GFP construct. The experiment was conducted identically to those previously described in this thesis, with three days of entrainment and four days of constant darkness for free-running conditions.

Only the power of rhythmicity was extracted from the DAM data and is reported in the figure below. During the free-running period, a one-way ANOVA detected a significant difference in the power of rhythmicity between the genotypes ($F_{2, 70} = 36.65$, $p < 0.001$). Flies expressing the expanded form of *Htt* in PDF neurons (PDF>Q138) demonstrated a sharp decrease in the rhythmicity which was statistically different when compared to the parental group PDFGal4 ($p < 0.001$, Tukey's *post-hoc* test). Expressing GFP in these flies (PDF> UAS GFP; Q138) led to a significant 66% decrease in the power of rhythmicity compared to the PDF>Q138 group ($p = 0.04$, Tukey's *post-hoc* test). The PDF>UAS GFP; Q138 group was also significantly different to its parental group PDFGal4 ($p < 0.001$, Tukey's *post-hoc* test). No difference was detected during the entrainment period ($F_{2, 70} = 1.787$, $p = 0.1751$, one-way ANOVA).

Although these are preliminary experiments, the results suggest that the presence of two UAS constructs is not the origin of a possible phenotypic rescue. However, future experiments should repeat this test with the expression of a mock RNAi instead, as the expression of the GFP protein may affect the PDF neurons independently of the *Htt*Q138 transgene.

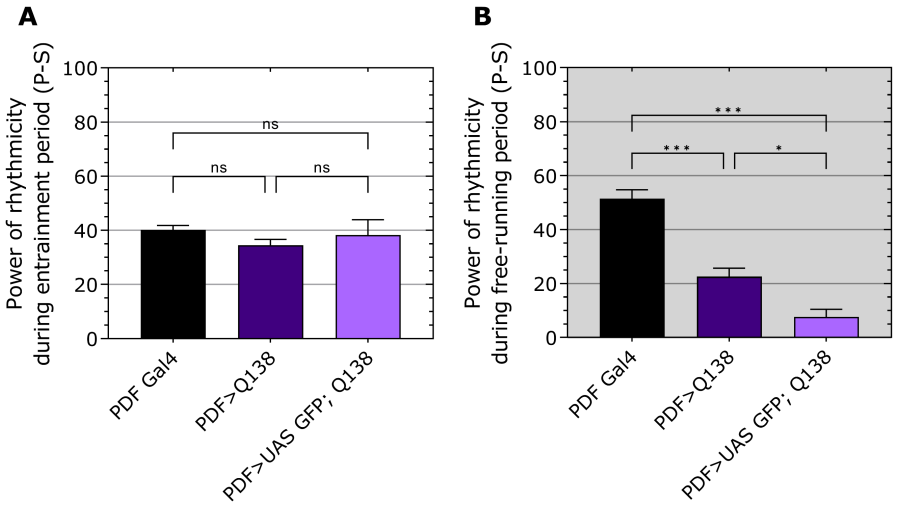

Appendix 1 Presence of two UAS constructs does not alleviate toxicity induced by HttQ138.

*Average power of rhythmicity during the entrainment period (A) and the free-running period (B) conditions. Power of rhythmicity corresponds to Power – Significance (P-S). Mean value calculated using individual fly values from SleepMat (Sisobhan et al., 2022). Data presented as mean ± SEM, *p < 0.05, **p < 0.01, and ***p < 0.001, Tukey's multiple comparison post-hoc test.*

Appendix 2. *Rin* knockdown does not affect stress-induced transcription

The overarching aim of this experiment was to determine whether stress-granule (SG) formation contributed to stress-induced transcriptional changes. For this purpose, I conducted an O-propargyl-puromycin incorporation assay to examine whether global translational repression induced by sodium arsenite was affected when *rin* was knocked-down and SGs were not observed.

Wild-type *Drosophila* S2 cells were depleted for *rin* mRNA by dsRNA. Briefly, 5 x 10^5 cells were transfected with 5 µg of dsRNA at 0 h and again at 48 h, and were harvested at 96 h. Knockdown of Rin was confirmed using Western blotting, and RNA was isolated using TRIzol reagent (Invitrogen) as per the manufacturer's protocol. For puromycylation assays, 93 h after mock and Rin dsRNA transfections, cells were subjected to 0.5 mM sodium arsenite in S2 media for 3 h at room temperature on a rocking shaker. After 3 h, arsenite containing S2 media was removed by centrifugation at 2000 rpm for 5 min, the cells were washed three times with fresh media and kept for recovery in fresh complete S2 media. Puromycin was added during the final 15 min at a final concentration of 4 µg/ml. Cells were immediately harvested and analysed for the knockdown of Rin and for puromycin incorporation. Cells were lysed and normalised for protein concentration using the Bio-Rad Protein Assay Kit (Bio-Rad Laboratories, # 5000001) and a spectrophotometer. Western blotting was performed using rabbit anti-Rin (1:1000), mouse anti-puromycin (1:2000, MABE343 Sigma-Aldrich), and mouse anti-tubulin (1:4000, E7c DSHB). Goat anti-rabbit HRP (sc-2004) and goat anti-mouse HRP (sc-2005) HRP–conjugated secondary antibodies were used at 1:10000 dilution. The band intensities for p-eIF2α under various treatments were acquired by measuring the mean grey value in ImageJ (https://imagej.net/software/fiji). Eight-bit images were used for quantification and hence the mean grey values were subtracted from 255 (which corresponds to the number of pixels) to obtain inverted pixel densities. Background subtraction was performed to eliminate non-specific signals and the resultant values were then normalized to the corresponding numbers obtained for total eIF2α. The same protocol was followed to quantify the levels of Rin in mock RNAi and Rin RNAi cells except that the normalization was done against the levels of tubulin. GraphPad Prism 9 was used

to plot the normalized values as a bar plot and unpaired Student's t test was used for statistical analysis ($p< 0.05$).

Strikingly, cells that were knocked-down for *rin* still exhibited stress-induced attenuation of global translation. In addition, cells treated with a mock RNAi displayed an increased expression of *rin* when treated with sodium arsenite. These results were in agreement with the hypothesis that the transcriptional response after oxidative stress is uncoupled from SG assembly.

More information can be found in: Singh, A., Kandi, A. R., Jayaprakashappa, D., Thuery, G., Purohit, D. J., Huelsmeier, J., Singh, R., Pothapragada, S. S., Ramaswami, M., & Bakthavachalu, B. (2022). The transcriptional response to oxidative stress is independent of stress-granule formation. *Mol Biol Cell*, *33*(3), ar25. https://doi.org/10.1091/mbc.E21-08-0418

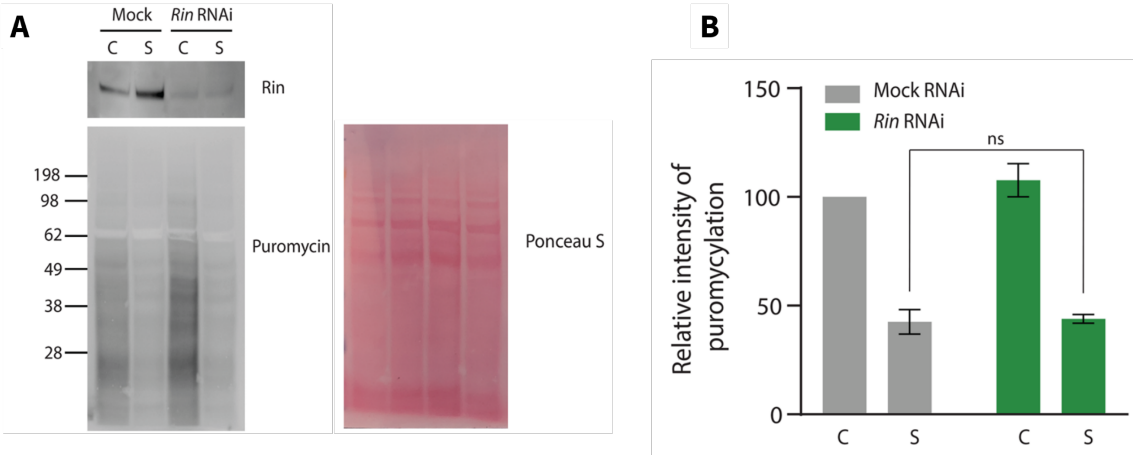

Appendix 2 Rin knockdown does not affect stress-induced transcription.

(A) O-propargyl-puromycin incorporation assays in mock and Rin RNAi cells. Western analyses using total cell lysates from mock RNAi and Rin RNAi cells under control and stress conditions were used for puromycin incorporation. Anti-puromycin and Anti-Rin antibodies were used at 1:1000 and 1:500 dilutions, respectively. A representative blot of four independent experiments is shown. Ponceau S staining depicts the protein levels in the different cell lysates. (B) Bar graphs showing the relative intensity of puromycylation in mock RNAi and Rin RNAi cells under control and stress conditions. Mann–Whitney U test shows that there was no significant difference in puromycylation between mock RNAi stress and Rin RNAi stress cells. Error bars show ± SEM (ns: $p > 0.05$).

Appendix 3. Novel RNA-binding protein alignments, and RNAi targets

A

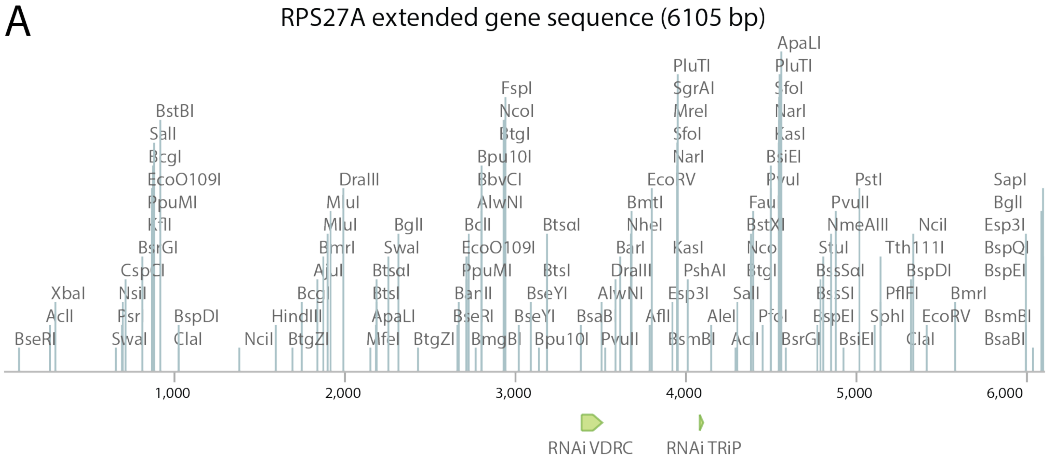

B

```
Fly      1 MQIFVKTLTGKTITLEVEPSDTIENVKAKIQDKEGIPPDQQRLIFAGKQLEDGRTLSDYNIQKES 65
           ||||||||||||||||||||||||||||||||||||||||||||||||||||||||||||||||||||
Human    1 MQIFVKTLTGKTITLEVEPSDTIENVKAKIQDKEGIPPDQQRLIFAGKQLEDGRTLSDYNIQKES 65

Fly     66 TLHLVLRLRGGAKKRKKKNYSTPKKIKHKRKKVKLAVLKYYKVDENGKIHRLRRECPGENCGAGV 130
           ||||||||||||||||||:|:||||.|||||||||||||||||||.|||||||.:.|||||
Human    66 TLHLVLRLRGGAKKRKKKSYTTPKKNKHKRKKVKLAVLKYYKVDENGKISRLRRECPSDECGAGV 130

Fly     131 FMAAHEDRHYCGKCNLTFVFSKPEEK 156
           |||:|.||||||||.||:.|:|||:|
Human   131 FMASHFDRHYCGKCCLTYCFNKPEDK 156
```

Appendix 3 – 1 RPS27A extended gene sequence and protein alignment.

(A) Extended gene sequence for Drosophila RPS27A, with RNAi target location in the locus labelled with green arrows. (B) Protein sequence alignment between Drosophila and H. Sapiens using the DRSC Integrative Ortholog Prediction Tool (DIOPT) (Hu et al., 2011). Sequence 1: NP_476778.1 (RpS27A), sequence 2: NP_001129064.1 (RPS27A). Alignment length: 156; Identity: 142/156 (91%); Similarity: 159/156 (95%); Gaps: 0/156 (0%).

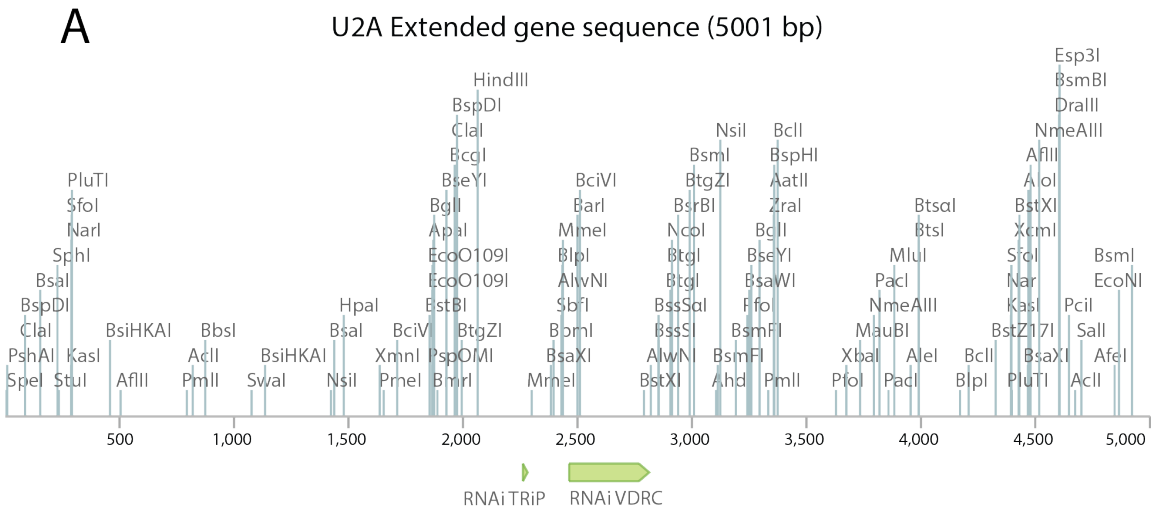

B

```
  Fly     1 MVKLTPELINQSMQYINPCRERELDLRGYKIPQIENLGATLDQFDTIDLSDNDLRKLDNLPHLPR 65
            |||||.|||.|:.||.|..|:||||||||||.||||||||||.||.|||::||||..|.|.|
Human     1 MVKLTAELIEQAAQYTNAVRDRELDLRGYKIPVIENLGATLDQFDAIDFSDNEIRKLDGFPLLRR 65

  Fly    66 LKCLLLNNNRILRISEGLEEAVPNLGSIILTGNNLQELSDLEPLVGFTKLETICLLINPVSTKPN 130
            ||.||:|||||.||.|||::|:|.|..:|||.|:|.||.||:||.....|..:.:|.|||:.|.:
Human    66 LKTLLVNNNRICRIGEGLDQALPCLTELILTNNSLVELGDLDPLASLKSLTYLSILRNPVTNKKH 130

  Fly   131 YREYMAYKFPQLRLLDFRKIKQKDRQAAQEFFRTKQGKDVLKEISRKSK-MSAAAAIAAEAGNGK 194
            ||.|:.||.||:|:|||:|:|.|:||.|::.|:.|:|..:.|:|:|:|| .:..|.:..:.
Human   131 YRLYVIYKVPQVRVLDFQKVKLKERQEAEKMFKGKRGAQLAKDIARRSKTFNPGAGLPTDK---- 191

  Fly   195 GRGSEGGRLANPQDMQRIREAIKRASSLAEVERLSQILQSGQLP---------DKFQHEMEA-VA 249
               .:||  .:|.|::.|:.||..||:|||||..:|||||:|         |..:.|||. ..
Human   192 ---KKGG--PSPGDVEAIKNAIANASTLAEVERLKGLLQSGQIPGRERRSGPTDDGEEEMEEDTV 251

  Fly   250 QNGA 253
            .||:
Human   252 TNGS 255
```

Appendix 3 – 2 U2A extended gene sequence and protein alignment.

(A) Extended gene sequence for Drosophila U2A, with RNAi target location in the locus labelled with green arrows. (B) Protein sequence alignment between Drosophila and H. Sapiens using the DRSC Integrative Ortholog Prediction Tool (DIOPT) (Hu et al., 2011). Sequence 1: NP_610315.1 (U2A), sequence 2: NP_003081.2 (SNRPA1). Alignment length: 264; Identity: 136/264 (51%); Similarity: 178/264 (67%); Gaps: 20/264 (7%).

A

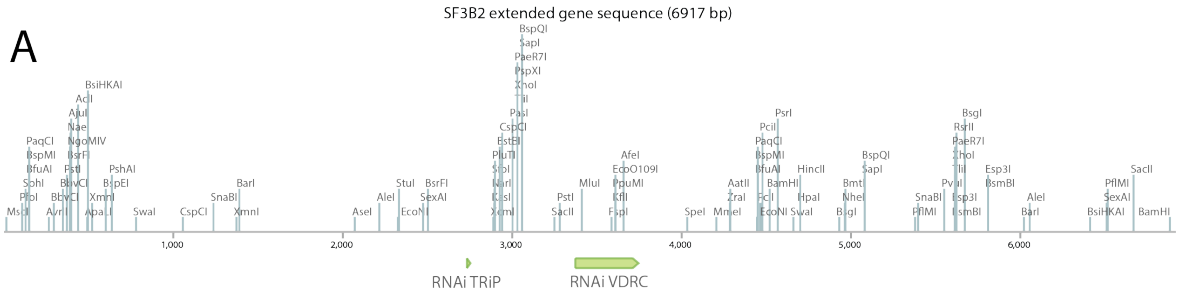

B

```
  Fly    44 GDASEDAVDAEKTPGELVLPKALEDVLALKDQRAAEFTVDADSQGGSGGATQDGDEADVGEDSEE 108
            ||.:.:..|....|   .:|:|||.:|.||:.|..|.....:.                 |:.|.
Human   254 GDENREMDDPSVGP---KIPQALEKILQLKESRQEEMNSQQEE----------------EEMET 298

  Fly   109 DADNQVNGSASQKTGKQSKAERNKKKKKRKKQNRKIRHQIEFARQQQLAQAEENEPEAKDSETKA 173
            ||.:.:..|||:.  ::.....:||:|.||::|||
Human   299 DARSSLGQSASET--EEDTVSVSKKEKNRKRRNRK---------------------------- 331

  Fly   174 HGSEDEQVAEKEKKDKR-----KESRSKRRKDRSDEKDTDKKAGEANDENVTIEYVPEKITIADL 233
                        |:||.:|     .||...|.||.:..:.:|..|.:     |.||||.|:..|.:
Human   332 ----------KKKKPQRVRGVSSESSGDREKDSTRSRGSDSPAAD-----VEIEYVTEEPEIYE- 380

  Fly   234 APMYRQFYRVFEIFKL------ENKPKPVEKDKSSHDSESHPRDKKATDKQLEDEDDDGDDDEER 292
             |.:..|.|:||.|||       |.:.:|.:.||.  ::.:.|:.|...::..:.:||..||::|:
Human   381 -PNFIFFKRIFEAFKLTDDVKKEKEKEPEKLDKL--ENSAAPKKKGFEEEHKDSDDDSSDDEQEK 442

  Fly   293 KEDKEKLSKRKLKKLTRLSVAELKQLVSRPDVVEMHDVTARDPKLLVQLKAYRNTVQVPRHWCFK 357
            |.:..||||:||:::.|.:||||||||:||||||||||||:||||||.|||.||:|.||||||||
Human   443 KPEAPKLSKKKLRRMNRFTVAELKQLVARPDVVEMHDVTAQDPKLLVHLKATRNSVPVPRHWCFK 507

  Fly   358 RKYLQGKRGIEKPPFDLPAFIKKTGIMEMRESLQEREDAKTLKAKMRERVRPKMGKIDIDYQKLH 422
            |||||||||||||:||.|||:|||.||||:|||:|:.||:|:|||||:|||||||||||||||||
Human   508 RKYLQGKRGIEKPPFELPDFIKRTGIQEMREALQEKEEQKTMKSKMREKVRPKMGKIDIDYQKLH 572

  Fly   423 DAFFKWQTKPRMTIHGDLYYEGKEFETRLKEKKPGDLSEELRIALGMPVGPNSHKIPPPWLIAQQ 487
            ||||||||||::|||||||||||||||||||||||:||||:||||||||:||:|||||||.|
Human   573 DAFFKWQTKPKLTIHGDLYYEGKEFETRLKEKKPGDLSDELRISLGMPVGPNAHKVPPPWLIAMQ 637

  Fly   488 RYGPPPSYPNLKIPGLNAPIPDGTSFGYHAGGWGKPPVDENGKPLYGDVFGTNILDLDNGVDEAD 552
            |||||||||||||||:|||:..|||||||||||||||.||||||||||||..:.....:|.:
Human   638 RYGPPPSYPNLKIPGLNSPIPESCSFGYHAGGWGKPPVDETGKPLYGDVFGTNAAEFQTKTEEEE 702

  Fly   553 IERNQWGELESESEESSEEEEEDGEDLGDQQDETGLVTPVE-GLVTPSGLTSVPAGMETPENIEL 616
            |:|..|||||...|||||||||:..| .|:|.||||.:||.: ||:||.|.:|||||||||.|||
Human   703 IDRTPWGELEPSDEESSEEEEEEESD-EDKPDETGFITPADSGLITPGGFSSVPAGMETPELIEL 766

  Fly   617 RKKKIEAEMEDNETPVLYQVLPEKRTDRIGASMMGSTHVYDVSGSGANKQPPVRSTTDREGIVEL 681
            ||||||..|:.:|||.|:.||||||..:|.:||||||:||:|...:.|.|    ..:.:| ||:
Human   767 RKKKIEEAMDGSETPQLFTVLPEKRTATVGGAMMGSTHIYDMSTVMSRKGP----APELQG-VEV 826

  Fly   682 ALDPSELDLDNDAMAQRYEQQMREQQNHLQKEDLSDMLAEHVARQK-SKRKRQQTDPAKTTKKYK 745
            ||.|.||:||..||.|:||:.:||||..::|||.|||:|||.|:|| .|||.|..|....:||||
Human   827 ALAPEELELDPMAMTQKYEEHVREQQAQVEKEDFSDMVAEHAAKQKQKKRKAQPQDSRGGSKKYK 891

  Fly   746 EFKF 749
            ||||
Human   892 EFKF 895
```

Appendix 3 – 3 SF3B2 extended gene sequence and protein alignment.

(A) Extended gene sequence for Drosophila SF3B2, with RNAi target location in the locus labelled with green arrows. (B) Protein sequence alignment between Drosophila and H. Sapiens using the DRSC Integrative Ortholog Prediction Tool (DIOPT) (Hu et al., 2011). Sequence 1: NP_001259979.1 (Sf3b2), sequence 2: NP_006833.2 (SF3B2). Alignment length: 719; Identity: 390/719 (54%); Similarity: 486/719 (67%); Gaps: 90/719 (12%).

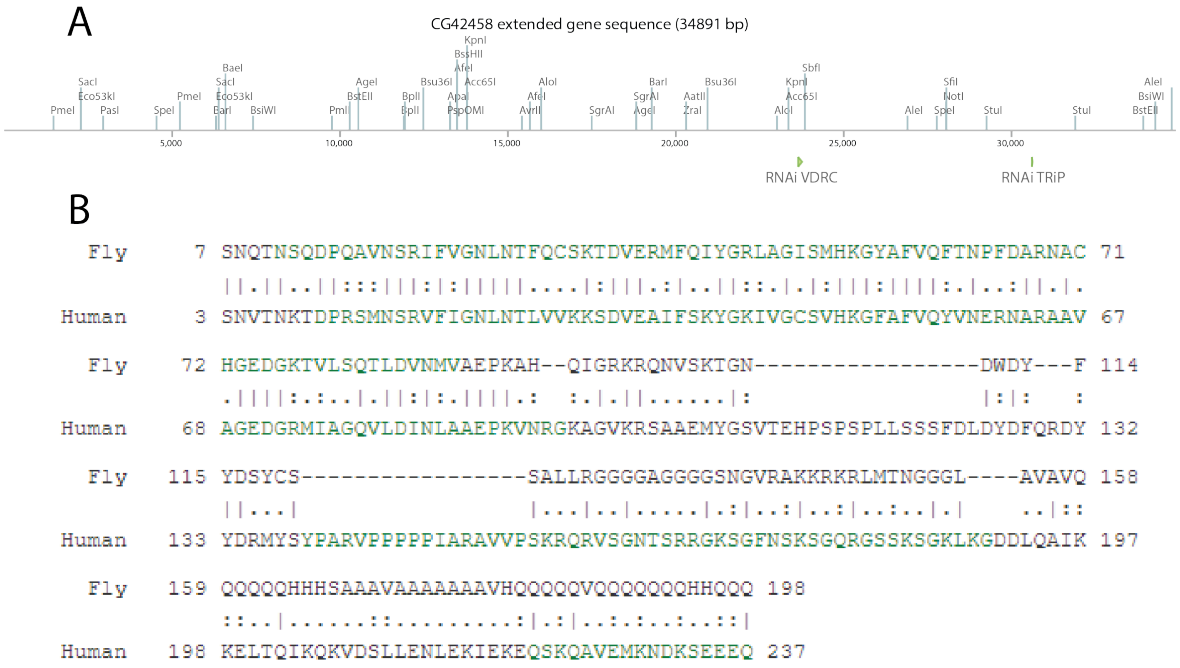

Appendix 3 – 4 CG42458 extended gene sequence and protein alignment

(A) Extended gene sequence for Drosophila CG42458, with RNAi target location in the locus labelled with green arrows. (B) Protein sequence alignment between Drosophila and H. Sapiens using the DRSC Integrative Ortholog Prediction Tool (DIOPT) (Hu et al., 2011). Sequence 1: NP_996010.2 (CG42458), sequence 2: NP_996010.2 (HNRNPC). Alignment length: 235; Identity: 70/235 (29%); Similarity: 110/235 (46%); Gaps: 43/235 (18%).